Tran-SET

Transportation Consortium of South-Central States

Solving Emerging Transportation Resiliency, Sustainability, and Economic Challenges through the Use of Innovative Materials and Construction Methods: From Research to Implementation

Enhancing the Durability and the Service Life of Asphalt Pavements through Innovative Light-Induced Self-Healing Materials

Project No. 17BLSU02

Lead University: Louisiana State University

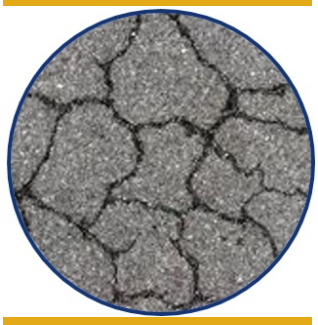

Enhancing Durability and Service Life of Infrastructure

Final Report

October 2018

Disclaimer

The contents of this report reflect the views of the authors, who are responsible for the facts and the accuracy of the information presented herein. This document is disseminated in the interest of information exchange. The report is funded, partially or entirely, by a grant from the U.S. Department of Transportation's University Transportation Centers Program. However, the U.S. Government assumes no liability for the contents or use thereof.

Acknowledgments

This study was funded by the Transportation Consortium of South-Central States (Tran-SET) and the Louisiana Transportation Research Center (LTRC). The authors would also like to acknowledge the laboratory support from LTRC and the Thermogravimetric Analysis (TGA) work from the USDA S-1041 program.

TECHNICAL DOCUMENTATION PAGE

1. **Project No.** 17BLSU02	**2. Government Accession No.**	**3. Recipient's Catalog No.**

4. Title and Subtitle Enhancing the Durability and the Service Life of Asphalt Pavements Through Innovative Light-Induced Self-Healing Materials	**5. Report Date** Oct. 2018 **6. Performing Organization Code**
7. Author(s) PI: Marwa Hassan https://orcid.org/0000-0001-8087-8232 GRA: Sharareh Shirzad https://orcid.org/0000-0001-5493-0690	**8. Performing Organization Report No.**
9. Performing Organization Name and Address Transportation Consortium of South-Central States (Tran-SET) University Transportation Center for Region 6 3319 Patrick F. Taylor Hall, Louisiana State University, Baton Rouge, LA 70803	**10. Work Unit No. (TRAIS)** **11. Contract or Grant No.** 69A3551747106
12. Sponsoring Agency Name and Address United States of America Department of Transportation Research and Innovative Technology Administration	**13. Type of Report and Period Covered** Final Research Report May 2017 – May 2018 **14. Sponsoring Agency Code**

15. Supplementary Notes

Report uploaded and accessible at: Tran-SET's website (http://transet.lsu.edu/)

16. Abstract

The objective of this study was to evaluate the efficiency of a new generation of Ultraviolet (UV) light-induced self-healing polymers in enhancing the durability and self-healing properties of asphalt mixtures. Self-healing polymers were successfully synthesized in the laboratory and were characterized using Fourier Transform Infrared Spectroscopy (FTIR). In addition, Thermogravimetric Analysis (TGA) results showed that the synthesized polymers achieved the required thermal stability to resist asphalt mixture production processes. Viscosity results showed that addition of 5% Recycled Asphalt Shingle (RAS) and/or 20% Reclaimed Asphalt Pavement (RAP) caused an increase in the viscosity of the binder blends. However, a reduction in viscosity of the binder blends containing recycled asphalt materials was observed when adding self-healing polymers.

Semi-Circular Bending (SCB) test results showed that addition of recycled asphalt materials negatively affected the cracking performance of mixtures. However, incorporation of self-healing polymer (SHP) and 48h of UV light exposure improved the cracking resistance. This behavior was more evident with mixtures prepared with an unmodified binder. Loaded-Wheel Test (LWT) results showed that the addition of the self-healing polymer led to an increase in the rut depth of the samples prepared with an unmodified binder. However, the final rut depth was less than 6 mm, which is an acceptable rutting performance. Thermal-Stress Restrained Specimen Test (TSRST) results showed that addition of 5% RAS negatively affected the low-temperature cracking performance of the mix. In contrast, 5% SHP enhanced the low-temperature cracking performance of the mix by increasing the fracture load and decreasing the fracture temperature.

For mixtures prepared with an unmodified binder, the optimum crack healing efficiency was observed for the mixtures containing 5% RAS and 5% self-healing polymer and exposed to 48h of UV light. Yet, self-healing polymer did not perform well in mixtures prepared with PG 70-22M polymer-modified binder. This may be due to the interaction between the polymer in the binder and the self-healing polymer.

17. Key Words	**18. Distribution Statement**
Self-healing polymer, Recycled asphalt material, Cracking, Asphalt binder	No restrictions.

19. Security Classif. (of this report)	**20. Security Classif. (of this page)**	**21. No. of Pages**	**22. Price**
Unclassified	Unclassified	150	

Form DOT F 1700.7 (8-72) **Reproduction of completed page authorized.**

SI* (MODERN METRIC) CONVERSION FACTORS

APPROXIMATE CONVERSIONS TO SI UNITS

Symbol	When You Know	Multiply By	To Find	Symbol
		LENGTH		
in	inches	25.4	millimeters	mm
ft	feet	0.305	meters	m
yd	yards	0.914	meters	m
mi	miles	1.61	kilometers	km
		AREA		
in^2	square inches	645.2	square millimeters	mm^2
ft^2	square feet	0.093	square meters	m^2
yd^2	square yard	0.836	square meters	m^2
ac	acres	0.405	hectares	ha
mi^2	square miles	2.59	square kilometers	km^2
		VOLUME		
fl oz	fluid ounces	29.57	milliliters	mL
gal	gallons	3.785	liters	L
ft^3	cubic feet	0.028	cubic meters	m^3
yd^3	cubic yards	0.765	cubic meters	m^3
		NOTE: volumes greater than 1000 L shall be shown in m^3		
		MASS		
oz	ounces	28.35	grams	g
lb	pounds	0.454	kilograms	kg
T	short tons (2000 lb)	0.907	megagrams (or "metric ton")	Mg (or "t")
		TEMPERATURE (exact degrees)		
^oF	Fahrenheit	5 (F-32)/9 or (F-32)/1.8	Celsius	^oC
		ILLUMINATION		
fc	foot-candles	10.76	lux	lx
fl	foot-Lamberts	3.426	$candela/m^2$	cd/m^2
		FORCE and PRESSURE or STRESS		
lbf	poundforce	4.45	newtons	N
lbf/in^2	poundforce per square inch	6.89	kilopascals	kPa

APPROXIMATE CONVERSIONS FROM SI UNITS

Symbol	When You Know	Multiply By	To Find	Symbol
		LENGTH		
mm	millimeters	0.039	inches	in
m	meters	3.28	feet	ft
m	meters	1.09	yards	yd
km	kilometers	0.621	miles	mi
		AREA		
mm^2	square millimeters	0.0016	square inches	in^2
m^2	square meters	10.764	square feet	ft^2
m^2	square meters	1.195	square yards	yd^2
ha	hectares	2.47	acres	ac
km^2	square kilometers	0.386	square miles	mi^2
		VOLUME		
mL	milliliters	0.034	fluid ounces	fl oz
L	liters	0.264	gallons	gal
m^3	cubic meters	35.314	cubic feet	ft^3
m^3	cubic meters	1.307	cubic yards	yd^3
		MASS		
g	grams	0.035	ounces	oz
kg	kilograms	2.202	pounds	lb
Mg (or "t")	megagrams (or "metric ton")	1.103	short tons (2000 lb)	T
		TEMPERATURE (exact degrees)		
^oC	Celsius	1.8C+32	Fahrenheit	^oF
		ILLUMINATION		
lx	lux	0.0929	foot-candles	fc
cd/m^2	$candela/m^2$	0.2919	foot-Lamberts	fl
		FORCE and PRESSURE or STRESS		
N	newtons	0.225	poundforce	lbf
kPa	kilopascals	0.145	poundforce per square inch	lbf/in^2

TABLE OF CONTENTS

LIST OF FIGURES VI

LIST OF TABLES X

ACRONYMS, ABBREVIATIONS, AND SYMBOLS XI

EXECUTIVE SUMMARY XIII

IMPLEMENTATION STATEMENT XV

1. INTRODUCTION 1

1.1. Background 1

1.1.1. Recycled Asphalt Materials (RAM) 2

1.1.2. Light-Activated Self-Healing Polymers 3

2. OBJECTIVE 5

3. SCOPE 6

4. METHODOLOGY 7

4.1. Self-Healing Polymer Synthesis and Characterization 7

4.1.1. Materials 7

4.1.2. Self-Healing Polymer Production Procedure 7

4.1.3. Light Activated Self-Healing Polymer Characterization 7

4.2. Effect of Self-Healing Polymer on Asphalt Binder Properties 9

4.2.1. Test Materials 9

4.2.2. Chemical Tests 10

4.2.3. Rheological Tests 11

4.3. Effect of Self-Healing Polymer on Self-Healing properties of Asphalt Mixture 13

4.3.1. Test Materials 13

4.3.2. Crack Healing Efficiency Test 14

4.4. Effect of Self-Healing Polymer on the Performance of the Mixtures 16

4.4.1. Statistical Analysis 19

5. RESULTS 20

5.1. Light Activated Self-Healing Polymer Characterization 20

5.1.1. Fourier Transform Infrared (FTIR) Spectroscopy 20

5.1.2. Thermal Stability 22

5.2. Effect of Self-Healing Polymer on the Asphalt Binder Properties 23

5.2.1. High-Pressure Gel Permeation Chromatography Results 23
5.2.2. Fourier Transform Infrared Spectroscopy Results 24
5.2.3. Rotational Viscometer (RV) 25
5.2.4. Superpave Performance Grade (PG-Grade) 26
5.2.5. Delta Tc 27
5.2.6. Useful Temperature Interval (UTI) 31
5.2.7. Multiple Stress Creep Recovery (MSCR) 34
5.2.8. Complex Shear Modulus, G* 35
5.2.9. Linear Amplitude Sweep Test Results 36
5.3. Effect of Self-Healing Polymers on Self-Healing Properties of Asphalt Mixture 40
5.3.1. Crack Healing Efficiency Test Results 40
5.4. Effect of Self-Healing Polymer on the Mechanical Performance of Asphalt Mixtures 59
5.4.1. Semi-Circular Bending Test Results 59
5.4.2. Loaded Wheel Tracking (LWT) Test Results 62
5.4.3. Thermal Stress Restrained Specimen Test (TSRST) 66
6. CONCLUSIONS 73
7. RECOMMENDATIONS 75
REFERENCES 76
APPENDIX A: PG-GRADING RESULTS 81
APPENDIX B: STATISTICAL ANALYSIS FOR BINDER TESTING 91
B.1. Statistical Analysis for DSR Results (G*/sinδ at 70°C) 91
B.2. Statistical Analysis for Calculated Delta Tc 92
B.3. Statistical Analysis for Calculated UTI 93
B.4. Statistical Analysis for MSCR Results (Percent Recovery (0.1 kPa)) 94
APPENDIX C: STATISTICAL ANALYSIS FOR MIXTURE TESTING 95
C.1. Statistical Analysis for Healing Efficiency 95
C.2. Statistical Analysis for Measured SERR 115
C.3. Statistical Analysis for SCB Results 127
C.4. Statistical Analysis for LWT Results 133
C.5. Statistical Analysis for TSRST Results 139

LIST OF FIGURES

Figure 1. Key phases of pavement life-cycle *(10).* 2

Figure 2. Chemical structure of Chitin and Chitosan *(44).* 3

Figure 3. (a) Undried and (b) dried prepared OXE-CHI. 8

Figure 4. Produced OXE-CHI-PUR polymer. 8

Figure 5. Structure of OXE-CHI-PUR *(7).* 8

Figure 6. Rectangular beams prepared for crack healing efficiency. 15

Figure 7. Crack induction at the bottom of beams. 15

Figure 8. Strain energy of the samples. 15

Figure 9. SCB samples. 16

Figure 10. SCB test setup. 17

Figure 11. Hamburg loaded wheel tracking test. 18

Figure 12. Thermal-stress restrained specimen test (TSRST). 19

Figure 13. FT-IR spectra of CHI. 20

Figure 14. FT-IR spectra of OXE-CHI (1:1). 21

Figure 15. FT-IR spectra of OXE-CHI (1:3). 21

Figure 16. FT-IR spectra of HDI. 21

Figure 17. FT-IR spectra of OXE-CHI-PUR (1:1). 22

Figure 18. FT-IR spectra of OXE-CHI-PUR (1:3). 22

Figure 19. TGA result of OXE-CHI-PUR (1:1). 23

Figure 20. TGA result of OXE-CHI-PUR (1:3). 23

Figure 21. HP-GPC results for HMW/LMW ratio. 24

Figure 22. FTIR test results. 25

Figure 23. Viscosity results for binder blends prepared with PG 67-22 binder. 25

Figure 24. Viscosity results for binder blends prepared with PG 70-22M binder. 26

Figure 25. Delta Tc results for PG 67-22 binder blends prepared with, (a) Virgin binder, (b) Virgin binder+5%RAS, (c) Virgin binder+20%RAP, and (d) Virgin binder+5%RAS+20%RAP. 29

Figure 26. Delta Tc results for PG 70-22M binder blends prepared with, (a) Virgin binder, (b) Virgin binder+5%RAS, (c) Virgin binder+20%RAP, and (d) Virgin binder+5%RAS+20%RAP. 30

Figure 27. Measured UTI for PG 67-22 Binder blends prepared with, (a) Virgin binder, (b) Virgin binder+5%RAS, (c) Virgin binder+20%RAP, and (d) Virgin Binder+5%RAS+20%RAP. 32

Figure 28. Measured UTI for PG 70-22M binder blends prepared with, (a) Virgin binder, (b) Virgin binder+5%RAS, (c) Virgin binder+20%RAP, and (d) Virgin binder+5%RAS+20%RAP. 33

Figure 29. G* results for PG 67-22 binder blends. 37

Figure 30. G* results for PG 70-22M binder blends. 38

Figure 31. LAS results for (a) PG 67-22 binder blends and (b) PG 70-22M Binder blends. . 39

Figure 32. Crack monitoring under different curing conditions; (a) Room temperature (25°C) and (b) High temperature (50°C)/ UV exposure. 40

Figure 33. Crack healing efficiency for PG 67-22 mixtures containing 5%RAS: (a) Room temperature conditioning and (b) High temperature or UV light conditioning. 42

Figure 34. Effect of curing conditions on healing efficiency of the PG 67-22 mixtures containing 5%RAS. 42

Figure 35. Crack healing efficiency for PG 70-22M mixtures containing 5%RAS: (a) Room temperature conditioning and (b) High temperature or UV light conditioning. 44

Figure 36. Effect of curing conditions on healing efficiency of the PG 70-22M mixtures containing 5%RAS. 44

Figure 37. Crack healing efficiency for PG 67-22 mixtures containing 20%RAP: (a) Room temperature conditioning and (b) High temperature or UV light conditioning. 45

Figure 38. Effect of curing conditions on healing efficiency of the PG 67-22 mixtures containing 20%RAP. 45

Figure 39. Crack healing efficiency for PG 70-22M mixtures containing 20%RAP: (a) Room temperature conditioning and (b) High temperature or UV light conditioning. 46

Figure 40. Effect of curing conditions on healing efficiency of the PG 70-22M mixtures containing 20%RAP. 47

Figure 41. Crack healing efficiency for PG 67-22 mixtures containing 5%RAS+20%RAP: (a) Room temperature conditioning and (b) High temperature or UV Light conditioning. 48

Figure 42. Effect of curing conditions on healing efficiency of the PG 67-22 mixtures containing 5%RAS+20%RAP..... 48

Figure 43. Crack healing efficiency for PG 70-22M mixtures containing 5%RAS+20%RAP: (a) Room temperature conditioning and (b) High temperature or UV light conditioning. 49

Figure 44. Effect of curing conditions on healing efficiency of the PG 70-22M mixtures containing 5%RAS+20%RAP..... 50

Figure 45. Strain energy recovery ratio for PG 67-22 mixtures containing 5%RAS: (a) Room temperature conditioning and (b) High temperature or UV light conditioning. 51

Figure 46. Effect of curing conditions on SERR of the PG 67-22 mixtures containing 5%RAS. 51

Figure 47. Strain energy recovery ratio for PG 70-22M mixtures containing 5%RAS: (a) Room temperature conditioning and (b) High temperature or UV light conditioning. 52

Figure 48. Effect of curing conditions on SERR of the PG 70-22M mixtures containing 5%RAS. 52

Figure 49. Strain energy recovery ratio for PG 67-22 mixtures containing 20%RAP: (a) Room temperature conditioning and (b) High temperature or UV light conditioning. 54

Figure 50. Effect of curing conditions on SERR of the PG 67-22 mixtures containing 20%RAP. 54

Figure 51. Strain energy recovery ratio for PG 70-22M mixtures containing 20%RAP: (a) Room temperature conditioning and (b) High temperature or UV light conditioning. 55

Figure 52. Effect of curing conditions on SERR of the PG 70-22M mixtures containing 20%RAP. 55

Figure 53. Strain energy recovery ratio for PG 70-22M mixtures containing 5%RAS+20%RAP: (a) Room temperature conditioning and (b) High temperature or UV light conditioning. 56

Figure 54. Effect of curing conditions on SERR of the PG 67-22 mixtures containing 5%RAS+20%RAP..... 57

Figure 55. Strain energy recovery ratio for PG 70-22M mixtures containing 5%RAS+20%RAP: (a) Room temperature conditioning and (b) High temperature or UV light conditioning. 57

Figure 56. Effect of curing conditions on SERR of the PG 70-22M mixtures containing 5%RAS+20%RAP..... 58

Figure 57. SCB results for PG 67-22 mixtures containing 5% RAS. 59

Figure 58. SCB results for PG 70-22M mixtures containing 5% RAS. 60

Figure 59. SCB results for PG 67-22 mixtures containing 20% RAP. 60

Figure 60. SCB results for PG 70-22M mixtures containing 20% RAP. 61

Figure 61. SCB results for PG 67-22 mixtures containing 5% RAS+ 20% RAP..... 61

Figure 62. SCB results for PG 70-22M mixtures containing 5% RAS+ 20% RAP. 62

Figure 63. LWT results for PG 67-22 mixtures containing 5% RAS. 62

Figure 64. LWT results for PG 70-22M mixtures containing 5% RAS. 63
Figure 65. LWT results for PG 67-22 mixtures containing 20% RAP. 63
Figure 66. LWT results for PG 70-22M mixtures containing 20% RAP. 64
Figure 67. LWT results for PG 67-22 mixtures containing 5%RAS+ 20% RAP. 64
Figure 68. LWT results for PG 70-22M mixtures containing 5%RAS+ 20% RAP. 65
Figure 69. LWT rut depth vs. number of passes for PG 67-22 mixtures. 65
Figure 70. LWT rut depth vs. number of passes for PG 70-22M mixtures. 66
Figure 71. TSRST results for PG 67-22 mixtures containing 5% RAS: (a) Fracture load and (b) Fracture temperature. 67
Figure 72. TSRST results for PG 70-22M mixtures containing 5% RAS: (a) Fracture load and (b) Fracture temperature. 68
Figure 73. TSRST results for PG 67-22 mixtures containing 20% RAP: (a) Fracture load and (b) Fracture temperature. 69
Figure 74. TSRST results for PG 67-22 mixtures containing 5% RAS+ 20% RAP: (a) Fracture load and (b) Fracture temperature. 70
Figure 75. TSRST results for PG 70-22M mixtures containing 20% RAP: (a) Fracture Load and (b) Fracture temperature. 71
Figure 76. TSRST results for PG 70-22M mixtures containing 5% RAS+ 20% RAP: (a) Fracture Load and (b) Fracture temperature. 72

LIST OF TABLES

Table 1. GPC results for RAS and RAP. 9
Table 2. Experimental test matrix for binder blends preparation. 9
Table 3. Binder blends compositions for PG 67-22. 10
Table 4. Binder blends compositions for PG 70-22M. 11
Table 5. Aggregate, RAP, and RAS gradation. 13
Table 6. Details of the prepared mixtures. 14
Table 7. Recycled asphalt materials binder availability. 14
Table 8. Summary of DSR and BBR results for PG 67-22 binder blends. 28
Table 9. Summary of DSR and BBR results for PG 70-22 M binder blends. 28
Table 10. Statistical significance of different variables on Delta Tc results. 31
Table 11. Statistical significance of different variables on UTI results. 34
Table 12. MSCR results for binder blends prepared with PG 67-22. 34
Table 13. MSCR results for binder blends prepared with PG 70-22M. 35
Table 14. Statistical significance of different variables on MSCR results. 35

ACRONYMS, ABBREVIATIONS, AND SYMBOLS

A	Notch depth
AASHTO	American Association of State Highway and Transportation Officials
ASTM	American Society for Testing and Materials
B	Sample thickness
BBR	Bending beam rheometer
CHI	Chitosan
DBTDL	Dibutyltin dilaurate
DMSO	Dimethyl sulfoxide
DSR	Dynamic shear rheometer
dU/da	Change of strain energy with a notch depth
EBA	Ethylene–butyl acrylate
EVA	Ethylene– vinyl acetate
FHWA	Federal Highway Administration
FTIR	Fourier transform infrared spectroscopy
G*	Complex modulus
HDI	Tri-functional homopolymer of hexamethylene diisocyanate
Jc	Critical strain energy release rate
kJ	Kilo Jules
LTRC	Louisiana Transportation Research Center
LWT	Loaded wheel tracking
NaOH	Sodium hydroxide
NAMS	Nominal maximum aggregate size
MSCR	Multiple stress creep recovery
m-value	Relaxation
OXE	Oxetane
OXE-CHI	Oxetane substituted Chitosan
OXE-CHI-PUR	Oxetane substituted Chitosan-Polyurethane
PAV	Pressure aging vessel
PCWS	Post-consumer waste shingles
PE	Polyethylene
PEG	Polyethylene glycol

PG	Performance Grading
PP	Polypropylene
PUR	PolyUrethane
RAM	Recycled asphalt materials
RAP	Reclaimed asphalt pavements
RAS	Recycled asphalt shingles
RTFO	Rolling thin film oven
RV	Rotational Viscometer
SBS	Styrene-butadiene-styrene
SEB	Styrene-ethylene butylene–styrene
SIS	Styrene-isoprene–styrene
SHP	Self-healing polymer
SRR	Strength recovery ratio
SCB	Semi-circular bending
TGA	Thermogravimetric analysis
TSRST	Thermal-stress restrained specimen test
U	Strain energy to failure
UV	Ultraviolet
δ	Phase angle
ΔTc	Difference between critical stiffness and critical m-value temperatures

EXECUTIVE SUMMARY

The objective of this study was to evaluate the efficiency of a new generation of light-induced self-healing polymers in enhancing the durability and self-healing properties of asphalt mixtures. The innovative UV light activated polymer is intended to delay crack propagation, and consequently, extend the service life of asphalt pavements.

Self-healing polymers (SHPs) were synthesized through a photocatalytic-based chemical method. Synthesized SHPs were characterized using Fourier Transform Infrared Spectroscopy (FTIR) and Thermogravimetric Analysis (TGA). Rheological tests such as Performance Grading (PG) and Multiple Stress Creep Recovery (MSCR) were used to find the optimum dosage of SHPs. Laboratory tests were conducted to study the performance of asphalt mixtures containing the optimum percentage of SHP against cracking (at intermediate and low-temperature) and rutting susceptibility. In addition, the healing efficiency of asphalt mixtures containing SHP was studied by inducing cracks on prismatic specimens and monitoring the healing of the cracks under different environmental conditions. Environmental conditions evaluated in this study were room temperature (25 ± 2°C) and high temperature (50 ± 2°C). Yet, for samples containing SHP, high-temperature conditioning was replaced by UV light exposure. Fracture energy of the mixtures was also measured for three conditions: undamaged, damaged, and healed to assess the fracture energy recovery of the samples.

Results of the FTIR analysis confirmed the successful synthesis of cross-linked networks of OXE-CHI-PUR polymer in the laboratory. In addition, TGA results showed that the synthesized polymers achieved the required thermal stability to resist asphalt mixture production processes. Viscosity results showed that the addition of 5% RAS and/or 20% RAP caused an increase in the viscosity of the binder blends. However, a reduction in viscosity of the binder blends containing recycled asphalt materials was observed when adding self-healing polymers.

Performance grading results showed an increase in the high-temperature grade of the binder blends containing recycled asphalt materials and recycled asphalt materials with SHP. However, the low-temperature grade was the same for all tested binder blends. The difference between the critical stiffness temperature and the m-value critical temperature (Delta Tc) showed an improvement at low service temperature for samples with 5% SHP when exposed to UV light. In addition, results of the MSCR test showed that the elastic behavior of the unmodified binder improved with the use of SHP. However, for the modified binder, the percent recovery decreased by increasing the contents of SHP.

Semi-Circular Bending (SCB) test results showed that the addition of recycled materials negatively affected the cracking performance of the mixtures. However, incorporation of SHP and 48h of UV light exposure improved the cracking resistance. This behavior was more evident with mixtures prepared with an unmodified binder. LWT test results showed that addition of the self-healing polymer led to an increase in the rut depth of the samples prepared with an unmodified binder. However, the final rut depth was less than 6 mm, which is an acceptable rutting performance. TSRST test results showed that the addition of 5% RAS negatively affected the low-temperature cracking performance of the mixture. In contrast, 5% SHP enhanced the low-temperature cracking performance of the mixture by increasing the fracture load and decreasing the fracture temperature.

The highest strength recovery ratio was observed for mixtures prepared without Recycled Asphalt Materials (RAM) and cured at high temperature. The addition of recycled asphalt materials (RAS and/or RAP) resulted in a decrease in the recovery ratio; yet, the addition of self-healing polymer and a 48h UV light exposure were both able to regain the recovery ratio of the control mixture cured at room temperature. For the mixtures prepared with an unmodified binder, the optimum crack healing efficiency was observed for the mixtures containing 5% RAS and 5% self-healing polymer and exposed to 48h of UV light. Yet, self-healing polymers did not perform well in mixtures prepared with PG 70-22M polymer-modified binder. This may be due to the interaction between the polymer in the binder and the self-healing polymer.

IMPLEMENTATION STATEMENT

This project investigated the implementation of a new generation of Ultraviolet (UV) light-activated self-healing polymers (SHPs) in asphalt mixture in the South-Central region. Results of this study demonstrated that using SHP is a promising approach to produce asphalt mixtures with enhanced cracking performance, and longer service life. In addition, the experimental data gathered throughout this research project has contributed to broaden the knowledge on the subject of innovative self-healing technologies in asphalt materials. The knowledge acquired from this investigation can be implemented in transportation materials courses at Louisiana State University (LSU) and other universities in the Transportation Consortium of South-Central States (Tran-SET) university consortium.

1. INTRODUCTION

Asphalt pavements performance is influenced by the rheological properties of asphalt binders, which can degrade with time leading to pavement failure *(1)*. For instance, age hardening of asphalt mixtures, caused by asphalt oxidation, leads to the appearance of micro-cracks and eventually results in advanced deterioration and failure *(2)*. Consequently, frequent rehabilitation of asphalt pavements leads to large amounts of aged asphalt waste and results in an increased consumption of virgin materials; thus, causing negative environmental and economic impacts.

The use of recycled materials such as Recycled Asphalt Shingles (RAS) and/or Reclaimed Asphalt Pavement (RAP) as a partial replacement of virgin materials can significantly reduce the use of virgin materials and the negative environmental effects of asphalt pavement reconstruction. However, the main challenge with this alternative is that the asphalt binder in the recycled materials has been subjected to severe oxidation during service. Consequently, this causes the binder to be hardened and brittle, which increases crack susceptibility and may affect the performance of asphalt mixtures adversely. One of the main sources of recycled asphalt materials is RAP. Hot mix asphalt (HMA) consists of asphalt binder and aggregate and is 100% recyclable. However, only 20% of RAP is commonly used in the mixture *(3)*. The second source of recycled materials is RAS, which is a roofing industry waste. RAS consists of approximately 28% binder, 58% of mineral aggregate and mineral filler and glass fibers *(4)*.

Polymers, which can be defined as large chains of repeated small molecules, can be added to asphalt mixtures to enhance the performance and extend its service life. Polymer modified binders have been often used to increase resistance to rutting, thermal cracking, fatigue, and to decrease stripping and temperature susceptibility. The use of polymers can also lead to greater elastic recovery, higher softening point, enhanced cohesive strength, and ductility *(5)*. On the other hand, the concept of self-healing was introduced as a solution to the cracking of asphalt mixtures. Self-healing of asphalt mixtures can be compared to the self-healing of an injured skin. When the skin is injured, it heals itself because nutrient supplies exist in the body and substitute the damaged parts. Self-healing properties may be defined as the recovery of the integrity of asphaltic materials by means of crack propagation arrest and closing. However, self-healing properties of asphalt binder are highly dependent on crack width, rest period, and temperature *(6)*.

Using polymer modification and self-healing concepts, a new generation of UV light-induced self-healing polymers was evaluated in the present study to enhance the elastic recovery of the binder and to increase the self-healing capabilities of asphalt mixtures. The propagation of micro-cracks due to aging and excessive loading cause the chemical breakage of polymer bonds and consequently produce free radicals. The free radicals would subsequently recombine through UV light exposure and close the micro-cracks *(7)*.

1.1. Background

Asphalt pavements are the most common type of pavements used around the world. For instance, about 90% of the 5.2 million kilometers of roads in Europe are surfaced with asphaltic materials, while 92% of the 4.0 million kilometers of US roads and highways are asphaltic. In addition, for airports and parking areas, the percentages of asphalt pavement were reported to

be 85%. In Canada and Mexico, asphalt paved roads account for 90% and 96% of the roads and highway networks, respectively *(8)*. However, the construction, maintenance, and rehabilitation of this huge network of roads and highways can result in considerable negative environmental and economic impacts. As a result, agencies, research institutes, and companies are embracing the concept of sustainable and resilient pavements. The objective of sustainable pavements is to achieve engineering goals while using resources more efficiently and preserving the surrounding ecosystem *(9)*. The life cycle of a pavement structure can be described by six key phases presented in Figure 1 *(10)*.

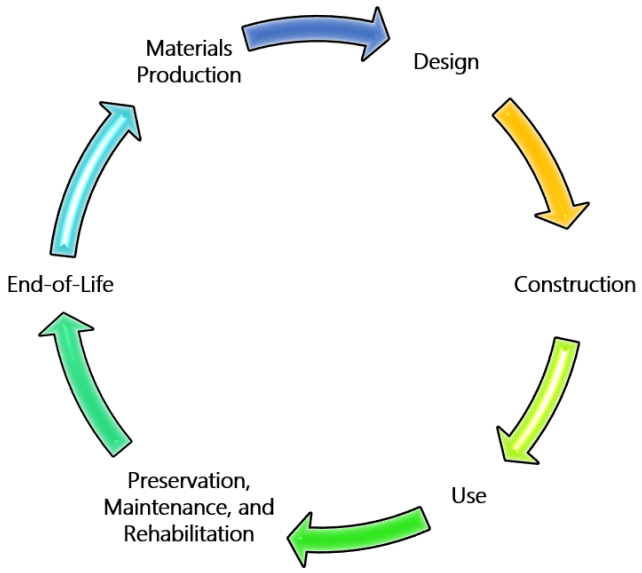

Figure 1. Key phases of pavement life-cycle *(10)*.

Different approaches may be used to design and construct a sustainable pavement. In general, sustainability is achieved by reconsidering priorities and reducing activities that result in green gas emission and ecological impacts of asphalt mixture production *(9)*. The acquisition, processing, and transportation of asphaltic materials cause significant energy consumption and green gas emissions. One of the main approaches to sustainable pavements is related to the reduction in materials consumption. This can be achieved by decreasing virgin materials consumption using recycled materials, byproducts or waste materials. This goal can also be achieved through the improvement of mix designs leading to an increase in the service life of the pavement.

1.1.1. Recycled Asphalt Materials (RAM)

The application of recycled asphalt materials as a partial replacement of virgin binders and aggregate can lead to a significant reduction in the required amount of virgin materials; thereby, decreasing the overall cost and environmental impacts of asphalt mixture production. The two main sources of recycled asphalt materials are reclaimed asphalt pavement and recycled asphalt shingles. RAP consists of approximately 95% aggregate and 5% asphalt binder; therefore, it is 100% recyclable *(11)*. On the other hand, RAS is a construction waste, which consists of approximately 28% binder, 58% of mineral aggregates and mineral filler and glass fibers. It is estimated that each year around 11 million tons of shingle wastes are generated in the United States and only 20% is reused *(12)*.

1.1.2. Light-Activated Self-Healing Polymers

A new generation of light-induced Self-Healing Polymer (SHP) was introduced by combining polyurethane and oxetane-substituted chitosan (OXE-CHI) into a crosslinked polymer. This new material has the ability to self-repair upon ultraviolet (UV) light exposure and through the remodeling of the damaged network. During this process, dormant oxonium ions are activated and react with accessible macromolecular ends that are caused by damage or cracks *(7).*

The main components of this novel light induced SHP are chitosan (CHI), oxetane (OXE), polyurethane (PUR) and Dibutyltin dilaurate (DBTDL). Chitosan is an important derivative of chitin. Chitin is a natural polysaccharide and is one of the most significant biopolymers in today's world. It is synthesized from different living organisms; it is also considered the second most abundant polymer after cellulose. Chitin is mostly exploited by the exoskeleton of insects, shrimp and crabs and cell walls of fungi *(43).* Because of Chitin's complicated structure and its insolubility, Chitosan is obtained by deacetylation of Chitin. Deacetylated Chitin or Chitosan is a natural polycationic linear polysaccharide, which is soluble in aqueous acidic media. Some characteristics of Chitosan can be listed as biodegradability, biocompatibility, and non-toxicity. Chitosan is being used in different shapes such as solutions, gels, fibers, and films in different applications. For example, it is used in water treatment, wound healing material, pharmaceutical applications and tissue engineering *(44).* The chemical structures of Chitin and Chitosan are presented in Figure 2.

Chitosan is used to provide UV light sensitivity, while Oxetane is a cyclic oxide compound and is used to deliver a four-member ring. Cleavage of the covalently attached four-member ring oxetane results in the production of free radicals. The other parameter affecting the selection of oxetane is its relatively low ring opening activation energy. Polyurethane is produced through an isocyanate-polyol (NCO-OH) crosslinking reaction between polyethylene glycol (PEG) and the tri-functional homopolymer of hexamethylene diisocyanate (HDI). Polyurethane is a thermosetting polymer with high-performance polymeric properties. The importance of PUR is to provide mechanical integrity, network heterogeneity and to facilitate the cleavage of the oxetane ring. The catalyst used is dibutyltin dilaurate (DBTDL), which influences the HDI and PEG crosslinking reactions *(7).*

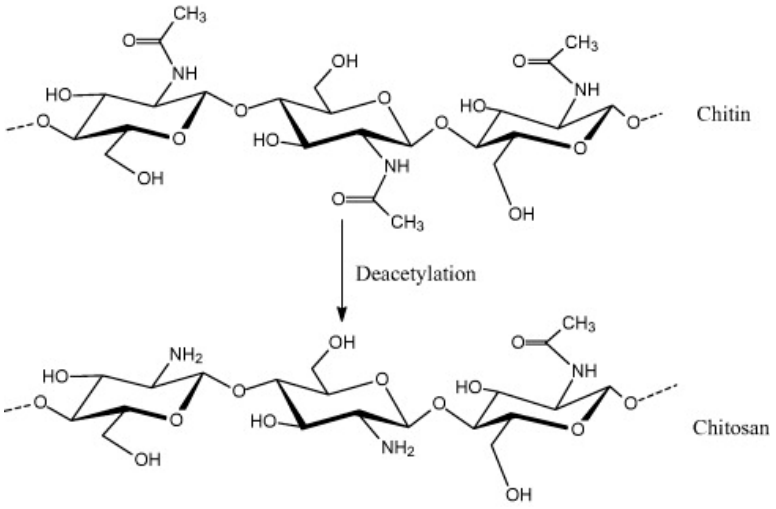

Figure 2. Chemical structure of Chitin and Chitosan *(44)*.

When asphalt is damaged, four different chemical bonds in OXE-CHI-PUR network are broken and two types of chemical bonds are produced: amide bond and ether bond. The amide bond is a covalent chemical bond linking two consecutive amino acid monomers along a peptide or protein chain. Ethers are a class of organic compounds that contain an ether group, which is an oxygen atom connected to two alkyl or aryl groups with the general formula of R–O–R′. The first bond is an ether bond. In this ether bond, hydroxyl of chitosan has a dehydration-condensation reaction with hydroxyl of oxetane, the bond is broken and produce the first kind of free radicals. The second kind of free radicals is created by breaking the amide bonds that are in the ureido and are generated from the reaction of the isocyanate of HDI with amino of CHI. The third radical is produced by breaking the ether bond that connects two naphthenic in the chitosan units. The fourth radical is produced by breaking the ether bond of oxetane. Breakage of the bonds generates unstable free radicals. These radicals recombine through UV light exposure and during the recombination; they repair the damaged areas in the asphalt mix. The increase in oxetane also leads to an increase of free radicals and therefore increases the rate of self-healing *(45).*

2. OBJECTIVE

A new generation of UV light-induced self-healing polymers was evaluated in the present study to enhance the elastic recovery of asphalt binder and to increase the self-healing capabilities of asphalt mixtures. To this end, the following tasks were achieved:

- Develop an optimized synthesis procedure for the production of UV light-induced SHP;
- Evaluate the thermal stability of the synthesized SHP during asphalt pavement mixing processes;
- Evaluate the effects of SHP on the rheological properties of the binder;
- Evaluate the effects of SHP on asphalt mixtures mechanical properties and laboratory performance; and
- Evaluate the effects of UV light-induced polymer on self-healing capabilities of asphalt mixtures.

3. SCOPE

Light-activated self-healing polymers were synthesized through an optimized photocatalytic-based chemical method. Fourier Transform Infrared Spectroscopy (FTIR) spectroscopy was used to confirm the successful synthesis of the polymers by comparing the obtained FTIR spectra of SHP's ingredients. Furthermore, the thermal stability of SHP was examined by conducting a Thermogravimetric Analysis (TGA).

Two binder types (unmodified PG 64-22 and polymer-modified PG 70-22), two sources of recycled asphalt materials (RAS and RAP) in addition to three different percentages of SHP were used to prepare the binder blends of this study. Performance of the binder blends was evaluated using asphalt binders rheological tests such as Performance Grading (PG) and Multiple Stress Creep Recovery (MSCR) test. Based on the results, the optimum percentage of SHP was selected and was used in asphalt mixture testing.

Fourteen asphalt mixtures were prepared to evaluate the effects of SHP on the mechanical and self-healing properties of the mix. The mechanical tests conducted evaluated intermediate- and low-temperature cracking in addition to rutting susceptibility in a controlled laboratory environment. Furthermore, healing efficiency of asphalt mixtures containing SHP was studied by inducing cracks and monitoring the healing of the cracks under two different environmental conditions. Finally, stiffness of undamaged, damaged, and healed mixtures was measured in order to assess the healing of the tested samples.

4. METHODOLOGY

4.1. Self-Healing Polymer Synthesis and Characterization

4.1.1. Materials

Chemicals required for the production of oxetane-substituted chitosan-polyurethane (OXE-CHI-PUR) can be listed as Chitosan (CHI), Sodium hydroxide (NaOH) beads, isopropanol alcohol, oxetane (OXE), dimethyl sulfoxide (DMSO), dibutyltin dilaurate (DBTDL), polyethylene glycol (PEG) and hexamethylene diisocyanate (HDI, Desmodur N 3900).

4.1.2. Self-Healing Polymer Production Procedure

The self-healing polymer production procedure consists of two phases. In the first phase, oxetane-substituted chitosan (OXE-CHI) network is prepared. Subsequently, in the second phase, OXE-CHI is reacted with isocyanate and polyethylene glycol to produce the final product of OXE-CHI-PUR.

In the first phase, Chitosan was added to 150 g of sodium hydroxide (NaOH) solution and stirred for 48 hours at 0ºC. Next, the solution was refrigerated at 0 ºC for another 48 hours. In the following step, 50 ml of pre-cooled isopropyl alcohol was added to the thawed solution and stirred for one hour. After adding pre-cooled 3-chloro-3-methyl oxetane (OXE) into the mixture, the temperature was raised to 80ºC and stirred for 12 hours. The prepared solution was then filtered and washed with methanol to provide a neutral pH. Next, the solution was dried at 60ºC for 12 hours to remove the excess methanol. The oxetane-substituted chitosan macromonomer (OXE-CHI) was polymerized by dispersing OXE-CHI in dimethyl sulfoxide (DMSO) with a pH of 6.8 and an exposure to UV radiation for 20 minutes. The product was then washed with methanol and dried. A non-acidic route was selected for the OXE-CHI macromonomer production in order to preserve the functionality of the amino group and maintain the un-opened ring structure of the OXE *(7).* Furthermore, SHP was produced with two different molar ratios of OXE-CHI; 1:1 (UV1) and 1:3 (UV2).

In the next phase, OXE-CHI was dispersed in DMSO and sonicated at 25ºC for 12 hours. Next, the solution was stirred at 80ºC for 48 hours. Finally, the self-healing polymer (OXE-CHI-PUR) was generated by reacting HDI with dispersed OXE-CHI and polyethylene glycol (PEG) under a nitrogen atmosphere at 25ºC for 10 min *(7).*

Figure 3 and Figure 4 present the produced self-healing polymer, while Figure 5 demonstrates its chemical structure.

4.1.3. Light Activated Self-Healing Polymer Characterization

Fourier Transform Infrared Spectroscopy: During FTIR spectroscopy, the self-healing polymer samples were exposed to infrared radiation. The infrared spectrum was obtained by determining the fraction of the incident radiation absorbed at a specific energy level. The produced OXE-CHI and OXE-CHI-PUR cross-linked networks were characterized by comparing the captured FTIR spectra of CHI with that of OXE-CHI, as well as HDI with that of OXE-CHI-PUR.

(a) **(b)**

Figure 3. (a) Undried and (b) dried prepared OXE-CHI.

Figure 4. Produced OXE-CHI-PUR polymer.

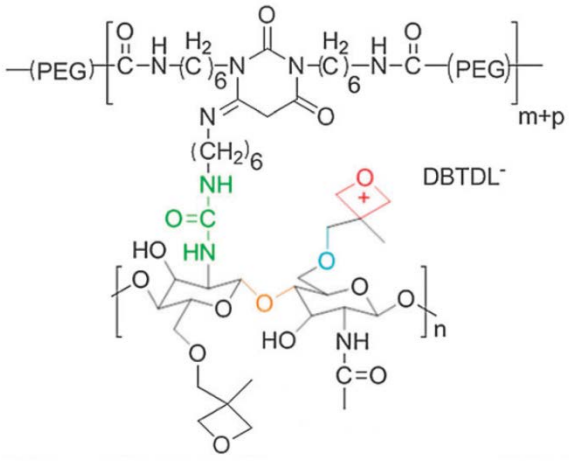

Figure 5. Structure of OXE-CHI-PUR *(7)*.

Thermal Stability: Asphalt mixture production includes heating the mixture at a temperature ranging from 135 to 165ºC. Thus, the produced polymer should have sufficient thermal stability to resist asphalt mixture production processes. The thermal stability of light-activated self-healing polymer was evaluated by Thermogravimetric Analysis (TGA), using a Universal V4.3A TA Instrument thermobalance. Results obtained from the TGA analysis measured changes in the properties of the SHP as a function of temperature (with a constant heating rate of 20ºC/min).

4.2. Effect of Self-Healing Polymer on Asphalt Binder Properties

4.2.1. Test Materials

To assess the effects of light-activated self-healing polymer on asphalt binder rheological properties, blends consisting of a virgin asphalt binder mixed with or without RAS, RAP, RAS+RAP, and SHP were prepared in the laboratory. This study considered both a straight (unmodified) binder and a styrene-butadiene-styrene (SBS) polymer-modified binder, which are classified as PG 64-22 and PG 70-22M in the Louisiana Specifications *(46).* RAS and RAP were the two sources of recycled asphalt materials. RAS was from post-consumer waste shingles (PCWS) with a 20% binder content (which was provided by a local contractor). On the other hand, the RAP used in this study had a 5% binder content. Asphalt binder was extracted from RAS and RAP based on AASHTO T 164 *(47)* and using trichloroethylene as a solvent. Afterward, the solvent (trichloroethylene) was removed based on the procedure described in AASHTO R 59 *(48).* A High-Pressure Gel Permeation Chromatography (GPC) was conducted on the extracted binder from RAS and RAP to obtain the molecular weight (MW) distribution. Results are presented in Table 1. Low molecular weight (LMW) represents the components with an MW less than 3,000 Daltons, while high molecular weight is considered between 3,000 and 50,000 Daltons.

Table 1. GPC results for RAS and RAP.

Components	Others MW	HMW	LMW
RAS (PCWS)	8.1%	26.69%	65.21%
RAP	13.31%	30.31%	56.38%

The extracted binders from RAS and RAP were added to the selected virgin asphalt binder blends at 5% and 20% of the weight of the binder, respectively. Four contents (0, 1%, 3%, and 5%) and two different types of SHP (UV1 and UV2) were used in the preparation of the binder blends. Furthermore, prepared binder samples (DSR and BBR samples) were exposed to two different durations of UV light (1h and 48h) to evaluate the effect of various UV exposures on the performance of the binder blends containing SHP. Results from the different binder blends were compared to the virgin asphalt binder. Table 2 presents the variables used in the binder experiment, while Table 3 and Table 4 describe the components of each binder blend in the experiment. In order to achieve a uniform distribution of the SHP in the binder blends, a mechanical stirrer with a high-shear rate of 3,600 rpm was used for 30 minutes. Laboratory test was performed for the 44 different binder blends (22 binder blends for PG 67-22 binder and 22 binder blends for PG 70-22M binder), under 3 conditions of 0, 1h and 48 h of UV light exposure, with three replicates. Due to a large number of tests required, a fractional factorial design was used to reduce the number of experiments.

Table 2. Experimental test matrix for binder blends preparation.

Variables	Level Description
Type of binder	PG 64-22 and PG 70-22 M
Type and percentage of Recycled Asphalt Materials (RAM)	0%, 5% RAS,20% RAP and 5% RAS+20% RAP
Type of SHP	UV1 (OXE-CHI=1:1) and UV2 (OXE-CHI=1:3)
Percentage of SHP	0, 1%, 3%, and 5%
Time of UV exposure	0, 1h, and 48h

4.2.2. Chemical Tests

In order to study aging and molecular characteristics of the different binder blends, HP-GPC and FTIR were conducted.

High-Pressure Gel Permeation Chromatography (GPC): High-pressure gel permeation chromatography provides a molecular weight (MW) distribution of the asphalt binder's components. The maltenes are low molecular weight (LMW) components with an average MW less than 3,000 Daltons while the MW for asphaltenes is between 3,000 and 50,000 Daltons. The polymers are high molecular weight (HMW) components with molecular weights significantly more than the MW of asphalt binder components making it feasible to be identified. Using this approach, the aging and brittleness levels can be evaluated through the change in the ratio of asphaltenes and maltenes molecular weights in the blends *(49).*

Fourier Transform Infrared Spectroscopy (FTIR): FTIR can be used to evaluate oxidative aging of asphalt binder through the formation of specific functional groups. Aging of asphalt binder causes an increase in the carbonyl (C=O) and sulfoxide (S=O) absorbance respectively around the 1695 cm^{-1} and 1030 cm^{-1} peaks. Carbonyl and sulfoxide index can be defined as the ratio of the area around these peaks divided by a reference area. The aliphatic group (around 1460 cm^{-1} and 1376 cm^{-1} peaks) is usually selected as a reference group since they are considered stable during the aging process. The increase in the ratio is an indication of higher levels of oxidation and therefore, a stiffer binder *(50).*

Table 3. Binder blends compositions for PG 67-22.

Binder Blend	Binder Type	RAM	SHP
67CO	PG 67-22	-	-
67-1P1	PG 67-22	-	1% UV1
67-3P1	PG 67-22	-	3% UV1
67-5P1	PG 67-22	-	5% UV1
67-1P2	PG 67-22	-	1% UV2
67-3P2	PG 67-22	-	3% UV2
67-5P2	PG 67-22	-	5% UV2
67-5RAS	PG 67-22	5% RAS	-
67-5RAS-1P1	PG 67-22	5% RAS	1% UV1
67-5RAS-3P1	PG 67-22	5% RAS	3% UV1
67-5RAS-5P1	PG 67-22	5% RAS	5% UV1
67-5RAS-1P2	PG 67-22	5% RAS	1% UV2
67-5RAS-3P2	PG 67-22	5% RAS	3% UV2
67-5RAS-5P2	PG 67-22	5% RAS	5% UV2
67-20RAP	PG 67-22	20% RAP	-
67-20RAP-1P1	PG 67-22	20% RAP	1% UV1
67-20RAP-3P1	PG 67-22	20% RAP	3% UV1
67-20RAP-5P1	PG 67-22	20% RAP	5% UV1
67-20RAP-1P2	PG 67-22	20% RAP	1% UV2
67-20RAP-3P2	PG 67-22	20% RAP	3% UV2
67-20RAP-5P2	PG 67-22	20% RAP	5% UV2
67-5RAS-20RAP	PG 67-22	5% RAS +20% RAP	-
67-5RAS-20RAP-1P1	PG 67-22	5% RAS +20% RAP	1% UV1
67-5RAS-20RAP-3P1	PG 67-22	5% RAS +20% RAP	3% UV1
67-5RAS-20RAP-5P1	PG 67-22	5% RAS +20% RAP	5% UV1
67-5RAS-20RAP-1P2	PG 67-22	5% RAS +20% RAP	1% UV2
67-5RAS-20RAP-3P2	PG 67-22	5% RAS +20% RAP	3% UV2
67-5RAS-20RAP-5P2	PG 67-22	5% RAS +20% RAP	5% UV2

Table 4. Binder blends compositions for PG 70-22M.

Binder Blend	Binder Type	RAM	SHP
70CO	PG 70-22M	-	-
70-1P1	PG 70-22M	-	1% UV1
70-3P1	PG 70-22M	-	3% UV1
70-5P1	PG 70-22M	-	5% UV1
70-1P2	PG 70-22M	-	1% UV2
70-3P2	PG 70-22M	-	3% UV2
70-5P2	PG 70-22M	-	5% UV2
70-5RAS	PG 70-22M	5% RAS	-
70-5RAS-1P1	PG 70-22M	5% RAS	1% UV1
70-5RAS-3P1	PG 70-22M	5% RAS	3% UV1
70-5RAS-5P1	PG 70-22M	5% RAS	5% UV1
70-5RAS-1P2	PG 70-22M	5% RAS	1% UV2
70-5RAS-3P2	PG 70-22M	5% RAS	3% UV2
70-5RAS-5P2	PG 70-22M	5% RAS	5% UV2
70-20RAP	PG 70-22M	20% RAP	-
70-20RAP-1P1	PG 70-22M	20% RAP	1% UV1
70-20RAP-3P1	PG 70-22M	20% RAP	3% UV1
70-20RAP-5P1	PG 70-22M	20% RAP	5% UV1
70-20RAP-1P2	PG 70-22M	20% RAP	1% UV2
70-20RAP-3P2	PG 70-22M	20% RAP	3% UV2
70-20RAP-5P2	PG 70-22M	20% RAP	5% UV2
70-5RAS-20RAP	PG 70-22M	5% RAS +20% RAP	-
70-5RAS-20RAP-1P1	PG 70-22M	5% RAS +20% RAP	1% UV1
70-5RAS-20RAP-3P1	PG 70-22M	5% RAS +20% RAP	3% UV1
70-5RAS-20RAP-5P1	PG 70-22M	5% RAS +20% RAP	5% UV1
70-5RAS-20RAP-1P2	PG 70-22M	5% RAS +20% RAP	1% UV2
70-5RAS-20RAP-3P2	PG 70-22M	5% RAS +20% RAP	3% UV2
70-5RAS-20RAP-5P2	PG 70-22M	5% RAS +20% RAP	5% UV2

4.2.3. Rheological Tests

To assess the effects of light-activated self-healing polymers on the rheological properties of asphalt binder, blends consisting of the binder with or without recycled asphalt materials, and SHP were prepared in the laboratory. The prepared blends were characterized using laboratory rheological tests (rotational viscometer, the dynamic shear rheometer and bending beam rheometer), and by comparing the Superpave Performance Grade (PG) of the modified binder blends to the unmodified binder. The Rolling Thin Film Oven (RTFO) and Pressure-Aging Vessel (PAV) were used for short- and long-term aging of the prepared binder samples, respectively *(51, 52).* Short-term aging simulates the production and construction phase of the asphalt mixture, while PAV simulates aging during the service life of the mixture.

The viscosity of the binder blends, with or without RAM, and with or without SHP, were measured using a rotational viscometer (RV), based on AASHTO T 316 *(53).* The RV is conducted at high temperature, in order to simulate the production and construction temperature. Test results relate to the workability required for pumping and mixing of the mixture. The DSR test was performed according to AASHTO T 315 to characterize the viscous and elastic behaviors of asphalt binders at intermediate to high temperatures *(54).* DSR was conducted on both unaged and RTFO aged samples to measure the complex shear modulus (G*) and phase angle (δ). The complex shear modulus is an indication of the binder's resistance to deformation, while the phase angle represents the lag between applied stress and the resulting strain. The rutting factor (G*/sin δ), which is the elastic portion of the complex modulus, should be high at high temperature for asphalt mixtures to resist rutting. In addition,

the greater the G*, the more resistant the binder is to permanent deformation. On the other hand, the lower the δ, the more enhanced elastic properties of the binder are. The BBR test was performed according to AASHTO T 313-06 *(55)* to evaluate the performance of the prepared binder blends at low service temperature. Parameters measured using BBR are creep stiffness and creep slope (m-value). Furthermore, ΔTc, which is defined as the difference between the critical stiffness temperature and the m-value critical temperature, was calculated for all binder blends.

Superpave Performance Grade (PG): All binder blends were graded according to AASHTO R 29, "Grading or Verifying the Performance Grade of an Asphalt Binder" and AASHTO M 320, "Standard Specification for Performance-Graded Asphalt Binder" *(56,57).* The high-temperature grade was obtained from DSR, while BBR provided the low-temperature grade. Moreover, the useful temperature interval (UTI) of the binder blends was calculated as the range between the minimum and maximum temperature of the binder blends where it is expected to have adequate performance.

Multiple Stress Creep Recovery (MSCR): A Multiple Stress Creep Recovery (MSCR) test was performed according to AASHTO TP 70, in order to evaluate the high service temperature properties and to assess the rutting susceptibility of the prepared asphalt binder blends. The MSCR test measures the percent recovery, which indicates the elastic response of an asphalt binder; the non-recoverable creep compliance, in turn, is an indicator of the asphalt binder's resistance to permanent deformation under a repeated loading. MSCR was performed at two stress levels, 0.1 kPa and 3.2 kPa with ten creep and recovery cycles applied at each stress level *(58).*

Complex Shear Modulus, G*: Master curves were constructed for binder blends prepared using 5% self-healing polymer to characterize the stiffness of the blends over a wide range of loading times and temperatures. In order to construct the master curves, the complex shear moduli of the binder blends were measured at various temperatures and were then combined into one master curve by horizontally shifting the separate curves along the time axis to a reference temperature.

Linear Amplitude Sweep (LAS): The Linear Amplitude Sweep (LAS) test was performed based on AASHTO TP 101, to measure the fatigue resistance of different binder blends, and to provide a quantitative assessment of the blends' fatigue resistance. The LAS test uses the following fatigue law to characterize the fatigue performance of asphalt binder:

$$N_f = A \times (\text{Applied Load})^{B} \qquad [1]$$

where *A* and *B* are VECD model coefficients that depend on the material characteristics, and N_f is the number of cycles to failure. The *A* parameter relates to the materials ability to preserve its integrity during loading cycles and is directly related to the storage modulus. The *B* parameter represents the sensitivity of the asphalt binder to change in strain level *(59).*

4.3. Effect of Self-Healing Polymer on Self-Healing properties of Asphalt Mixture

4.3.1. Test Materials

In order to evaluate the effects of polymer on the performance of asphalt mixture, samples were prepared using two types of asphalt binders (PG 70-22M and PG 67-22) and with or without RAM and SHP. The aggregate blend consisted of 5/8" gravel, 1/2" gravel, coarse sand and fine sand to satisfy the mix design for a 12.5-mm Nominal Maximum Aggregate Size (NAMS) asphalt mixture. The Superpave asphalt mixtures were prepared in accordance with AASHTO R35-09, "Standard Practice for Superpave Volumetric Design for Hot Mix Asphalt"; AASHTO M 323-07, "Standard Specification for Superpave Volumetric Mix Design"; and Section 502 of the 2006 Louisiana Standard Specifications for Roads and Bridges *(60, 61).* A Level 2 design ($N_{initial}$ = 8, N_{design} = 100, N_{final} = 160 gyrations) was utilized. The optimum asphalt content for each Superpave mixture was determined according to volumetric design criteria (air voids = 3 to 5%, voids in mineral aggregates ≥ 13%, voids filled with asphalt = 68%-78%) and densification requirements (%Gmm at $N_{initial}$ ≤ 89%, and %Gmm at N_{final} ≤ 98%). Gradations of the aggregate, RAS, and RAP used in this study are presented in Table 5.

Samples were prepared using the optimum percentage of SHP as determined from the binder experiment. Fourteen asphalt mixtures were prepared and tested to evaluate the effects of SHP on the self-healing and mechanical properties of the mixture. Descriptions of the prepared asphalt mixtures are presented in Table 6. Furthermore, Table 7 provides a summary of the virgin binder contents and the calculated recycled binder ratio (RBR) for the different asphalt mixtures.

Table 5. Aggregate, RAP, and RAS gradation.

Sieve Size inch (mm)	Agg.1 5/8 Cr. Gravel	Agg. 2 1/2 Cr. Gravel	Agg. 3 Coarse Sand	Agg. 4 Fine Sand	Agg. 5 RAP	Agg. 6 RAS
2" (50)	100.0	100.0	100.0	100.0	100.0	100.0
1 1/2" (37.5)	100.0	100.0	100.0	100.0	100.0	100.0
1" (25)	100.0	100.0	100.0	100.0	100.0	100.0
3/4" (19)	100.0	100.0	100.0	100.0	100.0	100.0
1/2" (12.5)	91.5	100.0	100.0	100.0	98.7	100.0
3/8" (9.5)	56.7	100.0	99.8	100.0	92.1	100.0
#4 (4.75)	14.7	66.8	98.2	99.5	71.4	99.2
#8 (2.36)	11.2	43.8	90.3	99.0	55.3	98.2
#16 (1.18)	10.1	25.1	78.7	98.3	44.9	81.0
#30 (0.600)	8.9	16.0	63.8	96.4	37.5	61.5
#50 (0.300)	6.7	10.1	23.1	85.0	28.2	55.1
#100 (0.150)	5.1	8.2	3.6	0.0	13.9	47.4
#200 (0.075)	3.8	5.0	1.1	0.0	10.3	36.1
Gsb (Dry)	2.465	2.465	2.607	2.379	2.629	3.098
Gsa (Dry)	2.616	2.639	2.656	2.745	2.631	2.667

Table 6. Details of the prepared mixtures.

Binder Blend	Binder Type	Content of RAP/RAS	SHP
67CO	PG 67-22	-	-
67-5RAS	PG 67-22	5% RAS	-
67-5RAS-5P	PG 67-22	5% RAS	5% UV1
67-20RAP	PG 67-22	20% RAP	-
67-20RAP-5P	PG 67-22	20% RAP	5% UV1
67-5RAS-20RAP	PG 67-22	5% RAS +20% RAP	-
67-5RAS-20RAP-5P	PG 67-22	5% RAS +20% RAP	5% UV1
70CO	PG 70-22 M	-	-
70-5RAS	PG 70-22 M	5% RAS	-
70-5RAS-5P	PG 70-22 M	5% RAS	5% UV1
70-20RAP	PG 70-22 M	20% RAP	-
70-20RAP-5P	PG 70-22 M	20% RAP	5% UV1
70-5RAS-20RAP	PG 70-22 M	5% RAS +20% RAP	-
70-5RAS-20RAP-5P	PG 70-22 M	5% RAS +20% RAP	5% UV1

Table 7. Recycled asphalt materials binder availability.

Mixture Type[1]	Design AC (%)	Virgin AC (%)	V/D AC (%)	Available Binder RAS	Available Binder RAP	Actual Binder from RAS/RAP	Actual Available Ratio (%)	RBR (%)
67CO	6.3	6.3	100	0	0	0	0	0
67-5RAS	6.3	5.5	87	1	0	0.8	80	13
67-5RAS-5P	6.3	5.9	94	1	0	0.4	40	6
67-20RAP	6.3	5.2	83	0	1	1.0	100	16
67-20RAP-5P	6.3	5.6	89	0	1	0.7	70	11
67-5RAS-20RAP	6.3	4.4	70	1	1	1.9	95	15
67-5RAS-20RAP-5P	6.3	4.8	76	1	1	1.5	75	12

[1]Presented values are also valid for mixtures prepared with PG 70-22M binder

4.3.2. Crack Healing Efficiency Test

Rectangular beams were prepared to evaluate the healing behavior of asphalt mixtures with and without SHP. Slab specimens were compacted, and rectangular beams with dimensions of 40 mm × 40 mm × 160 mm were cut from slab specimens (Figure 6). Using a three-point bending set up, a monotonic load was applied at the midpoint of the beam in a strain-controlled mode (0.25 mm/min) until cracks were induced at the bottom of the prepared beams. Loading was continued for 100 seconds after reaching the peak load, and was then stopped (Figure 7). Cracking healing efficiency was monitored using two different approaches; crack width analysis and the Strain Energy Recovery Ratio (SERR).

Crack Width Analysis: Crack healing efficiency of the different mixtures was examined by monitoring various cracks with varying widths, using light microscopy and image analysis. Images were captured and analyzed at day 0, day 1, day 2, day 5 and day 6. For self-healing quantification, an image analysis was performed to calculate crack width for day 0, day 1, day 2, day 5 and day 6. Healing efficiency was calculated as follows:

$$\text{Healing Efficiency} = \frac{\text{Initial crack width-crack width after curing}}{\text{Initial crack width}} \times 100 \qquad [2]$$

Figure 6. Rectangular beams prepared for crack healing efficiency.

Figure 7. Crack induction at the bottom of beams.

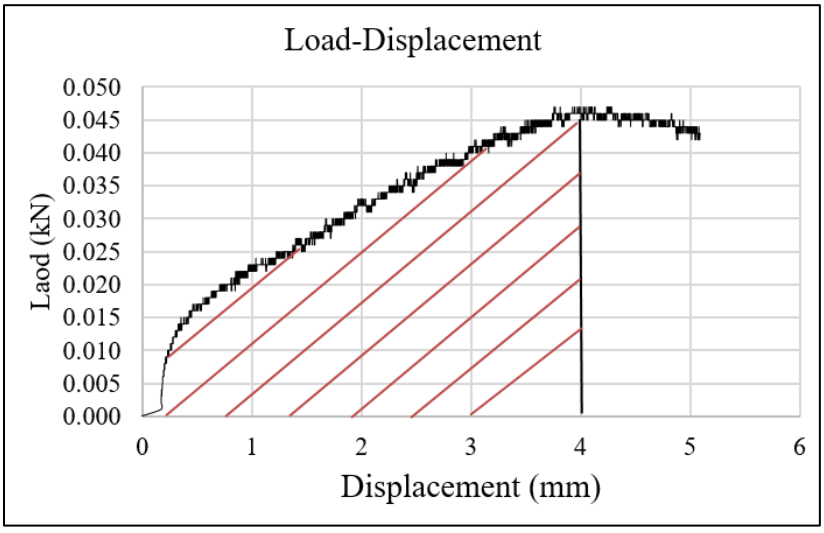

Figure 8. Strain energy of the samples.

Strain Energy Recovery Ratio: For strain energy recovery ratio, the area under the load-deflection curve until peak load was defined as the strain energy of the samples (Figure 8).

This value was measured for undamaged samples (initial strain energy), and after 6 days of healing (healed stain energy). Self-healing efficiency of the mixtures was compared using the Strain Energy Recovery Ratio (SERR), which was calculated as follows:

$$SERR = \frac{\text{Healed Strain Energy}}{\text{Initial Strain Energy}} \quad [3]$$

4.4. Effect of Self-Healing Polymer on the Performance of the Mixtures

Performance of the prepared asphalt mixtures was tested using Semi-Circular Bending (SCB) test, Loaded Wheel Tracking (LWT) test, and Thermal-Stress Restrained Specimen Test (TSRST).

Semi-Circular Bending Test: the SCB test was used to examine the effect of SHP on the cracking resistance of the mixtures containing recycled asphalt materials. SCB was conducted according to ASTM D 8044, "Evaluation of Asphalt Mixture Cracking Resistance using the Semi-Circular Bend Test (SCB) at Intermediate Temperatures" *(62).* Cylindrical samples were compacted to 7.0 ± 0.5% air voids using a Superpave Gyratory Compactor. Samples were compacted with a 150 mm diameter, and 57 mm height. The circular specimens were then cut along the diameter resulting in two semi-circular specimens. For this test, three sets of samples with three different notch depths (25.4, 31.8, and 38.1 mm) are required. Each set includes four semi-circular samples, resulting in 12 semi-circular notched samples *(62)* (Figure 9).

Figure 9. SCB samples.

Using a three-point bending set up (Figure 10), semi-circular samples were loaded monotonically at a deformation rate of 0.5 mm/min. The test was performed at the intermediate temperature of 25 ± 0.3°C. The critical strain energy release rate (kJ/m^2) value was calculated for all the samples based on the following equation:

$$Jc = \frac{1}{b}\left(\frac{dU}{da}\right) \quad [4]$$

where:
J_c = critical strain energy release rate (kJ/m^2);
b = sample thickness (m);

a = notch depth (m);
U = strain energy to failure (kJ); and
dU/da = change of strain energy with notch depth (kJ/m).

Based on Louisiana's specification, a J_c value of 0.5 kJ/m^2 is recommended for adequate cracking performance *(46)*. In order to gain a better understanding of the polymer's effect on the cracking performance of the mixture, SCB was conducted with and without UV light exposure.

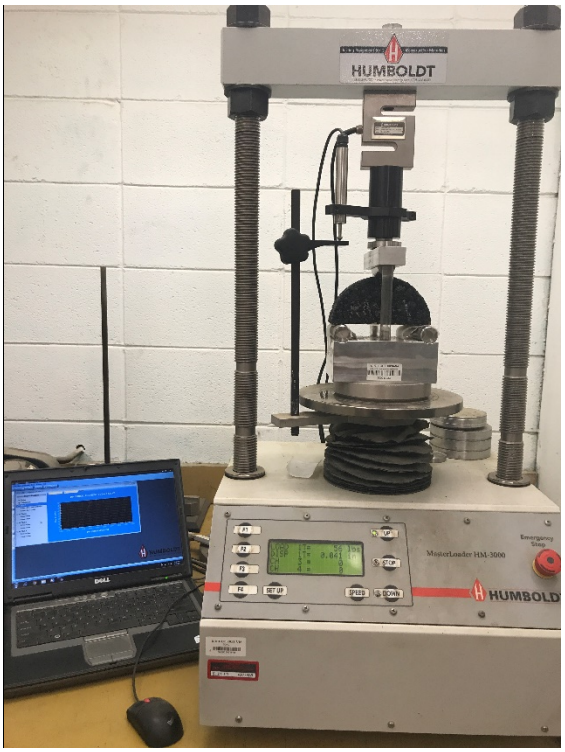

Figure 10. SCB test setup.

Loaded Wheel Tracking (LWT) Test: The resistance to permanent deformation of the mixtures was evaluated using the LWT, where cylindrical specimens were submerged at 50°C, and a 703-N steel wheel was passed across the surface until attainment of 20,000 cycles at a rate of 56 passes per minute. Two circular samples with an air void of 7.0 ± 0.5% were used for each mixture type (Figure 11).

Figure 11. Hamburg loaded wheel tracking test.

Thermal-Stress Restrained Specimen Test (TSRST): The Thermal-Stress Restrained Specimen Test (TSRST) (AASHTO TP 10-93) was used to determine the tensile strength and temperature at fracture. Rectangular slab specimens were compacted with the following dimensions; 260.8 mm (10.25 in.) wide by 320.3 mm (12.5 in.) long by 50mm (2 in.). After compaction, specimens were cooled down to room temperature and were checked for the required air voids of 7 ± 0.5%. In the next step, the rectangular slab was cut to produce beam specimens with the dimensions of 50 ± 5 mm (2.0 ± 0.15 in.) square and 250 ± 5 mm (10.0± 0.25 in.) in length. The prepared beams were attached at each end to platens of the test machine and placed in an environmental chamber for conditioning. A tensile load of 50 ± 5 N (10 ± 1 lbs.) was applied to the sample while cooling the sampling at a rate of 10 ± 1°C per hour. Cooling was continued until fracture failure of the sample. The thermal contraction of the long axis of the sample was recorded electronically. TSRST is a strain-controlled test, therefore, the length of the sample was kept constant, and cooling was continued until failure. Low-temperature performance of the asphalt mixtures was compared based on the temperature at which thermal fracture occurred *(63).*

Figure 12. Thermal-stress restrained specimen test (TSRST).

4.4.1. Statistical Analysis

A statistical analysis was conducted to determine whether differences in the performance of asphalt mixtures were significant. A One-way Analysis of Variance (ANOVA) with a 95% confidence level and Tukey test were conducted to identify significant differences in the results. The analysis obtained from JMP software provided a grouping of the results using letters (A, B, C, D, and so forth). The letter A presented the highest mean, followed by the subsequent letters. Single letters such as A and B, demonstrate significant differences, while a double letter designation such as AB or BC, indicates that the difference between values can be assigned to either of those groups, and are not statistically different.

5. RESULTS

5.1. Light Activated Self-Healing Polymer Characterization

5.1.1. Fourier Transform Infrared (FTIR) Spectroscopy

FTIR spectroscopy was used to evaluate the synthesis of self-healing polymers by comparing the captured FTIR spectra of CHI with that of OXE-CHI, as well as the spectra of HDI with that of OXE-CHI-PUR. During the first step of the self-healing polymer preparation, chloromethyl oxetane (OXE-cl) was reacted with chitosan in order to attach the OXE ring to the -OH group of CHI at the C6 position of the CHI. In this study, OXE-CHI macromonomers were produced with two different molar ratios of (OXE-CHI= 1:1) and (OXE-CHI= 1:3). The FTIR spectra of CHI and OXE-CHI, presented in Figures 13 – 15 confirmed the hypothesized reactions. Characteristic bands of CHI, observed on both the FTIR spectra of CHI and OXE-CHI, may be listed as 1030 cm^{-1} and 1070 cm^{-1} corresponding to the C-O bond, 1148 cm^{-1} corresponds to the ether bond of CHI, 1371 cm^{-1}, and 1420 cm^{-1} corresponds to C-C and CH bonds, while 1583 cm^{-1} corresponds to Amide I. However, a new peak was observed at 1348 cm^{-1}, but only on the FTIR spectra of OXE-CHI (Figures 15 and 16). This new peak corresponds to C-CH3 of OXE, thereby confirming the successful reaction of OXE and CHI.

In the next step, macromonomers of OXE-CHI were used to produce cross-linked networks of OXE-CHI-PUR. PUR networks were produced, based on an adjusted stoichiometric of reactive groups of HDI, PEG, and OXE-CHI. During this reaction, amidogens of CHI react with an isocyanate group of HDI, thus producing a carbamide of self-healing polymer. Due to this reaction, the band at 2260 cm^{-1}, which corresponds to the isocyanate group of HDI (Figure 16), was removed in the FTIR spectra of OXE-CHI-PUR (Figures 17 and 18); the band at 1616 cm^{-1} was added, showing the presence of carbamide.

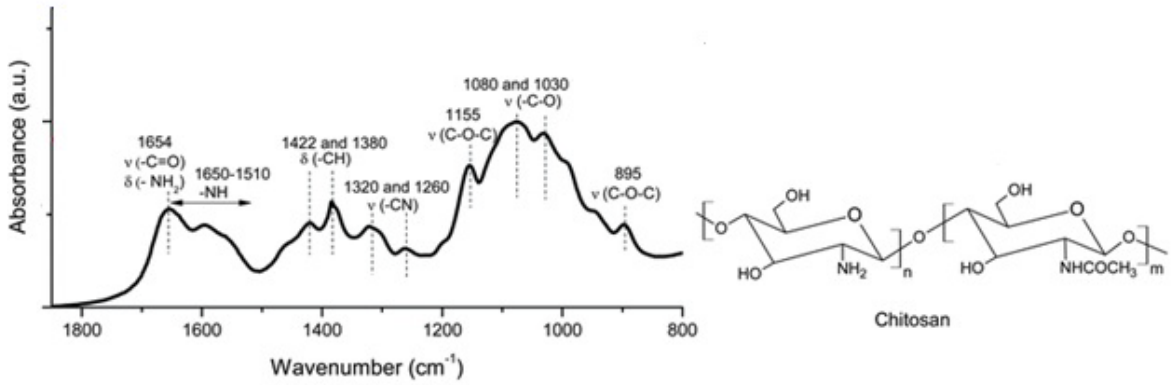

Figure 13. FT-IR spectra of CHI.

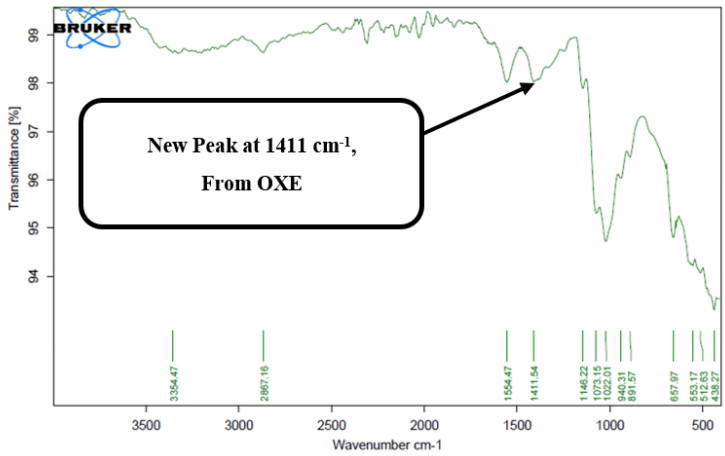

Figure 14. FT-IR spectra of OXE-CHI (1:1).

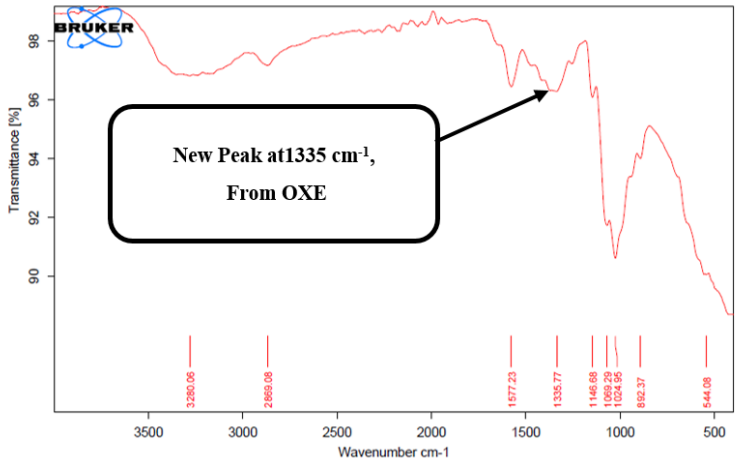

Figure 15. FT-IR spectra of OXE-CHI (1:3).

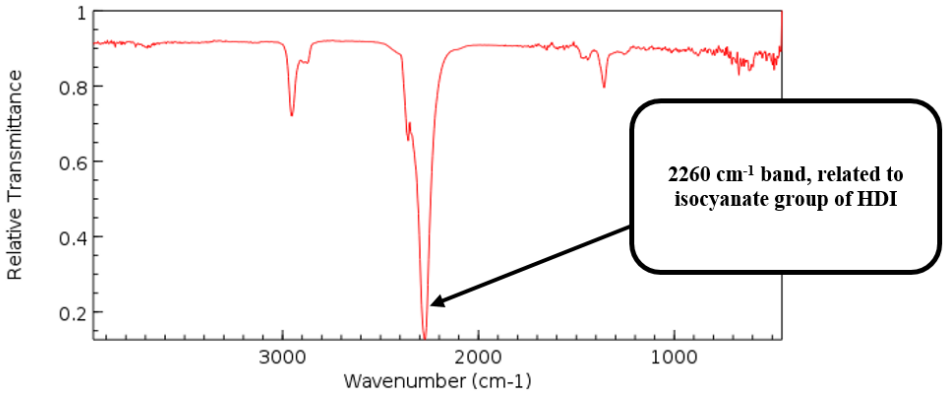

Figure 16. FT-IR spectra of HDI.

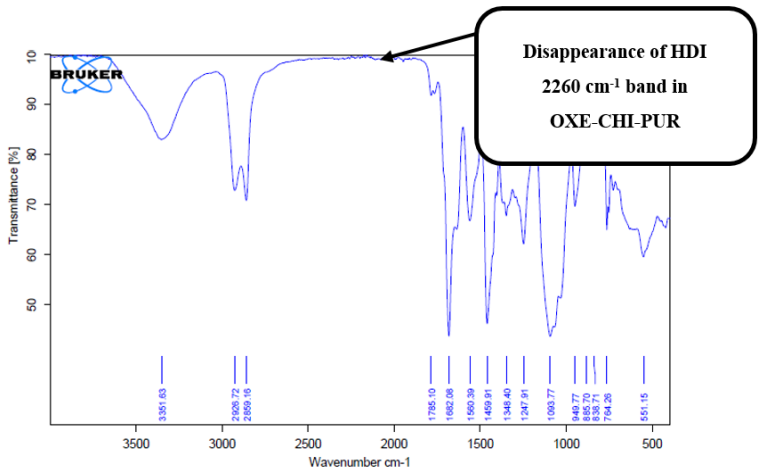

Figure 17. FT-IR spectra of OXE-CHI-PUR (1:1).

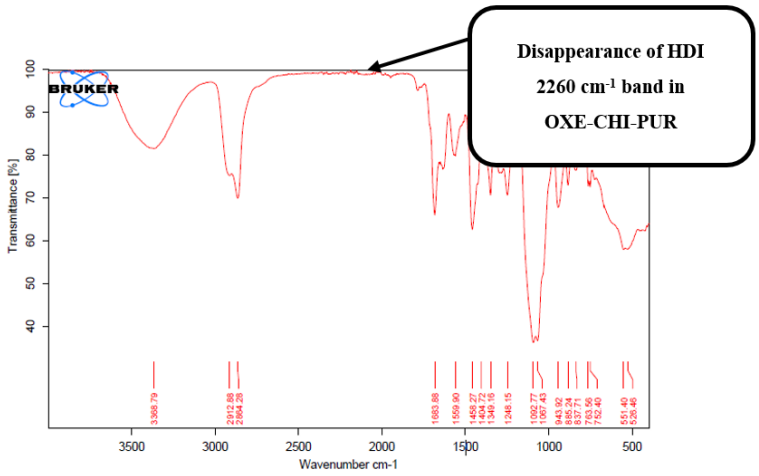

Figure 18. FT-IR spectra of OXE-CHI-PUR (1:3).

5.1.2. Thermal Stability

The thermal stability of the light-induced self-healing polymer was evaluated by TGA using a Universal V4.3A TA Instrument thermos-balance. Figures 19 and 20 present the thermogravimetric analysis of the produced OXE-CHI-PUR cross-linked networks for OXE-CHI-PUR with OXE-CHI molar ratios of 1:1 and 1:3, respectively. TGA results present the change, both in weight (%) and derivation weight (%/^{o}C) with the increase in the temperature. As shown in these figures, the weight loss for both of samples was less than 10% at around 163^{o}C. This initial weight loss can be related to evaporation of residual methanol used for washing and isolation of the OXE-CHI. Based on these results, it can be concluded that the produced SHP are suitable for use during the asphalt mixing process. Furthermore, a 50% weight loss was observed around 350^{o}C. The significant weight loss at high temperature is attributable to the disintegration and degradation of SHP polymer due to exposure to high temperature. In addition, the derivation weight (%/^{o}C) shows that the highest weight variation occurs at a temperature of around 460^{o}C, which can be identified as the point where SHP degradation starts.

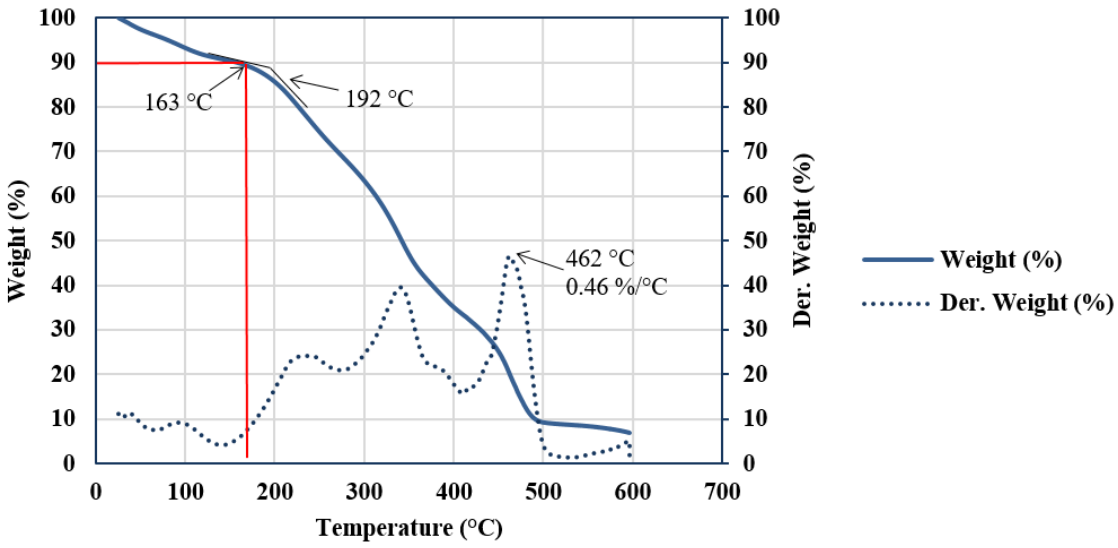

Figure 19. TGA result of OXE-CHI-PUR (1:1).

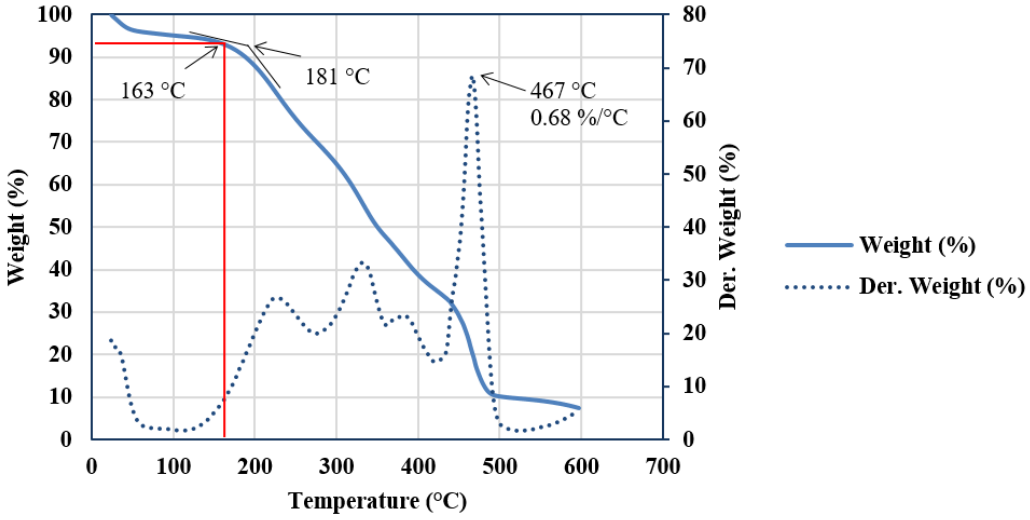

Figure 20. TGA result of OXE-CHI-PUR (1:3).

5.2. Effect of Self-Healing Polymer on the Asphalt Binder Properties

5.2.1. High-Pressure Gel Permeation Chromatography Results

Based on the HP-GPC results presented in Figure 21, the addition of 5% self-healing polymer caused an increase in the HMW/LMW ratio of 67CO and 70CO from 0.21 and 0.26 to 0.35 and 0.36. Furthermore, the addition of recycled materials led to an increase in HMW and a decrease in LMW, resulting in a higher HMW/LMW ratio compared to the control blends. The HMW/LMW ratio increased further through the addition of self-healing polymer to the blends.

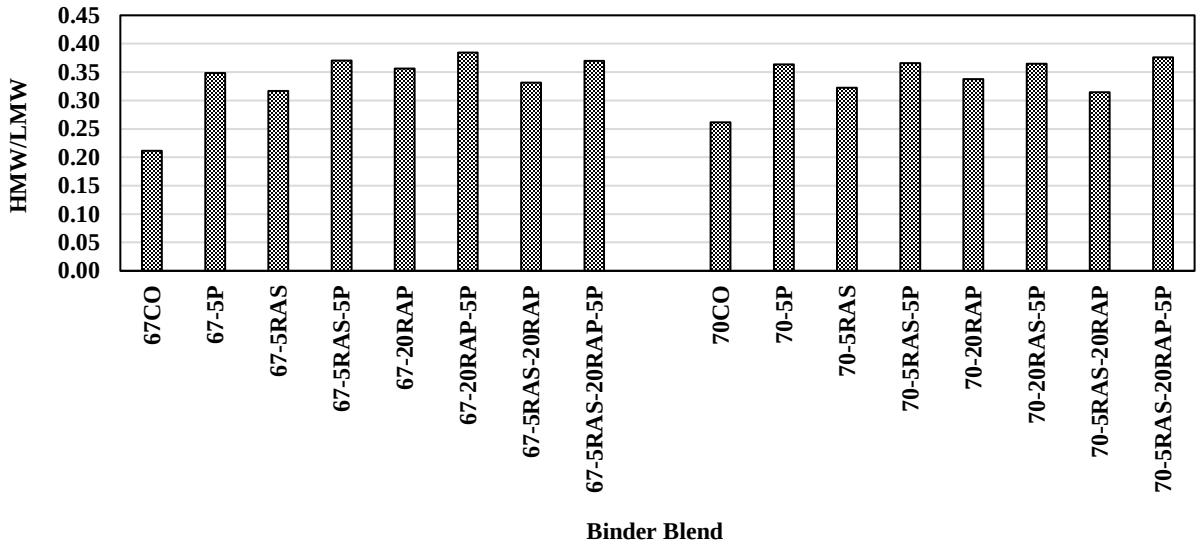

Figure 21. HP-GPC results for HMW/LMW ratio.

5.2.2. Fourier Transform Infrared Spectroscopy Results

Carbonyl and sulfoxide groups of different binder blends were obtained and were compared to examine the effect of recycled asphalt materials and self-healing polymer on the aging process in asphalt binder. The carbonyl and sulfoxide index was calculated based on Equations 5 and 6:

$$I_{CO} = \frac{\sum \text{Area of the carbonyl centered around 1700 cm}^{-1}}{\sum \text{Area of the spectral bands between 1350 and 1525 cm}^{-1}} \quad [5]$$

$$I_{SO} = \frac{\sum \text{Area of the carbonyl centered around 1030 cm}^{-1}}{\sum \text{Area of the spectral bands between 1350 and 1525 cm}^{-1}} \quad [6]$$

The results from the measured carbonyl and sulfoxide index are presented in Figure 22. When 5% self-healing polymer was added to the virgin binder, indices did not change significantly for 67-5P, while a decrease was observed for 70-5P carbonyl index. As expected, the addition of recycled materials and the incorporation of aged binder resulted in an increase in both carbonyl and sulfoxide indices. The addition of self-healing polymer resulted in an increase in the measured indices, which can be due to the reaction of polyurethane and polymer in the recycled materials, and also the absorption of the oil fraction in the binder, resulting in more HMW components in the blends.

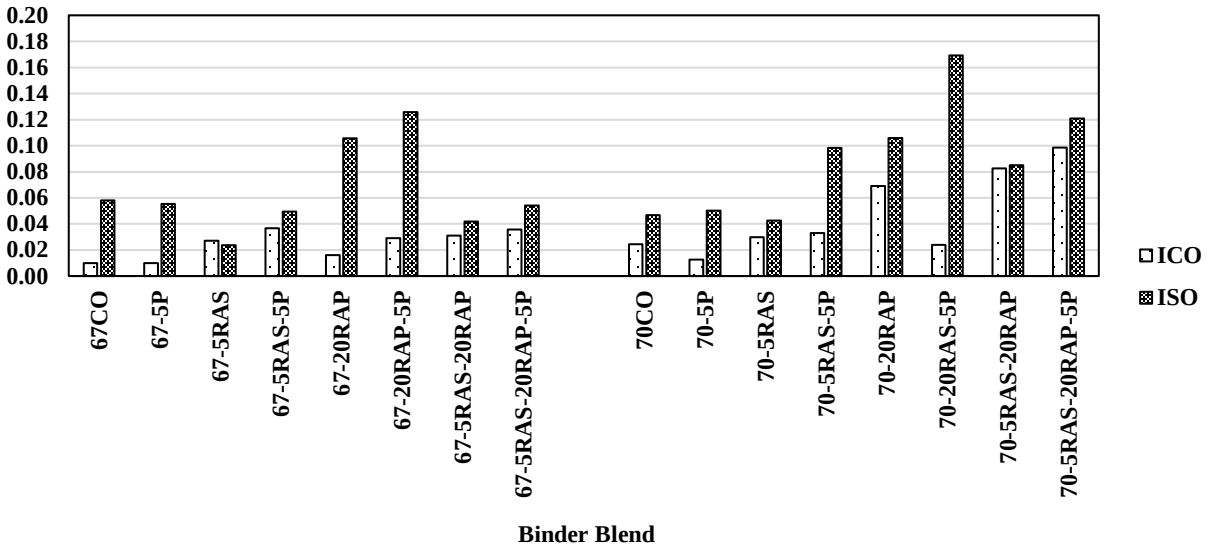

Figure 22. FTIR test results.

5.2.3. Rotational Viscometer (RV)

The viscosity of the prepared binder blends was measured at 135°C, using an RV. The results are presented in Figures 23 and 24. The viscosity of the unmodified and modified binders (i.e., 67CO and 70CO) increased due to the addition of recycled asphalt materials. For instance, the viscosity increased from 101 mPa.s to 122 mPa.s for the binder blend containing 5% RAS (i.e., 67-5RAS). However, a slight decrease was observed in the viscosity of the binder blends containing SHP. The viscosity of the binder blends containing 1%, 3%, and 5% SHP by weight of the binder (i.e., 67-5RAS-1P, 67-5RAS-3P, and 67-5RAS-5P) were measured at 110 mPa.s, 109 mPa.s, and 107 mPa.s, respectively. These trends indicate that the addition of polymer reduced the viscosity of the binder blends containing recycled asphalt materials. However, the viscosity of the virgin binder was not completely recovered.

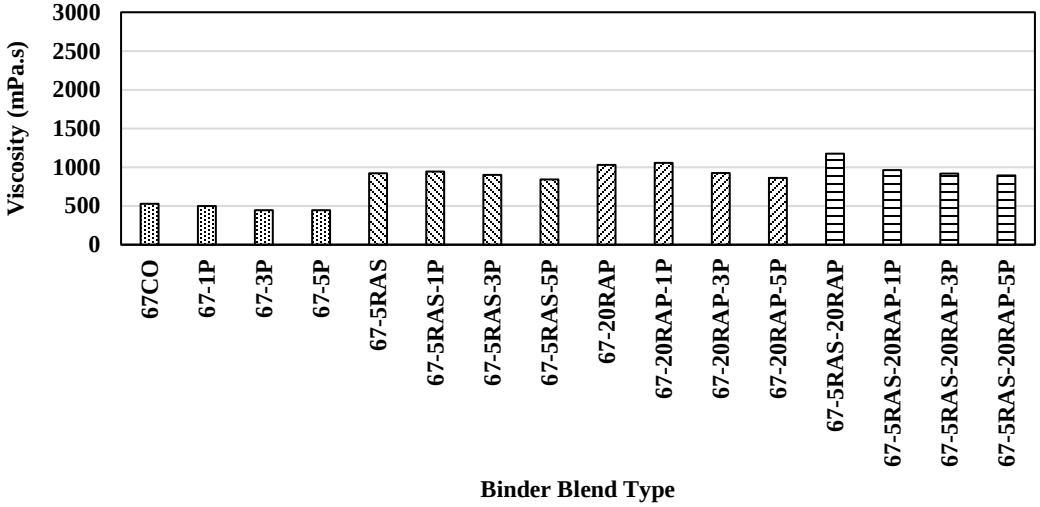

Figure 23. Viscosity results for binder blends prepared with PG 67-22 binder.

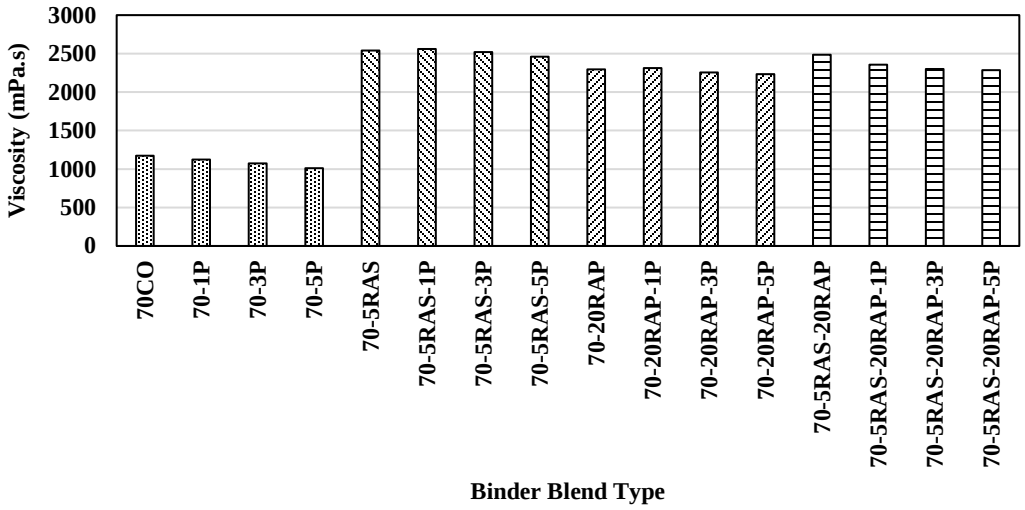

Figure 24. Viscosity results for binder blends prepared with PG 70-22M binder.

5.2.4. Superpave Performance Grade (PG-Grade)

Using DSR, two viscoelastic parameters were measured; the complex shear modulus (G*) and phase angle (δ). The G*/sinδ value of the virgin binders (67CO or 70CO) increased due to the addition of recycled asphalt materials. For example, G*/sinδ of 67CO at 70°C increased from 0.88 kPa to 1.24, 3.86 and 3.90 kPa, due to addition of 5% RAS, 20% RAP and 5% RAS+20% RAP, respectively. The increase in stiffness due to the addition of 5% RAS and 20% RAP was expected since these materials have been subjected to aging and therefore, they cause stiffening of the blends. Because of the age hardening, the attempts to perform DSR for extracted binders from RAS and RAP were not successful.

When 1% SHP was added to the blend containing an unmodified binder (PG 67-22) and recycled asphalt materials (5% RAS and or 20% RAP), the G*/sinδ value decreased from 1.21 to 1.08 kPa. The blends containing 3% and 5% SHP (i.e., 67-5RAS-3P and 67-5RAS-5P) showed slightly higher G*/sinδ values (1.09 and 1.15 kPa, respectively), compared to the blend with 1% SHP (i.e., 67-5RAS-1P). These values further increased with exposure to UV light for 1 and 48h. A G*/sinδ value of 1.87 kPa was measured for 67-5RAS-5P. As reported in the literature, when a polymer is blended with an asphalt binder, it absorbs the low molecular weight fraction (maltenes) from the binder and becomes swollen. Furthermore, polymers can make a network within the asphalt binder phase, which provides a binder with enhanced durability *(64)*. The absorption of the maltenes fraction and the formation of a network between the binder and the polymer leads to an increase in the complex modulus and stiffness of the binder. In summary, the addition of recycled asphalt materials caused an increase in G* and G*/sinδ, which is an indication of a stiffer binder. These values were reduced through the incorporation of 1% SHP but increased with the increase in SHP content and UV light exposure of the samples.

The BBR test was used to evaluate the low-temperature properties of the binder blends prepared with or without recycled asphalt materials and with or without SHP. Results obtained

from the BBR shows that the addition of recycled asphalt materials caused an increase in the stiffness and a decrease in the m-value of the binder blends. Incorporation of 20%RAP and 5% RAS + 20% RAP to PG 70-22M virgin binder, caused a decrease in the low-temperature grading of PG 70-22M from -22 to -16°C. However, changes caused by the addition of 5% RAS were not significant enough to change the low-temperature grade of the binder blend. The use of 5% SHP in the binder blends caused a decrease in the stiffness and an increase in the m-value for the binder blends prepared with PG 67-22 and PG 70-22M binders. As a result, SHP incorporation improved relaxation of the binder blends at low temperature, while decreasing its stiffness. It should be mentioned that the effect of the SHP was not significant enough to change the low-temperature grade of the binder blends. A summary of the DSR and BBR results for the different binder blends is presented in

Table 8 and Table 9, while detailed results are available in Appendix A.

5.2.5. Delta Tc

Aging of asphalt binder can result in loss of ductility, which is an important property affecting the cracking performance of the mix. Previous research showed that mixes with the same stiffness but different ductility showed different cracking performances; mixes with lower ductility had poor cracking performance *(65).* In addition, the relaxation loss had a more significant effect on cracking performance than stiffness. The current Superpave PG-grading system does not specify a direct measurement of ductility; however, it includes loss of relaxation parameters such as phase angle and m-value. The issue with these values is that they are not reliable indicators of the relationship between stiffness and ductility. Delta Tc is defined as the difference between the critical stiffness temperature and the critical m-value temperature and can be used for quantifying the loss of relaxation properties of asphalt binder.

A negative value of delta Tc presents a binder that is m-controlled while a positive Delta Tc is an indication of an S-controlled binder. When Delta Tc is negative, asphalt mixes become more prone to top-down cracking. Delta Tc results for binder blends prepared with PG 67-22 and PG 70-22M binders are presented in Figures 25 and 26, respectively. For binder blends prepared with virgin binders of PG 67-22 and PG 70-22M, delta Tc values of -2.7 and -0.7 were obtained, respectively. Both binder blends are m-controlled; however, as expected, the virgin binder PG 70-22M showed a better cracking performance at low temperature. Addition of the recycled asphalt materials (5%RAS and or 20%RAP) to the virgin binder, led to an increase in Delta Tc of the binder blends. The higher negative delta Tc is due to the loss of relaxation caused by the incorporation of the aged recycled binder.

Table 8. Summary of DSR and BBR results for PG 67-22 binder blends.

Binder Blend	Original G*/sinδ 70ºC (kPa)	RTFO G*/sinδ 70ºC (kPa)	PAV G*.sinδ 25ºC (kPa)	PAV Stiff 12ºC (MPa)	PAV m-value 12ºC
67CO	0.88	1.68	3920	197	0.312
67-1P	0.88	1.71	3650	226	0.316
67-3P	1.01	1.75	3660	226	0.318
67-5P	1.06	1.82	3680	227	0.312
67-5RAS	1.24	2.55	4885	190	0.302
67-5RAS-1P	1.10	2.26	4150	228	0.306
67-5RAS-3P	1.21	2.30	4150	218	0.312
67-5RAS-5P	1.24	2.45	4170	228	0.309
67-20RAP	3.86	9.69	5195	323	0.259
67-20RAP-1P	3.77	8.28	6580	269	0.273
67-20RAP-3P	3.78	8.29	6600	289	0.275
67-20RAP-5P	3.91	8.37	6640	307	0.273
67-5RAS-20RAP	3.90	9.47	6680	300	0.269
67-5RAS-20RAP-1P	2.80	8.53	6760	321	0.265
67-5RAS-20RAP-3P	2.82	8.57	6970	310	0.274
67-5RAS-20RAP-5P	2.95	8.65	6990	310	0.276

Table 9. Summary of DSR and BBR results for PG 70-22 M binder blends.

Binder Blend	Original G*/sinδ 76ºC (kPa)	RTFO G*/sinδ 76ºC (kPa)	PAV G*.sinδ 25ºC (kPa)	PAV Stiff 12ºC (MPa)	PAV m-value 12ºC
70CO	0.97	1.73	3180	178	0.336
70-1P	0.88	1.74	2830	183	0.339
70-3P	0.88	1.75	3030	188	0.340
70-5P	0.98	1.84	3230	179	0.342
70-5RAS	1.44	2.36	3030	161	0.330
70-5RAS-1P	1.27	2.06	3440	185	0.328
70-5RAS-3P	1.26	2.10	3430	165	0.329
70-5RAS-5P	1.30	2.15	3545	196	0.330
70-20RAP	3.02	5.12	4380	272	0.270
70-20RAP-1P	2.62	5.16	4075	254	0.274
70-20RAP-3P	2.71	5.21	4150	254	0.278
70-20RAP-5P	2.93	5.25	4380	252	0.282
70-5RAS-20RAP	3.60	6.12	6470	233	0.254
70-5RAS-20RAP-1P	2.71	5.35	6510	301	0.260
70-5RAS-20RAP-3P	2.74	6.10	6770	306	0.261
70-5RAS-20RAP-5P	2.86	6.14	6810	319	0.262

For binder blends prepared with PG 67-22 binder, when 1% SHP was added to the binder blend, a decrease in Delta Tc was observed. This decrease was observed in all binder blends except binder blends containing 20% RAP and SHP. In this case, an increase in Delta Tc was observed, which could relate to the reaction of the polymer with polymers originally present in the RAP. Delta Tc of the binder blends decreased with the increase in SHP content and exposure to UV light. The binder blends with 5% RAS and 5% SHP, exposed to UV light showed the best low-temperature cracking performance with a delta Tc of -0.6.

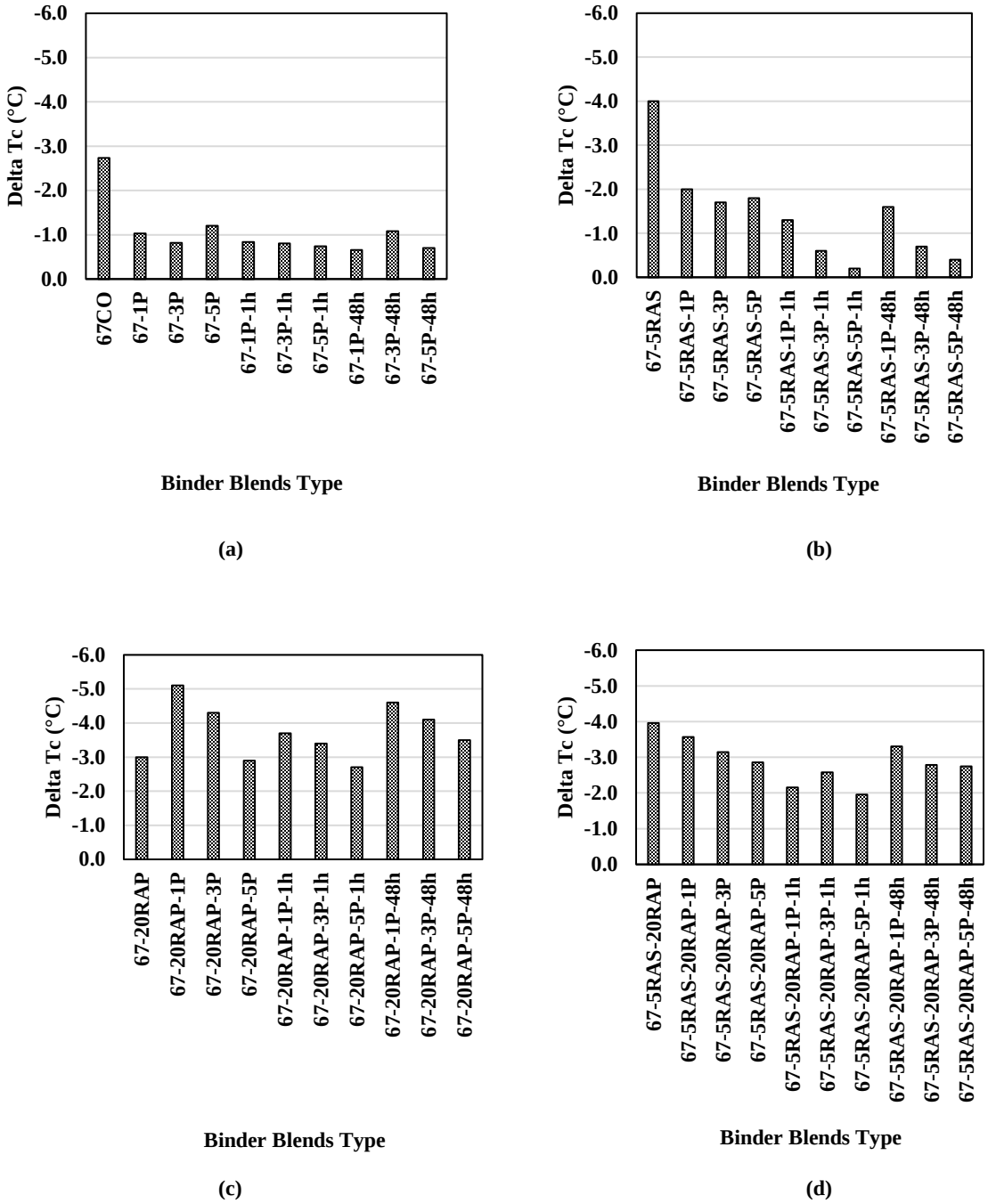

Figure 25. Delta Tc results for PG 67-22 binder blends prepared with, (a) Virgin binder, (b) Virgin binder+5%RAS, (c) Virgin binder+20%RAP, and (d) Virgin binder+5%RAS+20%RAP.

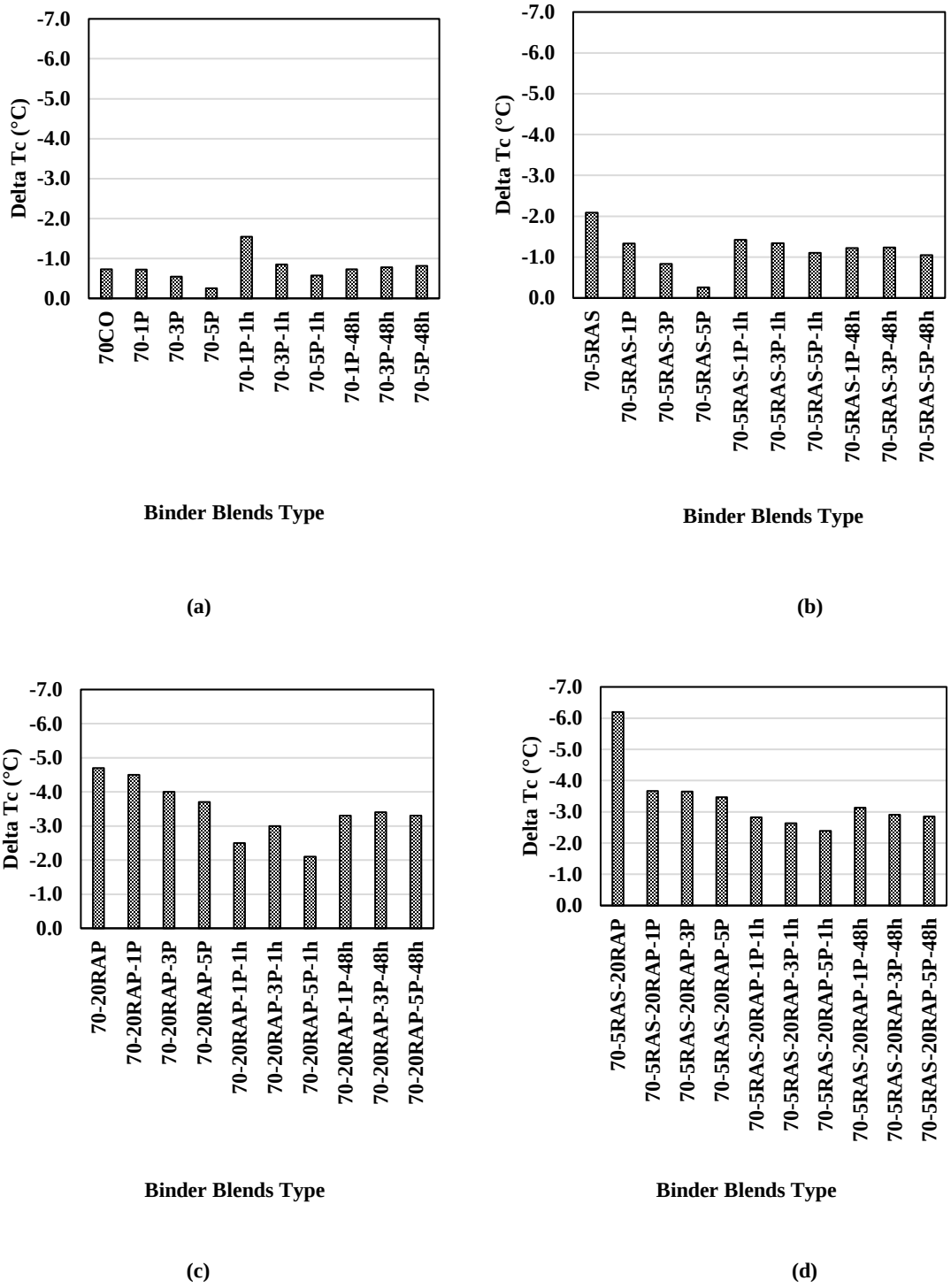

Figure 26. Delta Tc results for PG 70-22M binder blends prepared with, (a) Virgin binder, (b) Virgin binder+5%RAS, (c) Virgin binder+20%RAP, and (d) Virgin binder+5%RAS+20%RAP.

Similar behavior was observed in binder blends prepared with PG 70-22M binder. For all binder blends, incorporation of 1% SHP resulted in a decrease in Delta Tc value. Further reduction was observed due to the increase in self-healing polymer content to 3% and 5%. However, exposing samples to UV light caused an increase in Delta Tc. This loss of relaxation

through UV light exposure can be due to aging caused by UV light. In other words, aging that occurred through UV light exposure was greater than the enhancement provided by SHP.

Statistical Analysis of Delta Tc: A statistical analysis was performed to study the effect of different variables on low-temperature cracking performance of the prepared binder blends using the measured Delta Tc. Based on the results presented in Table 10, it can be concluded that the addition of 20%RAP had the most significant effect, while SHP type, binder type, and 5%RAS were the least influential variables.

Table 10. Statistical significance of different variables on Delta Tc results.

Source	LogWorth	P-Value	Significance
RAP	24.609	< 0.0005	Significant
UV Exposure	2.150	0.00708	Significant
%SHP	1.908	0.01237	Not significant
SHP Type	0.792	0.16144	Not significant
Binder Type	0.284	0.52033	Not significant
RAS	0.064	0.86368	Not significant

5.2.6. Useful Temperature Interval (UTI)

Using the continuous high- and low-temperature grading of the tested samples, the useful temperature interval (UTI) was calculated as the range of temperature that the binder would perform adequately. Figures 27 and 28 presents the measured UTI for PG 67-22 and PG 70-22M binder blends. For PG 67-22 binder blends, the addition of 5% RAS caused a decrease in the UTI of the binder blend from 94.4°C to 93.5°C; however, 20% RAP and 5% RAS+20% RAP increased the UTI to 103.2 and 99.8°C, respectively. In addition, SHP and UV light exposure increased the UTI. Addition of 5% SHP and 48h of UV light exposure increased the UTI value of the virgin binder from 94.4 to 94.8, 97.9, 104.4, and 100.7°C for binder blends containing no recycled materials, 5% RAS, 20% RAP, and 5% RAS+20% RAP, respectively.

For the PG 70-22M binder blends, the UTI increased from 101.2°C to 103.5°C, 107.2°C, and 107.0°C for the blends containing no recycled materials, 5% RAS, 20% RAP, and 5% RAS+20% RAP. The addition of 1% SHP caused a decrease in UTI, but 3% and 5% SHP and then UV light exposure increased the UTI. Binder blends containing 20% RAP and 5% SHP showed the highest UTI while binder blends with no recycled materials and SHP had the lowest UTI. From these results, SHP did not substantially affect the low-temperature grade of the binder blends; therefore, SHP did not significantly improve the thermal cracking resistance of the binder. However, based on the continuous grading results, SHP application followed by UV light exposure increased the UTI and therefore, temperature susceptibility of the virgin binder was improved.

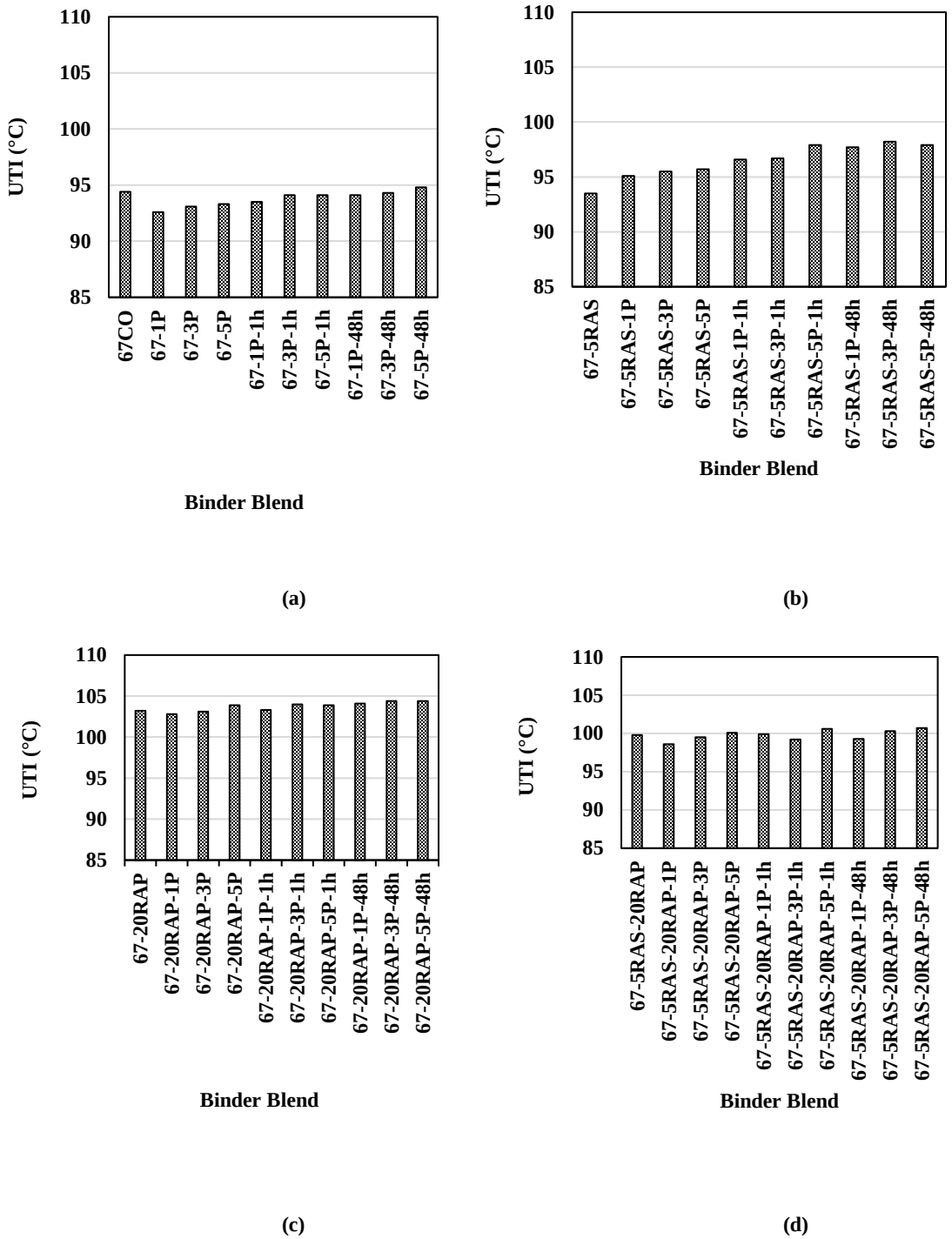

Figure 27. Measured UTI for PG 67-22 Binder blends prepared with, (a) Virgin binder, (b) Virgin binder+5%RAS, (c) Virgin binder+20%RAP, and (d) Virgin Binder+5%RAS+20%RAP.

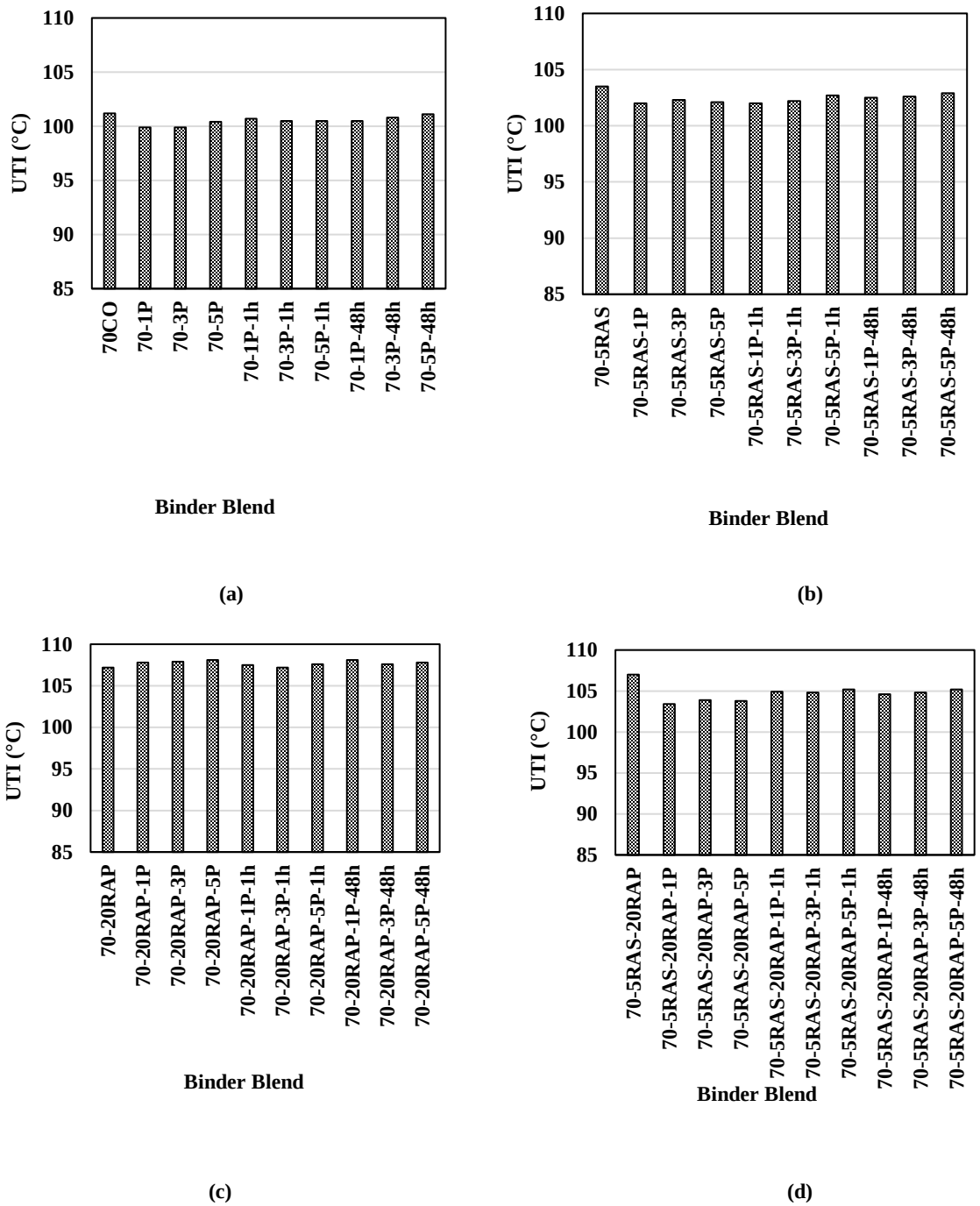

Figure 28. Measured UTI for PG 70-22M binder blends prepared with, (a) Virgin binder, (b) Virgin binder+5%RAS, (c) Virgin binder+20%RAP, and (d) Virgin binder+5%RAS+20%RAP.

Statistical Analysis of UTI Results: Statistical analysis was conducted to study the effect of various factors on the measured UTI of the binder blends. Results are presented in Table 11. Based on these results, RAP had the highest effect while SHP type was the least influential parameter.

Table 11. Statistical significance of different variables on UTI results.

Source	LogWorth	P-Value	Significance
RAP	21.931	< 0.0005	Significant
Binder Type	21.011	< 0.0005	Significant
UV Exposure	0.858	0.13861	Not significant
RAS	0.794	0.16052	Not significant
%SHP	0.152	0.70452	Not significant
SHP Type	0.103	0.78843	Not significant

5.2.7. Multiple Stress Creep Recovery (MSCR)

The MSCR test was conducted at 67ºC and the results are presented in Table 12 and Table 13. Detailed results are available in Appendix A. For binder blends prepared with PG 67-22 virgin binder, a percent recovery of 1.6% was measured, while the addition of 5% RAS, 20% RAP and 5% RAS+20% RAP resulted in 12.3%, 19.8%, and 22.2% percent recovery. Polymer modifiers improve the elastic and recovery properties of the asphalt binder *(66).* As a result, it can be concluded that the increase in percent recovery of the binder blends containing 5% RAS and 20% RAP may be caused by the polymer detected in the recycled materials. Furthermore, the percent recovery and the non-recoverable creep compliance (J_{nr}) of the binder blends increased by increasing the percentage of SHP followed by UV light exposure. The results obtained from the MSCR test for PG 67-22 binder blends indicate an improvement in the rutting susceptibility of the binder blends. However, the percentage recovery and the non-recoverable creep compliance (J_{nr}) of the binder blends prepared with polymer modified virgin binder (PG 70-22M) decreased with SHP modification. Therefore, the addition of SHP improved the performance of unmodified binder, while it failed to enhance the properties of polymer modified binder blends. The lack of enhancement in the case of the PG 70-22M binder blends may be due to the interaction of SBS polymer with polyurethane in the SHP polymer and the polymer in the recycled materials.

Table 12. MSCR results for binder blends prepared with PG 67-22.

Binder Blend	Percent Recovery (0.1 kPa)	Percent Recovery (3.2 kPa)	Jnr
67CO	1.62%	-0.50%	8.65%
67-5P	2.90%	-0.33%	12.42%
67-5P-1h	3.17%	-0.01%	12.46%
67-5P-48h	4.20%	0.13%	13.78%
67-5RAS	4.86%	0.58%	12.31%
67-5RAS-5P	6.69%	0.81%	17.12%
67-5RAS-5P-1h	8.64%	1.50%	16.88%
67-5RAS-5P-48h	6.52%	0.90%	16.66%
67-20RAP	19.80%	13.59%	15.00%
67-20RAP-5P	26.34%	12.99%	25.73%
67-20RAP-5P-1h	25.61%	13.39%	21.81%
67-20RAP-5P-48h	29.57%	16.24%	26.31%
67-5RAS-20RAP	22.22%	13.08%	16.23%
67-5RAS-20RAP-5P	22.94%	12.89%	16.92%
67-5RAS-20RAP-5P-1h	23.76%	12.82%	16.82%
67-5RAS-20RAP-5P-48h	25.11%	14.79%	18.98%

Table 13. MSCR results for binder blends prepared with PG 70-22M.

Binder Blend	Percent Recovery (0.1 kPa)	Percent Recovery (3.2 kPa)	Jnr
70CO	49.10%	30.17%	48.82%
70-5P	46.05%	27.97%	44.58%
70-5P-1h	45.88%	27.68%	44.49%
70-5P-48h	47.01%	28.58%	48.97%
70-5RAS	45.47%	28.36%	41.52%
70-5RAS-5P	41.88%	24.38%	40.42%
70-5RAS-5P-1h	42.29%	25.83%	37.54%
70-5RAS-5P-48h	44.51%	27.86%	36.25%
70-20RAP	59.54%	48.75%	31.58%
70-20RAP-5P	56.17%	44.74%	32.30%
70-20RAP-5P-1h	56.35%	44.89%	32.93%
70-20RAP-5P-48h	58.16%	47.15%	32.96%
70-5RAS-20RAP	63.57%	53.78%	31.38%
70-5RAS-20RAP-5P	53.68%	43.37%	25.22%
70-5RAS-20RAP-5P-1h	54.45%	44.18%	26.10%
70-5RAS-20RAP-5P-48h	55.59%	45.69%	24.89%

Statistical Analysis of MSCR Results: Table 14 presents the statistical analysis of the MSCR test results. Binder type and RAP usage had significant effects on MSCR test results while, SHP type, RAS usage, and SHP content were not significant.

Table 14. Statistical significance of different variables on MSCR results.

Source	LogWorth	P-Value	Significance
Binder Type	64.110	< 0.0005	Significant
RAP	36.953	< 0.0005	Significant
UV Exposure	2.209	0.00617	Significant
SHP Type	1.911	0.01226	Not significant
RAS	0.942	0.11420	Not significant
%SHP	0.168	0.67858	Not significant

As previously noted, two types of polymer were used in this study with two different molar ratios of OXE: CHI; 1:1 and 1:3. By performing statistical analysis for Delta Tc, UTI and MSCR results (Table 10, Table 11, and Table 14), it was shown that changing the molar ratio of OXE: CHI, which was depended on the SHP type, was not significant in all mentioned cases and therefore, did not significantly affect the rheological properties of the binder. Based on the results obtained from the statistical analysis and in order to reduce the cost of the polymer, materials produced with 1:3 molar ratio were used in the mechanical testing of the asphalt mixtures. The complete statistical analysis conducted on the PG-grading results is presented in Appendix B.

*5.2.8. Complex Shear Modulus, G**

Figure 29 presents the complex shear modulus (G*) for the prepared binder blends with PG 67-22, with and without recycled materials and 5% self-healing polymer at various test temperatures and frequencies. When self-healing polymer was added to the virgin binder (67-5P), the stiffness decreased at low frequency while it did not change significantly at high frequency. For binder blends containing 5% RAS, the 67-5RAS blend showed the highest stiffness at high frequency. The addition of self-healing polymer into the binder blends containing 5%RAS (67-5RAS-5P) did not affect the stiffness at low frequency, while it caused a decrease at high frequency. As it was expected, the addition of 20% RAP stiffened the binder.

In this case, self-healing polymer led to a decrease in stiffness at low frequency while achieving the same stiffness as 67-20RAP at high frequency. For binder blends with both type of recycled materials (67-5RAS-20RAP), the addition of self-healing polymer and 48h UV exposure resulted in a decrease in stiffness at low frequency and an increase at high frequency. In summary, self-healing polymer application caused a decrease at low frequency (high-temperature), while at high frequency (low-temperature), it caused an increase or did not affect the stiffness significantly.

For PG 70-22M blends (Figure 29), the addition of self-healing polymer and UV exposure caused a decrease in the stiffness. However, when self-healing polymer was added to the binder blend containing 5% RAS, followed by 48h of UV light exposure, the highest G* was obtained at high frequency. For binder blends with 20% RAP and 5% RAS+20% RAP, recycled material and self-healing polymer increased the stiffness at low frequency (high-temperature).

5.2.9. Linear Amplitude Sweep Test Results

The LAS test was performed in accordance with AASHTO TP 101 at a testing temperature of 18°C and 21°C for PG 67-22 and PG 70-22M binder blends, respectively. These temperatures were selected based on the binders' average climate PG minus 3°C. The fatigue characteristics of the binder blends obtained from LAS test are presented in Figure 30. Based on the equation of the fatigue law, a higher "A" parameter indicates an increase in fatigue life, while a higher "B" parameter indicates a decrease in fatigue life at a constant A. The results for number of cycles to failure (N_f) at two strain levels (2.5% and 5%) are presented in Figure 31. For PG 67-22 binder blends, the addition of 5% polymer increased the fatigue life (N_f) while the addition of 5%RAS, 20% RAP, and 5% RAS+ 20% RAP resulted in a decrease in fatigue life (N_f). Furthermore, the addition of self-healing polymer to the binder blends containing recycled materials caused a further decrease in the fatigue life (N_f). Exposure to UV light also led to a decrease in the fatigue life of the binder. When 5% RAS was added to PG 70-22M binder blends, the fatigue life was not affected significantly. However, the addition of 5% self-healing polymer and UV exposure negatively affected the fatigue life. It should be mentioned that UV light can negatively affect the fatigue properties of the blend through aging of the samples.

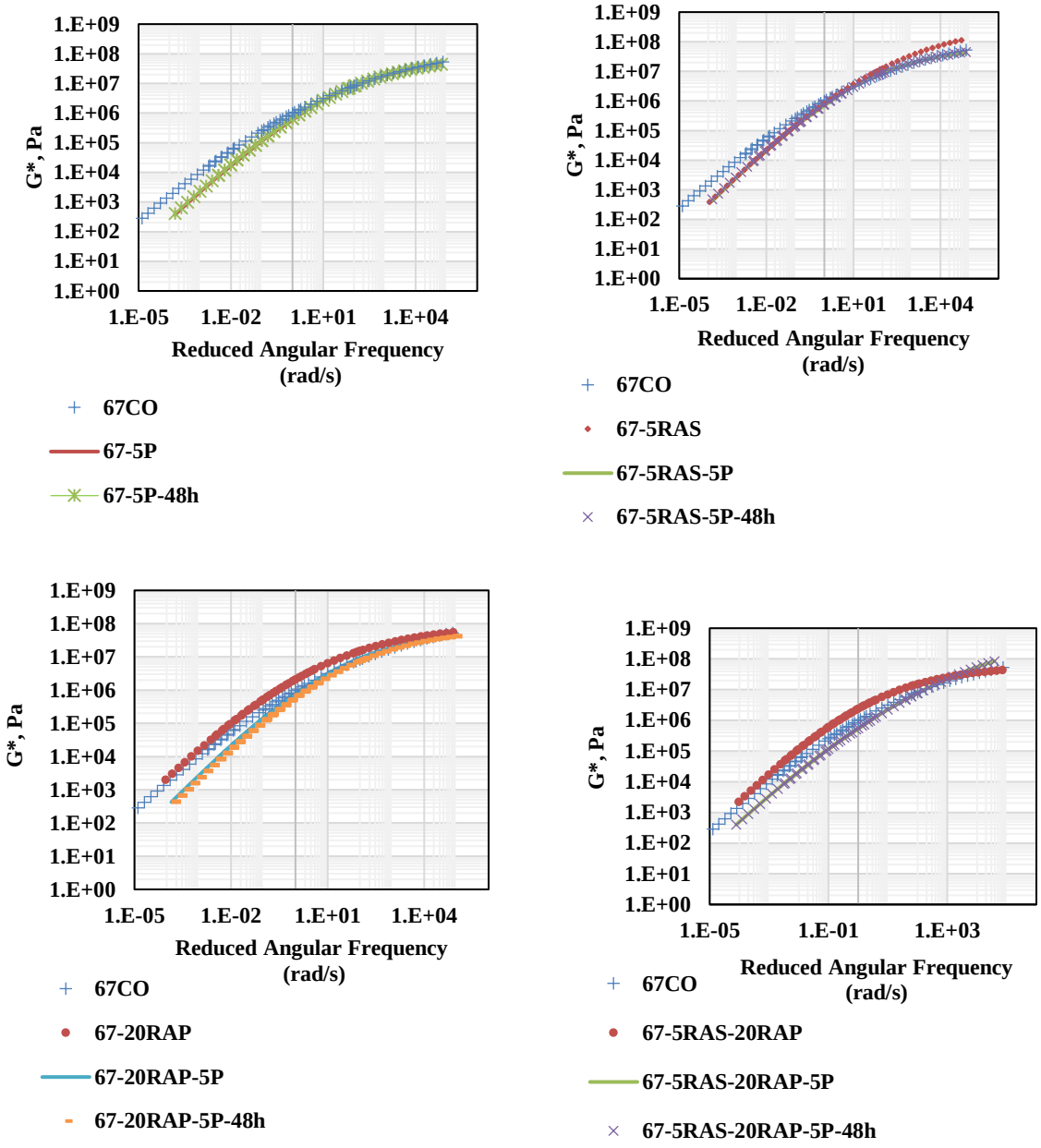

Figure 29. G* results for PG 67-22 binder blends.

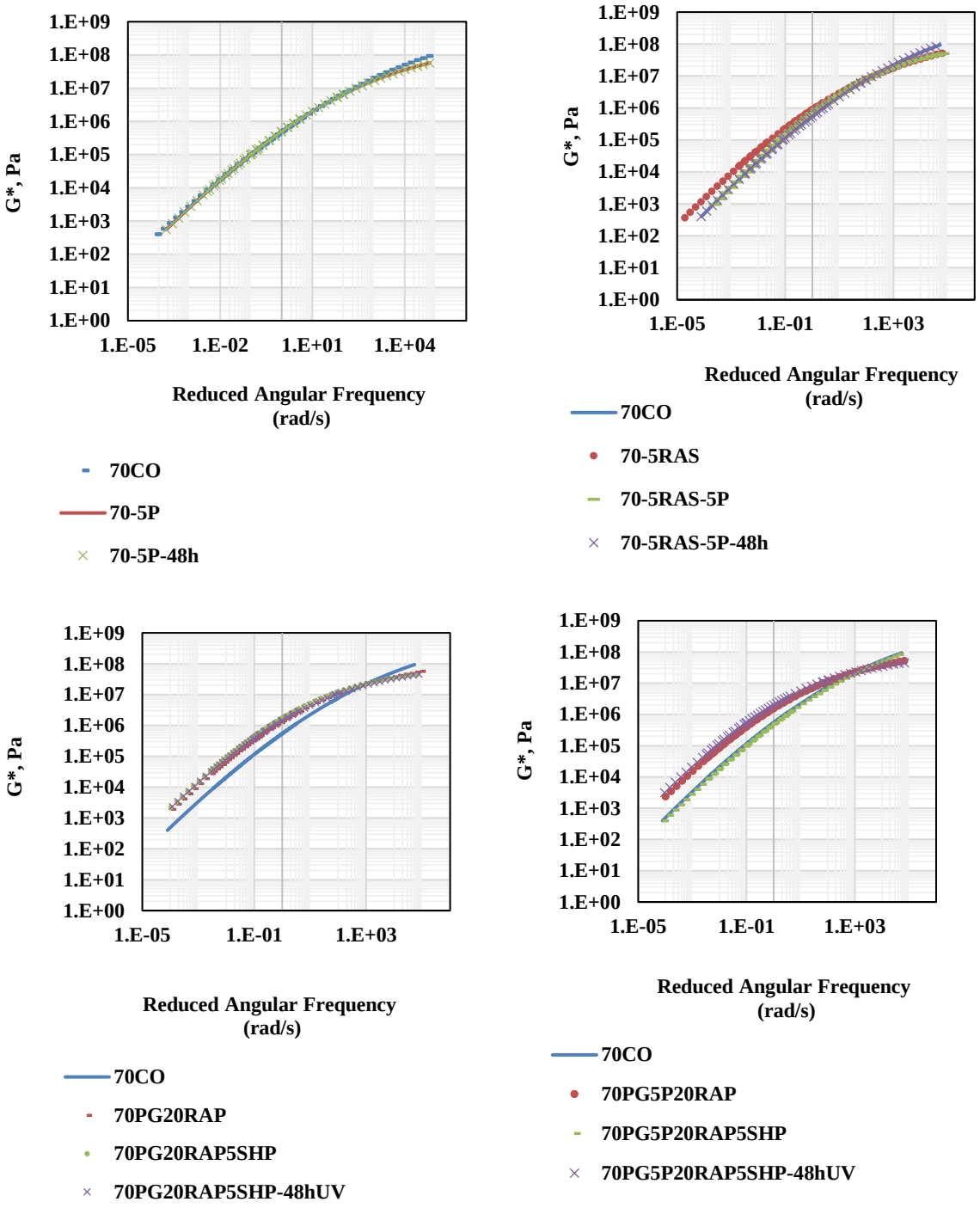

Figure 30. G* results for PG 70-22M binder blends.

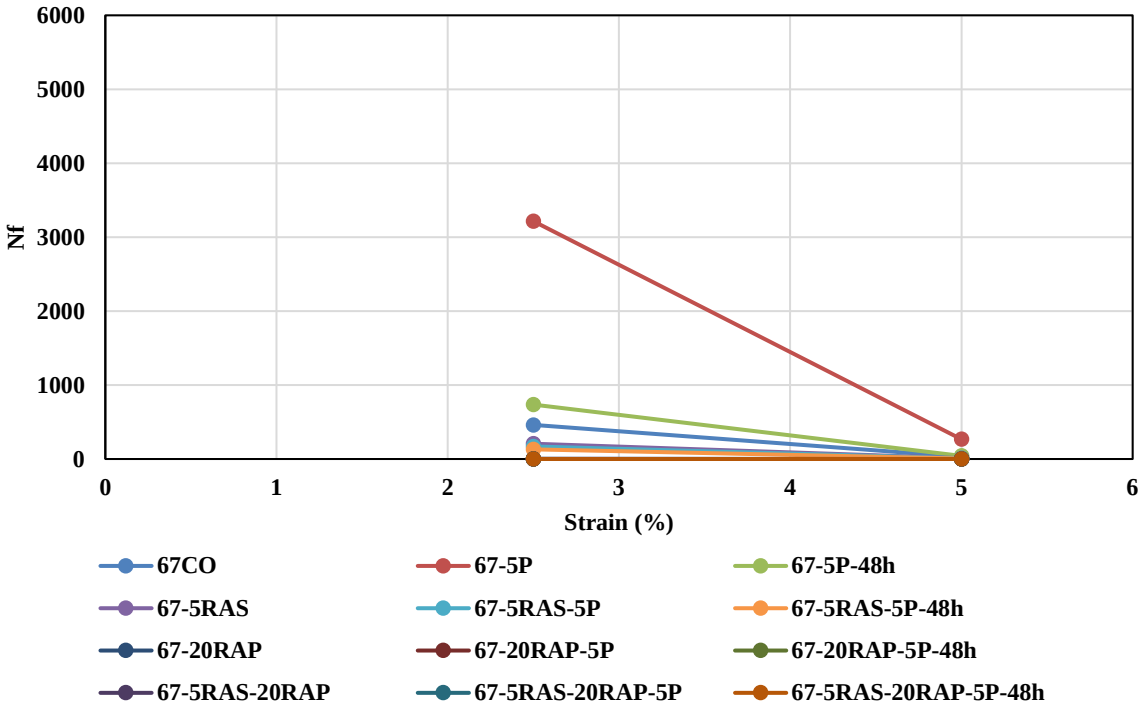

(a)

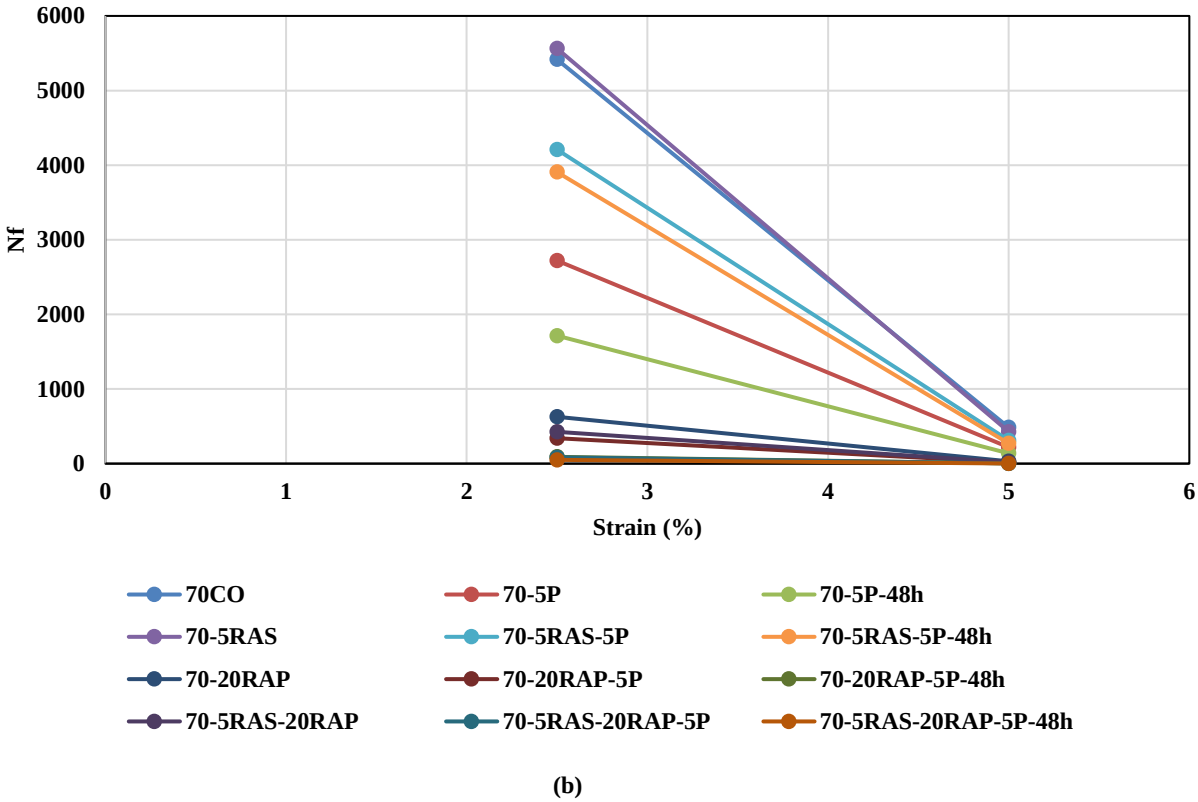

(b)

Figure 31. LAS results for (a) PG 67-22 binder blends and (b) PG 70-22M Binder blends.

5.3. Effect of Self-Healing Polymers on Self-Healing Properties of Asphalt Mixture

5.3.1. Crack Healing Efficiency Test Results

Fourteen asphalt mixtures were prepared using two binders, two recycled asphalt materials (5% RAS and/or 20% RAP), and with or without 5% SHP. Cracks were induced at the bottom of the prepared rectangular beams, and healing was monitored under two different healing conditions; room temperature (25 ± 2°C) and high temperature (50 ± 2°C) for samples without SHP and room temperature (25 ± 2°C) and UV light exposure for samples containing SHP. Crack healing was evaluated using two approaches; crack width analysis and strength recovery ratio. In the first approach, the width of the crack at the bottom of the prepared beams was monitored by crack analysis. Pictures were captured and analyzed at day 0, day 1, day 2, day 5 and day 6. Examples of pictures captured on day 0 and day 6 are presented in Figure 32.

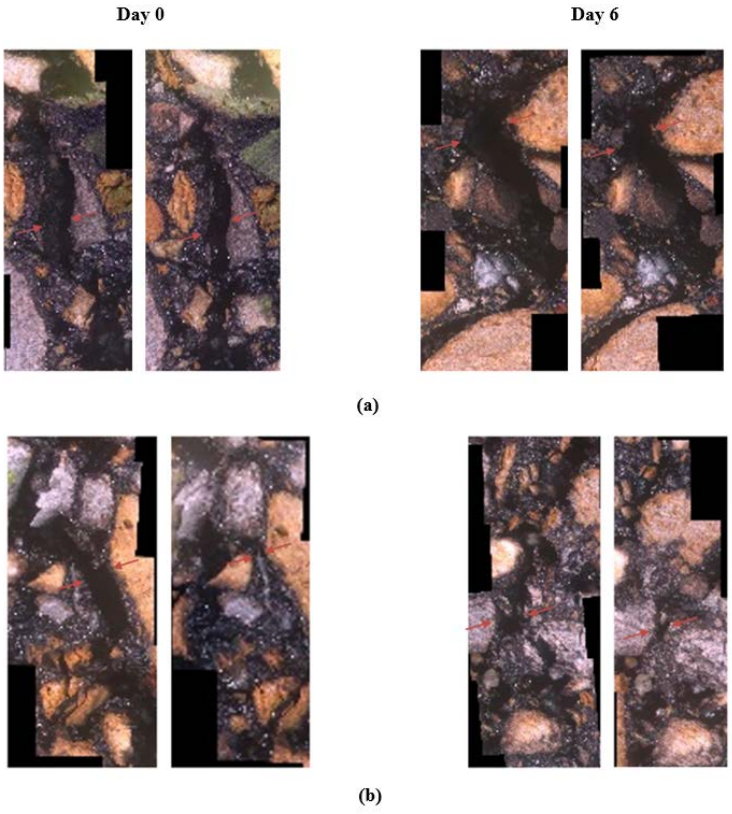

Figure 32. Crack monitoring under different curing conditions; (a) Room temperature (25°C) and (b) High temperature (50°C)/ UV exposure.

Crack Width Analysis for Mixtures Containing 5% RAS: Results from mixtures prepared with or without 5% RAS, and with or without 5% SHP are presented in Figures 33 and 34 respectively for mixtures prepared with an unmodified binder (PG 67-22) and polymer-modified binder (PG 70-22M).

PG 67-22 Binder Blends: For samples prepared with PG 67-22 binder and healed at room temperature, the control mixture (67CO) showed the highest healing efficiency at day 6 with 64% healing efficiency. When 5% SHP was added to the control mixture (67-5P), healing

efficiency decreased to 54%. Furthermore, the addition of RAS negatively affected the self-healing efficiency of the control mixture by reducing the healing efficiency of day 6 from 64% (67CO) to 45% (67-5RAS). This may due to the aged and brittle binder in the RAS. The application of SHP improved crack healing of the samples; however, it was not significant enough to achieve the healing efficiency of the control mixture. Results obtained from the statistical analysis indicated that the healing efficiency of mixtures with or without 5% RAS and 5% SHP were not significantly different at room temperature.

When the control mixture was subjected to a high-temperature healing condition, healing efficiency of the mixture marginally increased from 64% at room temperature to 67% at high temperature. The high temperature may stimulate the capillary flow of the binder and increase the rate of crack healing. An increase in the healing efficiency was observed due to UV light exposure of the mixture containing 5% SHP. On the other hand, the addition of RAS decreased the healing efficiency, even at high temperature. When samples containing 5% RAS and 5% SHP were subjected to UV light exposure, the healing efficiency increased to 69.5% at day 6. These results show that the reaction of unstable bonds of polymer activated through UV light exposure was able to increase the crack-healing rate and therefore, improve self-healing properties of the mixtures containing RAS.

Figure 34 shows the results from the statistical analysis conducted to evaluate the effect of healing conditions on the crack healing of the mixtures. Altering healing condition from room temperature to UV exposure/high temperature did not cause a significant change in the crack healing efficiency for the control mixture (67CO), and the mixture with RAS (67-5RAS). However, the addition of 5% SHP and exposure to UV light significantly improved the healing performance of the mixture without recycled materials (67-5P) and mixture with 5% RAS (67-5RAS-5P).

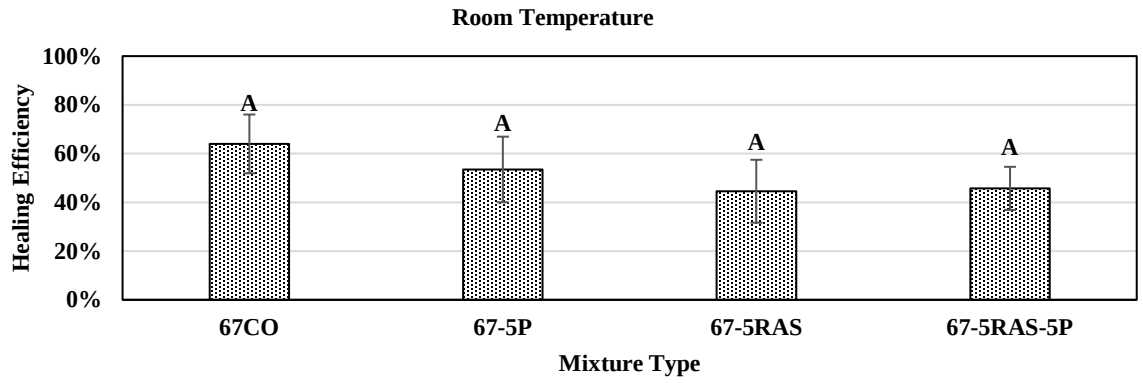

(a)

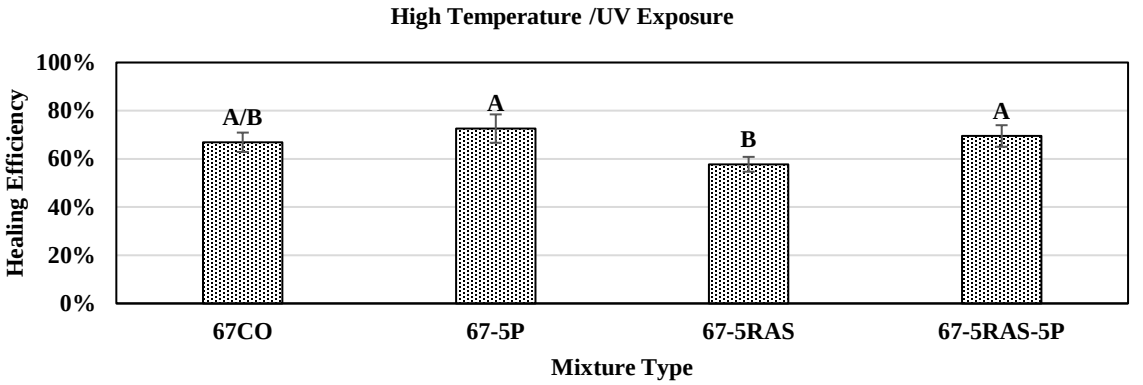

(b)

Figure 33. Crack healing efficiency for PG 67-22 mixtures containing 5%RAS: (a) Room temperature conditioning and (b) High temperature or UV light conditioning.

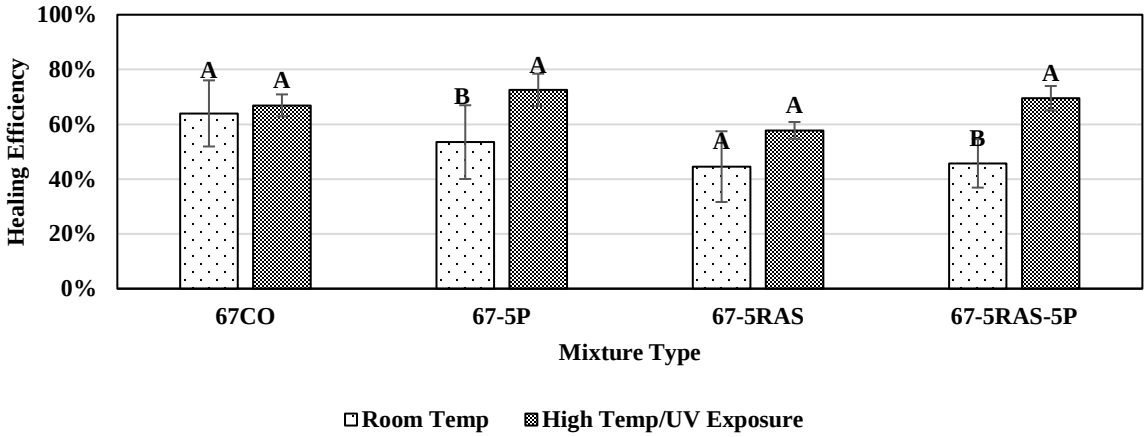

Figure 34. Effect of curing conditions on healing efficiency of the PG 67-22 mixtures containing 5%RAS.

PG 70-22M Binder Blends: For mixtures prepared with PG 70-22M, the control mixture (70CO) and mixtures containing 5% RAS (70-5RAS) had similar healing performances when conditioned at room temperature. A significant decrease in self-healing efficiency of the mixture was observed when 5% SHP was added to the control mixture and mixtures containing 5% RAS (Figure 35a). The decrease in healing efficiency may be attributed to the increase in stiffness through the undesirable interactions of SBS polymer in PG 70-22M and polyurethane in SHP. In addition, chemical reactions in the polymer require UV light exposure to be activated. Using UV exposure/high temperature, the healing efficiency of the control mix, mixture with 5% SHP, mixture containing 5% RAS, and mixture containing 5%RAS and 5% SHP, increased from 55%, 31%, 53%, and 41% to 64%, 44%, 55% to 54%, respectively. However, based on the conducted statistical analysis, performances of these mixtures at high-temperature curing conditions or UV exposure were not significantly different.

Statistical analysis results for the effect of curing conditions presented in Figure 36 indicate that the change in healing temperature from 25°C to 50°C did not have a significant effect on crack healing efficiency of the control mixture and the mixture containing 5%RAS. The same results were observed for a mixture containing 5% RAS and 5% SHP, which showed the insignificant difference in crack healing performance due to UV light exposure. The only mixture with significant improvement in crack healing was the mixture with 5% SHP (70-5P) and exposure to UV light.

Crack Width Analysis for Mixtures Containing 20% RAP: The crack width healing efficiency was evaluated in mixtures prepared with an unmodified binder (PG 67-22) and a polymer modified binder (PG 70-22M) with and without 20% RAP and 5% SHP.

PG 67-22 Binder Blends: Figure 37 presents the healing efficiency of the control mixture (67CO), mixture with 5% SHP (67-5P), mixture with 20% RAP (67-20RAP) and mixture containing 20% RAP and 5% SHP (67-20RAP-5P) at day 6. As shown in these results, the control mixture had the highest healing efficiency at room temperature with a healing efficiency of 64% at day 6. The healing efficiency of mixture containing SHP, mixture containing RAP and mixture containing RAP and SHP were measured as 54%, 53%, and 35%, respectively. The addition of 20% RAP and the use of aged binder negatively affected the crack-healing performance. Moreover, the use of SHP led to a decrease in the healing efficiency of the mixtures, which may be due to the increase in stiffness of the mixture.

When the healing condition was changed from room temperature to high temperature, the healing efficiency of the control mixture (67CO) and the mixture containing RAP (67-20RAP) was improved; however, based on the statistical analysis conducted, this increase was not significant (Figure 38). On the other hand, the UV exposure of mixture with 5% SHP and the mixture containing 20% RAP and 5% SHP significantly increased the healing efficiency from 54% and 35% at room temperature to 72% and 58%. As a result, it can be stated that UV exposure successfully activated the reaction of unstable free radicals and therefore, enhanced the healing efficiency of the mix.

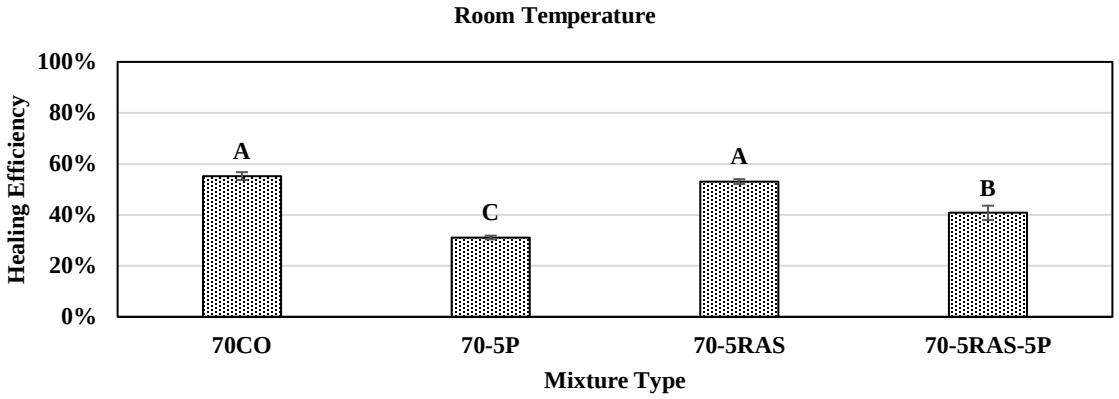

(a)

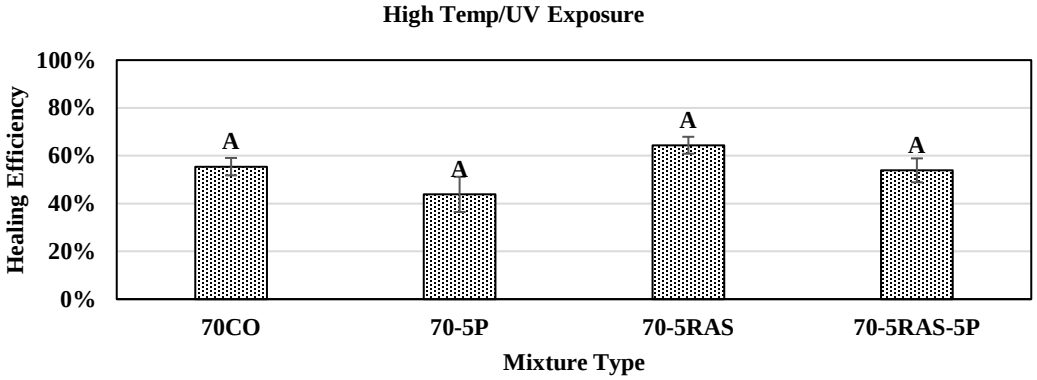

(b)

Figure 35. Crack healing efficiency for PG 70-22M mixtures containing 5%RAS: (a) Room temperature conditioning and (b) High temperature or UV light conditioning.

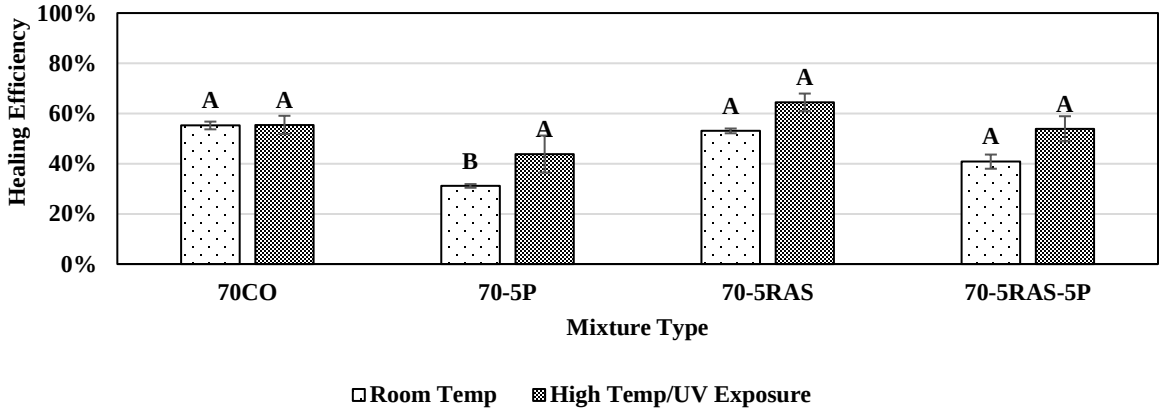

Figure 36. Effect of curing conditions on healing efficiency of the PG 70-22M mixtures containing 5%RAS.

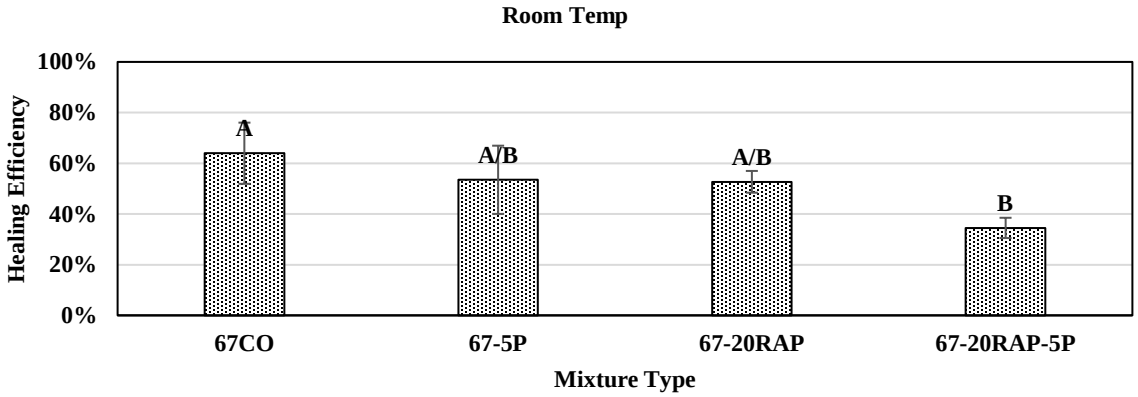

(a)

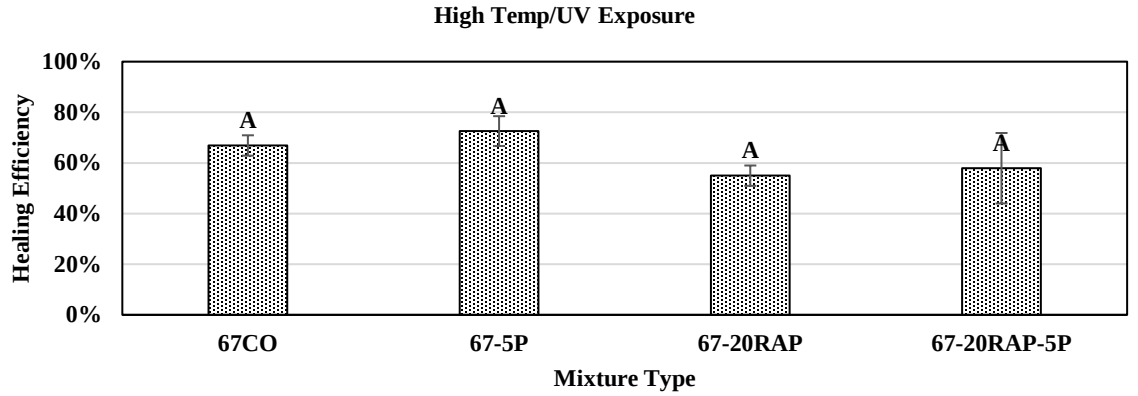

(b)

Figure 37. Crack healing efficiency for PG 67-22 mixtures containing 20%RAP: (a) Room temperature conditioning and (b) High temperature or UV light conditioning.

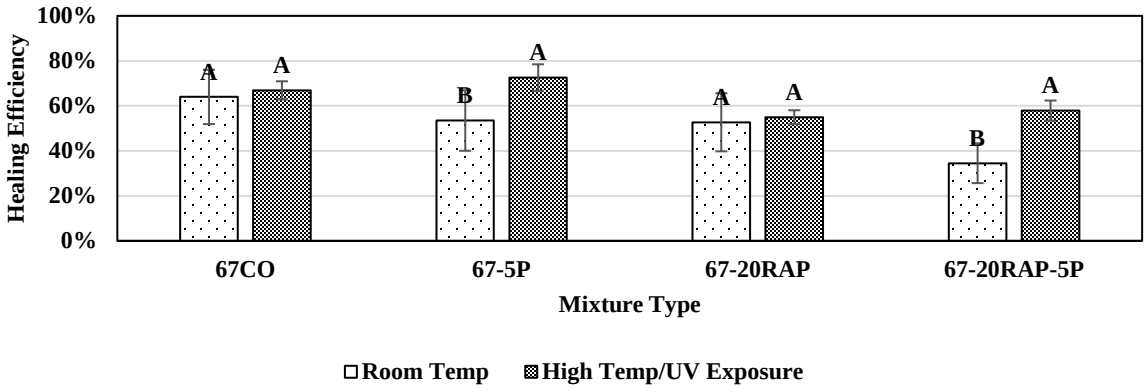

Figure 38. Effect of curing conditions on healing efficiency of the PG 67-22 mixtures containing 20%RAP.

PG 70-22M Binder Blends: Asphalt mixtures were prepared using polymer modified binder (PG 70-22M), with or without 20% RAP and 5% SHP. The healing efficiency results are presented in Figure 39. As shown in these results, the addition of 20% RAP to the mixture prepared with PG 70-22M binder improved the healing efficiency of the mixture; however, this improvement was not significant. In addition, the use of 5% SHP led to a significant decrease in healing efficiency. The same behavior was observed with a mixture prepared with PG 67-22 binder, 20% RAP, and 5% SHP. When the healing condition was changed from room temperature to high temperature or UV exposure, all mixtures, 70CO, 70-5P, 70-20RAP, and 70-20RAP-5P, had statistically equivalent healing efficiency at day 6, as shown in Figure 39b.

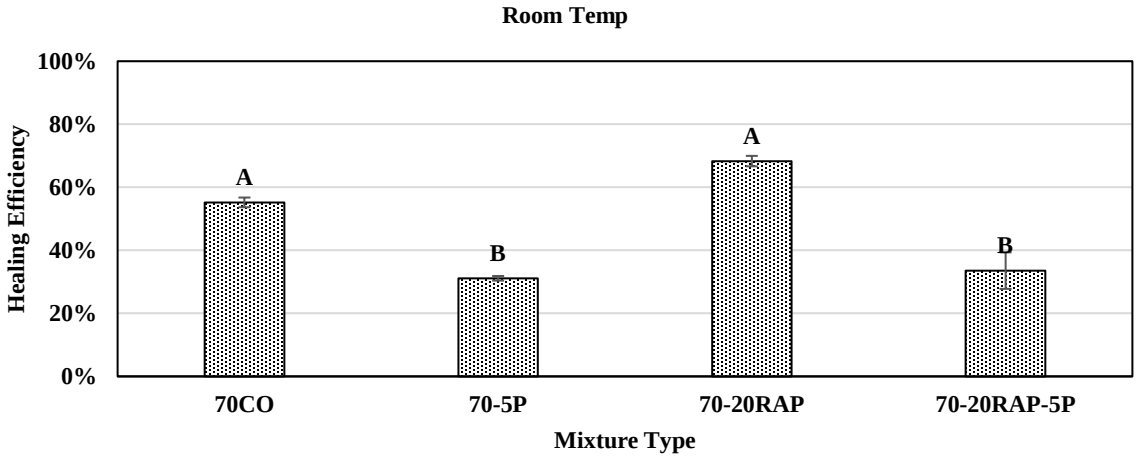

(a)

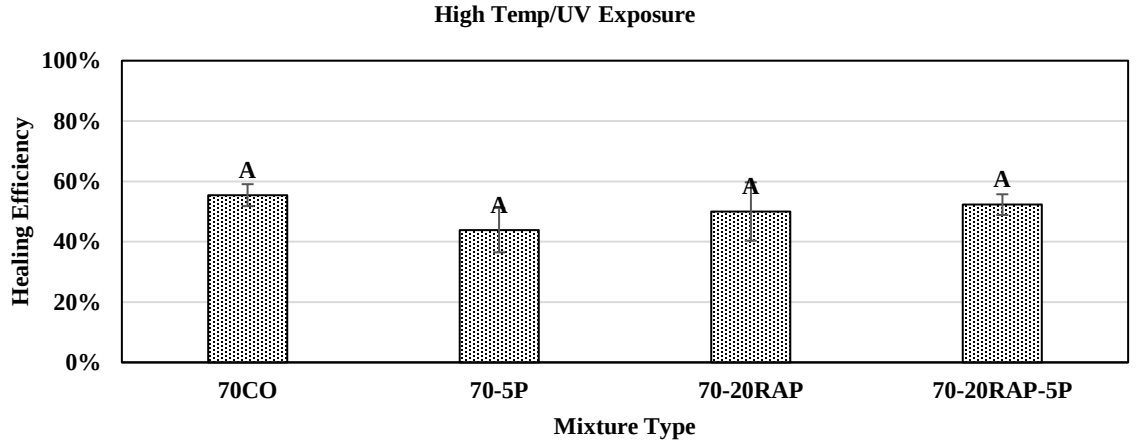

(b)

Figure 39. Crack healing efficiency for PG 70-22M mixtures containing 20%RAP: (a) Room temperature conditioning and (b) High temperature or UV light conditioning.

Figure 40 presents the results of the statistical analysis conducted to compare the healing efficiency at different temperatures. Based on the results, the healing efficiency of the control mixture (70CO) was the same at room temperature and at high temperature. The healing

efficiency of the mixture with 5% SHP significantly increased due to the exposure to the UV light. The mixture containing 20% RAP had significantly different healing efficiency at different healing conditions, with the healing efficiency of 68% at room temperature and 50% healing efficiency at high temperature. The mixture containing 20% RAP and 5% SHP had a significantly different performance with or without 48 h UV light exposure; the healing efficiency of this mixture was increased from 34% to 52% via UV light exposure.

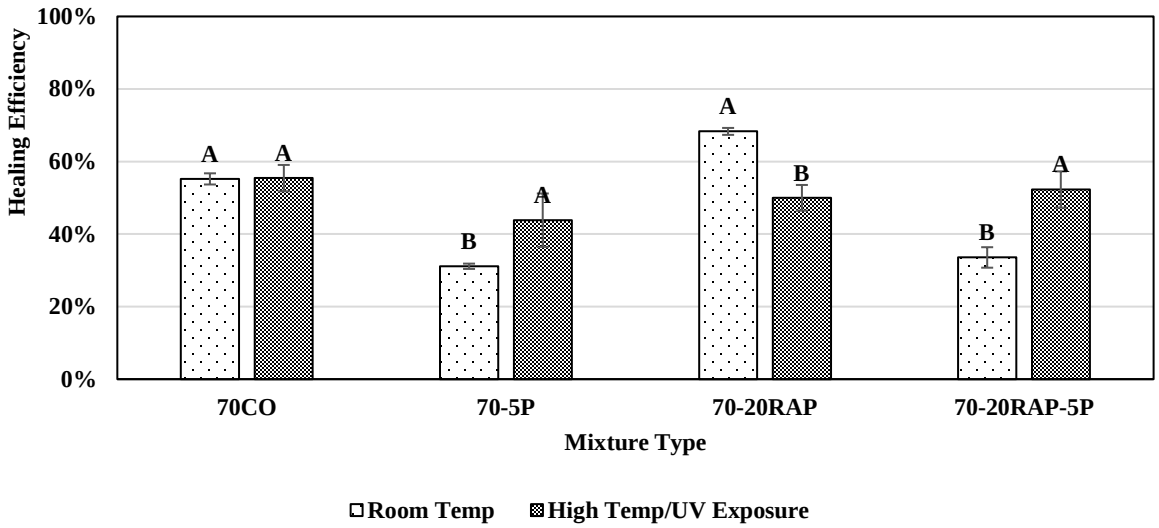

Figure 40. Effect of curing conditions on healing efficiency of the PG 70-22M mixtures containing 20%RAP.

Crack Width Analysis for Mixtures Containing 5% RAS+20%RAP

PG 67-22 Binder Blends: Based on the crack healing analysis performed for different mixtures with or without 5%RAS+20% RAP, the performance of the mixtures was negatively affected by the addition of recycled materials. However, based on the statistical analysis, all mixtures had similar crack healing efficiency at room temperature curing condition (Figure 41a). On the other hand, a significant decrease was observed in the healing efficiency of the mixtures containing 5%RAS+20% RAP, when samples were subjected to high temperature or UV exposure conditions. Figure shows the changes in healing efficiency performance when curing condition was altered from room temperature to high temperature/UV exposure. Based on these results, changes were insignificant for mixtures with 5%RAS+20%RAP, both without SHP (67-5RAS-20RAP) and with SHP (67-5RAS-20RAP-5P).

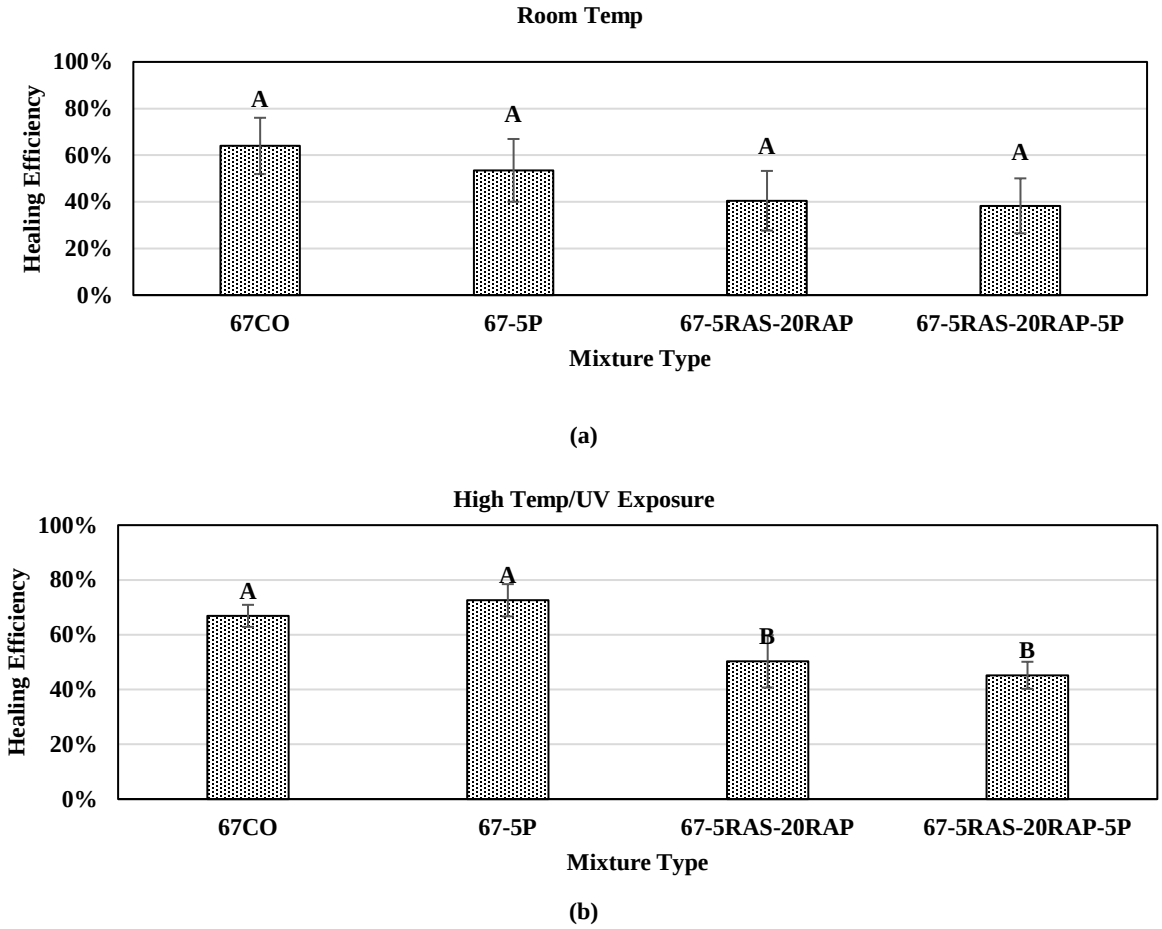

Figure 41. Crack healing efficiency for PG 67-22 mixtures containing 5%RAS+20%RAP: (a) Room temperature conditioning and (b) High temperature or UV Light conditioning.

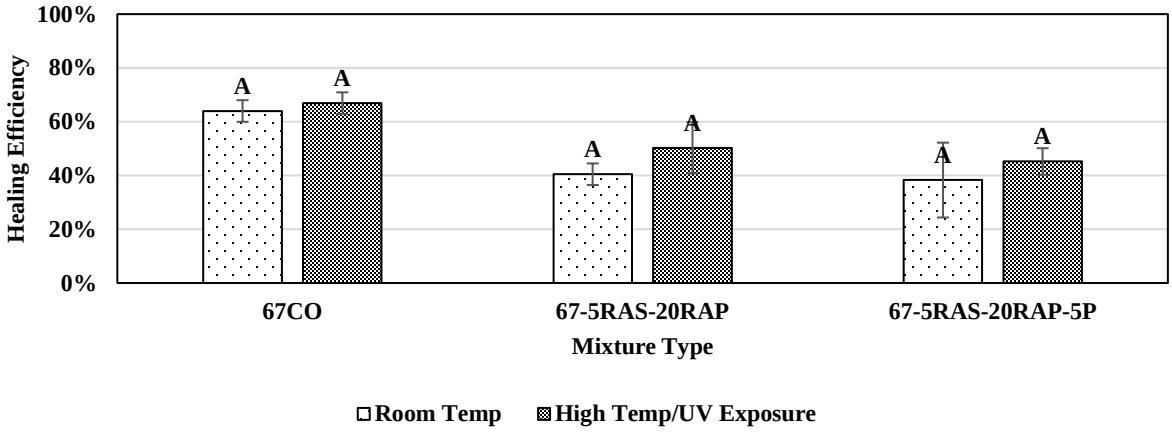

Figure 42. Effect of curing conditions on healing efficiency of the PG 67-22 mixtures containing 5%RAS+20%RAP.

PG 70-22M Binder Blends: Results for healing efficiency of the mixtures prepared with PG 70-22M, with or without 5%RAS+20%RAP are presented in Figure 43. Compared to the control (70CO), the addition of recycled materials led to a significant decrease in healing

efficiency of the mixtures at room temperature. The healing efficiency further decreased with the addition of 5% SHP. However, the decrease caused by SHP addition was statistically insignificant. For high temperature/UV exposure curing condition, all mixtures showed a similar performance, based on the statistical analysis. For the effect of curing conditions shown in Figure 44, altering the curing conditions from room temperature to high temperature did not have a significant effect while replacing the room temperature condition with UV exposure showed a significant improvement in the healing efficiency of the mixture containing 5%RAS+20% RAP and 5%SHP (70-5RAS-20RAP-5P).

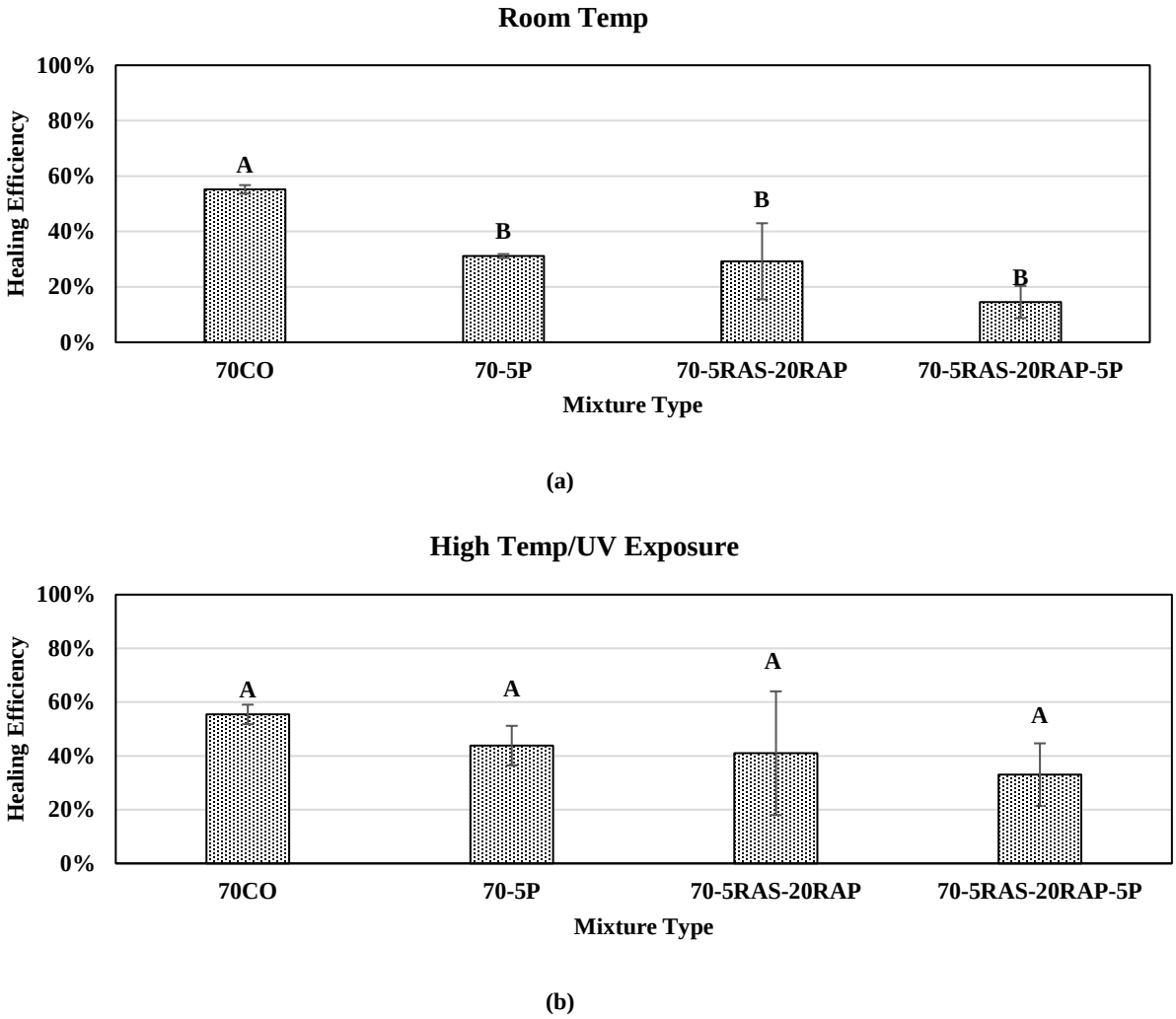

Figure 43. Crack healing efficiency for PG 70-22M mixtures containing 5%RAS+20%RAP: (a) Room temperature conditioning and (b) High temperature or UV light conditioning.

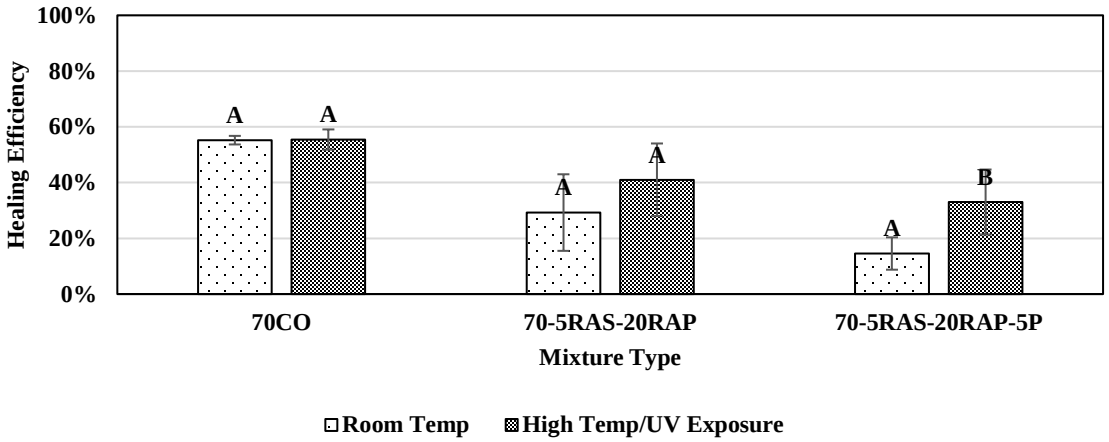

Figure 44. Effect of curing conditions on healing efficiency of the PG 70-22M mixtures containing 5%RAS+20%RAP.

Strain Energy Recovery Analysis for Mixtures Containing 5% RAS: The strain energy recovery of the beams was measured at three different stages; undamaged, and healed (after 6 days of healing).

PG 67-22 Binder Blends: Results from SERR measurements of the samples are presented in Figure 45. Statistical analysis conducted using JMP software to evaluate the effect of 5% RAS, 5% SHP, and different healing conditions are presented in Figures 46 and 47. Adding 5% SHP led to an increase in the measured SERR, while the addition of 5% RAS to asphalt mixtures prepared with PG 67-22 led to a decrease in the healed SERR at room temperature. Furthermore, the use of SHP in a mixture containing 5% RAS increased the healed SRR; however, this increase was insignificant. For samples healed at high temperature, the addition of 5% RAS increased the SERR, while the incorporation of 5% SHP, resulted in a lower SERR. Based on the statistical analysis, none of the changes caused by the addition of RAS and/or SHP were significant. In order to study the effect of healing conditions, the measured damaged SERR were statistically compared. Results showed that changing the healing conditions did not significantly affect the measured SERR (Figure 48).

PG 70-22M Binder Blends: For mixtures prepared with a polymer-modified binder (PG 70-22M), the addition of 5% SHP did not have a significant effect on SERR while RAS incorporation led to a significant decrease in the measured SERR at room temperature. The addition of 5% SHP and 48h exposure to UV light increased the SERR at high temperature or UV exposure, which may be due to the activation of SHP with UV exposure. For high temperature or UV light exposure conditioning, the best performance was obtained with the control mixture while the addition of 5% SHP resulted in the lowest recovery. Results presented in Figure indicate that changing the curing condition from room temperature to a high temperature significantly improved the SERR while the change from room temperature to UV exposure led to an insignificant increase in the SERR.

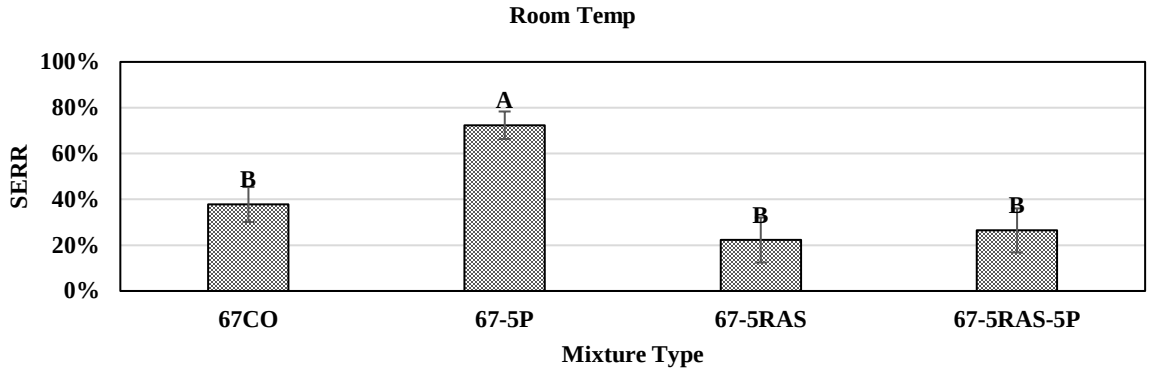

(a)

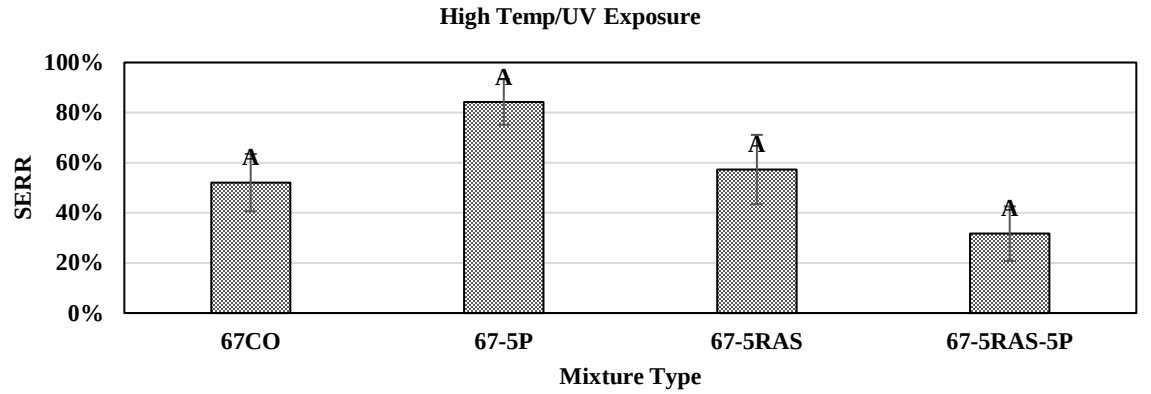

(b)

Figure 45. Strain energy recovery ratio for PG 67-22 mixtures containing 5%RAS: (a) Room temperature conditioning and (b) High temperature or UV light conditioning.

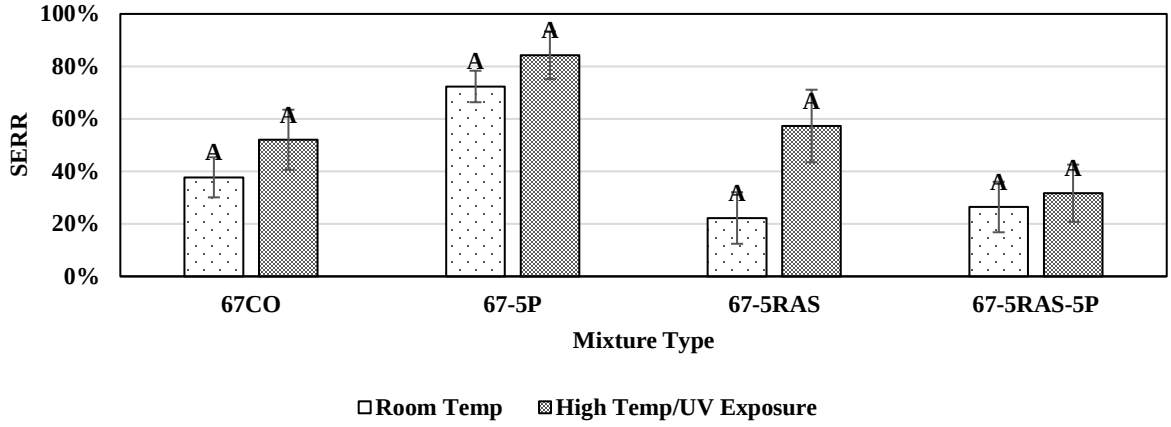

Figure 46. Effect of curing conditions on SERR of the PG 67-22 mixtures containing 5%RAS.

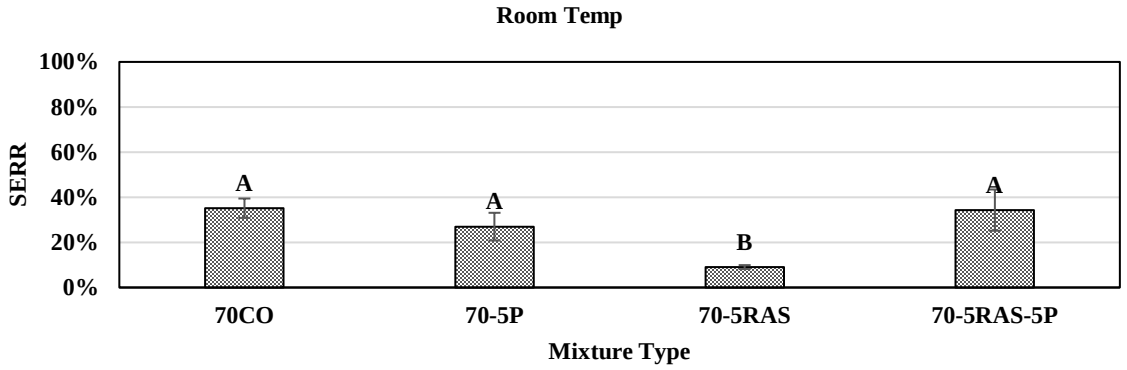

(a)

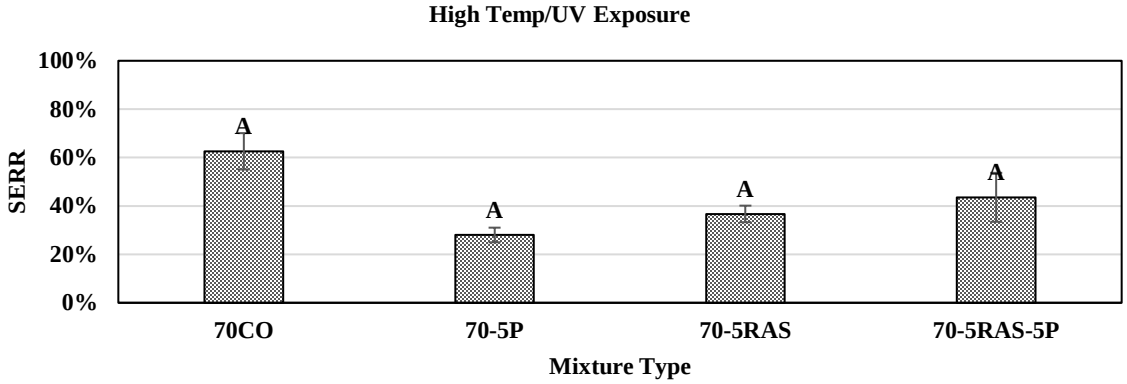

(b)

Figure 47. Strain energy recovery ratio for PG 70-22M mixtures containing 5%RAS: (a) Room temperature conditioning and (b) High temperature or UV light conditioning.

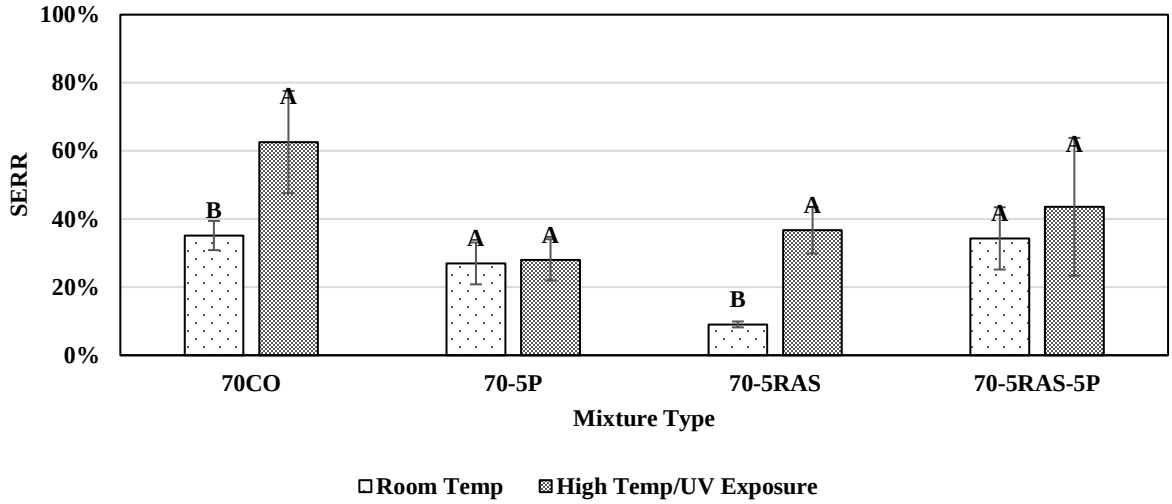

Figure 48. Effect of curing conditions on SERR of the PG 70-22M mixtures containing 5%RAS.

Strain Energy Recovery Analysis for Mixtures Containing 20% RAP

PG 67-22 Binder Blends: Figure 49 presents the measured healed SERR for the control mixture (67CO), mixture with 5% SHP (67-5P), mixture containing 20%RAP (67-20RAP), and mixture containing 20% RAP and 5% SHP (67-20RAP-5P), under two different healing conditions; room temperature and high temperature or UV exposure. As shown in this Figure, the addition of 5% SHP and 20% RAP to the mixtures resulted in an increase and a decrease in SERR respectively, under both healing conditions. Furthermore, the use of 5% SHP resulted in an improvement in strain energy recovery under both healing conditions. However, the increase in strain energy recovery, caused by 5% SHP application was not superior to the control mixture.

Figure 50 presents the statistical analysis conducted to evaluate the effects of 20% RAP and 5% SHP addition on the SERR of the mixtures prepared with PG 67-22 binder. The highest SERR at room temperature was for the mixture with 5% SHP, while the lowest SERR was observed for the mixture with 20% RAP. These results indicate that the aged binder in the RAP had a negative effect on the strain energy recovery of the mixtures at room temperature. The same behavior was observed for high temperature or UV exposure; the mixture with 5% SHP (67-5P), which had been exposed to UV light for 48 h, showed the best performance in strain energy recovery. Furthermore, it was observed that the addition of 5% SHP to mixtures containing 20% RAP and exposing the samples to UV light, activated the self-healing process of SHP and improved the mixture healing performance. Figure presents the effects of healing condition on the healed SERR. Results show that altering the healing conditions did not have a significant effect on the healed SERR.

PG 70-22M Binder Blends: The SERR measurements for mixtures prepared using PG 70-22M binder, with or without 20%RAP and 5%SHP, were evaluated (Figure 51). The healed SERR decreased when 20% RAP was added to the mixture at both healing conditions. Furthermore, the incorporation of 5% SHP to the mixtures healed at room temperature recovered the original strength of the mixtures. However, when samples were exposed to UV light, the strength recovery was affected neutrally for the healed SERR (Figure 52). Figure 52 statistically compared the effect of altering the curing condition from room temperature to UV exposure or high temperature. Based on the results, the change in healing conditions from room temperature to a high temperature significantly improved the performance of 70CO and 70-20RAP mixtures while for mixtures with 5% SHP (70-5P and 70-20RAP-5P), UV exposure did not have a significant effect on the healed SERR of the mixtures.

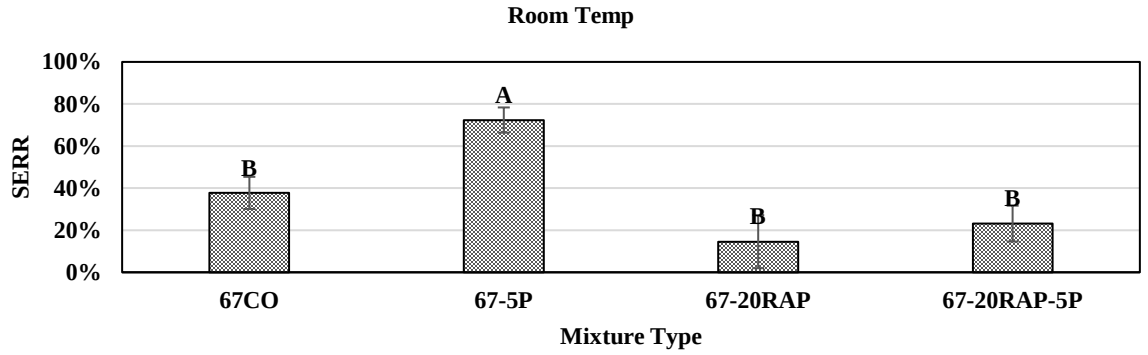

(a)

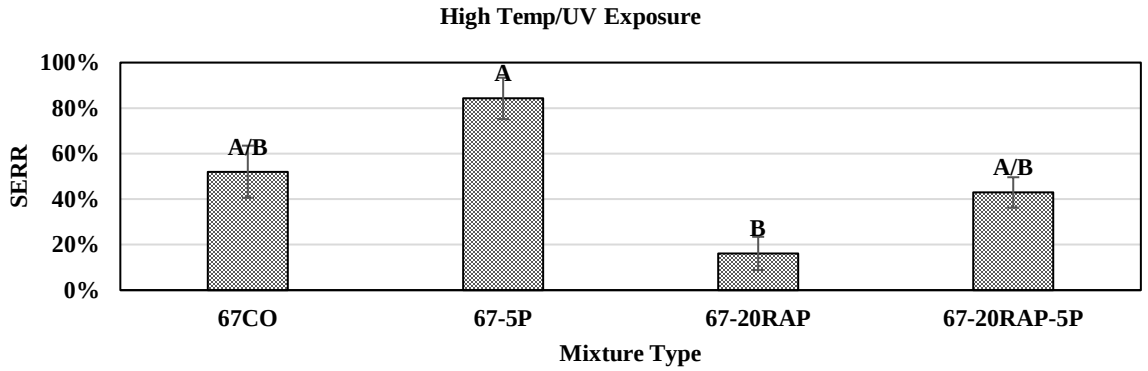

(b)

Figure 49. Strain energy recovery ratio for PG 67-22 mixtures containing 20%RAP: (a) Room temperature conditioning and (b) High temperature or UV light conditioning.

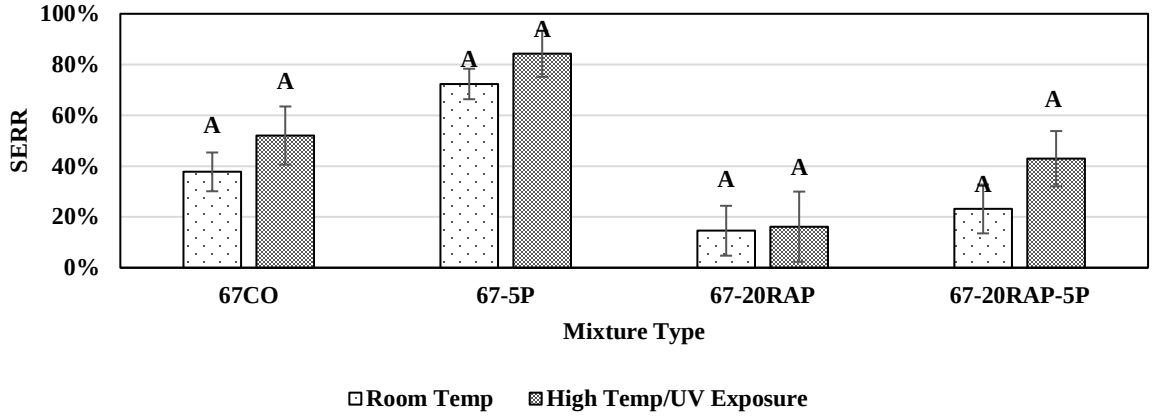

Figure 50. Effect of curing conditions on SERR of the PG 67-22 mixtures containing 20%RAP.

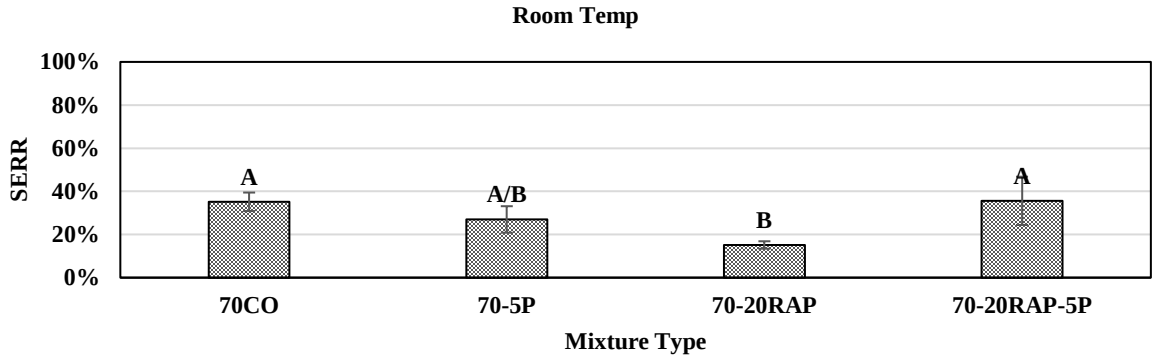

(a)

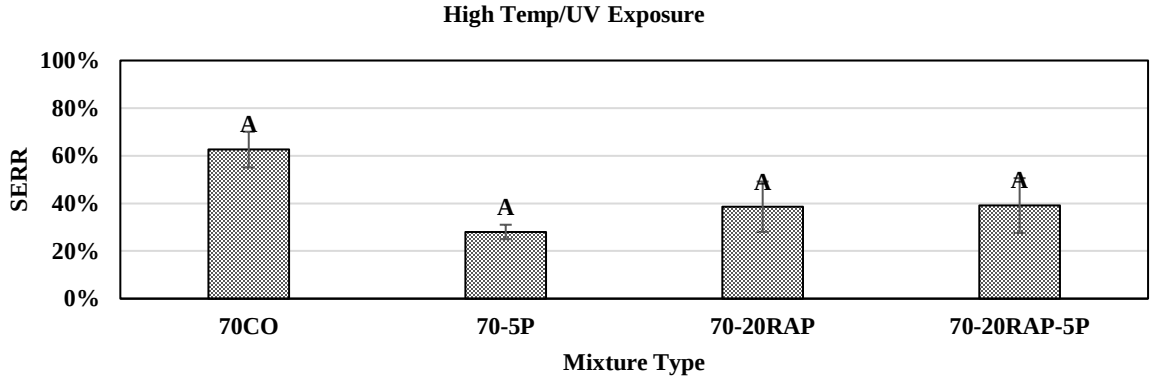

(b)

Figure 51. Strain energy recovery ratio for PG 70-22M mixtures containing 20%RAP: (a) Room temperature conditioning and (b) High temperature or UV light conditioning.

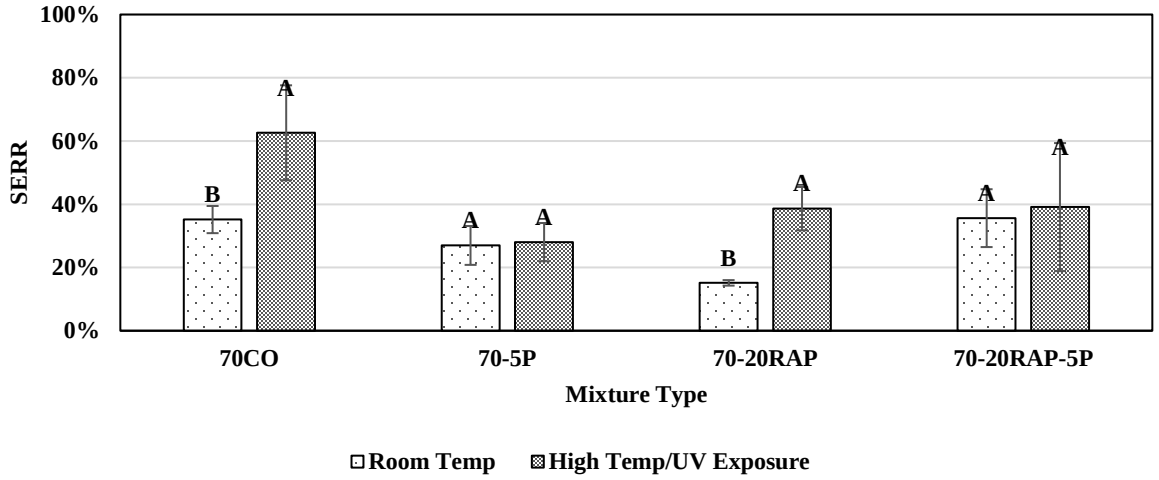

Figure 52. Effect of curing conditions on SERR of the PG 70-22M mixtures containing 20%RAP.

Strain Energy Recovery Analysis for Mixtures Containing 5%RAS+ 20% RAP: Strain energy was measured for mixtures containing 5%RAS+20%RAP, with or with 5% SHP.

PG 67-22 Binder Blends: Based on the results presented in Figure 53a, for samples cured at room temperature, the SERR significantly decreased when 5%RAS+20%RAP was added to the mixture (67-5RAS-20RAP). The incorporation of 5% SHP caused an increase in the calculated SERR; however, the increase was statistically insignificant. The same behavior was observed for samples exposed to high temperature or UV light for 6 days (Figure 54b). Furthermore, Figure 55 shows that changing the curing condition did not have a significant effect on the measured SERR of the samples with 5%RAS+20%RAP, with or without 5% SHP.

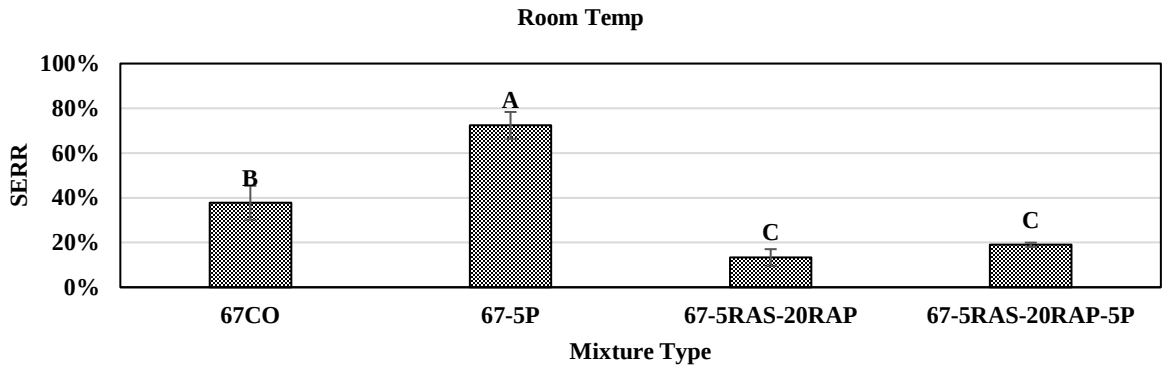

(a)

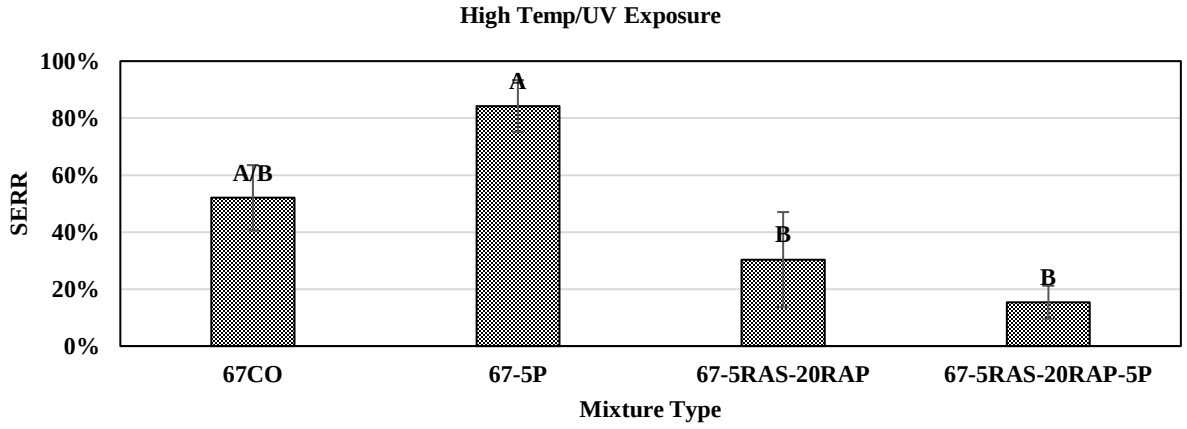

(b)

Figure 53. Strain energy recovery ratio for PG 70-22M mixtures containing 5%RAS+20%RAP: (a) Room temperature conditioning and (b) High temperature or UV light conditioning.

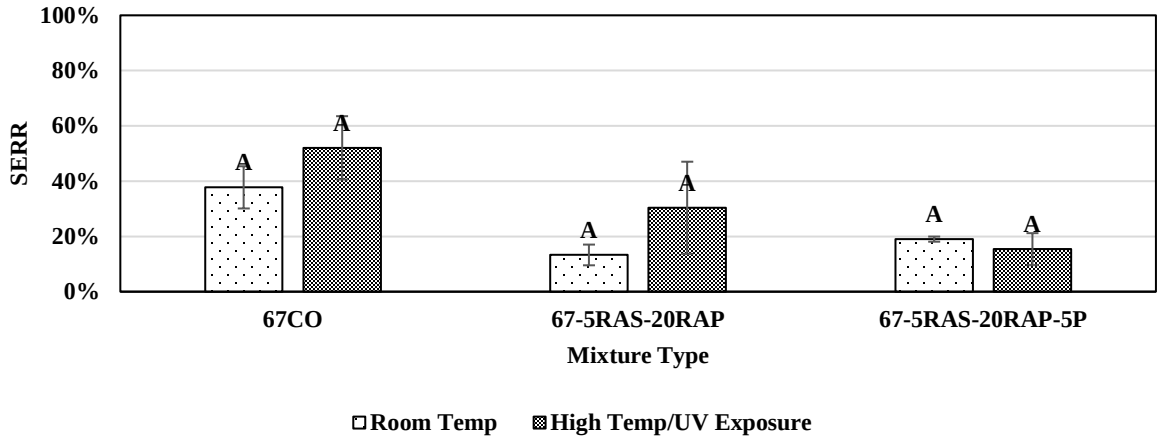

Figure 54. Effect of curing conditions on SERR of the PG 67-22 mixtures containing 5%RAS+20%RAP.

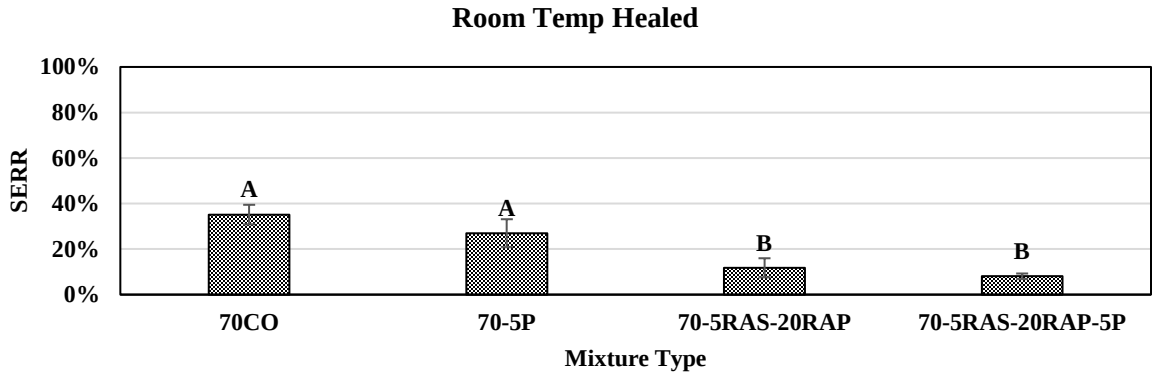

(a)

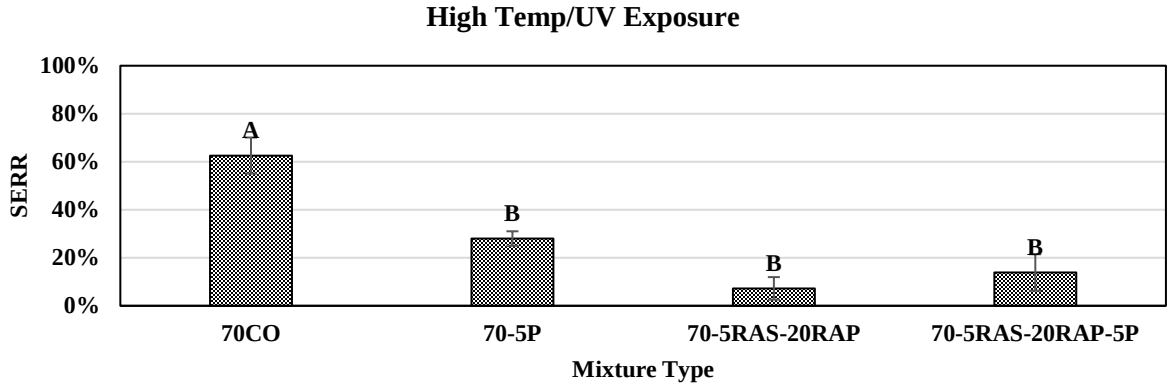

(b)

Figure 55. Strain energy recovery ratio for PG 70-22M mixtures containing 5%RAS+20%RAP: (a) Room temperature conditioning and (b) High temperature or UV light conditioning.

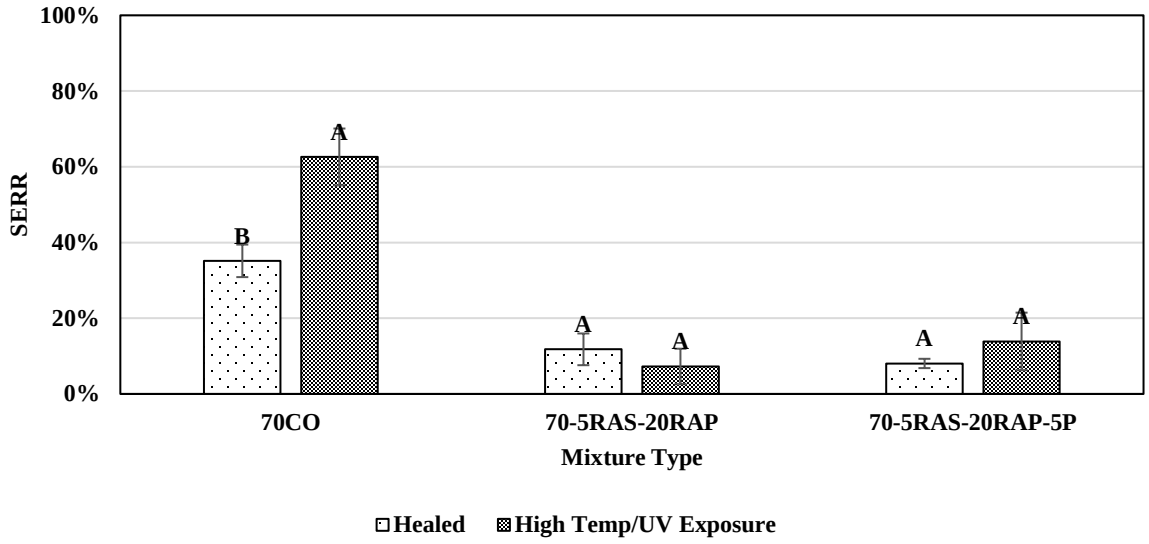

Figure 56. Effect of curing conditions on SERR of the PG 70-22M mixtures containing 5%RAS+20%RAP.

PG 70-22M Binder Blends: As it was expected, the addition of recycled materials (5%RAS+20%RAP) had a significant effect on reducing the SERR of the mixtures. The SERR of the control mixture (70CO) at room temperature and high temperature decreased from 35% and 63% to 12% and 7% due to the incorporation of 5% RAS and 20% RAP. Based on the statistical analysis, 5% SHP application had an insignificant effect on the SERR. Similar to the mixtures prepared with PG 67-22, altering the curing condition from room temperature to high temperature/ UV exposure led to insignificant changes in the calculated SERR (Figure 56).

5.4. Effect of Self-Healing Polymer on the Mechanical Performance of Asphalt Mixtures

Three laboratory tests were performed on seven different mixtures; semi-circular bending (SCB) test, Hamburg loaded wheel tracking (LWT) test and thermal stress restrained specimen test (TSRST). It should be noted that the complete details of the statistical analysis conducted for different mixture tests (Crack healing, SERR, SCB, LWT, and TSRST) is presented in Appendix C.

5.4.1. Semi-Circular Bending Test Results

SCB Results for Mixtures Containing 5%RAS

PG 67-22 Mixtures: The SCB test was used to compare the cracking susceptibility of different mixtures at intermediate temperature. The measured critical strain energy release rate (J_c) obtained for mixtures prepared using an unmodified binder (PG 67-22), with or without 5% RAS and 5% SHP is presented in Figure 57. The lowest J_c value was measured for the control mixture (i.e. 67CO) with a J_c value of 0.35 kJ/m^2. Due to the addition of 5% RAS, the J_c value of the mixture containing 5% RAS was similar at 0.38 kJ/m^2. Furthermore, when 5% SHP was added to the mixture, the J_c value increased to 0.48 kJ/m^2, and when the samples were exposed to 48h of UV light, the J_c value further increased to 0.52 kJ/m^2. In summary, the addition of 5% SHP to mixtures containing 5% RAS, improved the cracking performance at intermediate temperature. Based on the statistical analysis performed for SCB results, the J_c value measured for the control mixture (67CO) was significantly different, while the rest of the mixture demonstrated similar cracking performance.

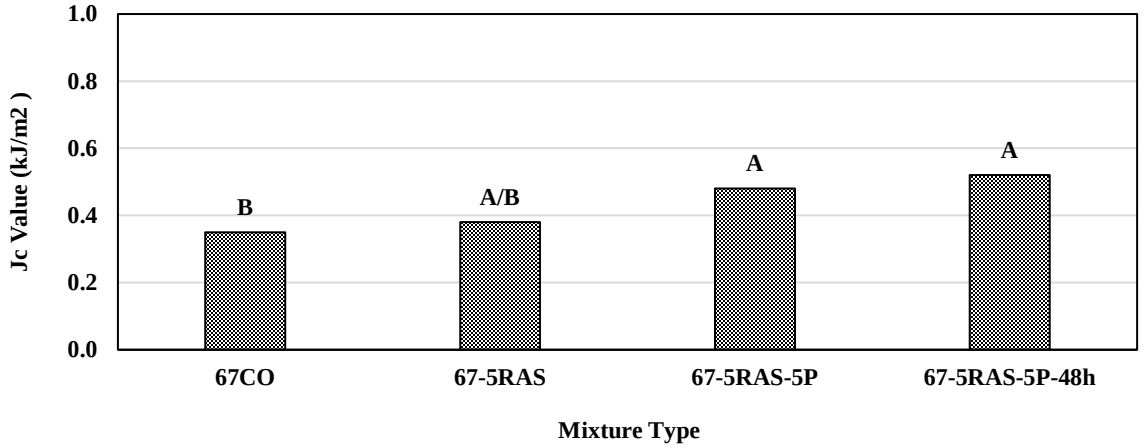

Figure 57. SCB results for PG 67-22 mixtures containing 5% RAS.

PG 70-22 Mixtures: The SCB test was conducted for mixtures containing 5% RAS and prepared with polymer modified binder, PG 70-22M. Figure 58 presents the measured J_c values. The control mixture, 70CO, had a J_c value 0.64 kJ/m^2. When 5% RAS was added to the mixtures, J_c decreased to 0.45 kJ/m^2. The addition of 5% SHP and 48h of UV light exposure increased J_c value (0.72 kJ/m^2), reaching a value higher than the control mixture (0.64 kJ/m^2). Based on the performed statistical analysis, the mixture containing 5% RAS and 5% SHP with 48 h of UV light exposure (70-5RAS-5P-48h) and the control mixture (70CO) had the best

cracking performance and were significantly different from the mixture with 5%RAS (70-5RAS).

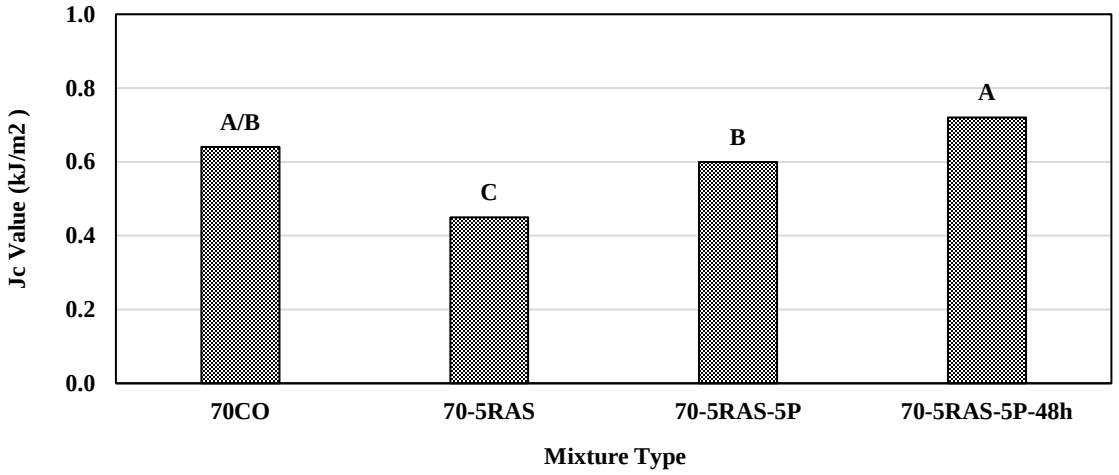

Figure 58. SCB results for PG 70-22M mixtures containing 5% RAS.

SCB Test Results for Mixtures Containing 20% RAP

PG 67-22 Mixtures: In case of RAP usage in the mixtures, the J_c value of the mixture prepared with unmodified binder decreased to 0.39 kJ/m^2 (Figure 59). This value increased to 0.62 and 0.68 kJ/m^2, respectively through 5% SHP application and 5% SHP application plus UV light exposure. The statistical analysis indicated the enhanced performance of the mix with SHP, especially when the samples were subjected to 48h of UV light.

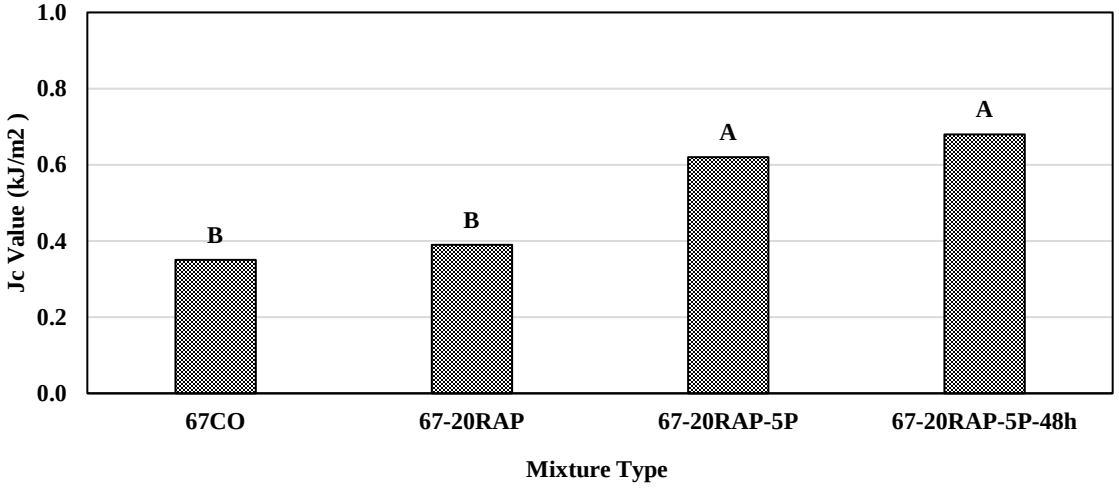

Figure 59. SCB results for PG 67-22 mixtures containing 20% RAP.

PG 70-22M Mixtures: SCB test results for mixtures with 20% RAP are presented in Figure 60. When 20% RAP was added to the mixture prepared with the PG 70-22M polymer-modified binder, the same cracking performance as the control mixture was observed. However, when 5% SHP was added to the mixture, a decrease in J_c value was observed, which could be caused by the undesirable interaction of polyurethane in SHP with the polymer from RAP or PG 70-

22M. The cracking performance of the mixture was improved through UV light exposure; however, the increase was not enough to reach the J_c value of the control mixture. These results were confirmed by the statistical analysis. The control mixture (70CO) and the mixture containing 20% RAP (70-20RAP) were significantly different from the mixtures containing 20% RAP and 5% SHP, with or without UV light exposure (70-20RAP-5P-25°C and 70-20RAP-5P-48h).

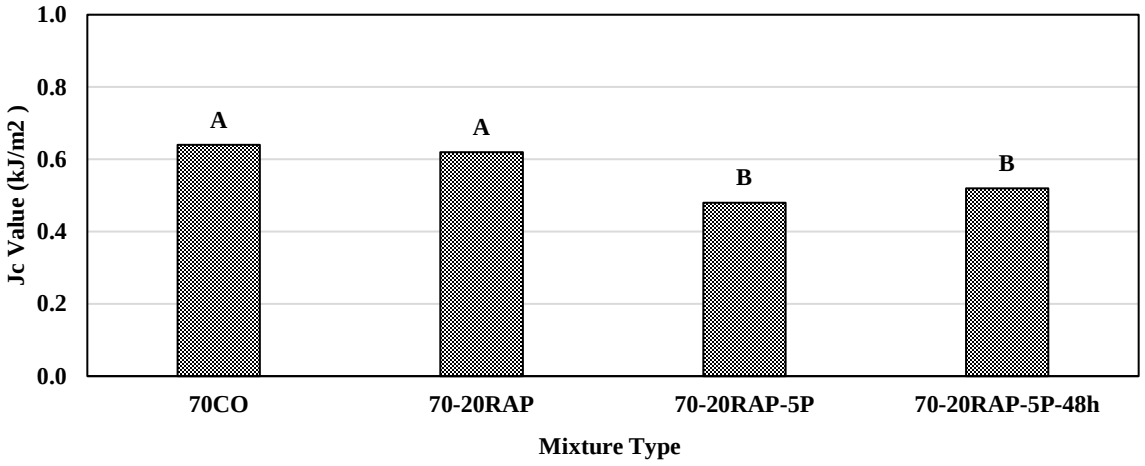

Figure 60. SCB results for PG 70-22M mixtures containing 20% RAP.

SCB Test Results for Mixtures Containing 5% RAS+ 20% RAP

PG 67-22 Mixtures: For the mixture containing both RAS and RAP (67-5RAS-5RAP), a Jc value of 0.48 kJ/m^2 was measured. The improved cracking performance can be related to the polymer in the recycled materials used in this study. The addition of SHP and the exposure to UV light did not have a significant effect on the performance of the mixtures.

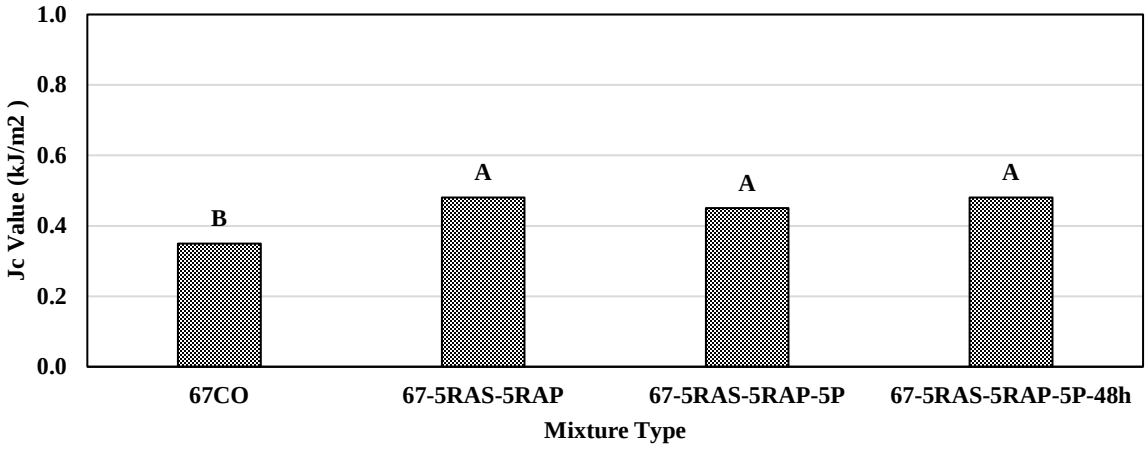

Figure 61. SCB results for PG 67-22 mixtures containing 5% RAS+ 20% RAP.

PG 70-22M Mixtures: Results from mixture with 5 RAS and 20% RAP, prepared with the polymer modified binder are presented in Figure 62. It can be stated that the addition of recycled materials resulted in a significant decrease in the measured J_c value. However, this decrease was recovered through the application of SHP and UV exposure.

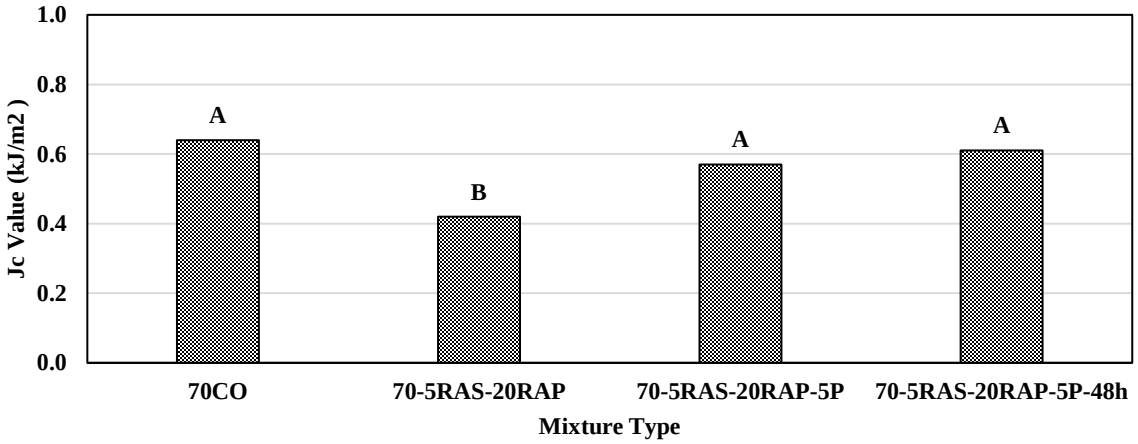

Figure 62. SCB results for PG 70-22M mixtures containing 5% RAS+ 20% RAP.

5.4.2. Loaded Wheel Tracking (LWT) Test Results

LWT Results for Mixtures Containing 5% RAS

PG 67-22 Mixtures: The loaded wheel-tracking test was used to evaluate the effects of recycled asphalt materials and SHP on the rutting performance of asphalt mixtures. Figure 63 presents the rut depth of the control mix (67CO), a mixture containing 5% RAS (67-5RAS), and a mixture containing 5% RAS and 5% SHP (67-5RAS-5P). Since the control mix has low stiffness, a large rut depth of 8.2 mm was measured. However, when aged and stiffened binder of RAS was added to the mixture, the rut depth decreased to 3.2mm. The use of 5% SHP increased the rut depth; however, the rut depth was below the failure criterion of 6mm. These results indicate that SHP can lead to a decrease in the mixture stiffness. Statistical analysis performed on the results shows that the addition of 5% RAS significantly enhanced the mix rutting performance. Furthermore, the use of 5% SHP led to a significant increase in rut depth.

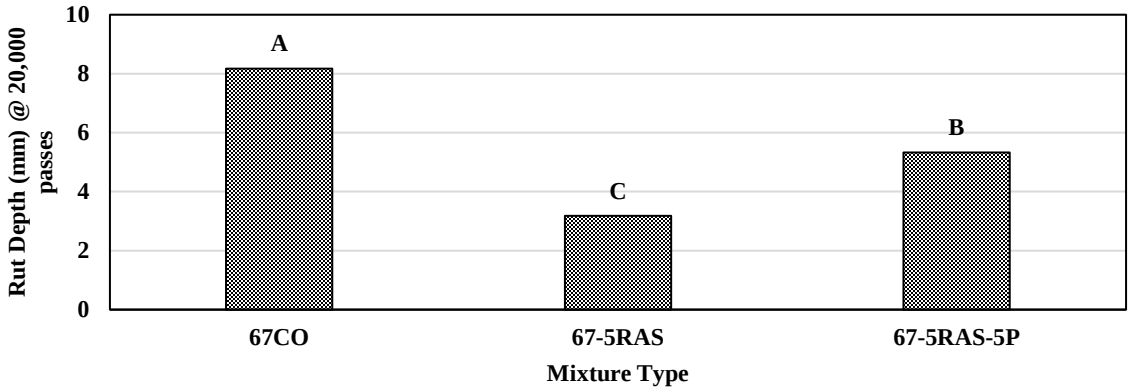

Figure 63. LWT results for PG 67-22 mixtures containing 5% RAS.

PG 70-22M Mixtures: PG 70-22M binder is a polymer-modified binder, which is known to enhance the mix rutting performance at high temperature. As shown in Figure 63, the control mixture prepared with PG 70-22M binder (70CO) had a lower rut depth compared to the mixture prepared with PG 67-22 (67CO) (Figure 64). The addition of 5% RAS decreased the rut depth even more as compared to the conventional mix. When 5% SHP was added to the mixture, the rut depth decreased to 2.1 mm. However, based on the results of the statistical analysis, changes caused by the addition of 5% RAS and 5% SHP to the mixture were insignificant.

LWT Results for Mixtures Containing 20% RAP

PG 67-22 Mixtures: Due to the presence of aged and hardened binder in the RAP, the rut depths of the mixtures were expected to decrease when 20% RAP was used in the mixtures. The addition of 5% SHP increased the rut depth of the mix to a value higher than the allowed rut depth of 6 mm. Based on these results, it was deduced that SHP application in mixtures prepared with an unmodified binder and recycled asphalt materials caused a decrease in stiffness of the mix and an increase in the rut depth. Furthermore, a statistical analysis was conducted on the LWT test results. Based on the results, 20% RAP and 5% SHP had both significant effects on the rutting performance of the asphalt mixture.

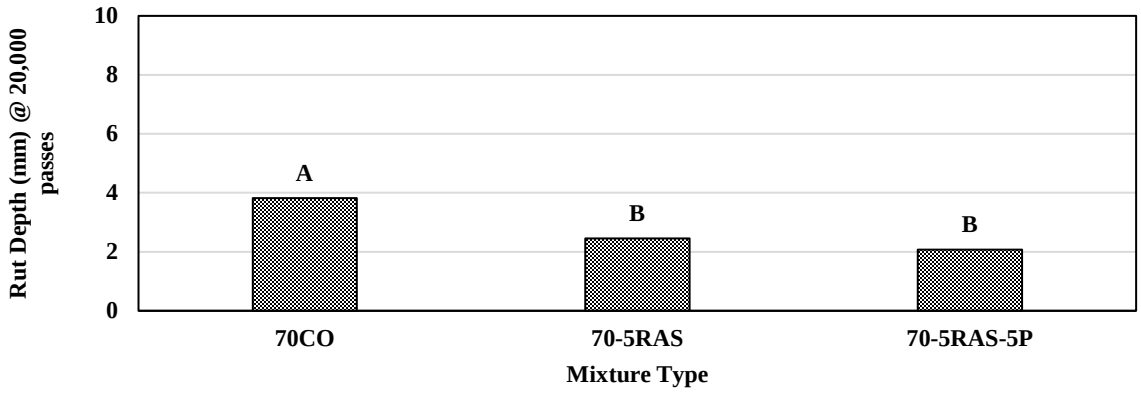

Figure 64. LWT results for PG 70-22M mixtures containing 5% RAS.

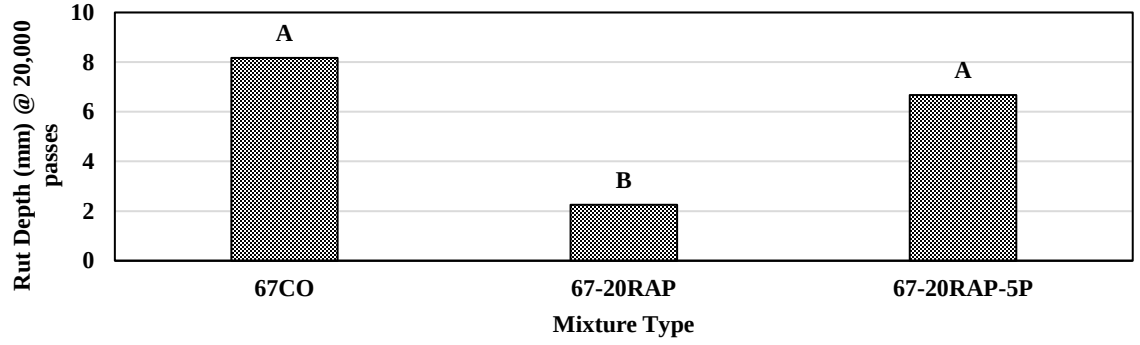

Figure 65. LWT results for PG 67-22 mixtures containing 20% RAP.

PG 70-22M Mixtures: The rut depths measured for the mixtures prepared using polymer modified binder (PG 70-22M), with or without 20% RAP and 5% SHP are presented in Figure 66. As shown in Figure 66, 20% RAP addition decreased the rut depth, while 5% SHP application increased the rut depth. However, it should be mentioned that the decrease caused by 20% RAP and the increase caused by 5% SHP were not statistically significant.

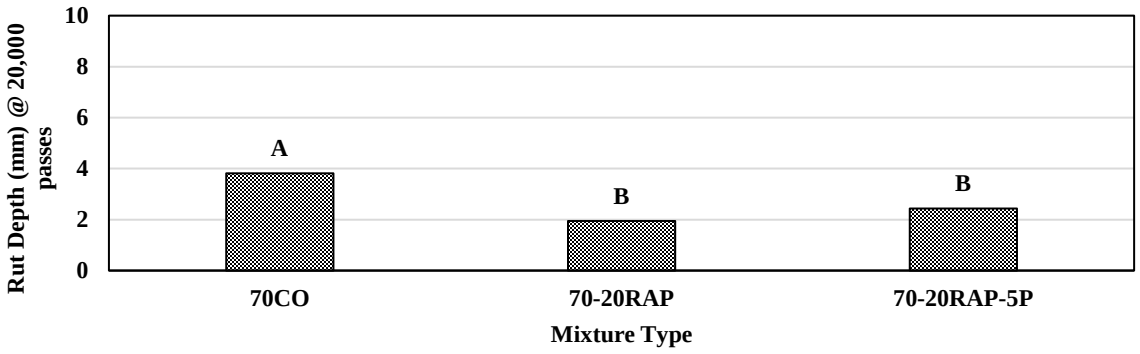

Figure 66. LWT results for PG 70-22M mixtures containing 20% RAP.

LWT Results for Mixtures Containing 5%RAS+ 20% RAP

PG 67-22 Mixtures: Figure 67 presents the measured rut depth for a mixture containing both 5%RAS and 20%RAP. The rut depth of the control mixture was decreased from 8.2 mm to 2.4 mm. This decrease was expected due to the incorporation of aged binder in the recycled materials. A further decrease was observed through the application of 5% SHP. However, based on the statistical analysis, the decrease was insignificant.

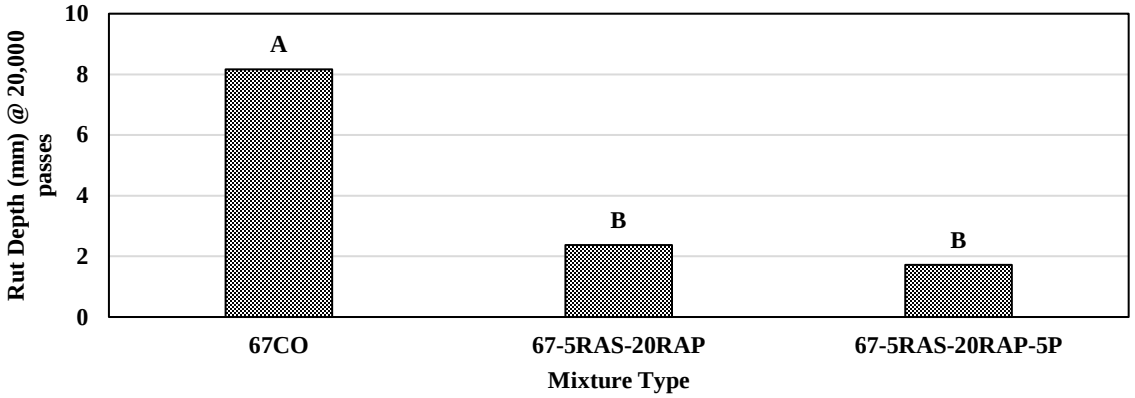

Figure 67. LWT results for PG 67-22 mixtures containing 5%RAS+ 20% RAP.

PG 70-22M Mixtures: The same trend was observed in PG 70-22M mixture; the addition of 5% RAS+20% RAP caused a decrease in the rut depth of the samples. However, in this case, the addition of 5% SHP led to an insignificant increase in the rut depth.

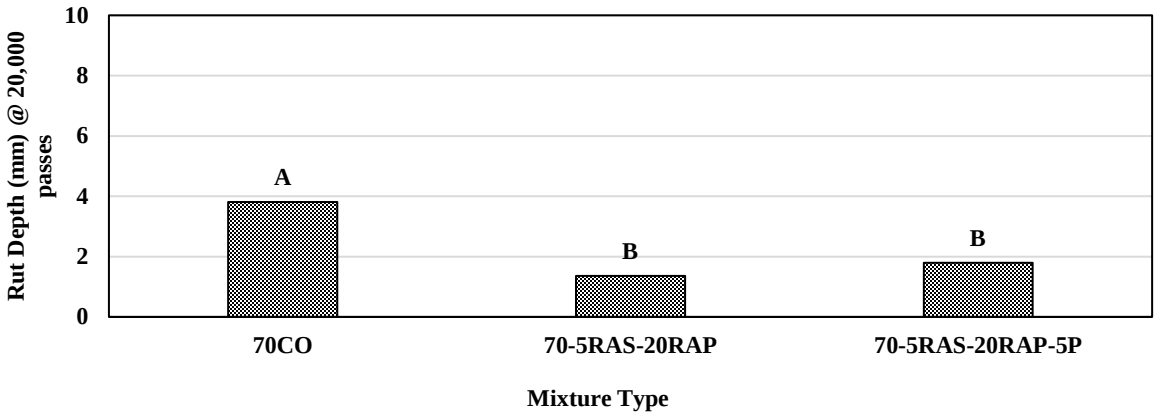

Figure 68. LWT results for PG 70-22M mixtures containing 5%RAS+ 20% RAP.

Moisture Susceptibility: Data obtained from LWT may also be used for assessing moisture susceptibility of the mix by measuring the stripping inflection point, which can be defined as the point where the slope of the rut lines begins to steepen. Figures 69 and 70 demonstrate the average permanent deformation of the various mixtures. Except for mixture 67CO, no stripping inflection points were detected, and it can be assumed that no moisture susceptibility was expected by LWT for the rest of the mixtures.

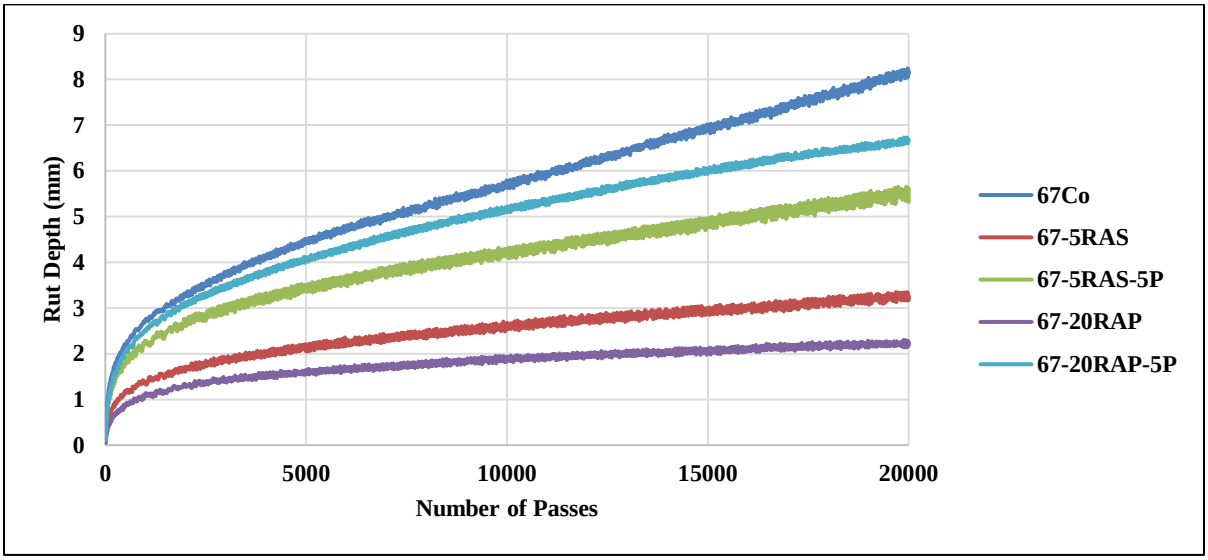

Figure 69. LWT rut depth vs. number of passes for PG 67-22 mixtures.

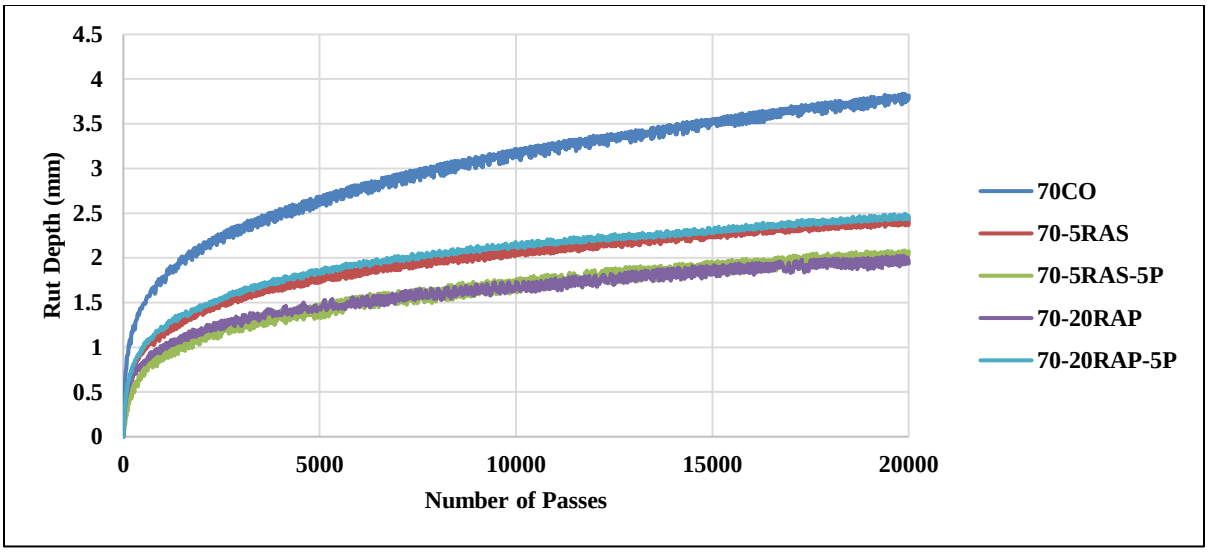

Figure 70. LWT rut depth vs. number of passes for PG 70-22M mixtures.

5.4.3. Thermal Stress Restrained Specimen Test (TSRST)

Low temperature cracking susceptibility of the asphalt mixtures was evaluated using TSRST. Tensile strength and temperature at fracture of samples were determined by measuring the tensile load while cooling the sample at a constant rate.

TSRST Results for Mixtures Containing 5% RAS

PG 67-22 Mixtures: TSRST test results for mixtures prepared using PG 67-22 binder, with or without 5% RAS and 5% SHP are presented in Figure 71. The addition of 5% RAS resulted in an increase in the fracture load and a decrease in the fracture temperature. Further increase in fracture load and a decrease in fracture temperature were observed with 5% SHP modification (Figure 71). Based on the statistical analysis, changes in fracture temperature, caused by the addition of 5% RAS and 5%SHP polymers were not statistically significant, while the increase in fracture load was significant.

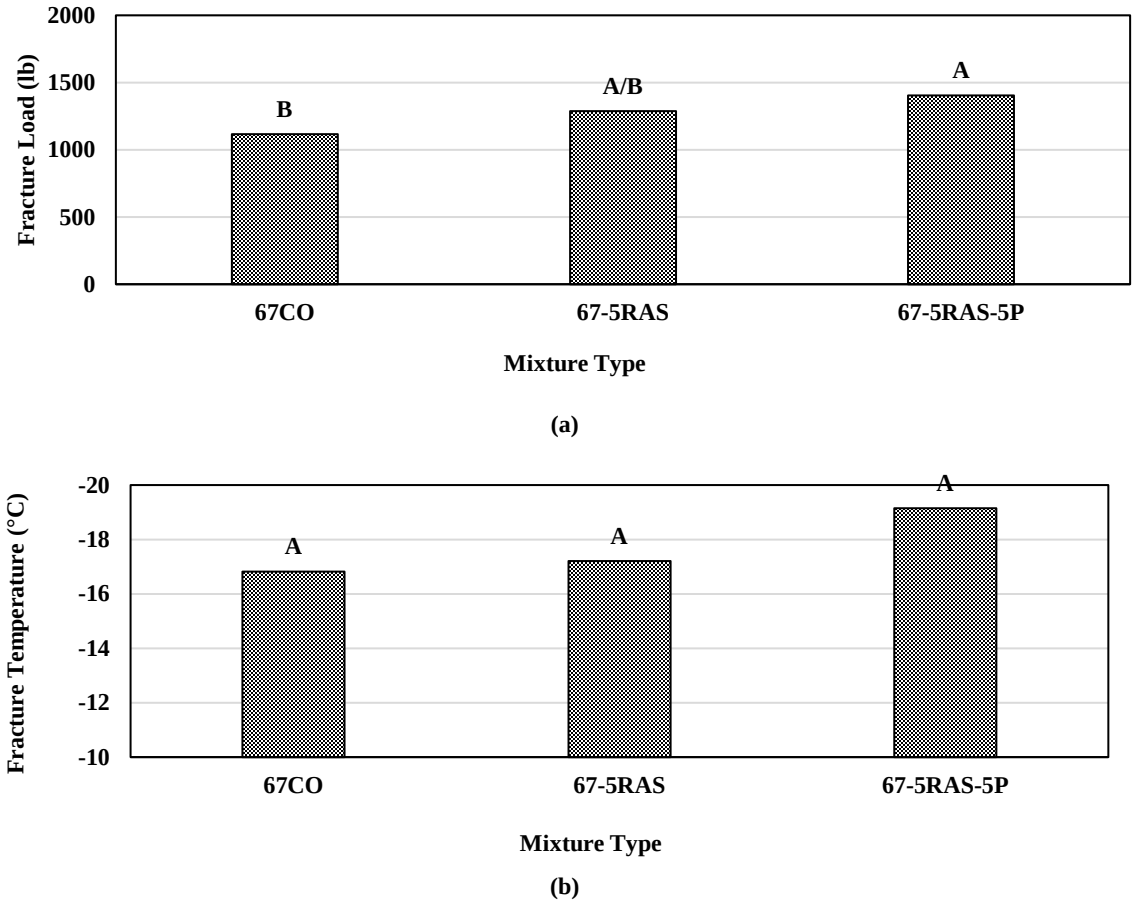

Figure 71. TSRST results for PG 67-22 mixtures containing 5% RAS: (a) Fracture load and (b) Fracture temperature.

PG 70-22M Mixtures: Figure 72 presents the fracture load and fracture temperature measured for mixtures prepared with a polymer-modified binder, with or without 5% RAS, and 5% SHP. When 5% RAS was added to the mixture, the fracture load increased due to the stiffening effect of RAS. An additional increase in load was observed with 5% SHP. Based on the statistical analysis, the addition of 5% RAS and 5% SHP significantly increased the fracture load. For the fracture temperature, the addition of 5% RAS caused an increase; however, the addition of 5% SHP resulted in a decrease in the fracture temperature. It should be noted that the changes in fracture temperature due to the addition of 5% RAS and 5% SHP were statistically insignificant.

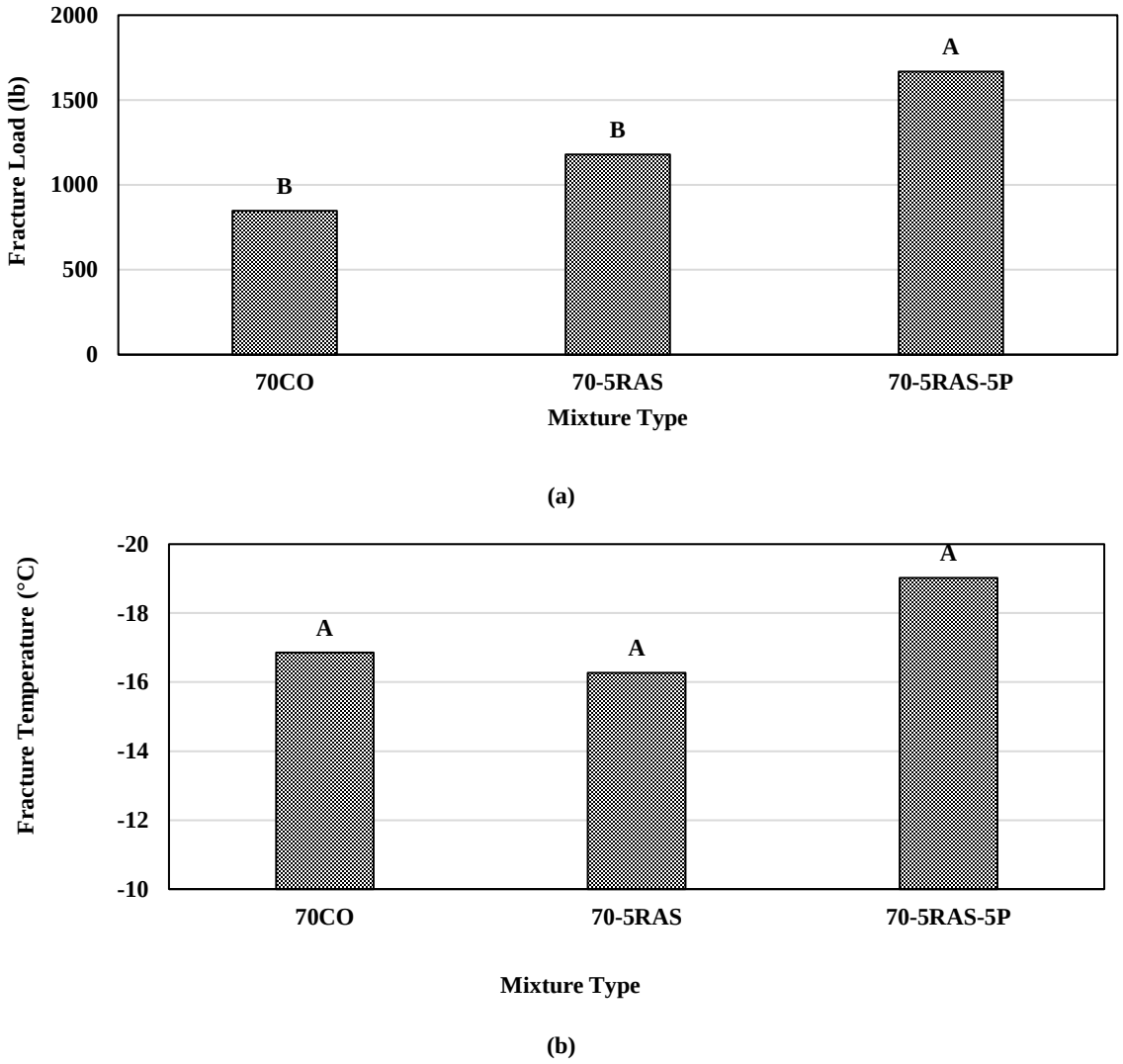

Figure 72. TSRST results for PG 70-22M mixtures containing 5% RAS: (a) Fracture load and (b) Fracture temperature.

TSRST Results for Mixtures Containing 20% RAP

PG 67-22 Mixtures: TSRST results for mixtures prepared with PG 67-22 binder, 20%RAP, and with or without SHP are presented in Figure 73. The addition of 20% RAP and the incorporation of 5% SHP led to an increase in the fracture load of the tested samples. Furthermore, the fracture temperature of the samples decreased with the addition of 20% RAP and 5% SHP. Based on the statistical analysis conducted, the use of 20% RAP and 5% SHP led to a significant improvement in the low temperature cracking performance of the mixes.

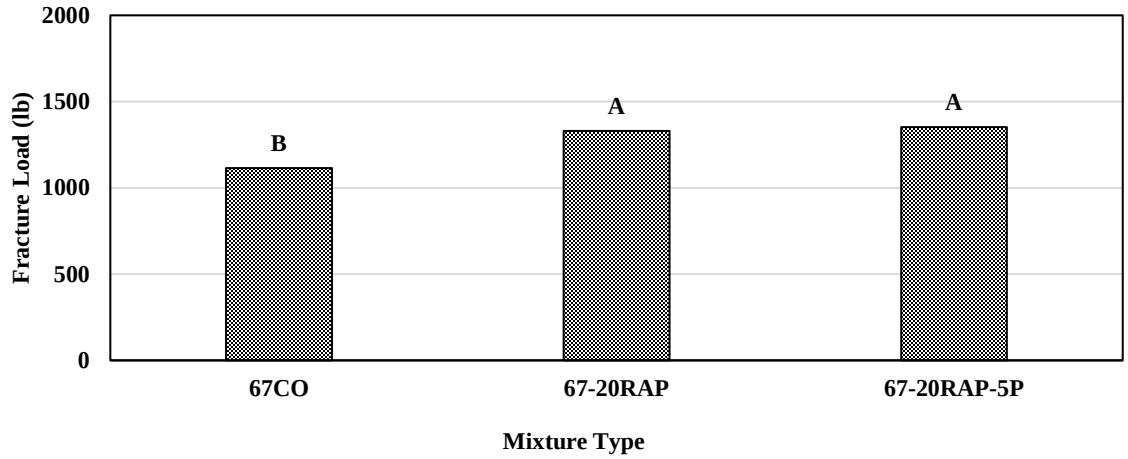

(a)

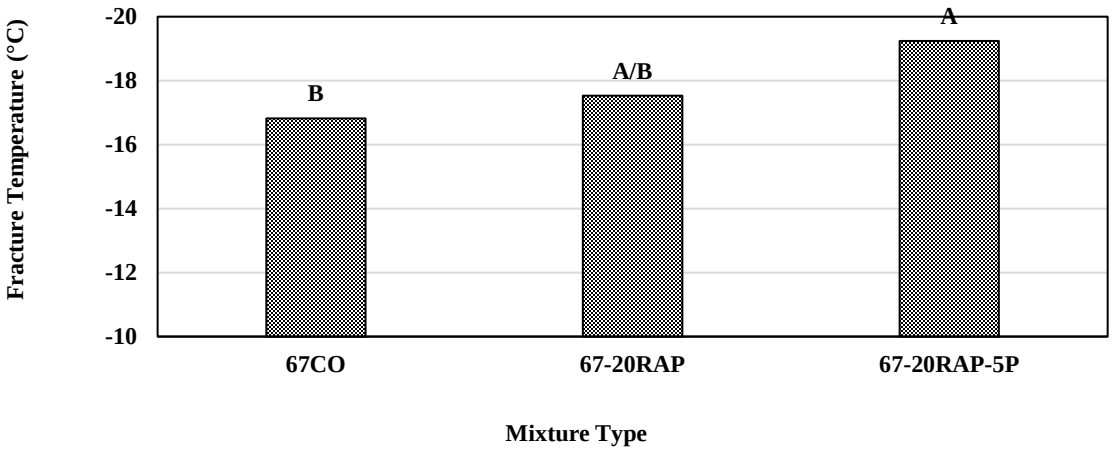

(b)

Figure 73. TSRST results for PG 67-22 mixtures containing 20% RAP: (a) Fracture load and (b) Fracture temperature.

PG 70-22M Mixtures: Results provided in Figure 74 presents the change in fracture load and fracture temperature of the asphalt mixtures when RAP and SHP were added to the mixture. The addition of 20% RAP and 5% SHP led to an increase in fracture load and a decrease in fracture temperature. However, based on the statistical analysis performed, 20% RAP and 5% SHP did not significantly affect the low temperature cracking performance of the mixtures.

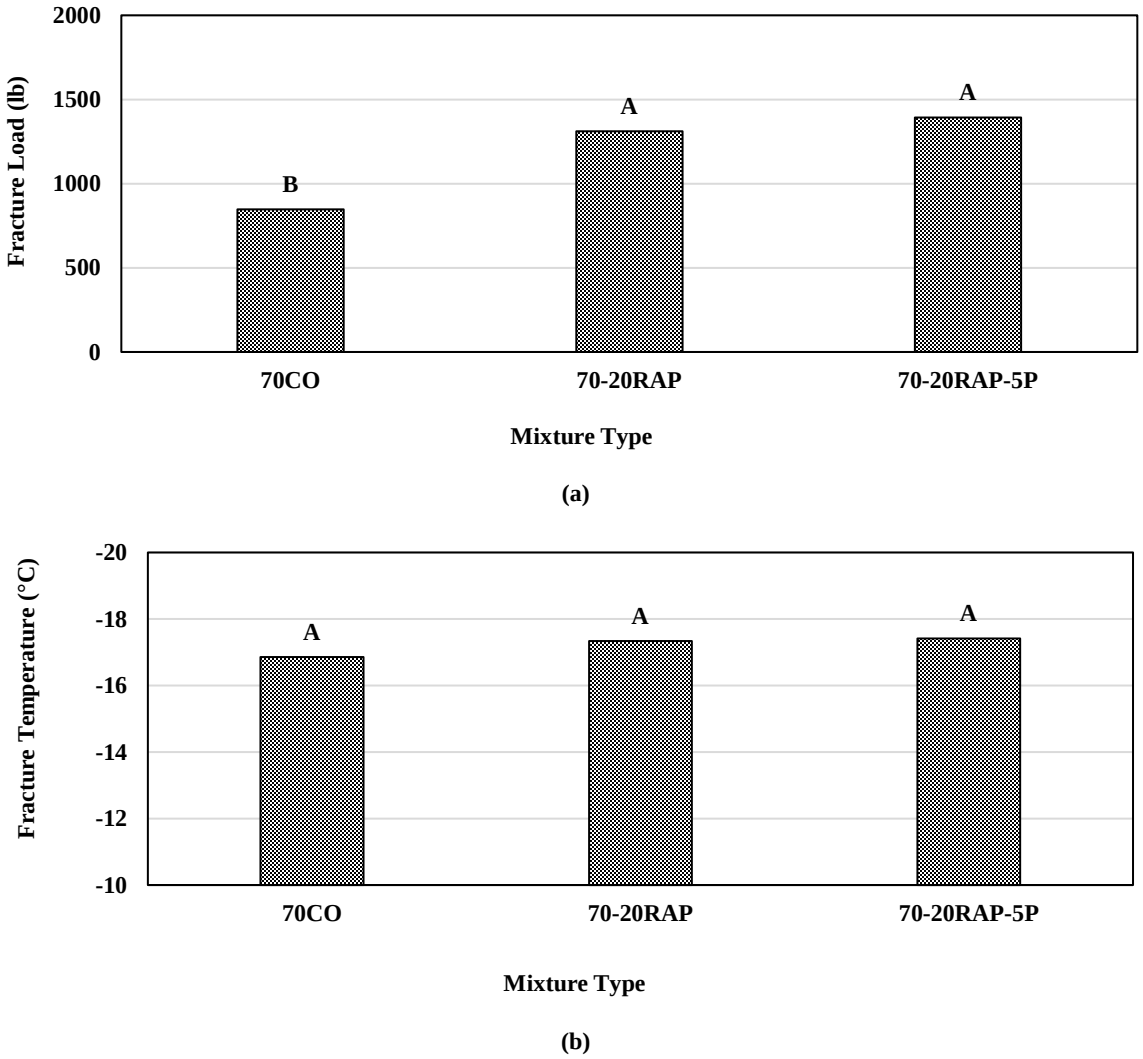

Figure 74. TSRST results for PG 67-22 mixtures containing 5% RAS+ 20% RAP: (a) Fracture load and (b) Fracture temperature.

TSRST Results for Mixtures Containing 5% RAS+ 20% RAP

PG 67-22 Mixtures: Figure 75 demonstrates the fracture load and fracture temperature for mixture with 5% RAS+ 20% RAP. Results show a decrease in both fracture load and temperature due to the addition of recycled materials; however, the decrease was statistically insignificant. The use of 5% SHP decreased the fracture load and increased the fracture temperature; however, the changes caused by SHP application were not significant.

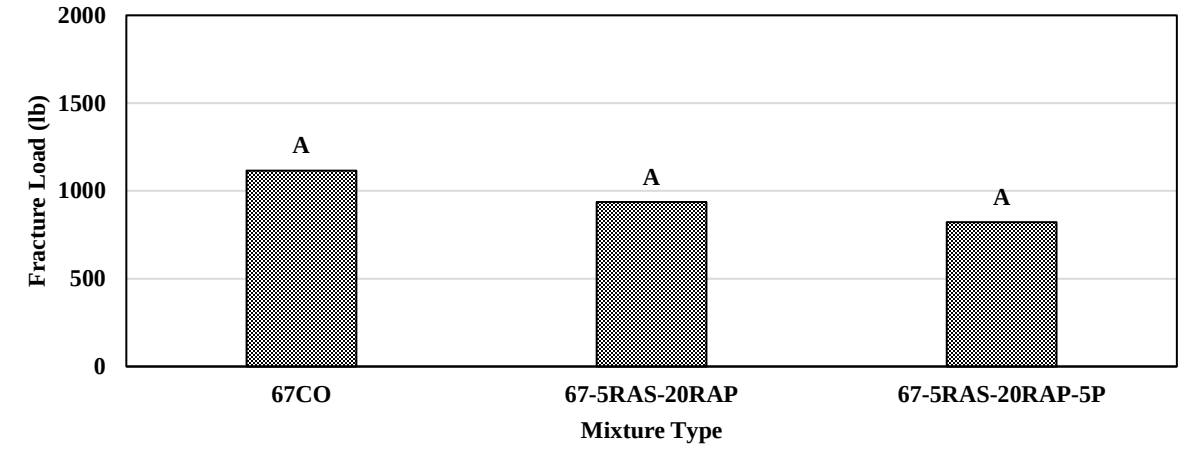

(a)

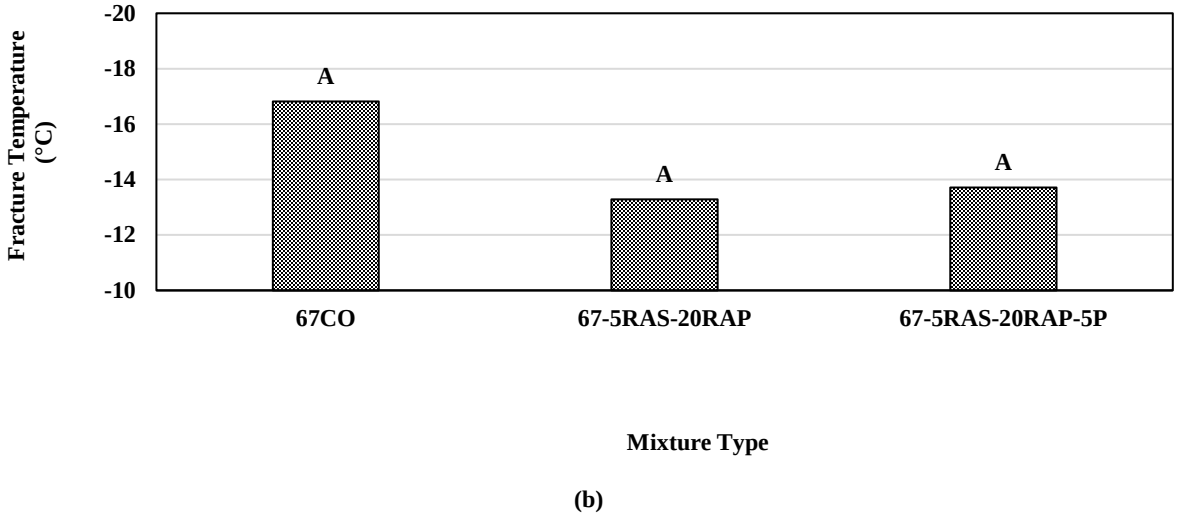

(b)

Figure 75. TSRST results for PG 70-22M mixtures containing 20% RAP: (a) Fracture Load and (b) Fracture temperature.

PG 70-22M Mixtures: The use of 5% RAS + 20% RAP negatively affected the cracking performance of the mixtures at low temperature. However, 5% SHP was able to improve mixtures performance. It should be mentioned that based on the statistical analysis performed, the performance of the all mixture at low temperature was the same.

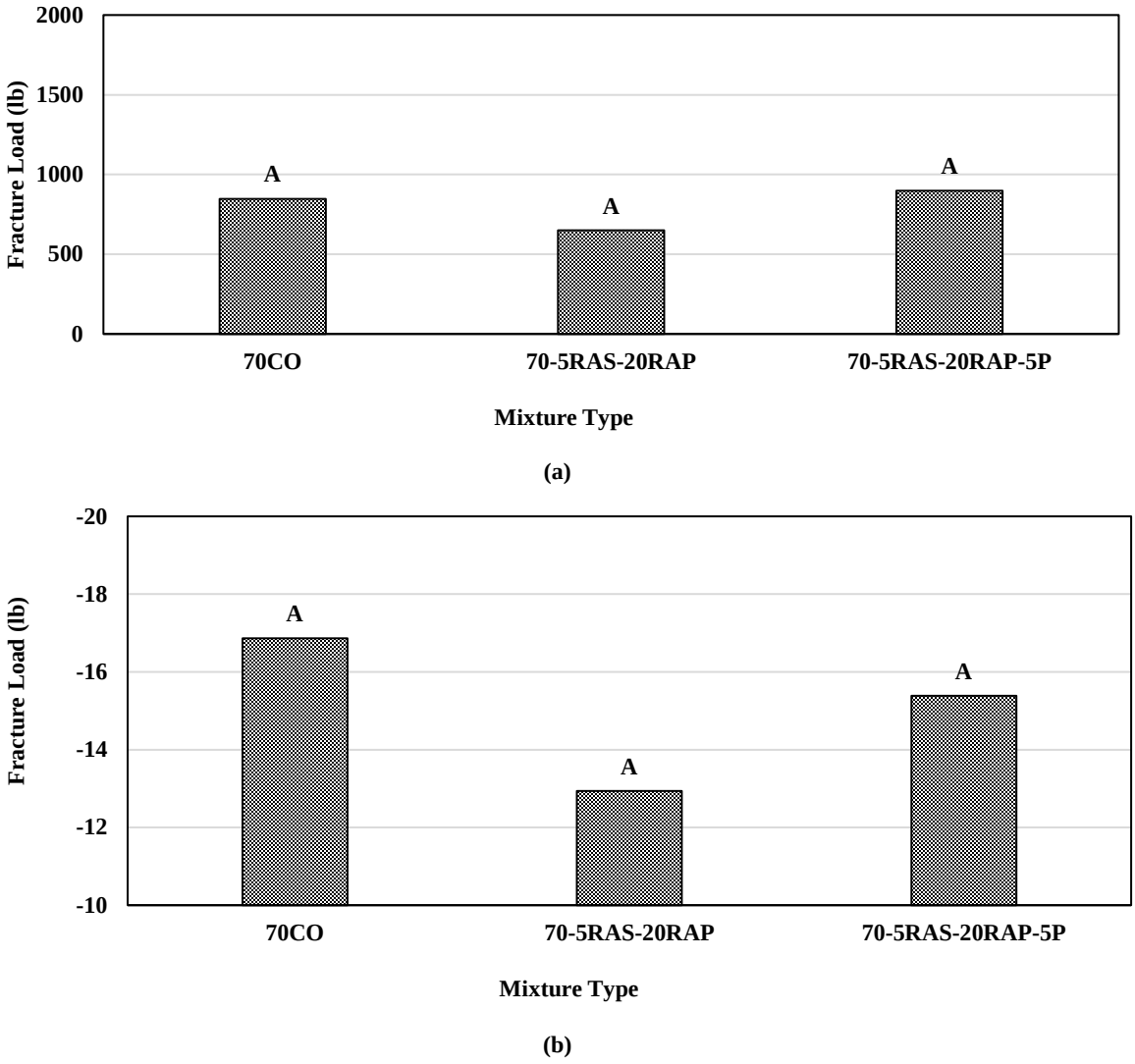

Figure 76. TSRST results for PG 70-22M mixtures containing 5% RAS+ 20% RAP: (a) Fracture Load and (b) Fracture temperature.

6. CONCLUSIONS

An innovative, light-activated, self-healing polymer was synthesized in the laboratory by means of a photocatalytic-based chemical method. The synthesis procedure of the self-healing polymers was evaluated using FTIR spectroscopy, while the thermal stability was analyzed by means of TGA. In addition, the effect of the light activated self-healing polymer on the rheological properties of asphalt binders was evaluated. Laboratory performance tests were also used to evaluate the cracking resistance at intermediate temperature, permanent deformation at high temperature, and cracking resistance at low temperature. Finally, self-healing properties of the mixtures were studied through fracture energy measurements and crack width monitoring. Based on the results of this study, the following conclusions may be drawn:

With respect to the synthesis of the self-healing polymers:

- The FTIR analysis confirmed the successful synthesis of cross-linked networks of OXE-CHI-PUR polymer in the laboratory. In addition, TGA results showed that the synthesized polymers achieved the required thermal stability to resist asphalt mixture production processes.

With respect to the effects of self-healing polymers on the binder rheological properties:

- HP-GPC results showed that asphaltenes/maltenes ratios of the binder blends were increased through the addition of recycled materials. Furthermore, self-healing polymer incorporation led to a further increase in the ratio, causing a higher stiffness.
- FTIR results showed that the addition of recycled materials led to an increase in stiffness. The measured indices further increased due to the addition of 5% SHP and the loss of oily fractions.
- Viscosity results showed that the addition of 5% RAS and/or 20% RAP led to an increase in the viscosity of the binder blends. However, a reduction in viscosity of the binder blends containing recycled asphalt materials was observed when adding self-healing polymers.
- Performance grading results showed an increase in the high-temperature grade of the binder blends containing recycled asphalt materials and recycled asphalt materials with SHP. However, the low-temperature grade was the same for all tested binder blends.
- The difference between the critical stiffness temperature and the m-value critical temperature (Delta Tc) showed an improvement at low service temperature for samples with 5% SHP when exposed to UV light.
- Based on the results of the MSCR test, the elastic behavior of the unmodified binder improved with the use of SHP. However, for modified binders, the percent recovery decreased by increasing the contents of SHP.
- The master curves showed that the addition of self-healing polymer to the virgin binder has an insignificant effect on the stiffness of the binder at various temperatures. However, the addition of recycled materials and self-healing polymer to PG 67-22 binder blends resulted in an increase in the stiffness at high frequency (low-temperature), while a decrease was observed at low frequency (high-temperature). The same behavior was observed with PG 70-22M containing 5% RAS, while the opposite trend was observed in PG 70-22M with 20% RAP and 5% RAS+20% RAP as an increase in stiffness was observed at low frequency and a decrease at high frequency.

- LAS showed that self-healing polymer improved the fatigue performance of the unmodified binder; however, when it was added to the binder blend containing recycled materials, negative effects were observed. Self-healing polymer addition to modified binder (PG 70-22M) resulted in a decrease in the N_f.

With respect to the effects of self-healing polymers on the mixture properties:

- SCB test results showed that the addition of recycled asphalt material negatively affected the cracking performance of the mixtures. However, incorporation of SHP and 48h of UV light exposure improved the cracking resistance. This behavior was more evident with mixtures prepared with unmodified binder.
- LWT test results showed that the addition of the self-healing polymer caused an increase in the rut depth of the samples prepared with unmodified binder in this study. However, the final rut depth was less than 6 mm, which is an acceptable rutting performance.
- TSRST test results showed that the addition of 5% RAS negatively affected the low temperature cracking performance of the mix. In contrast, 5% SHP enhanced the low temperature cracking performance of the mix by increasing the fracture load and decreasing the fracture temperature.

With respect to healing efficiency and strength recovery:

- As it was expected, the addition of recycled asphalt materials to mixtures prepared with an unmodified binder (PG 67-22) negatively affected the healing recovery at room temperature. RAS addition also deteriorated the self-healing properties of PG 70-22M mixture, while in some cases, RAP application resulted in improved properties. Self-healing properties of the mixtures were improved by increasing the curing condition temperature from 25°C to 50°C, which confirms the temperature dependency of the self-healing properties of the asphalt mixtures.
- The addition of 5% Self-healing polymer to the control mixture, followed by 48h of UV light exposure resulted in an increase in self-healing properties of the mixtures prepared with PG 67-22 binder. The highest healing recovery ratio (84%) was observed for mixtures prepared without recycled asphalt materials, containing 5% self-healing polymer, and exposed to UV light. On the other hand, the addition of self-healing polymer to PG 70-22M mixture resulted in a reduction in healing efficiency, which can be due to unwanted interactions of polyurethane in the self-healing polymer with SBS in the binder.

7. RECOMMENDATIONS

Based on the outcome of this study, the authors recommend conducting further research prior to implementing the developed SHP in practice. It is recommended to conduct further chemical analysis on the produced SHP and binder blends prepared with a virgin binder, and with or without recycled asphalt materials and SHP. In addition, softer binders (e.g., PG 58-22), and RAP and RAS from various sources should be used to evaluate SHP and their effects on the rheological properties of the binders and their enhancement of the mechanical properties of the mixtures. In addition, the possibility of using self-healing polymers in combination with other polymers should be investigated to avoid undesirable interaction between the polymer-modified binder and SHP. Finally, monitored field-testing is recommended to evaluate the performance of asphalt mixtures with SHP in a full-scale environment.

REFERENCES

1. Petersen, J. C., Harnsberger, P. M. and Robertson, R.E. 1996. ″Factors Affecting the Kinetics and Mechanisms of Asphalt Oxidation and the Relative Effects of Oxidation Products on Age Hardening.″ American Chemical Society Division of Fuel Chemistry, Preprints, 41(4), pp. 1232-1244.

2. Petersen, J. C. and Harnsberger, P.M. 1998. ″Asphalt Aging: Dual Oxidation Mechanism and Its Interrelationships with Asphalt Composition and Oxidative Age Hardening). ″ Transportation Research Board, No. 1638, pp. 47-55.

3. Zaumanis, M., Mallick, R., Poulikakos, L., Frank, R. ″Influence of six rejuvenators on the performance properties of Reclaimed Asphalt Pavement (RAP) binder and 100% recycled asphalt mixtures.″ Construction and Building Materials 71 (2014) 538–550.

4. Oldham, D., Fini, E., Chailleux, E. ″Application of a bio-binder as a rejuvenator for wet-processed asphalt shingles in pavement construction.″ Construction and Building Materials 86 (2015) 75–84.

5. Yildirim, Y. ″Polymer modified asphalt binders.″ Construction and Building Materials 21 (2007) 66–72.

6. Qiu, J., Ven, V., Wu, S., Yu, J. ″Investigation of self-healing behavior of asphalt mixes using the beam on elastic foundation setup.″ Materials and Structures, May 2012, volume 45, Issue 5, pp 777–791.

7. Ghosh, B., Chellappa, V., Urban, W. M. 2011. ″Self-healing inside a scratch of oxetane substituted chitosan-polyurethane networks.″ Journal of materials chemistry, 21, 14473.

8. Liseane Padilha Thives, Enedir Ghisi. 2017. “Asphalt mixtures emission and energy consumption: A review.” Renewable and Sustainable Energy Reviews 72 (2017) 473–484.

9. “Pavement sustainability.” OCTOBER 2014 FHWA-HIF-14-012

10. Santero, N. J. 2009. Pavements and the Environment: A Life-Cycle Assessment Approach. Ph.D. dissertation. University of California, Berkeley, CA.

11. “Use of Reclaimed Asphalt Pavement and Recycled Asphalt Shingles in Asphalt Mixtures: A Synthesis of Highway Practice.” NCHRP SYNTHESIS 495.

12. Willis, J. R. 2016. “Characterization of Asphalt Binder Extracted From Reclaimed Asphalt Shingles.” National Center for Asphalt Technology.

13. Zaumanis , M., Mallick, R.B. 2015. “Review of very high-content reclaimed asphalt use in plant-produced pavements: state of the art.” International Journal of Pavement Engineering, 2015 Vol. 16, No. 1, 39–55, Journal of Pavement Engineering (http://dx.doi.org/10.1080/10298436.2014.893331).

14. Waymen, M., et al., 2012. Life cycle assessment of reclaimed asphalt. european commission. WP3.2. Sponsored by European Commission, Grant SCP7-GA-2008-218747.

15. Copeland, A., 2011. Reclaimed asphalt pavement in asphalt mixtures: state of the practice. McLean, VA: Turner-Fairbank Highway Research Center, Report Number FHWA-HRT-11-021.

16. EAPA, 2012. Asphalt in figures [online]. Available from: EAPA Asphalt (http://eapa.org/usr_img/Asphalt%20in%20figures%20Version%) 2022-12-2011.pdf [Accessed: 3 Mar 2012].

17. West, R., et al., 2011. “A comparison of virgin and recycled asphalt pavements using long-term pavement performance SPS-5 data. In: Transportation research board 90th annual 54 M. Washington, DC: Transportation Research Board, Paper No. 22-3865.

18. Copeland, A., Hansen, K. R. 2016. “Asphalt Pavement Industry Survey on Recycled Materials and Warm-Mix Asphalt Usage.” Information Series 138 (7th edition).

19. Ongel, A., Hugener, M. Impact of rejuvenators on aging properties of bitumen. Construction and Building Materials 94 (2015) 467–474.

20. Yaghoubi, E., Ahadi, M.R., Alijanpour Sheshpoli, M., Jahanian Pahlevanloo, H. (2013).Evaluating the Performance of Hot Mix Asphalt with Reclaimed Asphalt Pavement and Heavy Vacuum Slops as Rejuvenator. International Journal of Transportation Engineering, Vol.1/ No.2.

21. Mogawer, W.S., Booshehrian, A., Vahidi, S., Austerman, A.J. (2013). Evaluating the effect of rejuvenators on the degree of blending and performance of high RAP, RAS, and RAP/RAS mixtures. Road Materials and Pavement Design. Vol. 14, No. S2, 193–213.

22. Grzybowski K.F. Recycled asphalt roofing materials - A multifunctional low cost hot – mix asphalt pavement additive. Use of waste materials in hot-mix asphalt, ASTM STP-1193; 1993. p. 159–79.

23. Button J.W, Williams D, Scherocman J A. Roofing shingles and toner in asphalt pavements. Texas Department of Transportation. Report No. FHWA/TX-96/ 1344-2F, 1995

24. Carpenter S, Wolosick J. Modifier influence in the characterization of hot-mix recycled material. Washington, DC: Transportation Research Record 777, TRB; 1980. p. 15–22.

25. Im, S., and Zhou, F. (2014). "Field Performance of RAS Test Sections and Laboratory Investigation of Impact of Rejuvenators on Engineering Properties of RAP/RAS Mixes." Texas A&M Transportation Institute, FHWA/TX-14/0-6614-3.

26. Martins Zaumanis, Rajib B. Mallick, Robert Frank, 100% recycled hot mix asphalt: a review and analysis, Resour. Conserv. Recycl. 92 (2014) 230–245.

27. Martins. Zaumanis, Rajib B. Mallick, Lily. Poulikakos, Robert. Frank, Influence of six rejuvenators on the performance properties of reclaimed asphalt pavement (RAP) binder and 100% recycled asphalt mixtures, Constr. Build. Mater. 71 (2014) 538–550.

28. Aybike Ongel, Martin Hugener, Impact of rejuvenators on aging properties of bitumen, Constr. Build. Mater. 94 (2015) 467–474.

29. Baaj, H., Moghaddam. T. B. (2016). The use of rejuvenating agents in production of recycled hot mix asphalt: A systematic review. Construction and Building Materials 114 (2016) 805–816.

30. M. Simonen, T. Blomberg, T. Pellinen, J. Valtonen, Physicochemical properties of bitumens modified with bioflux, Road Mater. Pavement Des. 14 (2012) 36–48

31. Dongliang Kuang, Jianying Yu, Huaxin Chen, Zhengang Feng, Rui Li, Hui Yang, Effect of rejuvenators on performance and microstructure of aged asphalt, J. Wuhan Univ. Technol. Mater. Sci. Ed. 29 (2014) 341–345.

32. Junan Shen, Serji Amirkhanian, Boming Tang, Effects of rejuvenator on performance-based properties of rejuvenated asphalt binder and mixtures, Constr. Build. Mater. 21 (2007) 958–964.

33. Hallizza Asli, Esmaeil Ahmadinia, Majid Zargar, Mohamed Rehan Karim, Investigation on physical properties of waste cooking oil – rejuvenated bitumen binder, Constr. Build. Mater. 37 (2012) 398–405.

34. M.N. Borhan, F. Suja, A. Ismail, R. Rahmat, The effects of used cylinder oil on asphalt mixes, Eur. J. Sci. Res. 28 (2009) 389–411.

35. Zhu, J. Birgisson, B., Kringos, N. 2014. “Polymer modification of bitumen: Advances and challenges.” European Polymer Journal 54 (2014) 18–38.

36. Qiu, J., Ven, V., Wu, S., Yu, J. ″Investigation of self-healing behavior of asphalt mixes using beam on elastic foundation setup.″ Materials and Structures, May 2012, Volume 45, Issue 5, pp 777−791.

37. Tabakovic . A., Schlangen . E. 2015. “Self-Healing Technology for Asphalt Pavements.” Adv Polym Sci. DOI: 10.1007/12_2015_335.

38. Qiu J et al (2009) Investigation of self-healing capability of bituminous binders. Road Mater Pavement Design 10(1):81–94, Special Issue on Asphalt Materials (ICAM 2009—China).

39. Fang C et al (2013) Nanomaterials applied in asphalt modification: a review. J Mater Sci Technol 29(7):589–594.

40. Liu Q (2012) Induction healing of porous asphalt concrete. Ph.D. thesis, Faculty of Civil Engineering and Geosciences, TU Delft, The Netherlands.

41. Aguirre. M.A., Hassan. M., Shirzad. S., Daly. W. H., Mohammad. L. N. (2016). "Micro-encapsulation of asphalt rejuvenators using melamine-formaldehyde." Construction and Building Materials 114 (2016) 29–39.

42. Yang. Y., Urban. Marek. 2013. "Self-healing polymeric materials." hem. Soc. Rev., 2013, 42, 7446.

43. "Chitin and chitosan: Properties and applications." Prog. Polym. Sci. 31 (2006) 603–632. Marguerite Rinaudo.

44. "Chitosan: An Update on Potential Biomedical and Pharmaceutical Applications." Marine Drugs 2015, 13, 5156-5186; doi:10.3390/md13085156. Randy Chi Fai Cheung, Tzi Bun Ng, Jack Ho Wong and Wai Yee Chan.

45. Li, R., Chen, J., Zhou, T., Pei. J. 2016. "Preparation and characterization of novel light induced self-healing materials for cracks in asphalt pavements." Construction and Building Materials 105 (2016) 336–342.

46. Louisiana Standard Specifications for Roads and Bridges. Louisiana Department of Transportation and Development, Baton Rouge, 2006.

47. AASHTO. (2014). "Standard Method of Test for Quantitative Extraction of Asphalt Binder from Hot Mix Asphalt (HMA)." AASHTO T 164, Washington, DC.

48. AASHTO. (2014). Standard Specification for Recovery of Asphalt Binder from Solution by Abson Method." AASHTO R 59, Washington, DC.

49. Daly, William H., Negulescu, Ioan., Balamurugan, Sreelatha S. 2013. Implementation of GPC Characterization of Asphalt Binders at Louisiana Materials Laboratory. FHWA/LA.13/505.

50. Cooper, Samuel B., Negulescu, Ioan., Balamurugan, Sreelatha S., Mohammad, Louay Daly, William H., Baumgardner, Gaylon L. 2017. Asphalt mixtures containing RAS and/or RAP: Relationships amongst binder composition analysis and mixture intermediate temperature cracking performance. Road Materials and Pavement Designs. 10.1080/14680629.2015.1266758.

51. AASHTO. (2013). "Effect of Heat and Air on a Moving Film of Asphalt (Rolling Thin-film Oven Test)." AASHTO T 240, Washington, DC.

52. AASHTO. (2016). "Accelerated Aging of Asphalt Binder Using a Pressurized Aging Vessel (PAV)." AASHTO R 28-12, Washington, DC.

53. AASHTO. (2013). "Standard Method of Test for Viscosity Determination of Asphalt Binder Using Rotational Viscometer." AASHTO T 316, Washington, DC.

54. AASHTO. (2016). ″Determining the Rheological Properties of Asphalt Binder Using a Dynamic Shear Rheometer (DSR).″ AASHTO T 315-12, Washington, DC.

55. AASHTO. (2-16) ″Determining the Flexural Creep Stiffness of Asphalt Binder Using the Bending Beam Rheometer (BBR).″ AASHTO T 313-12, Washington, DC.

56. AASHTO. (2015). ″Standard Practice for Grading or Verifying the Performance Grade of an Asphalt Binder.″ AASHTO R 29, Washington, DC.

57. AASHTO. (2015). ″Standard specification for performance-graded for asphalt binder.″ AASHTO M320, Washington, DC.

58. AASHTO. (2014). ″Standard Specification for Performance-Graded Asphalt Binder Using Multiple Stress Creep Recovery (MSCR) Test.″ AASHTO M332-14, Washington, DC.

59. Sabouri, M., Mirzaiyan, D., Moniri, A. (2018). "Effectiveness of Linear Amplitude Sweep (LAS) asphalt binder test in predicting asphalt mixtures fatigue performance." Construction and Building Materials 171 (2018) 281–290.

60. AASHTO. (2015). ″Standard Practice for Superpave Volumetric Design for Hot Mix Asphalt.″ AASHTO R35-09, Washington, DC.

61. AASHTO. (2015). ″Standard Specification for Superpave volumetric Mix design.″ AASHTO M 323-07, Washington, DC.

62. ASTM. (2016). "Evaluation of Asphalt Mixture Cracking Resistance using the Semi-Circular Bend Test (SCB) at Intermediate Temperatures", ASTM 8044.

63. AASHTO. ″Standard Test Method for Thermal Stress Restrained Specimen Tensile Strength.″ AASHTO TP 10-93, Washington, DC.

64. Mazumder. M., Kim. H., Lee. S. J. (2016). "Performance properties of polymer modified asphalt binders containing wax additives." International Journal of Pavement Research and Technology 9 (2016) 128–139.

65. Rowe. G. M., King. G., Anderson. M. (2014). "The Influence of Binder Rheology in the Cracking of Asphalt Mixes in Airport and Highway Projects." Journal of Testing and Evaluation. DOI: 10.1520/JTE20130245.

66. Nasra. D., Pakshirb., A., H. (2017). "Rheology and storage stability of modified binders with waste polymers composites." Road Materials and Pavement Design, Road Materials and Pavement Design (https://doi.org/10.1080/14680629.2017.1417152).

APPENDIX A: PG-GRADING RESULTS

Table A1. PG-Grading results for PG 67-22 binder blends+5%SHP.

Test	Specification	Temperature	67CO	67PG1SHP	67PG3SHP	67PG5SHP
RV at 20 rpm	<3.0 Pa.s	135 ºC	527 mPa.s	498 mPa.s	447 mPa.s	445 mPa.s
DSR (G*/sinδ) on Original Binder	>1.0 kPa	64 ºC	1.92 kPa	1.90 kPa	2.15 kPa	2.23 kPa
DSR (G*/sinδ) on Original Binder	>1.0 kPa	70 ºC	0.88 kPa	0.882 kPa	1.01 kPa	1.06 kPa
DSR (G*/sinδ) on Original Binder	>1.0 kPa	76 ºC	-	-	0.511 kPa	0.665 kPa
DSR (G*/sinδ) on RTFO	>2.2 kPa	64 ºC	3.75 kPa	4.01 kPa	4.05 kPa	4.13 kPa
DSR (G*/sinδ) on RTFO	>2.2 kPa	70 ºC	1.68 kPa	1.71 kPa	1.75 kPa	1.82 kPa
DSR (G^*./sinδ) on RFTO+PAV	<5000 kPa	25 ºC	3920 kPa	3650 kPa	3660 kPa	3680 kPa
DSR (G^*./sinδ) on RFTO+PAV	<5000 kPa	22 ºC	5795 kPa	5300 kPa	5360 kPa	5390 kPa
BBR-S on RFTO+PAV	<300 MPa	-6	92.05 Mpa	95 Mpa	96 Mpa	102 Mpa
BBR-S on RFTO+PAV	<300 MPa	-12	197 Mpa	226 Mpa	226 Mpa	227 Mpa
BBR-S on RFTO+PAV	<300 MPa	-18	351 Mpa	423 Mpa	424 Mpa	425 Mpa
BBR-m on RFTO+PAV	>0.3	-6	0.374	0.385	0.383	0.377
BBR-m on RFTO+PAV	>0.3	-12	0.312	0.316	0.318	0.312
BBR-m on RFTO+PAV	>0.3	-18	0.268	0.259	0.265	0.264
PG- Grading	--------	--------	**64-22**	**64-22**	**70-22**	**70-22**

Table A2. PG-Grading results for PG 67-22 binder blends+5%RAS+5%SHP.

Test	Specification	Temperature	67CO	67-5RAS	67-5RAS1SHP	67-5RAS3SHP	67-5RAS-5P
RV at 20 rpm on Original Binder	<3.0 Pa.s	135 ºC	527 mPa.s	922 mPa.s	944 mPa.s	901 mPa.s	842 mPa.s
DSR (G*/sinδ) on Original Binder	>1.0 kPa	64 ºC	1.92 kPa	2.73 kPa	2.39 kPa	2.60 kPa	2.66 kPa
DSR (G*/sinδ) on Original Binder	>1.0 kPa	70 ºC	0.88 kPa	1.24 kPa	1.10 kPa	1.21 kPa	1.24 kPa
DSR (G*/sinδ) on Original Binder	>1.0 kPa	76 ºC	-	0.61 kPa	0.53 kPa	0.61 kPa	0.63 kPa
DSR (G*/sinδ) on RTFO	>2.2 kPa	64 ºC	3.75 kPa	-	5.02 kPa	5.15 kPa	5.49 kPa
DSR (G*/sinδ) on RTFO	>2.2 kPa	70 ºC	1.68 kPa	2.55 kPa	2.26 kPa	2.30 kPa	2.45 kPa
DSR (G*/sinδ) on RTFO	>2.2 kPa	76 ºC	-	1.21 kPa	1.08 kPa	1.09 kPa	1.15 kPa
DSR (G^*.sinδ) on RFTO+PAV	<5000 kPa	25 ºC	3920 kPa	4885 kPa	4150 kPa	4150 kPa	4170 kPa
DSR (G^*.sinδ) on RFTO+PAV	<5000 kPa	22 ºC	5795 kPa	6925 kPa	5855 kPa	5850 kPa	5950 kPa
BBR-S on RFTO+PAV	<300 MPa	-6	92.05	97.95 Mpa	110 Mpa	110 Mpa	115 Mpa
BBR-S on RFTO+PAV	<300 MPa	-12	197 Mpa	189.5 Mpa	228 Mpa	218 Mpa	228 Mpa
BBR-S on RFTO+PAV	<300 MPa	-18	351 Mpa	360 Mpa	401 Mpa	397 Mpa	401 Mpa
BBR-m on RFTO+PAV	>0.3	-6	0.374	0.357	0.363	0.370	0.365
BBR-m on RFTO+PAV	>0.3	-12	0.312	0.302	0.306	0.312	0.309
BBR-m on RFTO+PAV	>0.3	-18	0.268	0.264	0.265	0.265	0.259
PG-Grading	--------	--------	**64-22**	**70-22**	**70-22**	**70-22**	**70-22**

Table A3. PG-Grading results for PG 67-22 binder blends+20%RAP+5%SHP.

Test	Specification	Temperature	67-20RAP	67-20RAP1SHP	67-20RAP3SHP	67-20RAP-5P
RV at 20 rpm on Original Binder	<3.0 Pa.s	135 ºC	1030 mPa.s	1056 mPa.s	925 mPa.s	862 mPa.s
DSR (G*/sinδ) on Original Binder	>1.0 kPa	70 ºC	3.86 kPa	3.77 kPa	3.78 kPa	3.91 kPa
DSR (G*/sinδ) on Original Binder	>1.0 kPa	76 ºC	1.82 kPa	1.82 kPa	1.84 kPa	1.90 kPa
DSR (G*/sinδ) on Original Binder	>1.0 kPa	82 ºC	0.896 kPa	0.94 kPa	0.945 kPa	0.954 kPa
DSR (G*/sinδ) on RTFO	>2.2 kPa	70 ºC	9.69 kPa	8.28 kPa	8.29 kPa	8.37 kPa
DSR (G*/sinδ) on RTFO	>2.2 kPa	76 ºC	4.5 kPa	3.88 kPa	3.89 kPa	3.91 kPa
DSR (G*/sinδ) on RTFO	>2.2 kPa	82 ºC	2.15 kPa	1.87 kPa	1.87 kPa	1.89 kPa
DSR (G^*.sinδ) on RFTO+PAV	<5000 kPa	28 ºC	6835 kPa	6580 kPa	6600 kPa	6640 kPa
DSR (G^*.sinδ) on RFTO+PAV	<5000 kPa	25 ºC	5195 kPa	4690 kPa	5190 kPa	5050 kPa
DSR (G^*.sinδ) on RFTO+PAV	<5000 kPa	22 ºC	-	-	3790 kPa	3710 kPa
BBR-S on RFTO+PAV	<300 MPa	-6	139 Mpa	159 Mpa	161 Mpa	168 Mpa
BBR-S on RFTO+PAV	<300 MPa	-12	323 Mpa	269 Mpa	289 Mpa	307 Mpa
BBR-S on RFTO+PAV	<300 MPa	-18	646 Mpa	475 Mpa	481 Mpa	520 Mpa
BBR-m on RFTO+PAV	>0.3	-6	0.326	0.314	0.314	0.325
BBR-m on RFTO+PAV	>0.3	-12	0.259	0.273	0.275	0.273
BBR-m on RFTO+PAV	>0.3	-18	0.179	0.232	0.224	0.225
PG-Grading	--------	--------	**76-16**	**76-16**	**76-16**	**76-16**

Table A4. PG-Grading results for PG 67-22 binder blends +5%RAS+20%RAP+5%SHP.

Test	Specification	Temperature	67CO	67-5RAS20RAP	67-5RAS20RAP1SHP	67-5RAS20RAP3SHP	67-5RAS20RAP5SHP
RV at 20 rpm on Original Binder	<3.0 Pa.s	135 ºC	527mPa.s	1175 mPa.s	962.5 mPa.s	917.5 mPa.s	893.75
DSR (G*/sinδ) on Original Binder	>1.0 kPa	70 ºC	0.88 kPa	3.9 kPa	2.8 kPa	2.82 kPa	2.95 kPa
DSR (G*/sinδ) on Original Binder	>1.0 kPa	76 ºC	-	1.84 kPa	1.31 kPa	1.34 kPa	1.37 kPa
DSR (G*/sinδ) on Original Binder	>1.0 kPa	82 ºC	-	0.906 kPa	0.643 kPa	0.669 kPa	0.679 kPa
DSR (G*/sinδ) on RTFO	>2.2 kPa	70 ºC	1.68 kPa	9.47 kPa	8.53 kPa	8.57 kPa	8.65 kPa
DSR (G*/sinδ) on RTFO	>2.2 kPa	76 ºC	-	4.44 kPa	3.96 kPa	4.01 kPa	4.09 kPa
DSR (G*/sinδ) on RTFO	>2.2 kPa	82 ºC	-	2.14 kPa	1.9 kPa	1.94 kPa	2.02 kPa
DSR (G^*.sinδ) on RFTO+PAV	<5000 kPa	28 ºC	-	5020 kPa	5190 kPa	5330 kPa	5540 kPa
DSR (G^*.sinδ) on RFTO+PAV	<5000 kPa	25 ºC	3920 kPa	6680 kPa	6760 kPa	6970 kPa kPa	6990 kPa
BBR-S on RFTO+PAV	<300 MPa	-6	92.05 Mpa	162 Mpa	169 Mpa	169 Mpa	150 Mpa
BBR-S on RFTO+PAV	<300 MPa	-12	197 Mpa	300 Mpa	321 Mpa	310 Mpa	310 Mpa
BBR-S on RFTO+PAV	<300 MPa	-18	351 Mpa	511 Mpa	566 Mpa	597 Mpa	594 Mpa
BBR-m on RFTO+PAV	>0.3	-6	0.374	0.316	0.315	0.319	0.322
BBR-m on RFTO+PAV	>0.3	-12	0.312	0.269	0.265	0.274	0.276
BBR-m on RFTO+PAV	>0.3	-18	0.268	0.231	0.23	0.221	0.23
PG-Grading	--------	--------	**64-22**	**76-16**	**76-16**	**76-16**	**76-16**

Table A5. PG-Grading results for PG 70-22M binder blends +5% SHP.

Test	Specification	Temperature	70Co	70PG1SHP	70PG3SHP	70PG5SHP
RV at 20 rpm on Original Binder	<3.0 Pa.s	135 ºC	1173 mPa.s	1125 mPa.s	1075 mPa.s	1012 mPa.s
DSR (G*/sinδ) on Original Binder	>1.0 kPa	70 ºC	1.77 kPa	1.61 kPa	1.62 kPa	1.75 kPa
DSR (G*/sinδ) on Original Binder	>1.0 kPa	76 ºC	0.97 kPa	0.884 kPa	0.884 kPa	0.984 kPa
DSR (G*/sinδ) on RTFO	>2.2 kPa	70 ºC	3.23 kPa	3.22 Kpa	3.24 kPa	3.41 kPa
DSR (G*/sinδ) on RTFO	>2.2 kPa	76 ºC	1.73 kPa	1.74 Kpa	1.75 Kpa	1.84 kPa
DSR (G*/sinδ) on RTFO	<5000 kPa	25 ºC	3180 kPa	2830 kPa	3030 kPa	3230 kPa
DSR (G^*.sinδ) on RFTO+PAV	<5000 kPa	22 ºC	4660 kPa	4220 kPa	4570 kPa	4770 kPa
DSR (G^*.sinδ) on RFTO+PAV	<5000 kPa	19 ºC	6620 kPa	6160 kPa	6710 kPa	6930 kPa
BBR-S on RFTO+PAV	<300 MPa	-6	83 Mpa	79.5 Mpa	78.6 Mpa	84.2 Mpa
BBR-S on RFTO+PAV	<300 MPa	-12	178 Mpa	183 Mpa	188 Mpa	179 Mpa
BBR-S on RFTO+PAV	<300 MPa	-18	317 Mpa	370 Mpa	371 Mpa	383 Mpa
BBR-S on RFTO+PAV	>0.3	-6	0.396	0.402	0.402	0.405
BBR-m on RFTO+PAV	>0.3	-12	0.336	0.339	0.34	0.342
BBR-m on RFTO+PAV	>0.3	-18	0.290	0.272	0.273	0.276
PG-Grading	--------	--------	**70-22**	**70-22**	**70-22**	**70-22**

Table A6. PG-Grading results for PG 70-22M binder blends + 5%RAS+5%SHP.

Test	Specification	Temperature	70-5RAS	70-5RAS1SHP	70-5RAS3SHP	70-5RAS-5P
RV at 20 rpm on Original Binder	<3.0 Pa.s	135 ºC	2450 mPa	2560 mPa	2520 mPa	2460 mPa
DSR (G*/sinδ) on Original Binder	>1.0 kPa	64 ºC	4.99 kPa	4.54 kPa	4.58 kPa	4.71 kPa
DSR (G*/sinδ) on Original Binder	>1.0 kPa	70 ºC	2.65 kPa	2.34 kPa	2.35 kPa	2.4 kPa
DSR (G*/sinδ) on Original Binder	>1.0 kPa	76 ºC	1.44 kPa	1.27 kPa	1.26 kPa	1.3 kPa
DSR (G*/sinδ) on RTFO	>2.2 kPa	70 ºC	4.39 kPa	3.88 kPa	3.96 kPa	4.07 kPa
DSR (G*/sinδ) on RTFO	>2.2 kPa	76 ºC	2.36 kPa	2.06 kPa	2.10 kPa	2.15 kPa
DSR (G^*.sinδ) on RFTO+PAV	<5000 kPa	25 ºC	3030 kPa	3440 kPa	3430 kPa	3545 kPa
DSR (G^*.sinδ) on RFTO+PAV	<5000 kPa	22 ºC	4525 kPa	5080 kPa	5085 kPa	5175 kPa
BBR-S on RFTO+PAV	<300 MPa	-6	81.2 Mpa	83 Mpa	80.4 Mpa	84.6 Mpa
BBR-S on RFTO+PAV	<300 MPa	-12	161 Mpa	185 Mpa	165 Mpa	196 Mpa
BBR-S on RFTO+PAV	<300 MPa	-18	323 Mpa	334 Mpa	364 Mpa	399 Mpa
BBR-S on RFTO+PAV	>0.3	-6	0.38	0.386	0.388	0.389
BBR-m on RFTO+PAV	>0.3	-12	0.33	0.328	0.329	0.330
BBR-m on RFTO+PAV	>0.3	-18	0.275	0.281	0.282	0.260
PG-Grading	--------	--------	**76-22**	**76-22**	**76-22**	**76-22**

Table A7. PG-Grading results for PG 70-22M binder blends+ 20%RAP+5%SHP.

Test	Specification	Temperature	70CO	70PG20RAP	70PG20RAP1SHP	70PG20RAP3SHP	70PG20RAP5SHP
RV at 20 rpm on Original Binder	<3.0 Pa.s	135 ºC	1173 mPa.s	2295 mPa.s	2312 mPa.s	2255 mPa.s	2233 mPa.s
DSR (G*/sinδ) on Original Binder	>1.0 kPa	76 ºC	1.77 kPa	3.02 kPa	2.62 kPa	2.71kPa	2.93 kPa
DSR (G*/sinδ) on Original Binder	>1.0 kPa	82 ºC	0.97 kPa	1.66 kPa	1.43 kPa	1.49 kPa	1.57 kPa
DSR (G*/sinδ) on Original Binder	>1.0 kPa	86ºC	-	0.939 kPa	0.816 kPa	0.847 kPa	0.878 kPa
DSR (G*/sinδ) on RTFO	>2.2 kPa	76 ºC	1.73 kPa	5.12 kPa	5.16 kPa	5.21 kPa	5.25 kPa
DSR (G*/sinδ) on RTFO	>2.2 kPa	82 ºC	-	2.77 kPa	2.78 kPa	2.80 kPa	2.85 kPa
DSR (G*/sinδ) on RTFO	>2.2 kPa	86 ºC	-	1.53 kPa	1.54 kPa	1.54 kPa	1.55 kPa
DSR (G^*.sinδ) on RFTO+PAV	<5000 kPa	28 ºC	-	4380 kPa	4075 kPa	4150 kPa	4380 kPa
DSR (G^*.sinδ) on RFTO+PAV	<5000 kPa	25 ºC	3180 kPa	5945 kPa	5660 kPa	5710 kPa	5880 kPa
BBR-S on RFTO+PAV	<300 MPa	-6	83 Mpa	149.5 Mpa	128 Mpa	136 Mpa	140 Mpa
BBR-S on RFTO+PAV	<300 MPa	-12	178 Mpa	272 Mpa	254 Mpa	254 Mpa	252 Mpa
BBR-S on RFTO+PAV	<300 MPa	-18	317 Mpa	476 Mpa	476 Mpa	485 Mpa	488 Mpa
BBR-S on RFTO+PAV	>0.3	-6	0.396	0.32	0.33	0.332	0.332
BBR-m on RFTO+PAV	>0.3	-12	0.336	0.27	0.274	0.278	0.282
BBR-m on RFTO+PAV	>0.3	-18	0.290	0.24	0.232	0.229	0.224
PG-Grading	--------		**70-22**	**82-16**	**82-16**	**82-16**	**82-16**

Table A8. PG-Grading results for PG 70-22M binder blends+5%RAS+20%RAP+ 5%SHP.

Test	Specification	Temperature	70-5RAS20RAP	70-5RAS20RAP1SHP	70-5RAS20RAP3SHP	70-5RAS20RAP5SHP
RV at 20 rpm on Original Binder	<3.0 Pa.s	135 ºC	2485 mPa.s	2356 mPa.s	2300 mPa.s	2285 mPa.s
DSR (G*/sinδ) on Original Binder	>1.0 kPa	76 ºC	3.60 kPa	2.71 kPa	2.74 kPa	2.86 kPa
DSR (G*/sinδ) on Original Binder	>1.0 kPa	82 ºC	1.91 kPa	1.28 kPa	1.46 kPa	1.34 kPa
DSR (G*/sinδ) on Original Binder	>1.0 kPa	88 ºC	1.08 kPa	0.71 kPa	0.804 kPa	1.05 kPa
DSR (G*/sinδ) on RTFO	>2.2 kPa	70 ºC	11.9 kPa	11.1 kPa	11.9 kPa	12.2 kPa
DSR (G*/sinδ) on RTFO	>2.2 kPa	76 ºC	6.12 kPa	5.35 kPa	6.11 kPa	6.14 kPa
DSR (G*/sinδ) on RTFO	>2.2 kPa	82 ºC	3.25 kPa	2.89 kPa	3.23 kPa	3.29 kPa
DSR (G*/sinδ) on RTFO	>2.2 kPa	88 ºC	1.80 kPa	1.55 kPa	1.67 kPa	1.74 kPa
DSR (G^*.sinδ) on RFTO+PAV	<5000 kPa	28 ºC	4830 kPa	4910 kPa	5200 kPa	5230 kPa
DSR (G^*.sinδ) on RFTO+PAV	<5000 kPa	25 ºC	6470 kPa	6510 kPa	6770 kPa	6810 kPa
BBR-S on RFTO+PAV	<300 MPa	-6	121 Mpa	159 Mpa	164 Mpa	160 Mpa
BBR-S on RFTO+PAV	<300 MPa	-12	233 Mpa	301 Mpa	306 Mpa	319 Mpa
BBR-S on RFTO+PAV	<300 MPa	-18	443 Mpa	515 Mpa	578 Mpa	573 Mpa
BBR-S on RFTO+PAV	>0.3	-6	0.326	0.318	0.322	0.319
BBR-m on RFTO+PAV	>0.3	-12	0.254	0.271	0.261	0.262
BBR-m on RFTO+PAV	>0.3	-18	0.23	0.227	0.213	0.217
PG-Grading	--------		**88-16**	**88-16**	**88-16**	**88-16**

Table A9. MSCR results for PG 67-22 binder blends.

Binder Blend	Percent Recovery (0.1)	Percent Recovery (3.2)	Jnr
67CO	1.62%	-0.50%	8.65%
67-1P	2.99%	-0.19%	11.27%
67-3P	2.92%	-0.21%	11.51%
67-5P	2.90%	-0.33%	12.42%
67-1P-1h	2.98%	-0.23%	11.79%
67-3P-1h	3.05%	-0.19%	11.39%
67-5P-1h	3.17%	-0.01%	12.46%
67-1P-48h	3.65%	0.13%	12.45%
67-3P-48h	3.75%	0.13%	12.59%
67-5P-48h	4.20%	0.13%	13.78%
67-5RAS	4.86%	0.58%	12.31%
67-5RAS-1P	4.63%	0.29%	13.18%
67-5RAS-3P	5.17%	0.56%	14.09%
67-5RAS-5P	6.69%	0.81%	17.12%
67-5RAS-1P-1h	5.76%	0.81%	13.92%
67-5RAS-3P-1h	5.40%	0.69%	13.52%
67-5RAS-5P-1h	8.64%	1.50%	16.88%
67-5RAS-1P-48h	6.33%	1.14%	13.87%
67-5RAS-3P-48h	6.80%	1.01%	15.99%
67-5RAS-5P-48h	6.52%	0.90%	16.66%
67-20RAP	19.80%	13.59%	15.00%
67-20RAP-1P	20.14%	11.27%	16.51%
67-20RAP-3P	20.96%	11.41%	18.67%
67-20RAP-5P	26.34%	12.99%	25.73%
67-20RAP-1P-1h	20.14%	11.22%	16.58%
67-20RAP-3P-1h	21.12%	11.61%	19.10%
67-20RAP-5P-1h	25.61%	13.39%	21.81%
67-20RAP-1P-48h	23.80%	14.46%	18.67%
67-20RAP-3P-48h	24.43%	14.90%	26.84%
67-20RAP-5P-48h	29.57%	16.24%	26.31%
67-5RAS-20RAP	22.22%	13.08%	16.23%
67-5RAS-20RAP-1P	18.98%	9.72%	15.07%
67-5RAS-20RAP-3P	20.35%	11.36%	15.13%
67-5RAS-20RAP-5P	22.94%	12.89%	16.92%
67-5RAS-20RAP-1P-1h	18.99%	10.49%	15.25%
67-5RAS-20RAP-3P-1h	20.16%	11.22%	15.81%
67-5RAS-20RAP-5P-1h	23.76%	12.82%	16.82%
67-5RAS-20RAP-1P-48h	19.56%	11.55%	14.72%
67-5RAS-20RAP-3P-48h	22.60%	13.11%	17.41%
67-5RAS-20RAP-5P-48h	25.11%	14.79%	18.98%

Table A10. MSCR results for PG 70-22M binder blends

Binder Blend	Percent Recovery (0.1)	Percent Recovery (3.2)	Jnr
70CO	49.10%	30.17%	48.82%
70-1P	47.68%	28.95%	47.15%
70-3P	46.22%	26.77%	47.93%
70-5P	46.05%	27.97%	44.58%
70-1P-1h	47.78%	28.98%	47.63%
70-3P-1h	46.51%	27.36%	47.82%
70-5P-1h	45.88%	27.68%	44.49%
70-1P-48h	50.19%	31.18%	50.22%
70-3P-48h	48.82%	28.95%	49.41%
70-5P-48h	47.01%	28.58%	48.97%
70-5RAS	45.47%	28.36%	41.52%
70-5RAS-1P	42.36%	25.02%	40.50%
70-5RAS-3P	42.50%	24.48%	42.50%
70-5RAS-5P	41.88%	24.38%	40.42%
70-5RAS-1P-1h	43.81%	27.27%	38.08%
70-5RAS-3P-1h	41.56%	23.75%	40.94%
70-5RAS-5P-1h	42.29%	25.83%	37.54%
70-5RAS-1P-48h	46.28%	29.87%	39.36%
70-5RAS-3P-48h	44.48%	26.50%	40.83%
70-5RAS-5P-48h	44.51%	27.86%	36.25%
70-20RAP	59.54%	48.75%	31.58%
70-20RAP-1P	57.99%	45.78%	34.84%
70-20RAP-3P	58.07%	45.23%	31.95%
70-20RAP-5P	56.17%	44.74%	32.30%
70-20RAP-1P-1h	57.30%	45.51%	33.65%
70-20RAP-3P-1h	57.01%	45.26%	32.12%
70-20RAP-5P-1h	56.35%	44.89%	32.93%
70-20RAP-1P-48h	62.05%	50.58%	37.12%
70-20RAP-3P-48h	60.08%	49.30%	34.85%
70-20RAP-5P-48h	58.16%	47.15%	32.96%
70-5RAS-20RAP	63.57%	53.78%	31.38%
70-5RAS-20RAP-1P	57.44%	47.27%	25.38%
70-5RAS-20RAP-3P	55.40%	45.83%	23.75%
70-5RAS-20RAP-5P	53.68%	43.37%	25.22%
70-5RAS-20RAP-5P-1h	54.45%	44.18%	26.10%
70-5RAS-20RAP-1P-48h	61.84%	52.12%	28.97%
70-5RAS-20RAP-3P-48h	58.46%	49.11%	25.51%
70-5RAS-20RAP-5P-48h	55.59%	45.69%	24.89%

APPENDIX B: STATISTICAL ANALYSIS FOR BINDER TESTING

B.1. Statistical Analysis for DSR Results (G*/sinδ at 70°C)

Table B1. Singularity details for DSR results.

Term	Details
Intercept	=SHP Type[0] - 0.5*SHP Type[1] + 1.5*%SHP[1-0]

Table B2. Effect summary for DSR results.

Source	LogWorth	PValue
RAP	63.151	0.00000
Binder	27.878	0.00000
RAS	9.252	0.00000
UV	5.706	0.00000
SHP Type	2.256	0.00555
%SHP	1.705	0.01971

Table B3. Summary of fit for DSR results.

RSquare	0.984824
RSquare Adj	0.982873
Root Mean Square Error	0.493351
Mean of Response	6.586375
Observations (or Sum Wgts)	80

Table B4. Analysis of variance for DSR results.

Source	DF	Sum of Squares	Mean Square	F Ratio
Model	9	1105.6510	122.850	504.7342
Error	70	17.0377	0.243	**Prob > F**
C. Total	79	1122.6886		<.0001*

Table B5. Parameter estimates for DSR results.

Term		Estimate	Std Error	t Ratio	Prob>|t|
Intercept	Biased	2.3478333	0.130298	18.02	<.0001*
Binder[67]		-1.018125	0.055158	-18.46	<.0001*
RAS[5-0]		0.79325	0.110317	7.19	<.0001*
RAP[20-0]		7.06525	0.110317	64.05	<.0001*
SHP Type[0]	Biased	0.3366667	0.145032	2.32	0.0232*
SHP Type[1]	Biased	-0.001944	0.092946	-0.02	0.9834
%SHP[1-0]	Zeroed	0	0	.	.
%SHP[3-1]		0.1291667	0.142418	0.91	0.3675
%SHP[5-3]		0.2729167	0.142418	1.92	0.0594
UV[1-0]		0.1375	0.142418	0.97	0.3376
UV[48-1]		0.6175	0.142418	4.34	<.0001*

Table B6. Effect tests for DSR results.

Source	Nparm	DF	Sum of Squares	F Ratio	Prob > F	
Binder	1	1	82.92628	340.7057	<.0001*	
RAS	1	1	12.58491	51.7056	<.0001*	
RAP	1	1	998.35515	4101.779	<.0001*	
SHP Type	2	1	1.99334	8.1897	0.0056*	LostDFs
%SHP	3	2	2.02271	4.1552	0.0197*	LostDFs
UV	2	2	7.76190	15.9450	<.0001*	

B.2. Statistical Analysis for Calculated Delta Tc

Table B7. Singularity details for Delta Tc results.

Term	Details
Intercept	=SHP Type[0] - 0.5*SHP Type[1] + 1.5*%SHP[1-0]

Table B8. Effect summary for calculated Delta Tc results.

Source	LogWorth	P-Value
RAP	24.609	0.00000
UV	2.150	0.00708
%SHP	1.908	0.01237
SHP Type	0.792	0.16144
binder	0.284	0.52033
RAS	0.064	0.86368

Table B9. Summary of fit for Delta Tc results.

RSquare	0.818752
RSquare Adj	0.795449
Root Mean Square Error	0.624012
Mean of Response	-2.23617
Observations (or Sum Wgts)	80

Table B10. Analysis of variance for Delta Tc.

Source	DF	Sum of Squares	Mean Square	F Ratio
Model	9	123.13010	13.6811	35.1346
Error	70	27.25741	0.3894	**Prob > F**
C. Total	79	150.38751		<.0001*

Table B11. Parameter estimates for Delta Tc results.

Term		Estimate	Std Error	t Ratio	Prob>|t|
Intercept	Biased	-1.791945	0.164807	-10.87	<.0001*
binder[67]		-0.045075	0.069767	-0.65	0.5203
RAS[5-0]		0.0240458	0.139533	0.17	0.8637
RAP[20-0]		-2.256232	0.139533	-16.17	<.0001*
SHP Type[0]	Biased	-0.517658	0.183442	-2.82	0.0062*
SHP Type[1]	Biased	0.1547532	0.117563	1.32	0.1924
%SHP[1-0]	Zeroed	0	0	.	.
%SHP[3-1]		0.2310666	0.180137	1.28	0.2038
%SHP[5-3]		0.3177935	0.180137	1.76	0.0821
UV[1-0]		0.5868114	0.180137	3.26	0.0017*
UV[48-1]		-0.317908	0.180137	-1.76	0.0820

Table B12. Effect tests for Delta Tc results.

Source	Nparm	DF	Sum of Squares	F Ratio	Prob > F	
binder	1	1	0.16254	0.4174	0.5203	
RAS	1	1	0.01156	0.0297	0.8637	
RAP	1	1	101.81163	261.4634	<.0001*	
SHP Type	2	1	0.77989	2.0028	0.1614	LostDFs
%SHP	3	2	3.64505	4.6804	0.0124*	LostDFs
UV	2	2	4.14178	5.3183	0.0071*	

B.3. Statistical Analysis for Calculated UTI

Table B12. Singularity details for UTI results.

Term	Details
Intercept	=SHP Type[0] - 0.5*SHP Type[1] + 1.5*%SHP[1-0]

Table B13. Effect summary for UTI results.

Source	LogWorth	PValue
RAP	21.931	0.00000
binder	21.011	0.00000
UV	0.858	0.13861
RAS	0.794	0.16052
%SHP	0.152	0.70452
SHP Type	0.103	0.78843

Table B14. Summary of fit for UTI results.

RSquare	0.853204
RSquare Adj	0.83433
Root Mean Square Error	1.749927
Mean of Response	101.1575
Observations (or Sum Wgts)	80

Table B15. Analysis of variance for UTI results.

Source	DF	Sum of Squares	Mean Square	F Ratio
Model	9	1245.8784	138.431	45.2057
Error	70	214.3571	3.062	**Prob > F**
C. Total	79	1460.2355		<.0001*

Table B16. Parameter estimates for UTI results.

Term		Estimate	Std Error	t Ratio	Prob>|t|
Intercept	Biased	98.135556	0.46217	212.34	<.0001*
binder[67]		-2.71	0.195648	-13.85	<.0001*
RAS[5-0]		-0.555	0.391296	-1.42	0.1605
RAP[20-0]		5.645	0.391296	14.43	<.0001*
SHP Type[0]	Biased	0.5444444	0.51443	1.06	0.2935
SHP Type[1]	Biased	-0.327778	0.329683	-0.99	0.3235
%SHP[1-0]	Zeroed	0	0	.	.
%SHP[3-1]		0.1666667	0.50516	0.33	0.7424
%SHP[5-3]		0.2541667	0.50516	0.50	0.6164
UV[1-0]		0.6291667	0.50516	1.25	0.2171
UV[48-1]		0.3791667	0.50516	0.75	0.4554

Table B17. Effect tests for UTI results.

Source	Nparm	DF	Sum of Squares	F Ratio	Prob > F	
binder	1	1	587.52800	191.8619	<.0001*	
RAS	1	1	6.16050	2.0118	0.1605	
RAP	1	1	637.32050	208.1220	<.0001*	
SHP Type	2	1	0.22222	0.0726	0.7884	LostDFs
%SHP	3	2	2.15583	0.3520	0.7045	LostDFs
UV	2	2	12.45083	2.0330	0.1386	

B.4. Statistical Analysis for MSCR Results (Percent Recovery (0.1 kPa))

Table B18. Singularity details for MSCR results (0.1 kPa).

Term	Details
Intercept	=SHP Type[0] - 0.5*SHP Type[1] + 1.5*%SHP[1-0]

Table B19. Effect summary for MSCR results (0.1 kPa).

Source	LogWorth	PValue
binder	64.110	0.00000
RAP	36.953	0.00000
UV	2.209	0.00617
SHP Type	1.911	0.01226
RAS	0.942	0.11420
%SHP	0.168	0.67858

Table B20. Summary of fit for MSCR results (0.1 kPa).

RSquare	0.986381
RSquare Adj	0.98463
Root Mean Square Error	0.025834
Mean of Response	0.325655
Observations (or Sum Wgts)	80

Table B21. Analysis of variance for MSCR results (0.1 kPa).

Source	DF	Sum of Squares	Mean Square	F Ratio
Model	9	3.3835794	0.375953	563.3300
Error	70	0.0467164	0.000667	**Prob > F**
C. Total	79	3.4302958		<.0001*

Table B22. Parameter estimates for MSCR results (0.1 kPa).

Term		Estimate	Std Error	t Ratio	Prob>|t|
Intercept	Biased	0.2517768	0.006823	36.90	<.0001*
binder[67]		-0.191003	0.002888	-66.13	<.0001*
RAS[5-0]		-0.00924	0.005777	-1.60	0.1142
RAP[20-0]		0.150105	0.005777	25.99	<.0001*
SHP Type[0]	Biased	0.0105157	0.007594	1.38	0.1705
SHP Type[1]	Biased	-0.013086	0.004867	-2.69	0.0090*
%SHP[1-0]	Zeroed	0	0	.	.
%SHP[3-1]		-0.003437	0.007458	-0.46	0.6463
%SHP[5-3]		0.0065833	0.007458	0.88	0.3804
UV[1-0]		0.0018208	0.007458	0.24	0.8078
UV[48-1]		0.0204042	0.007458	2.74	0.0079*

Table B23. Effect tests for MSCR results (0.1 kPa).

Source	Nparm	DF	Sum of Squares	F Ratio	Prob > F	
binder	1	1	2.9185564	4373.177	<.0001*	
RAS	1	1	0.0017076	2.5586	0.1142	
RAP	1	1	0.4506302	675.2262	<.0001*	
SHP Type	2	1	0.0044117	6.6106	0.0123*	LostDFs
%SHP	3	2	0.0005204	0.3899	0.6786	LostDFs
UV	2	2	0.0073088	5.4757	0.0062*	

APPENDIX C: STATISTICAL ANALYSIS FOR MIXTURE TESTING

C.1. Statistical Analysis for Healing Efficiency

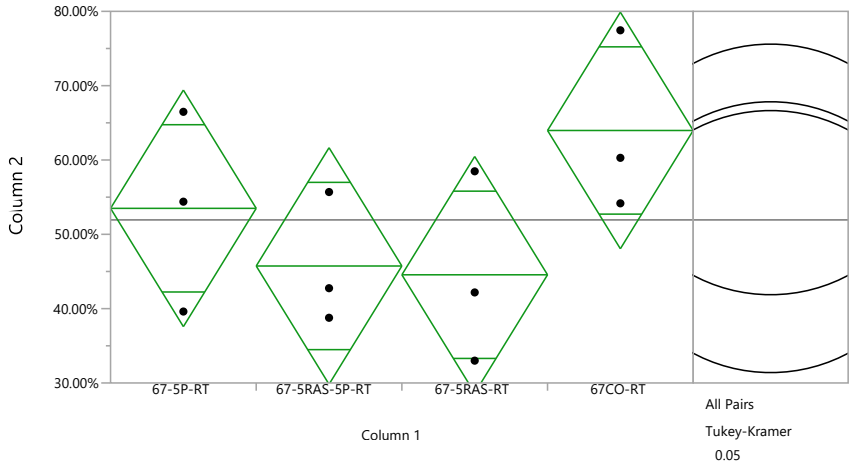

Figure C1. One-way analysis of crack healing at day 6 for PG 67-22 + 5%RAS (room temperature).

Table C1. Summary of fit of crack healing at day 6 for PG 67-22 + 5%RAS (room temperature).

Rsquare	0.386632
Adj Rsquare	0.156618
Root Mean Square Error	0.119535
Mean of Response	0.519383
Observations (or Sum Wgts)	12

Table C2. Analysis of variance of crack healing at day 6 for PG 67-22 + 5%RAS (room temperature).

Source	DF	Sum of Squares	Mean Square	F Ratio	Prob > F
Column 1	3	0.07205338	0.024018	1.6809	0.2475
Error	8	0.11430850	0.014289		
C. Total	11	0.18636188			

Table C3. Means for one-way ANOVA of crack healing at day 6 for PG 67-22 + 5%RAS (room temperature).

Level	Number	Mean	Std Error	Lower 95%	Upper 95%
67-5P-RT	3	0.534933	0.06901	0.37579	0.69408
67-5RAS-5P-RT	3	0.457367	0.06901	0.29822	0.61651
67-5RAS-RT	3	0.445533	0.06901	0.28639	0.60468
67CO-RT	3	0.639700	0.06901	0.48055	0.79885

Table C4. Connecting letters report of crack healing at day 6 for PG 67-22 + 5%RAS (room temperature).

Level		Mean
67CO-RT	A	0.63970000
67-5P-RT	A	0.53493333
67-5RAS-5P-RT	A	0.45736667
67-5RAS-RT	A	0.44553333

Table C5. Ordered differences report of crack healing at day 6 for PG 67-22 + 5%RAS (room temperature).

Level	- Level	Difference	Std Err Dif	Lower CL	Upper CL	p-Value
67CO-RT	67-5RAS-RT	0.1941667	0.0975997	-0.118381	0.5067146	0.2677
67CO-RT	67-5RAS-5P-RT	0.1823333	0.0975997	-0.130215	0.4948813	0.3122
67CO-RT	67-5P-RT	0.1047667	0.0975997	-0.207781	0.4173146	0.7141
67-5P-RT	67-5RAS-RT	0.0894000	0.0975997	-0.223148	0.4019479	0.7974
67-5P-RT	67-5RAS-5P-RT	0.0775667	0.0975997	-0.234981	0.3901146	0.8550
67-5RAS-5P-RT	67-5RAS-RT	0.0118333	0.0975997	-0.300715	0.3243813	0.9993

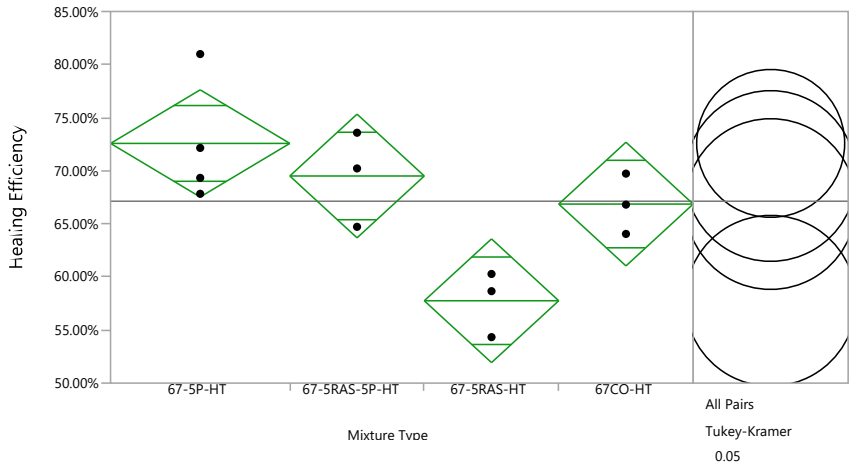

Figure C2. One-way analysis of crack healing at day 6 for PG 67-22 + 5%RAS (high temperature/UV exposure).

Table C6. Summary of fit of crack healing at day 6 for PG 67-22 + 5%RAS (high temperature/UV exposure).

Rsquare	0.690354
Adj Rsquare	0.587139
Root Mean Square Error	0.044611
Mean of Response	0.671292
Observations (or Sum Wgts)	13

Table C7. Analysis of variance of crack healing at day 6 for PG 67-22 + 5%RAS (high temperature/UV exposure).

Source	DF	Sum of Squares	Mean Square	F Ratio	Prob > F
Mixture Type	3	0.03993292	0.013311	6.6885	0.0114*
Error	9	0.01791117	0.001990		
C. Total	12	0.05784409			

Table C8. Means of one-way ANOVA of crack healing at day 6 for PG 67-22 + 5%RAS (high temperature/UV exposure).

Level	Number	Mean	Std Error	Lower 95%	Upper 95%
67-5P-HT	4	0.725750	0.02231	0.67529	0.77621
67-5RAS-5P-HT	3	0.695067	0.02576	0.63680	0.75333
67-5RAS-HT	3	0.577567	0.02576	0.51930	0.63583
67CO-HT	3	0.668633	0.02576	0.61037	0.72690

Table C9. Connecting letters report of crack healing at day 6 for PG 67-22 + 5%RAS (high temperature/UV exposure).

Level			Mean
67-5P-HT	A		0.72575000
67-5RAS-5P-HT	A		0.69506667
67CO-HT	A	B	0.66863333
67-5RAS-HT		B	0.57756667

Table C10. Ordered differences report of crack healing at day 6 for PG 67-22 + 5%RAS (high temperature/UV exposure).

Level	- Level	Difference	Std Err Dif	Lower CL	Upper CL	p-Value
67-5P-HT	67-5RAS-HT	0.1481833	0.0340721	0.041817	0.2545498	0.0082*
67-5RAS-5P-HT	67-5RAS-HT	0.1175000	0.0364246	0.003789	0.2312106	0.0428*
67CO-HT	67-5RAS-HT	0.0910667	0.0364246	-0.022644	0.2047772	0.1265
67-5P-HT	67CO-HT	0.0571167	0.0340721	-0.049250	0.1634832	0.3883
67-5P-HT	67-5RAS-5P-HT	0.0306833	0.0340721	-0.075683	0.1370498	0.8050
67-5RAS-5P-HT	67CO-HT	0.0264333	0.0364246	-0.087277	0.1401439	0.8844

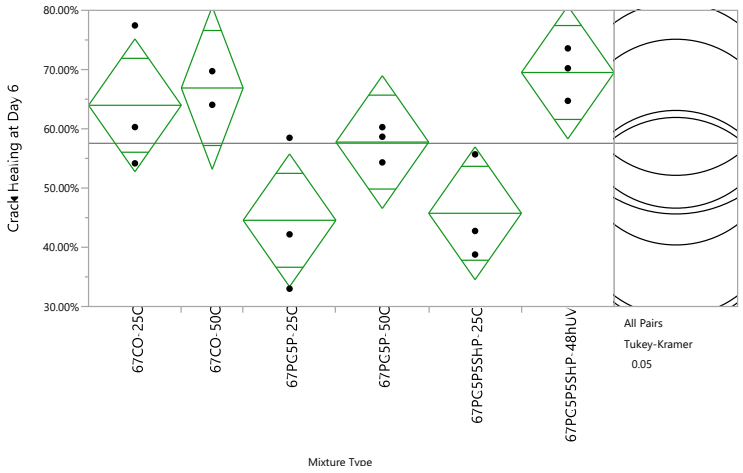

Figure C3. One-way analysis of crack healing at day 6 for PG 67-22 + 5%RAS (Effect of curing conditions).

Table C11. Summary of fit of crack healing at day 6 for PG 67-22 + 5%RAS (Effect of curing conditions).

Rsquare	0.658779
Adj Rsquare	0.503678
Root Mean Square Error	0.088212
Mean of Response	0.5755
Observations (or Sum Wgts)	17

Table C12. Analysis of variance of crack healing at day 6 for PG 67-22 + 5%RAS (Effect of curing conditions).

Source	DF	Sum of Squares	Mean Square	F Ratio	Prob > F
Mixture Type	5	0.16525387	0.033051	4.2474	0.0214*
Error	11	0.08559501	0.007781		
C. Total	16	0.25084888			

Table C13. Means for one-way ANOVA of crack healing at day 6 for PG 67-22 + 5%RAS (Effect of curing conditions).

Level	Number	Mean	Std Error	Lower 95%	Upper 95%
67CO-25C	3	0.639700	0.05093	0.52761	0.75179
67CO-50C	2	0.668900	0.06238	0.53161	0.80619
67-5RAS-25C	3	0.445533	0.05093	0.33344	0.55763
67-5RAS-50C	3	0.577567	0.05093	0.46547	0.68966
67-5RAS-5P-25C	3	0.457367	0.05093	0.34527	0.56946
67-5RAS-5P-48h	3	0.695067	0.05093	0.58297	0.80716

Table C14. Connecting letters report of crack healing at day 6 for PG 67-22 + 5%RAS (Effect of curing conditions).

Level			Mean
67-5RAS-5P-48h	A		0.69506667
67CO-50C	A	B	0.66890000
67CO-25C	A	B	0.63970000
67-5RAS-50C	A	B	0.57756667
67-5RAS-5P-25C	A	B	0.45736667
67-5RAS-25C		B	0.44553333

Table C15. Ordered differences report of crack healing at day 6 for PG 67-22 + 5%RAS (effect of curing conditions).

Level	- Level	Difference	Std Err Dif	Lower CL	Upper CL	p-Value
67-5RAS-5P-48h	67-5RAS-25C	0.2495333	0.0720248	0.003904	0.4951624	0.0458*
67-5RAS-5P-48h	67-5RAS-5P-25C	0.2377000	0.0720248	-0.007929	0.4833291	0.0596
67CO-50C	67-5RAS-25C	0.2233667	0.0805262	-0.051255	0.4979883	0.1360
67CO-50C	67-5RAS-5P-25C	0.2115333	0.0805262	-0.063088	0.4861550	0.1696
67CO-25C	67-5RAS-25C	0.1941667	0.0720248	-0.051462	0.4397957	0.1530
67CO-25C	67-5RAS-5P-25C	0.1823333	0.0720248	-0.063296	0.4279624	0.1952
67-5RAS-50C	67-5RAS-25C	0.1320333	0.0720248	-0.113596	0.3776624	0.4848
67-5RAS-50C	67-5RAS-5P-25C	0.1202000	0.0720248	-0.125429	0.3658291	0.5756
67-5RAS-5P-48h	67-5RAS-50C	0.1175000	0.0720248	-0.128129	0.3631291	0.5968
67CO-50C	67-5RAS-50C	0.0913333	0.0805262	-0.183288	0.3659550	0.8574
67CO-25C	67-5RAS-50C	0.0621333	0.0720248	-0.183496	0.3077624	0.9480
67-5RAS-5P-48h	67CO-25C	0.0553667	0.0720248	-0.190262	0.3009957	0.9675
67CO-50C	67CO-25C	0.0292000	0.0805262	-0.245422	0.3038216	0.9989
67-5RAS-5P-48h	67CO-50C	0.0261667	0.0805262	-0.248455	0.3007883	0.9994
67-5RAS-5P-25C	67-5RAS-25C	0.0118333	0.0720248	-0.233796	0.2574624	1.0000

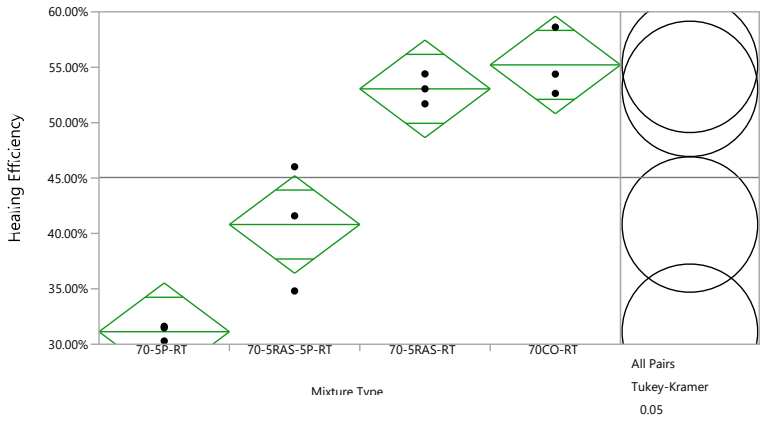

Figure C4. One-way analysis of crack healing at day 6 for PG 70-22M + 5%RAS (room temperature).

Table C16. Summary of fit of crack healing at day 6 for PG 70-22M + 5%RAS (room temperature).

Rsquare	0.928639
Adj Rsquare	0.901879
Root Mean Square Error	0.033051
Mean of Response	0.4505
Observations (or Sum Wgts)	12

Table C17. Analysis of variance of crack healing at day 6 for PG 70-22M + 5%RAS (room temperature).

Source	DF	Sum of Squares	Mean Square	F Ratio	Prob > F
Mixture Type	3	0.11371969	0.037907	34.7020	<.0001*
Error	8	0.00873875	0.001092		
C. Total	11	0.12245844			

Table C18. Means for one-way ANOVA of crack healing at day 6 for PG 70-22M + 5%RAS (room temperature).

Level	Number	Mean	Std Error	Lower 95%	Upper 95%
70-5P-RT	3	0.311300	0.01908	0.26730	0.35530
70-5RAS-5P-RT	3	0.408067	0.01908	0.36406	0.45207
70-5RAS-RT	3	0.530500	0.01908	0.48650	0.57450
70CO-RT	3	0.552133	0.01908	0.50813	0.59614

Table C19. Connecting letters report of crack healing at day 6 for PG 70-22M + 5%RAS (room temperature).

Level				Mean
70CO-RT	A			0.55213333
70-5RAS-RT	A			0.53050000
70-5RAS-5P-RT		B		0.40806667
70-5P-RT			C	0.31130000

Table C20. Ordered differences report of crack healing at day 6 for PG 70-22M + 5%RAS (room temperature).

Level	- Level	Difference	Std Err Dif	Lower CL	Upper CL	p-Value
70CO-RT	70-5P-RT	0.2408333	0.0269857	0.154416	0.3272509	<.0001*
70-5RAS-RT	70-5P-RT	0.2192000	0.0269857	0.132782	0.3056176	0.0002*
70CO-RT	70-5RAS-5P-RT	0.1440667	0.0269857	0.057649	0.2304842	0.0031*
70-5RAS-RT	70-5RAS-5P-RT	0.1224333	0.0269857	0.036016	0.2088509	0.0082*
70-5RAS-5P-RT	70-5P-RT	0.0967667	0.0269857	0.010349	0.1831842	0.0293*
70CO-RT	70-5RAS-RT	0.0216333	0.0269857	-0.064784	0.1080509	0.8519

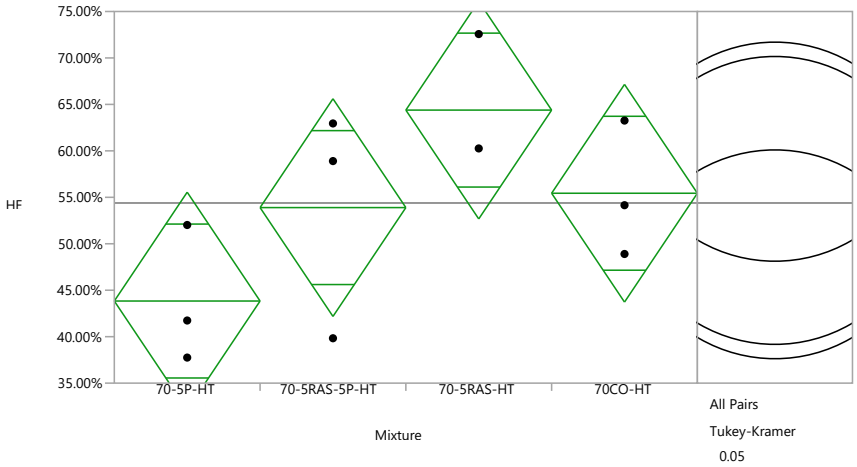

Figure C5. One-way analysis of crack healing at day 6 for PG 70-22M + 5%RAS (high temperature/UV exposure).

Table C21. Summary of fit of crack healing at day 6 for PG 70-22M + 5%RAS (high temperature/UV exposure).

Rsquare	0.507408
Adj Rsquare	0.322685
Root Mean Square Error	0.087986
Mean of Response	0.543883
Observations (or Sum Wgts)	12

Table C22. Analysis of variance of crack healing at day 6 for PG 70-22M + 5%RAS (high temperature/UV exposure).

Source	DF	Sum of Squares	Mean Square	F Ratio	Prob > F
Mixture	3	0.06379451	0.021265	2.7469	0.1126
Error	8	0.06193187	0.007741		
C. Total	11	0.12572638			

Table C23. Means for one-way ANOVA of crack healing at day 6 for PG 70-22M + 5%RAS (high temperature/UV exposure).

Level	Number	Mean	Std Error	Lower 95%	Upper 95%
70-5P-HT	3	0.438367	0.05080	0.32122	0.55551
70-5RAS-5P-HT	3	0.538933	0.05080	0.42179	0.65608
70-5RAS-HT	3	0.643867	0.05080	0.52672	0.76101
70CO-HT	3	0.554367	0.05080	0.43722	0.67151

Table C24. Connecting letters report of crack healing at day 6 for PG 70-22M + 5%RAS (high temperature/UV exposure).

Level		Mean
70-5RAS-HT	A	0.64386667
70CO-HT	A	0.55436667
70-5RAS-5P-HT	A	0.53893333
70-5P-HT	A	0.43836667

Table C25. Ordered differences report of crack healing at day 6 for PG 70-22M + 5%RAS (high temperature/UV exposure).

Level	- Level	Difference	Std Err Dif	Lower CL	Upper CL	p-Value
70-5RAS-HT	70-5P-HT	0.2055000	0.0718400	-0.024556	0.4355565	0.0810
70CO-HT	70-5P-HT	0.1160000	0.0718400	-0.114056	0.3460565	0.4228
70-5RAS-HT	70-5RAS-5P-HT	0.1049333	0.0718400	-0.125123	0.3349898	0.5006
70-5RAS-5P-HT	70-5P-HT	0.1005667	0.0718400	-0.129490	0.3306231	0.5330
70-5RAS-HT	70CO-HT	0.0895000	0.0718400	-0.140556	0.3195565	0.6180
70CO-HT	70-5RAS-5P-HT	0.0154333	0.0718400	-0.214623	0.2454898	0.9962

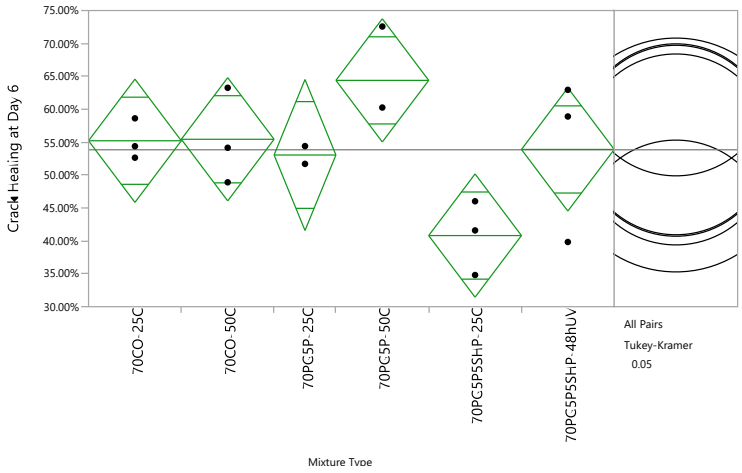

Figure C6. One-way analysis of crack healing at day 6 for PG 70-22M + 5%RAS (effect of curing condition).

Table C26. Summary of fit of crack healing at day 6 for PG 70-22M + 5%RAS (effect of curing condition).

Rsquare	0.58956
Adj Rsquare	0.402996
Root Mean Square Error	0.073684
Mean of Response	0.538418
Observations (or Sum Wgts)	17

Table C27. Analysis of variance of crack healing at day 6 for PG 70-22M + 5%RAS (effect of curing condition).

Source	DF	Sum of Squares	Mean Square	F Ratio	Prob > F
Mixture Type	5	0.08578627	0.017157	3.1601	0.0520
Error	11	0.05972275	0.005429		
C. Total	16	0.14550902			

Table C28. Means for one-way ANOVA of crack healing at day 6 for PG 70-22M + 5%RAS (effect of curing condition).

Level	Number	Mean	Std Error	Lower 95%	Upper 95%
70CO-25C	3	0.552133	0.04254	0.45850	0.64577
70CO-50C	3	0.554367	0.04254	0.46073	0.64800
70-5RAS-25C	2	0.530500	0.05210	0.41582	0.64518
70-5RAS-50C	3	0.643867	0.04254	0.55023	0.73750
70-5RAS-5P-25C	3	0.408067	0.04254	0.31443	0.50170
70-5RAS-5P-48	3	0.538933	0.04254	0.44530	0.63257

Table C29. Connecting letters report of crack healing at day 6 for PG 70-22M + 5%RAS (effect of curing condition).

Level			Mean
70-5RAS-50C	A		0.64386667
70CO-50C	A	B	0.55436667
70CO-25C	A	B	0.55213333
70-5RAS-5P-48	A	B	0.53893333
70-5RAS-25C	A	B	0.53050000
70-5RAS-5P-25C		B	0.40806667

Table C30. Ordered differences report of crack healing at day 6 for PG 70-22M + 5%RAS (effect of curing condition).

Level	- Level	Difference	Std Err Dif	Lower CL	Upper CL	p-Value
70-5RAS-50C	70-5RAS-5P-25C	0.2358000	0.0601628	0.030625	0.4409755	0.0221*
70CO-50C	70-5RAS-5P-25C	0.1463000	0.0601628	-0.058875	0.3514755	0.2253
70CO-25C	70-5RAS-5P-25C	0.1440667	0.0601628	-0.061109	0.3492421	0.2375
70-5RAS-5P-48	70-5RAS-5P-25C	0.1308667	0.0601628	-0.074309	0.3360421	0.3201
70-5RAS-25C	70-5RAS-5P-25C	0.1224333	0.0672640	-0.106960	0.3518265	0.4918
70-5RAS-50C	70-5RAS-25C	0.1133667	0.0672640	-0.116026	0.3427598	0.5663
70-5RAS-50C	70-5RAS-5P-48	0.1049333	0.0601628	-0.100242	0.3101088	0.5334
70-5RAS-50C	70CO-25C	0.0917333	0.0601628	-0.113442	0.2969088	0.6574
70-5RAS-50C	70CO-50C	0.0895000	0.0601628	-0.115675	0.2946755	0.6783
70CO-50C	70-5RAS-25C	0.0238667	0.0672640	-0.205526	0.2532598	0.9990
70CO-25C	70-5RAS-25C	0.0216333	0.0672640	-0.207760	0.2510265	0.9994
70CO-50C	70-5RAS-5P-48	0.0154333	0.0601628	-0.189742	0.2206088	0.9998
70CO-25C	70-5RAS-5P-48	0.0132000	0.0601628	-0.191975	0.2183755	0.9999
70-5RAS-5P-48	70-5RAS-25C	0.0084333	0.0672640	-0.220960	0.2378265	1.0000
70CO-50C	70CO-25C	0.0022333	0.0601628	-0.202942	0.2074088	1.0000

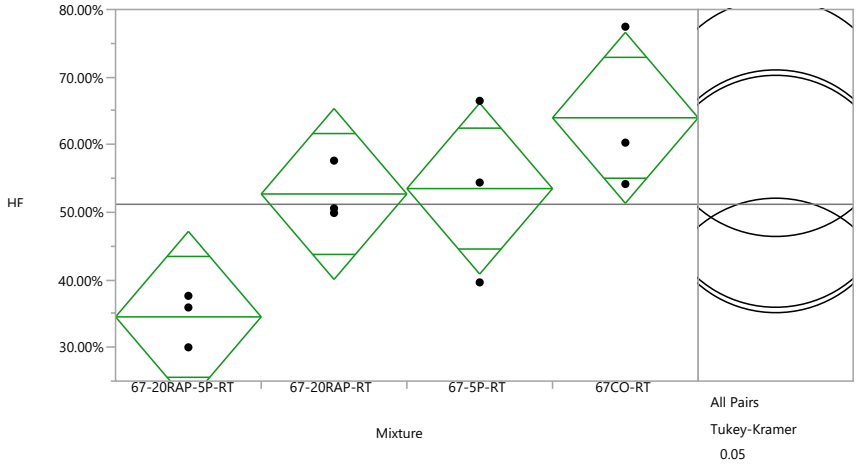

Figure C7. One-way analysis of crack healing at day 6 for PG 67-22 + 20%RAP (room temp).

Table C31. Summary of fit of crack healing at day 6 for PG 67-22 + 20%RAP (room temp).

Rsquare	0.651079
Adj Rsquare	0.520233
Root Mean Square Error	0.095015
Mean of Response	0.511658
Observations (or Sum Wgts)	12

Table C32. Analysis of variance of crack healing at day 6 for PG 67-22 + 20%RAP (room temp).

Source	DF	Sum of Squares	Mean Square	F Ratio	Prob > F
Mixture	3	0.13476751	0.044923	4.9759	0.0309*
Error	8	0.07222356	0.009028		
C. Total	11	0.20699107			

Table C33. Means for one-way ANOVA of crack healing at day 6 for PG 67-22 + 20%RAP (room temp).

Level	Number	Mean	Std Error	Lower 95%	Upper 95%
67-20RAP-5P-RT	3	0.345067	0.05486	0.21857	0.47157
67-20RAP-RT	3	0.526933	0.05486	0.40043	0.65343
67-5P-RT	3	0.534933	0.05486	0.40843	0.66143
67CO-RT	3	0.639700	0.05486	0.51320	0.76620

Table C34. Connecting letters report of crack healing at day 6 for PG 67-22 + 20%RAP (room temp).

Level			Mean
67CO-RT	A		0.63970000
67-5P-RT	A	B	0.53493333
67-20RAP-RT	A	B	0.52693333
67-20RAP-5P-RT		B	0.34506667

Table C35. Ordered differences report of crack healing at day 6 for PG 67-22 + 20%RAP (room temp).

Level	- Level	Difference	Std Err Dif	Lower CL	Upper CL	p-Value
67CO-RT	67-20RAP-5P-RT	0.2946333	0.0775798	0.046196	0.5430706	0.0219*
67-5P-RT	67-20RAP-5P-RT	0.1898667	0.0775798	-0.058571	0.4383040	0.1446
67-20RAP-RT	67-20RAP-5P-RT	0.1818667	0.0775798	-0.066571	0.4303040	0.1667
67CO-RT	67-20RAP-RT	0.1127667	0.0775798	-0.135671	0.3612040	0.5043
67CO-RT	67-5P-RT	0.1047667	0.0775798	-0.143671	0.3532040	0.5599
67-5P-RT	67-20RAP-RT	0.0080000	0.0775798	-0.240437	0.2564373	0.9996

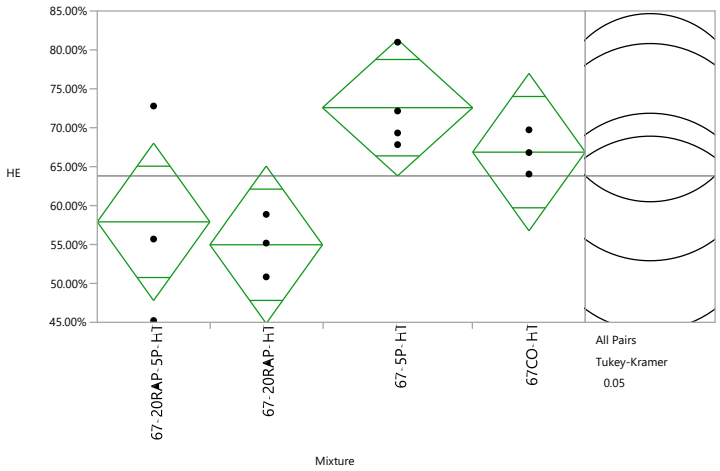

Figure C8. One-way analysis of crack healing at day 6 for PG 67-22 + 20%RAP (high temp/UV exposure).

Table C36. Summary of fit of crack healing at day 6 for PG 67-22 + 20%RAP (high temp/UV exposure).

Rsquare	0.555611
Adj Rsquare	0.407481
Root Mean Square Error	0.077428
Mean of Response	0.638077
Observations (or Sum Wgts)	13

Table C37. Analysis of variance of crack healing at day 6 for PG 67-22 + 20%RAP (high temp/UV exposure).

Source	DF	Sum of Squares	Mean Square	F Ratio	Prob > F
Mixture	3	0.06746079	0.022487	3.7508	0.0536
Error	9	0.05395651	0.005995		
C. Total	12	0.12141730			

Table C38. Means for one-way ANOVA of crack healing at day 6 for PG 67-22 + 20%RAP (high temp/UV exposure).

Level	Number	Mean	Std Error	Lower 95%	Upper 95%
67-20RAP-5P-HT	3	0.579067	0.04470	0.47794	0.68019
67-20RAP-HT	3	0.549633	0.04470	0.44851	0.65076
67-5P-HT	4	0.725750	0.03871	0.63817	0.81333
67CO-HT	3	0.668633	0.04470	0.56751	0.76976

Table C39. Connecting letters report of crack healing at day 6 for PG 67-22 + 20%RAP (high temp/UV exposure).

Level		Mean
67-5P-HT	A	0.72575000
67CO-HT	A	0.66863333
67-20RAP-5P-HT	A	0.57906667
67-20RAP-HT	A	0.54963333

Table C40. Ordered differences report of crack healing at day 6 for PG 67-22 + 20%RAP (high temp/UV exposure).

Level	- Level	Difference	Std Err Dif	Lower CL	Upper CL	p-Value
67-5P-HT	67-20RAP-HT	0.1761167	0.0591370	-0.008497	0.3607307	0.0621
67-5P-HT	67-20RAP-5P-HT	0.1466833	0.0591370	-0.037931	0.3312974	0.1302
67CO-HT	67-20RAP-HT	0.1190000	0.0632201	-0.078361	0.3163607	0.2999
67CO-HT	67-20RAP-5P-HT	0.0895667	0.0632201	-0.107794	0.2869274	0.5204
67-5P-HT	67CO-HT	0.0571167	0.0591370	-0.127497	0.2417307	0.7715
67-20RAP-5P-HT	67-20RAP-HT	0.0294333	0.0632201	-0.167927	0.2267941	0.9648

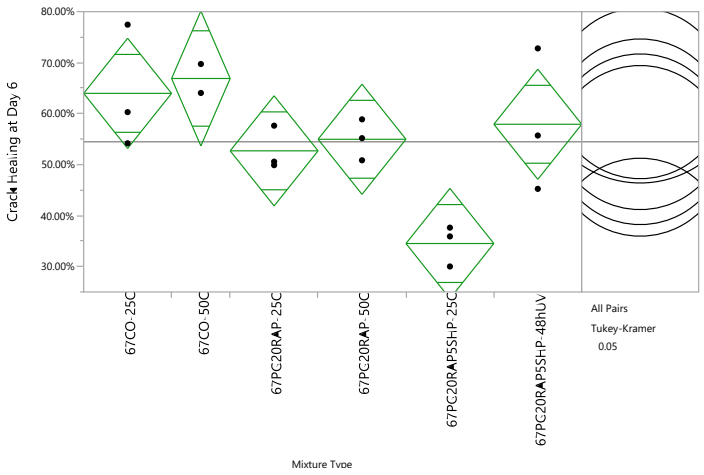

Figure C9. One-way analysis of crack healing at day 6 for PG 67-22 + 20%RAP (effect of curing conditions).

Table C41. Summary of fit of crack healing at day 6 for PG 67-22 + 20%RAP (effect of curing conditions).

Rsquare	0.695895
Adj Rsquare	0.557666
Root Mean Square Error	0.085043
Mean of Response	0.544647
Observations (or Sum Wgts)	17

Table C42. Analysis of variance of crack healing at day 6 for PG 67-22 + 20%RAP (effect of curing conditions).

Source	DF	Sum of Squares	Mean Square	F Ratio	Prob > F
Mixture Type	5	0.18204982	0.036410	5.0343	0.0121*
Error	11	0.07955541	0.007232		
C. Total	16	0.26160522			

Table C 43. Means for one-way ANOVA of crack healing at day 6 for PG 67-22 + 20%RAP (effect of curing conditions).

Level	Number	Mean	Std Error	Lower 95%	Upper 95%
67CO-25C	3	0.639700	0.04910	0.53163	0.74777
67CO-50C	2	0.668900	0.06013	0.53654	0.80126
67-20RAP-25C	3	0.526933	0.04910	0.41887	0.63500
67-20RAP-50C	3	0.549633	0.04910	0.44157	0.65770
67-20RAP-5P-25C	3	0.345067	0.04910	0.23700	0.45313
67-20RAP-5P-48h	3	0.579067	0.04910	0.47100	0.68713

Table C44. Connecting letters report of crack healing at day 6 for PG 67-22 + 20%RAP (effect of curing conditions).

Level			Mean
67CO-50C	A		0.66890000
67CO-25C	A		0.63970000
67-20RAP-5P-48h	A	B	0.57906667
67-20RAP-50C	A	B	0.54963333
67-20RAP-25C	A	B	0.52693333
67-20RAP-5P-25C		B	0.34506667

Table C45. Ordered differences report of crack healing at day 6 for PG 67-22 + 20%RAP (effect of curing conditions).

Level	- Level	Difference	Std Err Dif	Lower CL	Upper CL	p-Value
67CO-50C	67-20RAP-5P-25C	0.3238333	0.0776333	0.059078	0.5885891	0.0148*
67CO-25C	67-20RAP-5P-25C	0.2946333	0.0694373	0.057829	0.5314381	0.0132*
67-20RAP-5P-48h	67-20RAP-5P-25C	0.2340000	0.0694373	-0.002805	0.4708047	0.0533
67-20RAP-50C	67-20RAP-5P-25C	0.2045667	0.0694373	-0.032238	0.4413714	0.1043
67-20RAP-25C	67-20RAP-5P-25C	0.1818667	0.0694373	-0.054938	0.4186714	0.1716
67CO-50C	67-20RAP-25C	0.1419667	0.0776333	-0.122789	0.4067224	0.4872
67CO-50C	67-20RAP-50C	0.1192667	0.0776333	-0.145489	0.3840224	0.6509
67CO-25C	67-20RAP-25C	0.1127667	0.0694373	-0.124038	0.3495714	0.6010
67CO-25C	67-20RAP-50C	0.0900667	0.0694373	-0.146738	0.3268714	0.7811
67CO-50C	67-20RAP-5P-48h	0.0898333	0.0776333	-0.174922	0.3545891	0.8476
67CO-25C	67-20RAP-5P-48h	0.0606333	0.0694373	-0.176171	0.2974381	0.9455
67-20RAP-5P-48h	67-20RAP-25C	0.0521333	0.0694373	-0.184671	0.2889381	0.9705
67-20RAP-5P-48h	67-20RAP-50C	0.0294333	0.0694373	-0.207371	0.2662381	0.9977
67CO-50C	67CO-25C	0.0292000	0.0776333	-0.235556	0.2939558	0.9987
67-20RAP-50C	67-20RAP-25C	0.0227000	0.0694373	-0.214105	0.2595047	0.9993

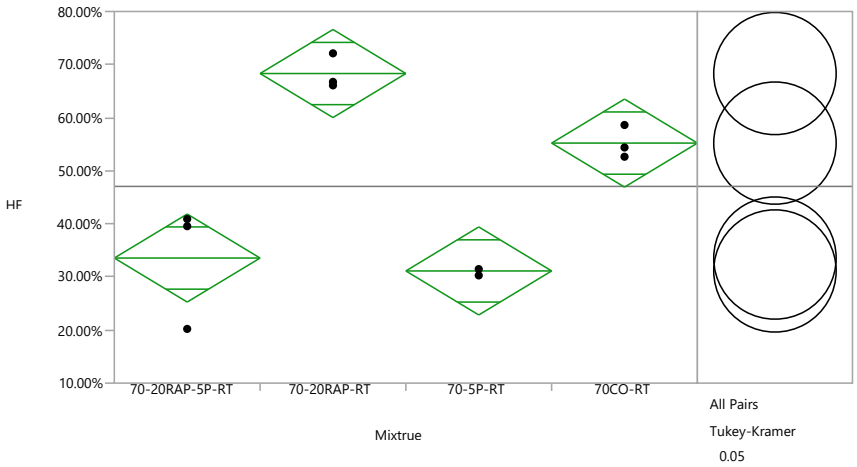

Figure C10. One-way analysis of crack healing at day 6 for PG 70-22M + 20%RAP (room temp).

Table C46. Summary of fit of crack healing at day 6 for PG 70-22M + 20%RAP (room temp).

Rsquare	0.902234
Adj Rsquare	0.865572
Root Mean Square Error	0.062268
Mean of Response	0.470542
Observations (or Sum Wgts)	12

Table C47. Analysis of variance of crack healing at day 6 for PG 70-22M + 20%RAP (room temp).

Source	DF	Sum of Squares	Mean Square	F Ratio	Prob > F
Mixtrue	3	0.28625874	0.095420	24.6094	0.0002*
Error	8	0.03101889	0.003877		
C. Total	11	0.31727763			

Table C48. Means for one-way ANOVA of crack healing at day 6 for PG 70-22M + 20%RAP (room temp).

Level	Number	Mean	Std Error	Lower 95%	Upper 95%
70-20RAP-5P-RT	3	0.335600	0.03595	0.25270	0.41850
70-20RAP-RT	3	0.683133	0.03595	0.60023	0.76604
70-5P-RT	3	0.311300	0.03595	0.22840	0.39420
70CO-RT	3	0.552133	0.03595	0.46923	0.63504

Table C49. Connecting letters report of crack healing at day 6 for PG 70-22M + 20%RAP (room temp).

Level			Mean
70-20RAP-RT	A		0.68313333
70CO-RT	A		0.55213333
70-20RAP-5P-RT		B	0.33560000
70-5P-RT		B	0.31130000

Table C50. Ordered differences report of crack healing at day 6 for PG 70-22M + 20%RAP (room temp).

Level	- Level	Difference	Std Err Dif	Lower CL	Upper CL	p-Value
70-20RAP-RT	70-5P-RT	0.3718333	0.0508420	0.209020	0.5346469	0.0004*
70-20RAP-RT	70-20RAP-5P-RT	0.3475333	0.0508420	0.184720	0.5103469	0.0006*
70CO-RT	70-5P-RT	0.2408333	0.0508420	0.078020	0.4036469	0.0064*
70CO-RT	70-20RAP-5P-RT	0.2165333	0.0508420	0.053720	0.3793469	0.0118*
70-20RAP-RT	70CO-RT	0.1310000	0.0508420	-0.031814	0.2938135	0.1208
70-20RAP-5P-RT	70-5P-RT	0.0243000	0.0508420	-0.138514	0.1871135	0.9619

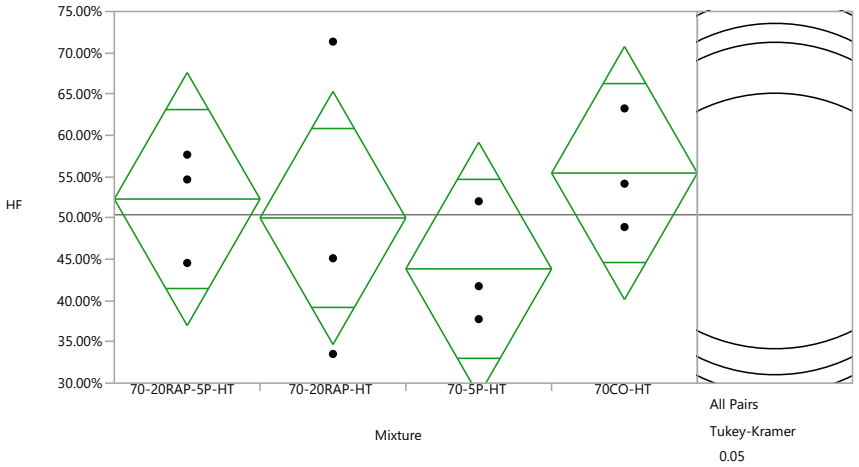

Figure C11. One-way analysis of crack healing at day 6 for PG 70-22M + 20%RAP (high temp/UV exposure).

Table C51. Summary of fit of crack healing at day 6 for PG 70-22M + 20%RAP (high temp/UV exposure).

Rsquare	0.169723
Adj Rsquare	-0.14163
Root Mean Square Error	0.115068
Mean of Response	0.503908
Observations (or Sum Wgts)	12

Table C52. Analysis of variance of crack healing at day 6 for PG 70-22M + 20%RAP (high temp/UV exposure).

Source	DF	Sum of Squares	Mean Square	F Ratio	Prob > F
Mixture	3	0.02165314	0.007218	0.5451	0.6651
Error	8	0.10592577	0.013241		
C. Total	11	0.12757891			

Table C53. Means for one-way ANOVA of crack healing at day 6 for PG 70-22M + 20%RAP (high temp/UV exposure).

Level	Number	Mean	Std Error	Lower 95%	Upper 95%
70-20RAP-5P-HT	3	0.522900	0.06643	0.36970	0.67610
70-20RAP-HT	3	0.500000	0.06643	0.34680	0.65320
70-5P-HT	3	0.438367	0.06643	0.28517	0.59157
70CO-HT	3	0.554367	0.06643	0.40117	0.70757

Table C54. Connecting letters report of crack healing at day 6 for PG 70-22M + 20%RAP (high temp/UV exposure).

Level		Mean
70CO-HT	A	0.55436667
70-20RAP-5P-HT	A	0.52290000
70-20RAP-HT	A	0.50000000
70-5P-HT	A	0.43836667

Table C55. Ordered differences report of crack healing at day 6 for PG 70-22M + 20%RAP (high temp/UV exposure).

Level	- Level	Difference	Std Err Dif	Lower CL	Upper CL	p-Value
70CO-HT	70-5P-HT	0.1160000	0.0939529	-0.184870	0.4168695	0.6242
70-20RAP-5P-HT	70-5P-HT	0.0845333	0.0939529	-0.216336	0.3854029	0.8055
70-20RAP-HT	70-5P-HT	0.0616333	0.0939529	-0.239236	0.3625029	0.9105
70CO-HT	70-20RAP-HT	0.0543667	0.0939529	-0.246503	0.3552362	0.9357
70CO-HT	70-20RAP-5P-HT	0.0314667	0.0939529	-0.269403	0.3323362	0.9861
70-20RAP-5P-HT	70-20RAP-HT	0.0229000	0.0939529	-0.277970	0.3237695	0.9945

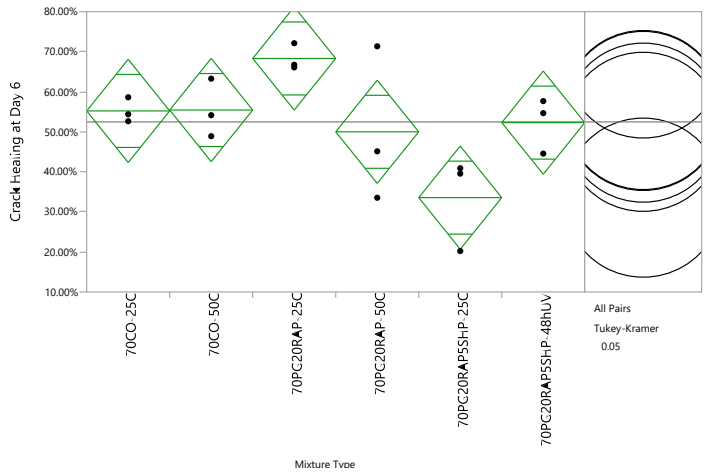

Figure C12. One-way analysis of crack healing at day 6 for PG 70-22M + 20%RAP (effect of curing conditions).

Table C56. Summary of fit of crack healing at day 6 for PG 70-22M + 20%RAP (effect of curing conditions).

Rsquare	0.600409
Adj Rsquare	0.433913
Root Mean Square Error	0.102468
Mean of Response	0.524689
Observations (or Sum Wgts)	18

Table C57. Analysis of variance of crack healing at day 6 for PG 70-22M + 20%RAP (effect of curing conditions).

Source	DF	Sum of Squares	Mean Square	F Ratio	Prob > F
Mixture Type	5	0.18931788	0.037864	3.6061	0.0319*
Error	12	0.12599680	0.010500		
C. Total	17	0.31531468			

Table C58. Means for one-way ANOVA of crack healing at day 6 for PG 70-22M + 20%RAP (effect of curing conditions).

Level	Number	Mean	Std Error	Lower 95%	Upper 95%
70CO-25C	3	0.552133	0.05916	0.42323	0.68103
70CO-50C	3	0.554367	0.05916	0.42547	0.68327
70-20RAP-25C	3	0.683133	0.05916	0.55423	0.81203
70-20RAP-50C	3	0.500000	0.05916	0.37110	0.62890
70-20RAP-5P-25C	3	0.335600	0.05916	0.20670	0.46450
70-20RAP-5P-48h	3	0.522900	0.05916	0.39400	0.65180

Table C59. Connecting letters report of crack healing at day 6 for PG 70-22M + 20%RAP (effect of curing conditions).

Level			Mean
70-20RAP-25C	A		0.68313333
70CO-50C	A	B	0.55436667
70CO-25C	A	B	0.55213333
70-20RAP-5P-48h	A	B	0.52290000
70-20RAP-50C	A	B	0.50000000
70-20RAP-5P-25C		B	0.33560000

Table C60. Ordered differences report of crack healing at day 6 for PG 70-22M + 20%RAP (effect of curing conditions).

Level	- Level	Difference	Std Err Dif	Lower CL	Upper CL	p-Value
70-20RAP-25C	70-20RAP-5P-25C	0.3475333	0.0836649	0.066514	0.6285525	0.0131*
70CO-50C	70-20RAP-5P-25C	0.2187667	0.0836649	-0.062252	0.4997858	0.1668
70CO-25C	70-20RAP-5P-25C	0.2165333	0.0836649	-0.064486	0.4975525	0.1738
70-20RAP-5P-48h	70-20RAP-5P-25C	0.1873000	0.0836649	-0.093719	0.4683192	0.2891
70-20RAP-25C	70-20RAP-50C	0.1831333	0.0836649	-0.097886	0.4641525	0.3094
70-20RAP-50C	70-20RAP-5P-25C	0.1644000	0.0836649	-0.116619	0.4454192	0.4129
70-20RAP-25C	70-20RAP-5P-48h	0.1602333	0.0836649	-0.120786	0.4412525	0.4384
70-20RAP-25C	70CO-25C	0.1310000	0.0836649	-0.150019	0.4120192	0.6331
70-20RAP-25C	70CO-50C	0.1287667	0.0836649	-0.152252	0.4097858	0.6484
70CO-50C	70-20RAP-50C	0.0543667	0.0836649	-0.226652	0.3353858	0.9844
70CO-25C	70-20RAP-50C	0.0521333	0.0836649	-0.228886	0.3331525	0.9870
70CO-50C	70-20RAP-5P-48h	0.0314667	0.0836649	-0.249552	0.3124858	0.9987
70CO-25C	70-20RAP-5P-48h	0.0292333	0.0836649	-0.251786	0.3102525	0.9991
70-20RAP-5P-48h	70-20RAP-50C	0.0229000	0.0836649	-0.258119	0.3039192	0.9997
70CO-50C	70CO-25C	0.0022333	0.0836649	-0.278786	0.2832525	1.0000

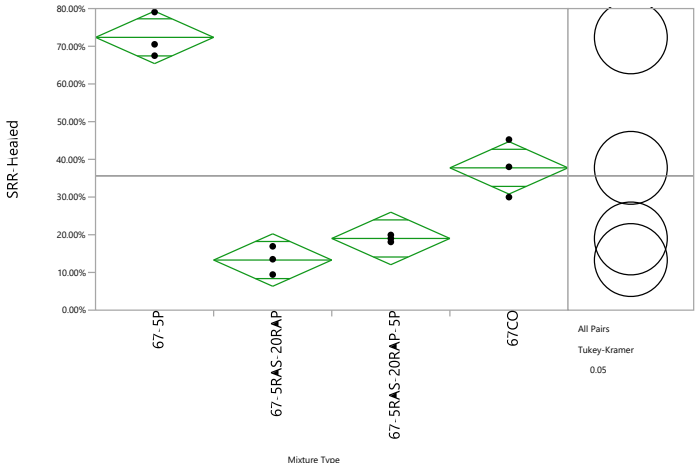

Figure C13. One-way analysis of crack healing at day 6 for PG 67-22 + 5%RAS+20%RAP (room temp).

Table C61. Summary of fit of crack healing at day 6 for PG 67-22 + 5%RAS+20%RAP (room temp).

Rsquare	0.966904
Adj Rsquare	0.954493
Root Mean Square Error	0.052271
Mean of Response	0.356033
Observations (or Sum Wgts)	12

Table C62. Analysis of variance of crack healing at day 6 for PG 67-22 + 5%RAS+20%RAP (room temp).

Source	DF	Sum of Squares	Mean Square	F Ratio	Prob > F
Mixture Type	3	0.63859463	0.212865	77.9068	<.0001*
Error	8	0.02185841	0.002732		
C. Total	11	0.66045305			

Table C63. Means for one-way ANOVA of crack healing at day 6 for PG 67-22 + 5%RAS+20%RAP (room temp).

Level	Number	Mean	Std Error	Lower 95%	Upper 95%
67-5P	3	0.723600	0.03018	0.65401	0.79319
67-5RAS-20RAP	3	0.132900	0.03018	0.06331	0.20249
67-5RAS-20RAP-5P	3	0.190167	0.03018	0.12057	0.25976
67CO	3	0.377467	0.03018	0.30787	0.44706

Table C64. Connecting letters report of crack healing at day 6 for PG 67-22 + 5%RAS+20%RAP (room temp).

Level				Mean
67-5P	A			0.72360000
67CO		B		0.37746667
67-5RAS-20RAP-5P			C	0.19016667
67-5RAS-20RAP			C	0.13290000

Table C65. Ordered differences report of crack healing at day 6 for PG 67-22 + 5%RAS+20%RAP (room temp).

Level	- Level	Difference	Std Err Dif	Lower CL	Upper CL	p-Value
67-5P	67-5RAS-20RAP	0.5907000	0.0426794	0.454026	0.7273742	<.0001*
67-5P	67-5RAS-20RAP-5P	0.5334333	0.0426794	0.396759	0.6701076	<.0001*
67-5P	67CO	0.3461333	0.0426794	0.209459	0.4828076	0.0002*
67CO	67-5RAS-20RAP	0.2445667	0.0426794	0.107892	0.3812409	0.0020*
67CO	67-5RAS-20RAP-5P	0.1873000	0.0426794	0.050626	0.3239742	0.0100*
67-5RAS-20RAP-5P	67-5RAS-20RAP	0.0572667	0.0426794	-0.079408	0.1939409	0.5646

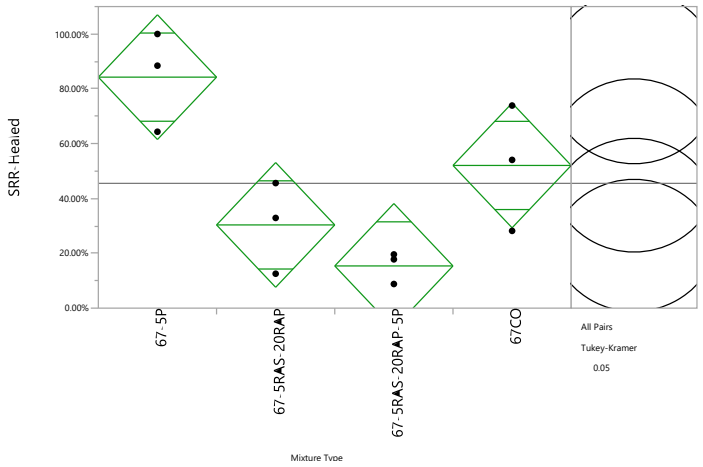

Figure C14. One-way analysis of crack healing at day 6 for PG 67-22 + 5%RAS + 20%RAP (high temp/UV exposure).

Table C66. Summary of fit of crack healing at day 6 for PG 67-22 + 5%RAS + 20%RAP (high temp/UV exposure).

Rsquare	0.774946
Adj Rsquare	0.69055
Root Mean Square Error	0.170865
Mean of Response	0.455125
Observations (or Sum Wgts)	12

Table C67. Analysis of variance of crack healing at day 6 for PG 67-22 + 5%RAS + 20%RAP (high temp/UV exposure).

Source	DF	Sum of Squares	Mean Square	F Ratio	Prob > F
Mixture Type	3	0.8042311	0.268077	9.1823	0.0057*
Error	8	0.2335593	0.029195		
C. Total	11	1.0377904			

Table C68. Means for one-way ANOVA of crack healing at day 6 for PG 67-22 + 5%RAS + 20%RAP (high temp/UV exposure).

Level	Number	Mean	Std Error	Lower 95%	Upper 95%
67-5P	3	0.842567	0.09865	0.6151	1.0701
67-5RAS-20RAP	3	0.303533	0.09865	0.0760	0.5310
67-5RAS-20RAP-5P	3	0.153933	0.09865	-0.0736	0.3814
67CO	3	0.520467	0.09865	0.2930	0.7480

Table C69. Connecting letters report of crack healing at day 6 for PG 67-22 + 5%RAS + 20%RAP (high temp/UV exposure).

Level			Mean
67-5P	A		0.84256667
67CO	A	B	0.52046667
67-5RAS-20RAP		B	0.30353333
67-5RAS-20RAP-5P		B	0.15393333

Table C70. Ordered differences report of crack healing at day 6 for PG 67-22 + 5%RAS + 20%RAP (high temp/UV exposure).

Level	- Level	Difference	Std Err Dif	Lower CL	Upper CL	p-Value
67-5P	67-5RAS-20RAP-5P	0.6886333	0.1395108	0.241872	1.135395	0.0050*
67-5P	67-5RAS-20RAP	0.5390333	0.1395108	0.092272	0.985795	0.0200*
67CO	67-5RAS-20RAP-5P	0.3665333	0.1395108	-0.080228	0.813295	0.1125
67-5P	67CO	0.3221000	0.1395108	-0.124662	0.768862	0.1750
67CO	67-5RAS-20RAP	0.2169333	0.1395108	-0.229828	0.663695	0.4521
67-5RAS-20RAP	67-5RAS-20RAP-5P	0.1496000	0.1395108	-0.297162	0.596362	0.7147

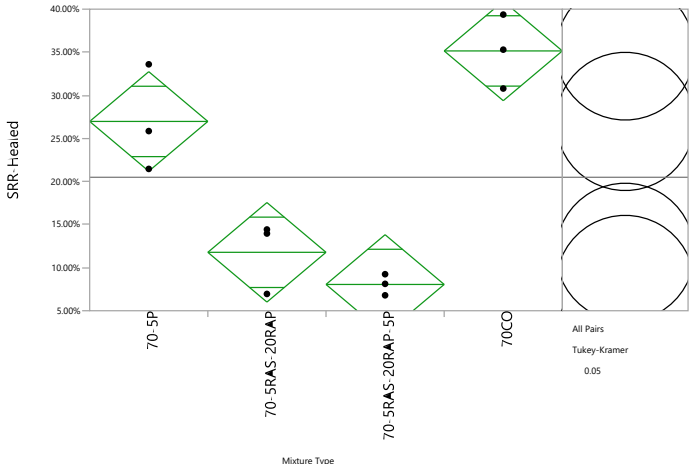

Figure C15. One-way analysis of crack healing at day 6 for PG 70-22M + 5%RAS + 20%RAP (room temp).

Table C71. Summary of fit of crack healing at day 6 for PG 70-22M + 5%RAS + 20%RAP (room temp).

Rsquare	0.906703
Adj Rsquare	0.871717
Root Mean Square Error	0.043377
Mean of Response	0.204883
Observations (or Sum Wgts)	12

Table C72. Analysis of variance of crack healing at day 6 for PG 70-22M + 5%RAS + 20%RAP (room temp).

Source	DF	Sum of Squares	Mean Square	F Ratio	Prob > F
Mixture Type	3	0.14628643	0.048762	25.9159	0.0002*
Error	8	0.01505243	0.001882		
C. Total	11	0.16133886			

Table C73. Means for one-way ANOVA of crack healing at day 6 for PG 70-22M + 5%RAS + 20%RAP (room temp).

Level	Number	Mean	Std Error	Lower 95%	Upper 95%
70-5P	3	0.269700	0.02504	0.21195	0.32745
70-5RAS-20RAP	3	0.117800	0.02504	0.06005	0.17555
70-5RAS-20RAP-5P	3	0.080500	0.02504	0.02275	0.13825
70CO	3	0.351533	0.02504	0.29378	0.40928

Table C74. Connecting letters report of crack healing at day 6 for PG 70-22M + 5%RAS + 20%RAP (room temp).

Level			Mean
70CO	A		0.35153333
70-5P	A		0.26970000
70-5RAS-20RAP		B	0.11780000
70-5RAS-20RAP-5P		B	0.08050000

Table C75. Ordered differences report of crack healing at day 6 for PG 70-22M + 5%RAS + 20%RAP (room temp).

Level	- Level	Difference	Std Err Dif	Lower CL	Upper CL	p-Value
70CO	70-5RAS-20RAP-5P	0.2710333	0.0354171	0.157616	0.3844510	0.0003*
70CO	70-5RAS-20RAP	0.2337333	0.0354171	0.120316	0.3471510	0.0008*
70-5P	70-5RAS-20RAP-5P	0.1892000	0.0354171	0.075782	0.3026176	0.0031*
70-5P	70-5RAS-20RAP	0.1519000	0.0354171	0.038482	0.2653176	0.0114*
70CO	70-5P	0.0818333	0.0354171	-0.031584	0.1952510	0.1746
70-5RAS-20RAP	70-5RAS-20RAP-5P	0.0373000	0.0354171	-0.076118	0.1507176	0.7252

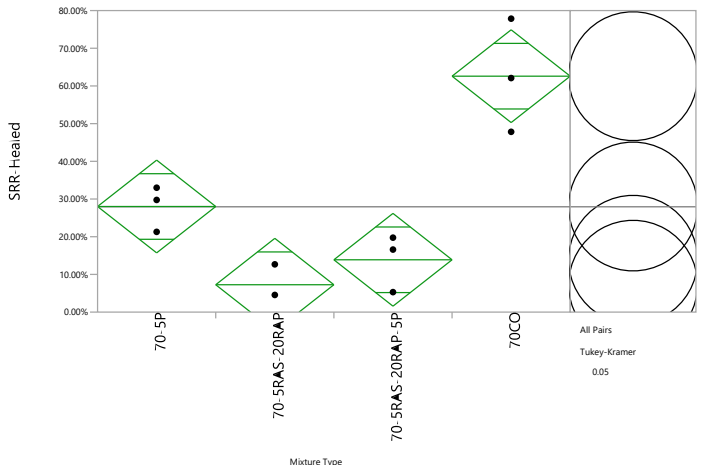

Figure C16. One-way analysis of crack healing at day 6 for PG 70-22M + 5%RAS + 20%RAP (high temp/UV exposure).

Table C76. Summary of fit of crack healing at day 6 for PG 70-22M + 5%RAS + 20%RAP (high temp/UV exposure).

Rsquare	0.88908
Adj Rsquare	0.847485
Root Mean Square Error	0.092427
Mean of Response	0.279367
Observations (or Sum Wgts)	12

Table C77. Analysis of variance of crack healing at day 6 for PG 70-22M + 5%RAS + 20%RAP (high temp/UV exposure).

Source	DF	Sum of Squares	Mean Square	F Ratio	Prob > F
Mixture Type	3	0.54779230	0.182597	21.3747	0.0004*
Error	8	0.06834157	0.008543		
C. Total	11	0.61613387			

Table C78. Means for one-way ANOVA of crack healing at day 6 for PG 70-22M + 5%RAS + 20%RAP (high temp/UV exposure).

Level	Number	Mean	Std Error	Lower 95%	Upper 95%
70-5P	3	0.280167	0.05336	0.1571	0.40322
70-5RAS-20RAP	3	0.072600	0.05336	-0.0505	0.19565
70-5RAS-20RAP-5P	3	0.138800	0.05336	0.0157	0.26185
70CO	3	0.625900	0.05336	0.5028	0.74895

Table C79. Connecting letters report of crack healing at day 6 for PG 70-22M + 5%RAS + 20%RAP (high temp/UV exposure).

Level			Mean
70CO	A		0.62590000
70-5P		B	0.28016667
70-5RAS-20RAP-5P		B	0.13880000
70-5RAS-20RAP		B	0.07260000

Table C80. Ordered differences report of crack healing at day 6 for PG 70-22M + 5%RAS + 20%RAP (high temp/UV exposure).

Level	- Level	Difference	Std Err Dif	Lower CL	Upper CL	p-Value
70CO	70-5RAS-20RAP	0.5533000	0.0754661	0.311632	0.7949684	0.0004*
70CO	70-5RAS-20RAP-5P	0.4871000	0.0754661	0.245432	0.7287684	0.0009*
70CO	70-5P	0.3457333	0.0754661	0.104065	0.5874017	0.0078*
70-5P	70-5RAS-20RAP	0.2075667	0.0754661	-0.034102	0.4492351	0.0946
70-5P	70-5RAS-20RAP-5P	0.1413667	0.0754661	-0.100302	0.3830351	0.3103
70-5RAS-20RAP-5P	70-5RAS-20RAP	0.0662000	0.0754661	-0.175468	0.3078684	0.8166

C.2. Statistical Analysis for Measured SERR

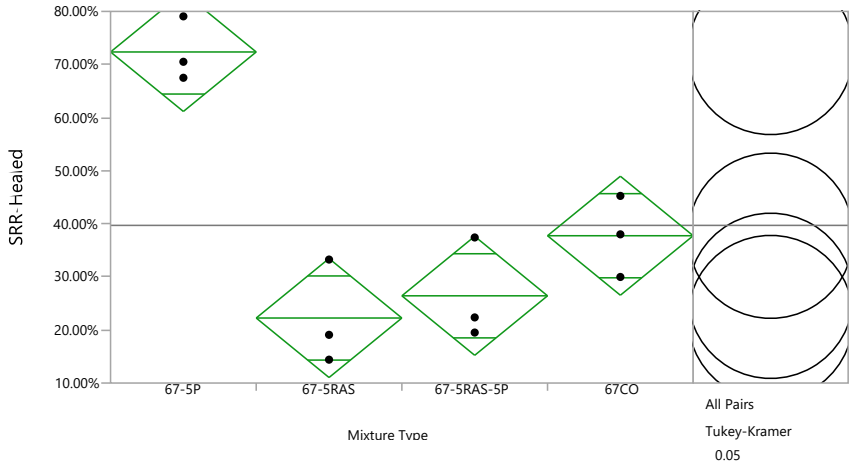

Figure C17. One-way analysis of SERR-Healed for PG 67-22 +5%RAS (room temp).

Table C81. Summary of fit of SERR-Healed for PG 67-22 +5%RAS (room temp).

Rsquare	0.891413
Adj Rsquare	0.850692
Root Mean Square Error	0.084178
Mean of Response	0.396958
Observations (or Sum Wgts)	12

Table C82. Analysis of variance of SERR-Healed for PG 67-22 +5%RAS (room temp).

Source	DF	Sum of Squares	Mean Square	F Ratio	Prob > F
Mixture Type	3	0.46536084	0.155120	21.8911	0.0003*
Error	8	0.05668795	0.007086		
C. Total	11	0.52204879			

Table C83. Means for one-way ANOVA of SERR-Healed for PG 67-22 +5%RAS (room temp).

Level	Number	Mean	Std Error	Lower 95%	Upper 95%
67-5P	3	0.723600	0.04860	0.61153	0.83567
67-5RAS	3	0.222467	0.04860	0.11039	0.33454
67-5RAS-5P	3	0.264300	0.04860	0.15223	0.37637
67CO	3	0.377467	0.04860	0.26539	0.48954

Table C84. Connecting letters report of SERR-Healed for PG 67-22 +5%RAS (room temp).

Level			Mean
67-5P	A		0.72360000
67CO		B	0.37746667
67-5RAS-5P		B	0.26430000
67-5RAS		B	0.22246667

Table C85. Ordered differences report of SERR-Healed for PG 67-22 +5%RAS (room temp).

Level	- Level	Difference	Std Err Dif	Lower CL	Upper CL	p-Value
67-5P	67-5RAS	0.5011333	0.0687313	0.281032	0.7212347	0.0004*
67-5P	67-5RAS-5P	0.4593000	0.0687313	0.239199	0.6794014	0.0007*
67-5P	67CO	0.3461333	0.0687313	0.126032	0.5662347	0.0044*
67CO	67-5RAS	0.1550000	0.0687313	-0.065101	0.3751014	0.1882
67CO	67-5RAS-5P	0.1131667	0.0687313	-0.106935	0.3332680	0.4077
67-5RAS-5P	67-5RAS	0.0418333	0.0687313	-0.178268	0.2619347	0.9265

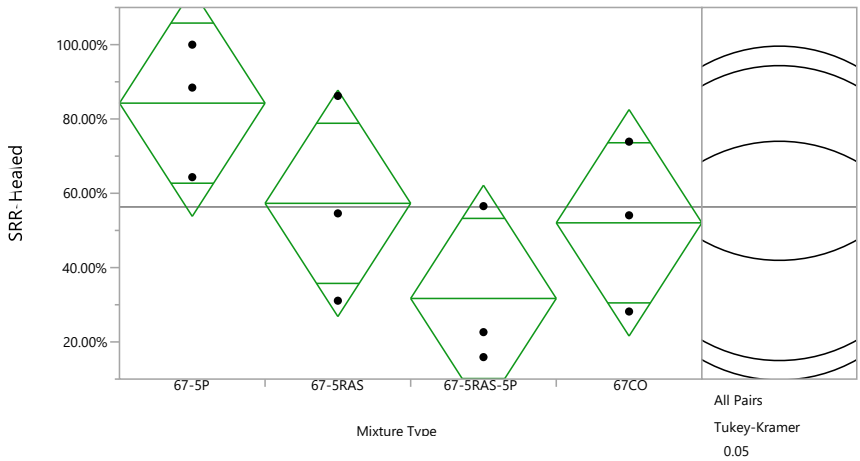

Figure C18. One-way analysis of SERR-Healed for PG 67-22 +5%RAs (high temp/UV exposure).

Table C86. Summary of fit of SERR-Healed for PG 67-22 +5%RAS (high temp/UV exposure).

Rsquare	0.501649
Adj Rsquare	0.314767
Root Mean Square Error	0.228875
Mean of Response	0.563225
Observations (or Sum Wgts)	12

Table C87. Analysis of variance of SERR-Healed for PG 67-22 +5%RAS (high temp/UV exposure).

Source	DF	Sum of Squares	Mean Square	F Ratio	Prob > F
Mixture Type	3	0.42184164	0.140614	2.6843	0.1175
Error	8	0.41906871	0.052384		
C. Total	11	0.84091034			

Table C88. Means for one-way ANOVA of SERR-Healed for PG 67-22 +5%RAS (high temp/UV exposure).

Level	Number	Mean	Std Error	Lower 95%	Upper 95%
67-5P	3	0.842567	0.13214	0.53785	1.1473
67-5RAS	3	0.572933	0.13214	0.26822	0.8777
67-5RAS-5P	3	0.316933	0.13214	0.01222	0.6217
67CO	3	0.520467	0.13214	0.21575	0.8252

Table C89. Connecting letters report of SERR-Healed for PG 67-22 +5%RAS (high temp/UV exposure).

Level		Mean
67-5P	A	0.84256667
67-5RAS	A	0.57293333
67CO	A	0.52046667
67-5RAS-5P	A	0.31693333

Table C90. Ordered differences report of SERR-Healed for PG 67-22 +5%RAS (high temp/UV exposure).

Level	- Level	Difference	Std Err Dif	Lower CL	Upper CL	p-Value
67-5P	67-5RAS-5P	0.5256333	0.1868753	-0.072806	1.124072	0.0867
67-5P	67CO	0.3221000	0.1868753	-0.276339	0.920539	0.3725
67-5P	67-5RAS	0.2696333	0.1868753	-0.328806	0.868072	0.5100
67-5RAS	67-5RAS-5P	0.2560000	0.1868753	-0.342439	0.854439	0.5492
67CO	67-5RAS-5P	0.2035333	0.1868753	-0.394906	0.801972	0.7054
67-5RAS	67CO	0.0524667	0.1868753	-0.545972	0.650906	0.9917

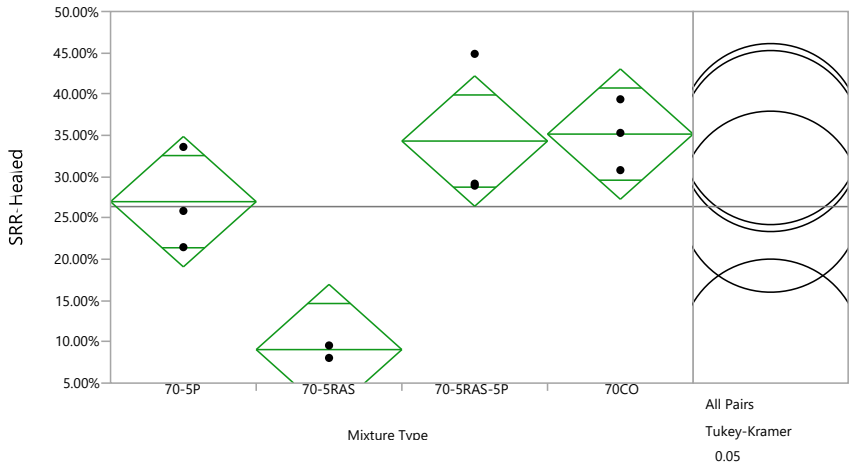

Figure C19. One-way analysis of SERR-Healed for PG 70-22M +5%RAS (room temp).

Table C90. Summary of fit of SERR-Healed for PG 70-22M +5%RAS (room temp).

Rsquare	0.824465
Adj Rsquare	0.758639
Root Mean Square Error	0.059291
Mean of Response	0.263725
Observations (or Sum Wgts)	12

Table C91. Analysis of variance of SERR-Healed for PG 70-22M +5%RAS (room temp).

Source	DF	Sum of Squares	Mean Square	F Ratio	Prob > F
Mixture Type	3	0.13209061	0.044030	12.5250	0.0022*
Error	8	0.02812311	0.003515		
C. Total	11	0.16021372			

Table C92. Means for one-way ANOVA of SERR-Healed for PG 70-22M +5%RAS (room temp).

Level	Number	Mean	Std Error	Lower 95%	Upper 95%
70-5P	3	0.269700	0.03423	0.19076	0.34864
70-5RAS	3	0.090567	0.03423	0.01163	0.16950
70-5RAS-5P	3	0.343100	0.03423	0.26416	0.42204
70CO	3	0.351533	0.03423	0.27260	0.43047

Table C93. Connecting letters report of SERR-Healed for PG 70-22M +5%RAS (room temp).

Level			Mean
70CO	A		0.35153333
70-5RAS-5P	A		0.34310000
70-5P	A		0.26970000
70-5RAS		B	0.09056667

Table C94. Ordered differences report of SERR-Healed for PG 70-22M +5%RAS (room temp).

Level	- Level	Difference	Std Err Dif	Lower CL	Upper CL	p-Value
70CO	70-5RAS	0.2609667	0.0484107	0.105939	0.4159943	0.0029*
70-5RAS-5P	70-5RAS	0.2525333	0.0484107	0.097506	0.4075610	0.0036*
70-5P	70-5RAS	0.1791333	0.0484107	0.024106	0.3341610	0.0250*
70CO	70-5P	0.0818333	0.0484107	-0.073194	0.2368610	0.3874
70-5RAS-5P	70-5P	0.0734000	0.0484107	-0.081628	0.2284276	0.4717
70CO	70-5RAS-5P	0.0084333	0.0484107	-0.146594	0.1634610	0.9980

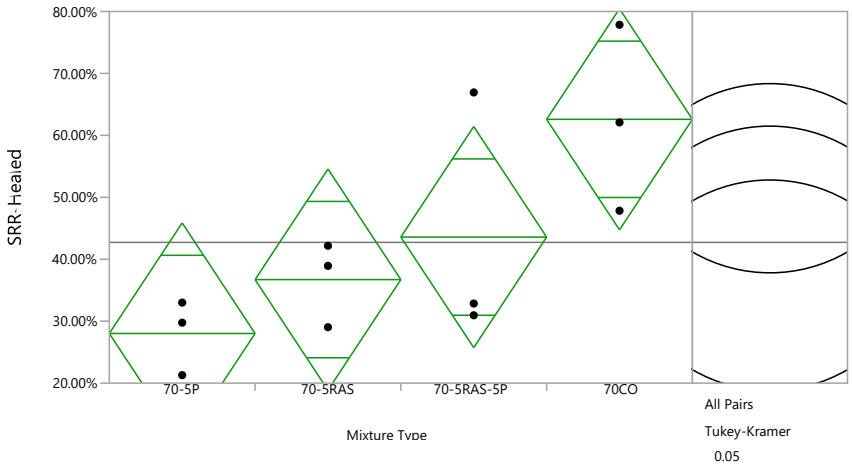

Figure C20. One-way analysis of SERR-Healed for PG 70-22M +5%RAS (high temp/UV exposure).

Table C95. Summary of fit of SERR-Healed for PG 70-22M +5%RAS (high temp/UV exposure).

Rsquare	0.574773
Adj Rsquare	0.415313
Root Mean Square Error	0.134062
Mean of Response	0.427242
Observations (or Sum Wgts)	12

Table C96. Analysis of variance of SERR-Healed for PG 70-22M +5%RAS (high temp/UV exposure).

Source	DF	Sum of Squares	Mean Square	F Ratio	Prob > F
Mixture Type	3	0.19434563	0.064782	3.6045	0.0653
Error	8	0.14378000	0.017973		
C. Total	11	0.33812563			

Table C97. Means for one-way ANOVA of SERR-Healed for PG 70-22M +5%RAS (high temp/UV exposure).

Level	Number	Mean	Std Error	Lower 95%	Upper 95%
70-5P	3	0.280167	0.07740	0.10168	0.45865
70-5RAS	3	0.367133	0.07740	0.18865	0.54562
70-5RAS-5P	3	0.435767	0.07740	0.25728	0.61425
70CO	3	0.625900	0.07740	0.44741	0.80439

Table C98. Connecting letters report of SERR-Healed for PG 70-22M +5%RAS (high temp/UV exposure).

Level		Mean
70CO	A	0.62590000
70-5RAS-5P	A	0.43576667
70-5RAS	A	0.36713333
70-5P	A	0.28016667

Table C100. Ordered differences report of SERR-Healed for PG 70-22M +5%RAS (high temp/UV exposure).

Level	- Level	Difference	Std Err Dif	Lower CL	Upper CL	p-Value
70CO	70-5P	0.3457333	0.1094608	-0.004798	0.6962645	0.0532
70CO	70-5RAS	0.2587667	0.1094608	-0.091764	0.6092978	0.1622
70CO	70-5RAS-5P	0.1901333	0.1094608	-0.160398	0.5406645	0.3666
70-5RAS-5P	70-5P	0.1556000	0.1094608	-0.194931	0.5061311	0.5213
70-5RAS	70-5P	0.0869667	0.1094608	-0.263564	0.4374978	0.8551
70-5RAS-5P	70-5RAS	0.0686333	0.1094608	-0.281898	0.4191645	0.9205

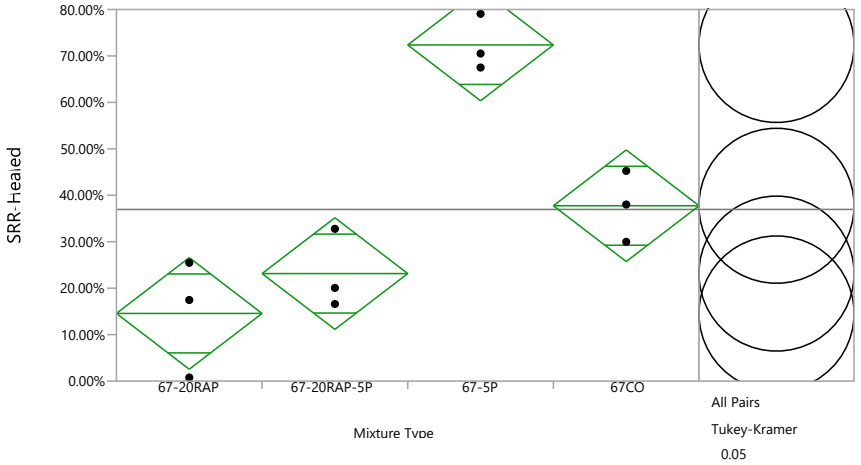

Figure C21. One-way analysis of SERR-Healed for PG 67-22 +20%RAP (room temp).

Table C99. Summary of fit of SERR-Healed for PG 67-22 +20%RAP (room temp).

Rsquare	0.899603
Adj Rsquare	0.861954
Root Mean Square Error	0.090246
Mean of Response	0.36955
Observations (or Sum Wgts)	12

Table C100. Analysis of variance of SERR-Healed for PG 67-22 +20%RAP (room temp).

Source	DF	Sum of Squares	Mean Square	F Ratio	Prob > F
Mixture Type	3	0.58381449	0.194605	23.8945	0.0002*
Error	8	0.06515462	0.008144		
C. Total	11	0.64896911			

Table C101. Means for one-way ANOVA of SERR-Healed for PG 67-22 +20%RAP (room temp).

Level	Number	Mean	Std Error	Lower 95%	Upper 95%
67-20RAP	3	0.145667	0.05210	0.02552	0.26582
67-20RAP-5P	3	0.231467	0.05210	0.11132	0.35162
67-5P	3	0.723600	0.05210	0.60345	0.84375
67CO	3	0.377467	0.05210	0.25732	0.49762

Table C102. Connecting letters report of SERR-Healed for PG 67-22 +20%RAP (room temp).

Level			Mean
67-5P	A		0.72360000
67CO		B	0.37746667
67-20RAP-5P		B	0.23146667
67-20RAP		B	0.14566667

Table C103. Ordered differences report of SERR-Healed for PG 67-22 +20%RAP (room temp).

Level	- Level	Difference	Std Err Dif	Lower CL	Upper CL	p-Value
67-5P	67-20RAP	0.5779333	0.0736855	0.341967	0.8138996	0.0002*
67-5P	67-20RAP-5P	0.4921333	0.0736855	0.256167	0.7280996	0.0007*
67-5P	67CO	0.3461333	0.0736855	0.110167	0.5820996	0.0067*
67CO	67-20RAP	0.2318000	0.0736855	-0.004166	0.4677663	0.0541
67CO	67-20RAP-5P	0.1460000	0.0736855	-0.089966	0.3819663	0.2705
67-20RAP-5P	67-20RAP	0.0858000	0.0736855	-0.150166	0.3217663	0.6636

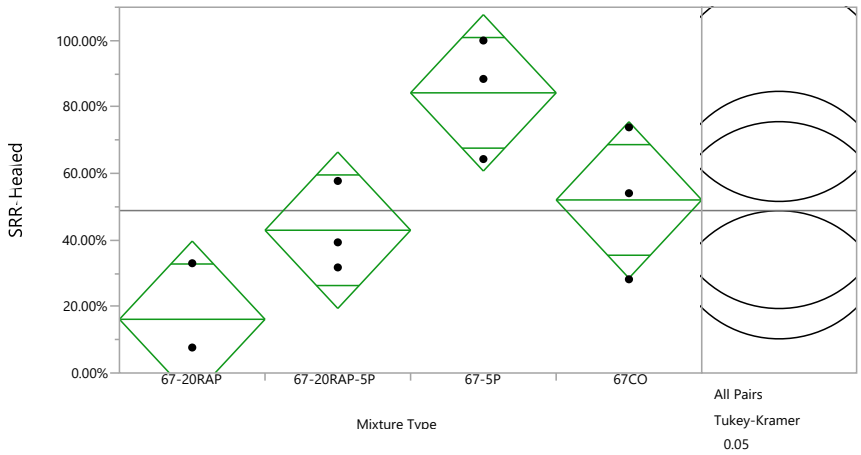

Figure C22. One-way analysis of SERR-Healed for PG 67-22 +20%RAP (high temp/UV exposure).

Table C104. Summary of fit of SERR-Healed for PG 67-22 +20%RAP (high temp/UV exposure).

Rsquare	0.739926
Adj Rsquare	0.642398
Root Mean Square Error	0.176675
Mean of Response	0.488467
Observations (or Sum Wgts)	12

Table C105. Analysis of variance of SERR-Healed for PG 67-22 +20%RAP (high temp/UV exposure).

Source	DF	Sum of Squares	Mean Square	F Ratio	Prob > F
Mixture Type	3	0.71044429	0.236815	7.5868	0.0100*
Error	8	0.24971220	0.031214		
C. Total	11	0.96015649			

Table C106. Means for one-way ANOVA of SERR-Healed for PG 67-22 +20%RAP (high temp/UV exposure).

Level	Number	Mean	Std Error	Lower 95%	Upper 95%
67-20RAP	3	0.161500	0.10200	-0.0737	0.3967
67-20RAP-5P	3	0.429333	0.10200	0.1941	0.6646
67-5P	3	0.842567	0.10200	0.6073	1.0778
67CO	3	0.520467	0.10200	0.2852	0.7557

Table C107. Connecting letters report of SERR-Healed for PG 67-22 +20%RAP (high temp/UV exposure).

Level			Mean
67-5P	A		0.84256667
67CO	A	B	0.52046667
67-20RAP-5P	A	B	0.42933333
67-20RAP		B	0.16150000

Table C108. Ordered differences report of SERR-Healed for PG 67-22 +20%RAP (high temp/UV exposure).

Level	- Level	Difference	Std Err Dif	Lower CL	Upper CL	p-Value
67-5P	67-20RAP	0.6810667	0.1442545	0.219114	1.143019	0.0065*
67-5P	67-20RAP-5P	0.4132333	0.1442545	-0.048719	0.875186	0.0805
67CO	67-20RAP	0.3589667	0.1442545	-0.102986	0.820919	0.1366
67-5P	67CO	0.3221000	0.1442545	-0.139852	0.784052	0.1940
67-20RAP-5P	67-20RAP	0.2678333	0.1442545	-0.194119	0.729786	0.3168
67CO	67-20RAP-5P	0.0911333	0.1442545	-0.370819	0.553086	0.9189

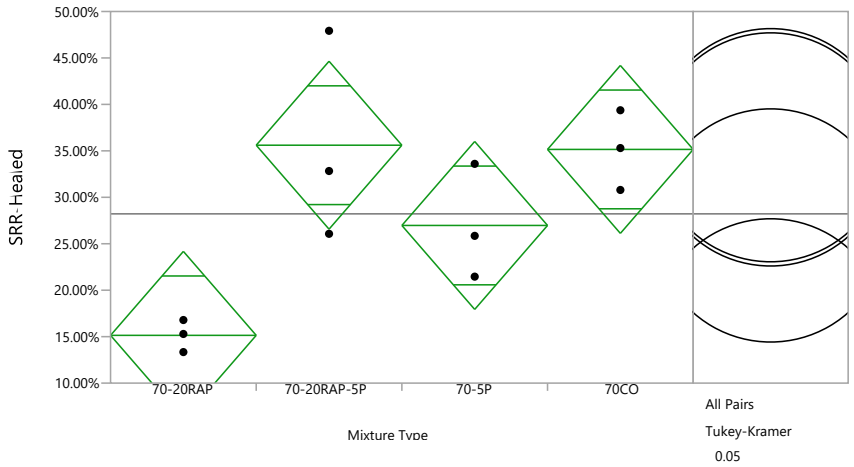

Figure C23. One-way analysis of SERR-Healed for PG 70-22M +20%RAP (room temp).

Table C109. Summary of fit of SERR-Healed for PG 70-22M +20%RAP (room temp).

Rsquare	0.691363
Adj Rsquare	0.575625
Root Mean Square Error	0.067885
Mean of Response	0.282175
Observations (or Sum Wgts)	12

Table C110. Analysis of variance of SERR-Healed for PG 70-22M +20%RAP (room temp).

Source	DF	Sum of Squares	Mean Square	F Ratio	Prob > F
Mixture Type	3	0.08258485	0.027528	5.9735	0.0194*
Error	8	0.03686729	0.004608		
C. Total	11	0.11945214			

Table C111. Means for one-way ANOVA of SERR-Healed for PG 70-22M +20%RAP (room temp).

Level	Number	Mean	Std Error	Lower 95%	Upper 95%
70-20RAP	3	0.151400	0.03919	0.06102	0.24178
70-20RAP-5P	3	0.356067	0.03919	0.26569	0.44645
70-5P	3	0.269700	0.03919	0.17932	0.36008
70CO	3	0.351533	0.03919	0.26115	0.44191

Table C112. Connecting letters report of SERR-Healed for PG 70-22M +20%RAP (room temp).

Level			Mean
70-20RAP-5P	A		0.35606667
70CO	A		0.35153333
70-5P	A	B	0.26970000
70-20RAP		B	0.15140000

Table C113. Ordered differences report of SERR-Healed for PG 70-22M +20%RAP (room temp).

Level	- Level	Difference	Std Err Dif	Lower CL	Upper CL	p-Value
70-20RAP-5P	70-20RAP	0.2046667	0.0554281	0.027167	0.3821665	0.0253*
70CO	70-20RAP	0.2001333	0.0554281	0.022633	0.3776332	0.0283*
70-5P	70-20RAP	0.1183000	0.0554281	-0.059200	0.2957999	0.2214
70-20RAP-5P	70-5P	0.0863667	0.0554281	-0.091133	0.2638665	0.4505
70CO	70-5P	0.0818333	0.0554281	-0.095667	0.2593332	0.4923
70-20RAP-5P	70CO	0.0045333	0.0554281	-0.172967	0.1820332	0.9998

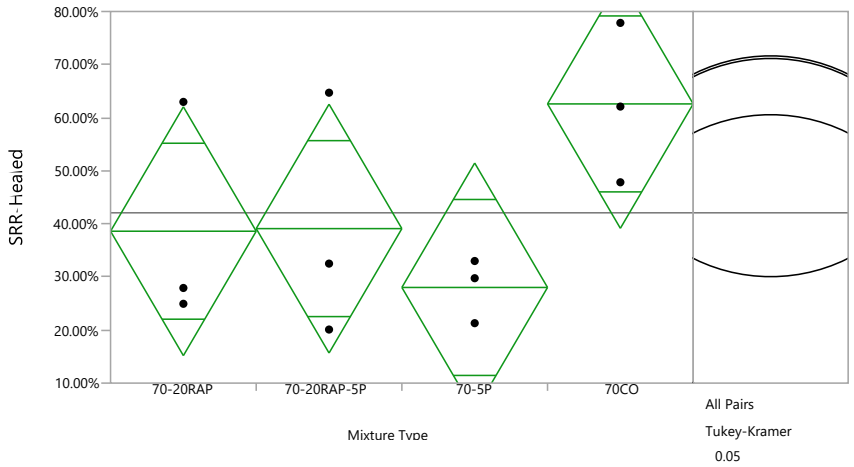

Figure C24. One-way analysis of SERR-Healed for PG 70-22M +20%RAP (high temp/UV exposure).

Table C114. Summary of fit of SERR-Healed for PG 70-22M +20%RAP (high temp/UV exposure).

Parameter	Value
Rsquare	0.436234
Adj Rsquare	0.224822
Root Mean Square Error	0.176026
Mean of Response	0.420792
Observations (or Sum Wgts)	12

Table C115. Analysis of variance of SERR-Healed for PG 70-22M +20%RAP (high temp/UV exposure).

Source	DF	Sum of Squares	Mean Square	F Ratio	Prob > F
Mixture Type	3	0.19180762	0.063936	2.0634	0.1836
Error	8	0.24788189	0.030985		
C. Total	11	0.43968951			

Table C116. Means for one-way ANOVA of SERR-Healed for PG 70-22M +20%RAP (high temp/UV exposure).

Level	Number	Mean	Std Error	Lower 95%	Upper 95%
70-20RAP	3	0.386100	0.10163	0.15174	0.62046
70-20RAP-5P	3	0.391000	0.10163	0.15664	0.62536
70-5P	3	0.280167	0.10163	0.04581	0.51452
70CO	3	0.625900	0.10163	0.39154	0.86026

Table C117. Connecting letters report of SERR-Healed for PG 70-22M +20%RAP (high temp/UV exposure).

Level		Mean
70CO	A	0.62590000
70-20RAP-5P	A	0.39100000
70-20RAP	A	0.38610000
70-5P	A	0.28016667

Table C118. Ordered differences report of SERR-Healed for PG 70-22M +20%RAP (high temp/UV exposure).

Level	- Level	Difference	Std Err Dif	Lower CL	Upper CL	p-Value
70CO	70-5P	0.3457333	0.1437248	-0.114523	0.8059897	0.1532
70CO	70-20RAP	0.2398000	0.1437248	-0.220456	0.7000563	0.3975
70CO	70-20RAP-5P	0.2349000	0.1437248	-0.225356	0.6951563	0.4134
70-20RAP-5P	70-5P	0.1108333	0.1437248	-0.349423	0.5710897	0.8653
70-20RAP	70-5P	0.1059333	0.1437248	-0.354323	0.5661897	0.8796
70-20RAP-5P	70-20RAP	0.0049000	0.1437248	-0.455356	0.4651563	1.0000

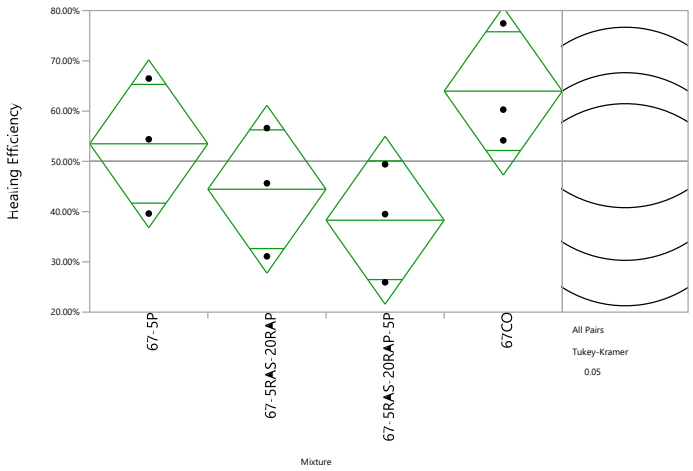

Figure C25. One-way analysis of SERR-Healed for PG 67-22 +5%RAS+20%RAP (room temp).

Table C119. Summary of fit of SERR-Healed for PG 67-22 +5%RAS+20%RAP (room temp).

Parameter	Value
Rsquare	0.472184
Adj Rsquare	0.274253
Root Mean Square Error	0.125443
Mean of Response	0.5005
Observations (or Sum Wgts)	12

Table C120. Analysis of variance of SERR-Healed for PG 67-22 +5%RAS+20%RAP (room temp).

Source	DF	Sum of Squares	Mean Square	F Ratio	Prob > F
Mixture	3	0.11262002	0.037540	2.3856	0.1448
Error	8	0.12588856	0.015736		
C. Total	11	0.23850858			

Table C121. Means for one-way ANOVA of SERR-Healed for PG 67-22 +5%RAS+20%RAP (room temp).

Level	Number	Mean	Std Error	Lower 95%	Upper 95%
67-5P	3	0.534933	0.07242	0.36792	0.70195
67-5RAS-20RAP	3	0.444533	0.07242	0.27752	0.61155
67-5RAS-20RAP-5P	3	0.382833	0.07242	0.21582	0.54985
67CO	3	0.639700	0.07242	0.47269	0.80671

Table C122. Connecting letters report of SERR-Healed for PG 67-22 +5%RAS+20%RAP (room temp).

Level		Mean
67CO	A	0.63970000
67-5P	A	0.53493333
67-5RAS-20RAP	A	0.44453333
67-5RAS-20RAP-5P	A	0.38283333

Table C123. Ordered differences report of SERR-Healed for PG 67-22 +5%RAS+20%RAP (room temp).

Level	- Level	Difference	Std Err Dif	Lower CL	Upper CL	p-Value
67CO	67-5RAS-20RAP-5P	0.2568667	0.1024242	-0.071131	0.5848641	0.1330
67CO	67-5RAS-20RAP	0.1951667	0.1024242	-0.132831	0.5231641	0.2980
67-5P	67-5RAS-20RAP-5P	0.1521000	0.1024242	-0.175897	0.4800975	0.4878
67CO	67-5P	0.1047667	0.1024242	-0.223231	0.4327641	0.7416
67-5P	67-5RAS-20RAP	0.0904000	0.1024242	-0.237597	0.4183975	0.8140
67-5RAS-20RAP	67-5RAS-20RAP-5P	0.0617000	0.1024242	-0.266297	0.3896975	0.9285

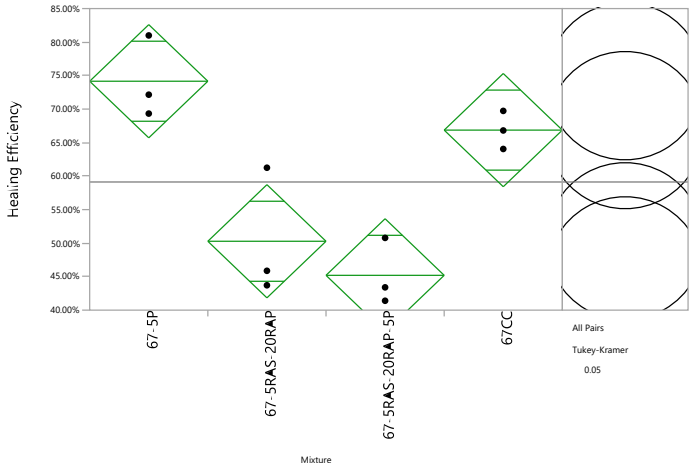

Figure C26. One-way analysis of SERR-Healed for PG 67-22 +5%RAS+20%RAP (high temp/UV exposure).

Table C124. Summary of fit of SERR-Healed for PG 67-22 +5%RAS+20%RAP (high temp/UV exposure).

Parameter	Value
Rsquare	0.838762
Adj Rsquare	0.778298
Root Mean Square Error	0.063435
Mean of Response	0.591225
Observations (or Sum Wgts)	12

Table C125. Analysis of variance of SERR-Healed for PG 67-22 +5%RAS+20%RAP (high temp/UV exposure).

Source	DF	Sum of Squares	Mean Square	F Ratio	Prob > F
Mixture	3	0.16746514	0.055822	13.8720	0.0016*
Error	8	0.03219235	0.004024		
C. Total	11	0.19965748			

Table C126. Means for one-way ANOVA of SERR-Healed for PG 67-22 +5%RAS+20%RAP (high temp/UV exposure).

Level	Number	Mean	Std Error	Lower 95%	Upper 95%
67-5P	3	0.741567	0.03662	0.65711	0.82602
67-5RAS-20RAP	3	0.502767	0.03662	0.41831	0.58722
67-5RAS-20RAP-5P	3	0.451933	0.03662	0.36748	0.53639
67CC	3	0.668633	0.03662	0.58418	0.75309

Table C127. Connecting letters report of SERR-Healed for PG 67-22 +5%RAS+20%RAP (high temp/UV exposure).

Level			Mean
67-5P	A		0.74156667
67CC	A		0.66863333
67-5RAS-20RAP		B	0.50276667
67-5RAS-20RAP-5P		B	0.45193333

Table C128. Ordered differences report of SERR-Healed for PG 67-22 +5%RAS+20%RAP (high temp/UV exposure).

Level	- Level	Difference	Std Err Dif	Lower CL	Upper CL	p-Value
67-5P	67-5RAS-20RAP-5P	0.2896333	0.0517947	0.123769	0.4554979	0.0023*
67-5P	67-5RAS-20RAP	0.2388000	0.0517947	0.072935	0.4046646	0.0075*
67CC	67-5RAS-20RAP-5P	0.2167000	0.0517947	0.050835	0.3825646	0.0130*
67CC	67-5RAS-20RAP	0.1658667	0.0517947	2.0716e-6	0.3317313	0.0500*
67-5P	67CC	0.0729333	0.0517947	-0.092931	0.2387979	0.5285
67-5RAS-20RAP	67-5RAS-20RAP-5P	0.0508333	0.0517947	-0.115031	0.2166979	0.7637

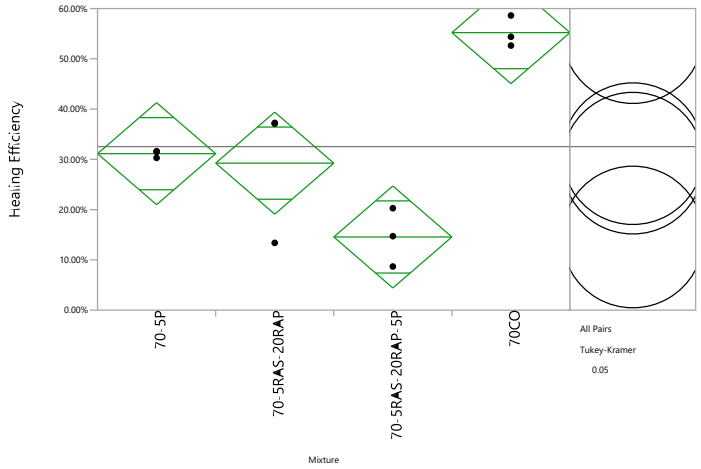

Figure C27. One-way analysis of SERR-Healed for PG 70-22M +5%RAS+20%RAP (room temp).

Table C129. Summary of fit of SERR-Healed for PG 70-22M +5%RAS+20%RAP (room temp).

Parameter	Value
Rsquare	0.845883
Adj Rsquare	0.788089
Root Mean Square Error	0.076222
Mean of Response	0.325358
Observations (or Sum Wgts)	12

Table C130. Analysis of variance of SERR-Healed for PG 70-22M +5%RAS+20%RAP (room temp).

Source	DF	Sum of Squares	Mean Square	F Ratio	Prob > F
Mixture	3	0.25510091	0.085034	14.6362	0.0013*
Error	8	0.04647846	0.005810		
C. Total	11	0.30157937			

Table C131. Means for one-way ANOVA of SERR-Healed for PG 70-22M +5%RAS+20%RAP (room temp).

Level	Number	Mean	Std Error	Lower 95%	Upper 95%
70-5P	3	0.311300	0.04401	0.20982	0.41278
70-5RAS-20RAP	3	0.292433	0.04401	0.19095	0.39391
70-5RAS-20RAP-5P	3	0.145567	0.04401	0.04409	0.24705
70CO	3	0.552133	0.04401	0.45065	0.65361

Table C132. Connecting letters report of SERR-Healed for PG 70-22M +5%RAS+20%RAP (room temp).

Level			Mean
70CO	A		0.55213333
70-5P		B	0.31130000
70-5RAS-20RAP		B	0.29243333
70-5RAS-20RAP-5P		B	0.14556667

Table C133. Ordered differences report of SERR-Healed for PG 70-22M +5%RAS+20%RAP (room temp).

Level	- Level	Difference	Std Err Dif	Lower CL	Upper CL	p-Value
70CO	70-5RAS-20RAP-5P	0.4065667	0.0622351	0.207269	0.6058648	0.0008*
70CO	70-5RAS-20RAP	0.2597000	0.0622351	0.060402	0.4589981	0.0132*
70CO	70-5P	0.2408333	0.0622351	0.041535	0.4401315	0.0199*
70-5P	70-5RAS-20RAP-5P	0.1657333	0.0622351	-0.033565	0.3650315	0.1070
70-5RAS-20RAP	70-5RAS-20RAP-5P	0.1468667	0.0622351	-0.052431	0.3461648	0.1632
70-5P	70-5RAS-20RAP	0.0188667	0.0622351	-0.180431	0.2181648	0.9896

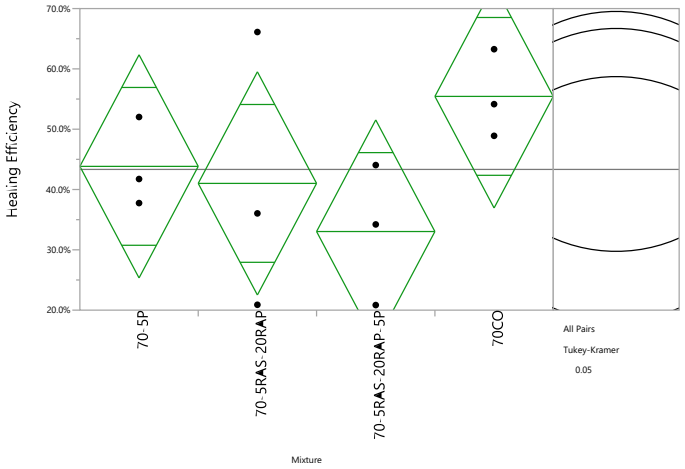

Figure C28. One-way analysis of SERR-Healed for PG 70-22M +5%RAS+20%RAP (high temp/UV exposure).

Table C134. Summary of fit of SERR-Healed for PG 70-22M +5%RAS+20%RAP (high temp/UV exposure).

Parameter	Value
Rsquare	0.333958
Adj Rsquare	0.084192
Root Mean Square Error	0.138967
Mean of Response	0.4333
Observations (or Sum Wgts)	12

Table C135. Analysis of variance of SERR-Healed for PG 70-22M +5%RAS+20%RAP (high temp/UV exposure).

Source	DF	Sum of Squares	Mean Square	F Ratio	Prob > F
Mixture	3	0.07746491	0.025822	1.3371	0.3289
Error	8	0.15449527	0.019312		
C. Total	11	0.23196018			

Table C136. Means for one-way ANOVA of SERR-Healed for PG 70-22M +5%RAS+20%RAP (high temp/UV exposure).

Level	Number	Mean	Std Error	Lower 95%	Upper 95%
70-5P	3	0.438367	0.08023	0.25335	0.62338
70-5RAS-20RAP	3	0.410133	0.08023	0.22512	0.59515
70-5RAS-20RAP-5P	3	0.330333	0.08023	0.14532	0.51535
70CO	3	0.554367	0.08023	0.36935	0.73938

Table C137. Connecting letters report of SERR-Healed for PG 70-22M +5%RAS+20%RAP (high temp/UV exposure).

Level		Mean
70CO	A	0.55436667
70-5P	A	0.43836667
70-5RAS-20RAP	A	0.41013333
70-5RAS-20RAP-5P	A	0.33033333

Table C138. Ordered differences report of SERR-Healed for PG 70-22M +5%RAS+20%RAP (high temp/UV exposure).

Level	- Level	Difference	Std Err Dif	Lower CL	Upper CL	p-Value
70CO	70-5RAS-20RAP-5P	0.2240333	0.1134663	-0.139325	0.5873915	0.2729
70CO	70-5RAS-20RAP	0.1442333	0.1134663	-0.219125	0.5075915	0.6038
70CO	70-5P	0.1160000	0.1134663	-0.247358	0.4793582	0.7419
70-5P	70-5RAS-20RAP-5P	0.1080333	0.1134663	-0.255325	0.4713915	0.7790
70-5RAS-20RAP	70-5RAS-20RAP-5P	0.0798000	0.1134663	-0.283558	0.4431582	0.8930
70-5P	70-5RAS-20RAP	0.0282333	0.1134663	-0.335125	0.3915915	0.9942

C.3. Statistical Analysis for SCB Results

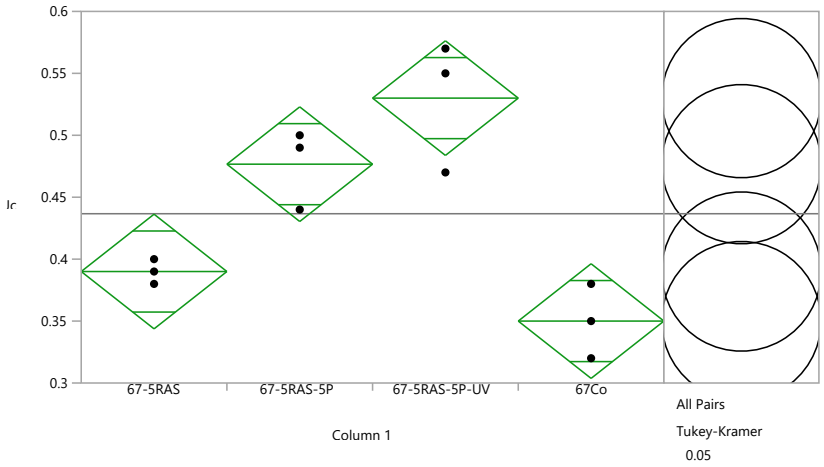

Figure C29. One-way analysis of Jc for PG 67-22 +5%RAS.

Table C139. Summary of fit of Jc for PG 67-22 +5%RAS.

Parameter	Value
Rsquare	0.861244
Adj Rsquare	0.809211
Root Mean Square Error	0.034761
Mean of Response	0.436667
Observations (or Sum Wgts)	12

Table C140. Analysis of variance of Jc for PG 67-22 +5%RAS.

Source	DF	Sum of Squares	Mean Square	F Ratio	Prob > F
Column 1	3	0.06000000	0.020000	16.5517	0.0009*
Error	8	0.00966667	0.001208		
C. Total	11	0.06966667			

Table C141. Means for One-way anova of Jc for PG 67-22 +5%RAS.

Level	Number	Mean	Std Error	Lower 95%	Upper 95%
67-5RAS	3	0.390000	0.02007	0.34372	0.43628
67-5RAS-5P	3	0.476667	0.02007	0.43039	0.52295
67-5RAS-5P-UV	3	0.530000	0.02007	0.48372	0.57628
67Co	3	0.350000	0.02007	0.30372	0.39628

Table C142. Connecting letters report of Jc for PG 67-22 +5%RAS.

Level				Mean
67-5RAS-5P-UV	A			0.53000000
67-5RAS-5P	A	B		0.47666667
67-5RAS		B	C	0.39000000
67Co			C	0.35000000

Table C143. Ordered differences report of Jc for PG 67-22 +5%RAS.

Level	- Level	Difference	Std Err Dif	Lower CL	Upper CL	p-Value
67-5RAS-5P-UV	67Co	0.1800000	0.0283823	0.089110	0.2708899	0.0010*
67-5RAS-5P-UV	67-5RAS	0.1400000	0.0283823	0.049110	0.2308899	0.0050*
67-5RAS-5P	67Co	0.1266667	0.0283823	0.035777	0.2175566	0.0091*
67-5RAS-5P	67-5RAS	0.0866667	0.0283823	-0.004223	0.1775566	0.0617
67-5RAS-5P-UV	67-5RAS-5P	0.0533333	0.0283823	-0.037557	0.1442233	0.3080
67-5RAS	67Co	0.0400000	0.0283823	-0.050890	0.1308899	0.5279

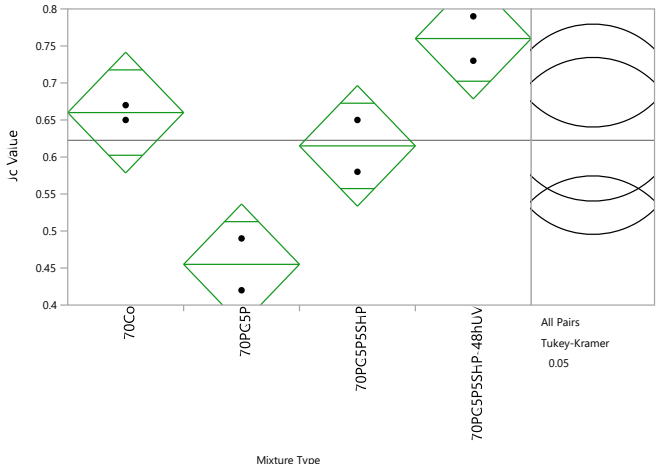

Figure C30. One-way analysis of Jc for PG 70-22M +5%RAS.

Table C144. Summary of fit of Jc for PG 70-22M +5%RAS.

Parameter	Value
Rsquare	0.933494
Adj Rsquare	0.883614
Root Mean Square Error	0.041533
Mean of Response	0.6225
Observations (or Sum Wgts)	8

Table C145. Analysis of variance of Jc for PG 70-22M +5%RAS.

Source	DF	Sum of Squares	Mean Square	F Ratio	Prob > F
Mixture Type	3	0.09685000	0.032283	18.7150	0.0081*
Error	4	0.00690000	0.001725		
C. Total	7	0.10375000			

Table C146. Means for one-way anova of Jc for PG 70-22M +5%RAS.

Level	Number	Mean	Std Error	Lower 95%	Upper 95%
70Co	2	0.660000	0.02937	0.57846	0.74154
70-5RAS	2	0.455000	0.02937	0.37346	0.53654
70-5RAS-5P	2	0.615000	0.02937	0.53346	0.69654
70-5RAS-5P-48	2	0.760000	0.02937	0.67846	0.84154

Table C147. Connecting letters report of Jc for PG 70-22M +5%RAS.

Level			Mean
70-5RAS-5P-48	A		0.76000000
70Co	A		0.66000000
70-5RAS-5P	A	B	0.61500000
70-5RAS		B	0.45500000

Table C148. Ordered differences report of Jc for PG 70-22M +5%RAS.

Level	- Level	Difference	Std Err Dif	Lower CL	Upper CL	p-Value
70-5RAS-5P-48	70-5RAS	0.3050000	0.0415331	0.135925	0.4740753	0.0063*
70Co	70-5RAS	0.2050000	0.0415331	0.035925	0.3740753	0.0264*
70-5RAS-5P	70-5RAS	0.1600000	0.0415331	-0.009075	0.3290753	0.0596
70-5RAS-5P-48	70-5RAS-5P	0.1450000	0.0415331	-0.024075	0.3140753	0.0805
70-5RAS-5P-48	70Co	0.1000000	0.0415331	-0.069075	0.2690753	0.2172
70Co	70-5RAS-5P	0.0450000	0.0415331	-0.124075	0.2140753	0.7169

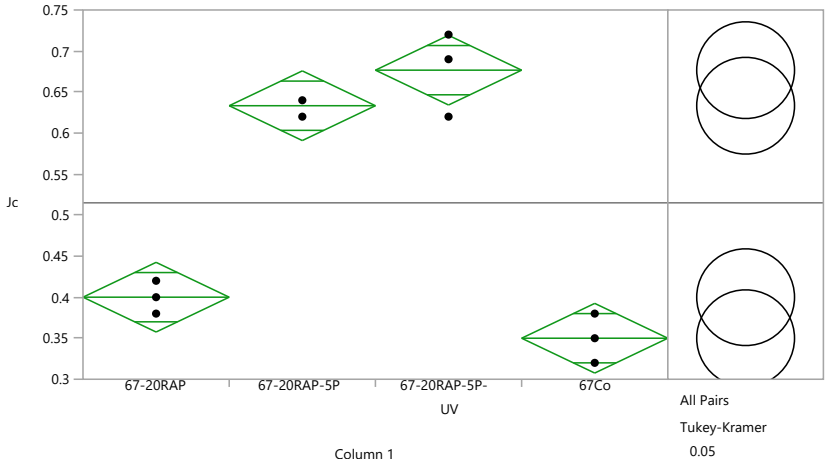

Figure C31. One-way analysis of Jc for PG 67-22 +20%RAP.

Table C149. Summary of fit of Jc for PG 67-22 +20%RAP.

Parameter	Value
Rsquare	0.967454
Adj Rsquare	0.955249
Root Mean Square Error	0.031885
Mean of Response	0.515
Observations (or Sum Wgts)	12

Table C150. Analysis of variance of Jc for PG 67-22 +20%RAP.

Source	DF	Sum of Squares	Mean Square	F Ratio	Prob > F
Column 1	3	0.24176667	0.080589	79.2678	<.0001*
Error	8	0.00813333	0.001017		
C. Total	11	0.24990000			

Table C151. Means for one-way anova of Jc for PG 67-22 +20%RAP.

Level	Number	Mean	Std Error	Lower 95%	Upper 95%
67-20RAP	3	0.400000	0.01841	0.35755	0.44245
67-20RAP-5P	3	0.633333	0.01841	0.59088	0.67578
67-20RAP-5P-UV	3	0.676667	0.01841	0.63422	0.71912
67Co	3	0.350000	0.01841	0.30755	0.39245

Table C152. Connecting letters report of Jc for PG 67-22 +20%RAP.

Level			Mean
67-20RAP-5P-UV	A		0.67666667
67-20RAP-5P	A		0.63333333
67-20RAP		B	0.40000000
67Co		B	0.35000000

Table C153. Ordered differences report of Jc for PG 67-22 +20%RAP.

Level	- Level	Difference	Std Err Dif	Lower CL	Upper CL	p-Value
67-20RAP-5P-UV	67Co	0.3266667	0.0260342	0.243296	0.4100370	<.0001*
67-20RAP-5P	67Co	0.2833333	0.0260342	0.199963	0.3667037	<.0001*
67-20RAP-5P-UV	67-20RAP	0.2766667	0.0260342	0.193296	0.3600370	<.0001*
67-20RAP-5P	67-20RAP	0.2333333	0.0260342	0.149963	0.3167037	<.0001*
67-20RAP	67Co	0.0500000	0.0260342	-0.033370	0.1333704	0.2923
67-20RAP-5P-UV	67-20RAP-5P	0.0433333	0.0260342	-0.040037	0.1267037	0.3993

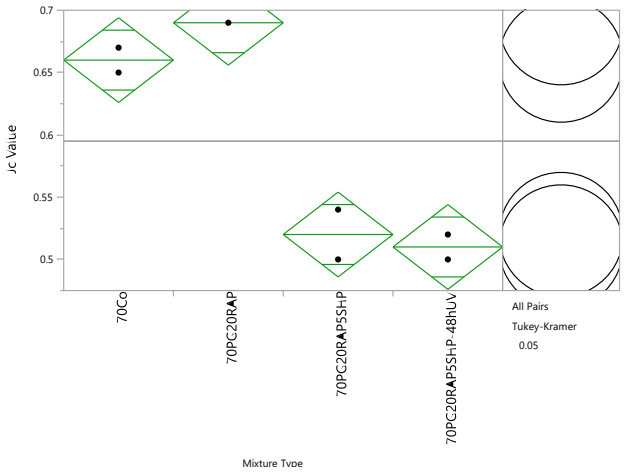

Figure C32. One-way analysis of Jc for PG 70-22M +20%RAP.

Table C154. Summary of fit of Jc for PG 70-22M +20%RAP.

Parameter	Value
Rsquare	0.977528
Adj Rsquare	0.960674
Root Mean Square Error	0.017321
Mean of Response	0.595
Observations (or Sum Wgts)	8

Table C155. Analysis of variance of Jc for PG 70-22M +20%RAP.

Source	DF	Sum of Squares	Mean Square	F Ratio	Prob > F
Mixture Type	3	0.05220000	0.017400	58.0000	0.0009*
Error	4	0.00120000	0.000300		
C. Total	7	0.05340000			

Table C156. Means for one-way anova of Jc for PG 70-22M +20%RAP.

Level	Number	Mean	Std Error	Lower 95%	Upper 95%
70Co	2	0.660000	0.01225	0.62600	0.69400
70-20RAP	2	0.690000	0.01225	0.65600	0.72400
70-20RAP-5P	2	0.520000	0.01225	0.48600	0.55400
70-20RAP-5P-48h	2	0.510000	0.01225	0.47600	0.54400

Table C157. Connecting letters report of Jc for PG 70-22M +20%RAP.

Level			Mean
70-20RAP	A		0.69000000
70Co	A		0.66000000
70-20RAP-5P		B	0.52000000
70-20RAP-5P-48h		B	0.51000000

Table C158. Ordered differences report of Jc for PG 70-22M +20%RAP.

Level	- Level	Difference	Std Err Dif	Lower CL	Upper CL	p-Value
70-20RAP	**70-20RAP-5P-48h**	0.1800000	0.0173205	0.109491	0.2505093	0.0017*
70-20RAP	70-20RAP-5P	0.1700000	0.0173205	0.099491	0.2405093	0.0021*
70Co	**70-20RAP-5P-48h**	0.1500000	0.0173205	0.079491	0.2205093	0.0034*
70Co	70-20RAP-5P	0.1400000	0.0173205	0.069491	0.2105093	0.0044*
70-20RAP	70Co	0.0300000	0.0173205	-0.040509	0.1005093	0.4153
70-20RAP-5P	**70-20RAP-5P-48h**	0.0100000	0.0173205	-0.060509	0.0805093	0.9339

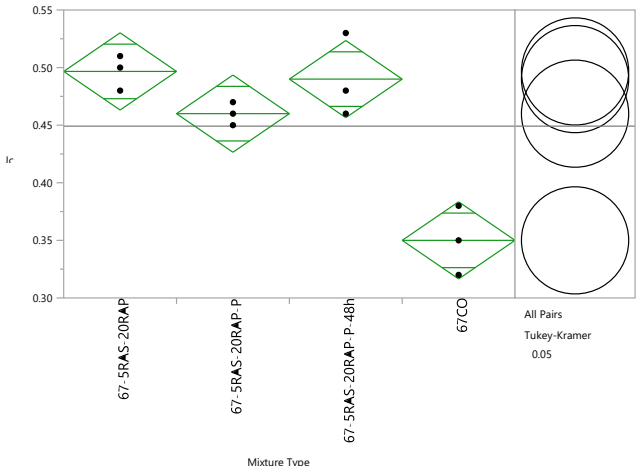

Figure C33. One-way analysis of Jc for PG 67-22 +5%RAS+20%RAP.

Table C159. Summary of fit of Jc for PG 67-22 +5%RAS+20%RAP.

Parameter	Value
Rsquare	0.891487
Adj Rsquare	0.850794
Root Mean Square Error	0.025166
Mean of Response	0.449167
Observations (or Sum Wgts)	12

Table C160. Analysis of variance of Jc for PG 67-22 +5%RAS+20%RAP.

Source	DF	Sum of Squares	Mean Square	F Ratio	Prob > F
Mixture Type	3	0.04162500	0.013875	21.9079	0.0003*
Error	8	0.00506667	0.000633		
C. Total	11	0.04669167			

Table C161. Means for one-way anova of Jc for PG 67-22 +5%RAS+20%RAP.

Level	Number	Mean	Std Error	Lower 95%	Upper 95%
67-5RAS-20RAP	3	0.496667	0.01453	0.46316	0.53017
67-5RAS-20RAP-P	3	0.460000	0.01453	0.42649	0.49351
67-5RAS-20RAP-P-48h	3	0.490000	0.01453	0.45649	0.52351
67CO	3	0.350000	0.01453	0.31649	0.38351

Table C162. Connecting letters report of Jc for PG 67-22 +5%RAS+20%RAP.

Level			Mean
67-5RAS-20RAP	A		0.49666667
67-5RAS-20RAP-P-48h	A		0.49000000
67-5RAS-20RAP-P	A		0.46000000
67CO		B	0.35000000

Table C163. Ordered differences report of Jc for PG 67-22 +5%RAS+20%RAP.

Level	- Level	Difference	Std Err Dif	Lower CL	Upper CL	p-Value
67-5RAS-20RAP	67CO	0.1466667	0.0205480	0.080865	0.2124686	0.0004*
67-5RAS-20RAP-P-48h	67CO	0.1400000	0.0205480	0.074198	0.2058019	0.0006*
67-5RAS-20RAP-P	67CO	0.1100000	0.0205480	0.044198	0.1758019	0.0030*
67-5RAS-20RAP	67-5RAS-20RAP-P	0.0366667	0.0205480	-0.029135	0.1024686	0.3462
67-5RAS-20RAP-P-48h	67-5RAS-20RAP-P	0.0300000	0.0205480	-0.035802	0.0958019	0.5009
67-5RAS-20RAP	67-5RAS-20RAP-P-48h	0.0066667	0.0205480	-0.059135	0.0724686	0.9873

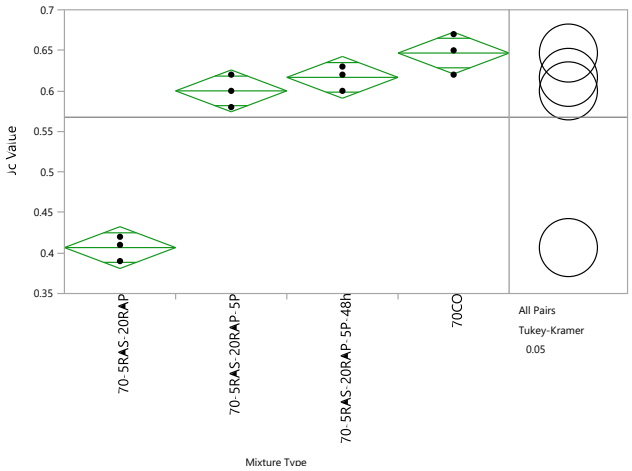

Figure C34. One-way analysis of Jc for PG 70-22M +5%RAS+20%RAP.

Table C164. Summary of fit of Jc for PG 70-22M +5%RAS+20%RAP.

Parameter	Value
Rsquare	0.972684
Adj Rsquare	0.96244
Root Mean Square Error	0.019365
Mean of Response	0.5675
Observations (or Sum Wgts)	12

Table C165. Analysis of variance of Jc for PG 70-22M +5%RAS+20%RAP.

Source	DF	Sum of Squares	Mean Square	F Ratio	Prob > F
Mixture Type	3	0.10682500	0.035608	94.9556	<.0001*
Error	8	0.00300000	0.000375		
C. Total	11	0.10982500			

Table C166. Means for one-way anova of Jc for PG 70-22M +5%RAS+20%RAP.

Level	Number	Mean	Std Error	Lower 95%	Upper 95%
70-5RAS-20RAP	3	0.406667	0.01118	0.38088	0.43245
70-5RAS-20RAP-5P	3	0.600000	0.01118	0.57422	0.62578
70-5RAS-20RAP-5P-48h	3	0.616667	0.01118	0.59088	0.64245
70CO	3	0.646667	0.01118	0.62088	0.67245

Table C167. Connecting letters report of Jc for PG 70-22M +5%RAS+20%RAP.

Level			Mean
70CO	A		0.64666667
70-5RAS-20RAP-5P-48h	A		0.61666667
70-5RAS-20RAP-5P	A		0.60000000
70-5RAS-20RAP		B	0.40666667

Table C168. Ordered differences report of Jc for PG 70-22M +5%RAS+20%RAP.

Level	- Level	Difference	Std Err Dif	Lower CL	Upper CL	p-Value
70CO	70-5RAS-20RAP	0.2400000	0.0158114	0.189366	0.2906335	<.0001*
70-5RAS-20RAP-5P-48h	70-5RAS-20RAP	0.2100000	0.0158114	0.159366	0.2606335	<.0001*
70-5RAS-20RAP-5P	70-5RAS-20RAP	0.1933333	0.0158114	0.142700	0.2439668	<.0001*
70CO	70-5RAS-20RAP-5P	0.0466667	0.0158114	-0.003967	0.0973002	0.0712
70CO	70-5RAS-20RAP-5P-48h	0.0300000	0.0158114	-0.020634	0.0806335	0.3010
70-5RAS-20RAP-5P-48h	70-5RAS-20RAP-5P	0.0166667	0.0158114	-0.033967	0.0673002	0.7247

C.4. Statistical Analysis for LWT Results

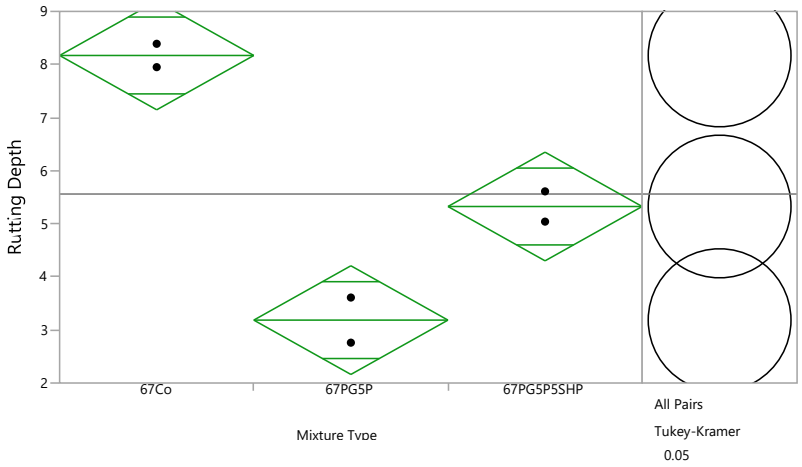

Figure C35. One-way analysis of rutting depth for PG 67-22 +5%RAS.

Table C169. Summary of fit for rutting depth for PG 67-22 +5%RAS.

Parameter	Value
Rsquare	0.975796
Adj Rsquare	0.95966
Root Mean Square Error	0.454789
Mean of Response	5.56
Observations (or Sum Wgts)	6

Table C170. Analysis of variance rutting depth for PG 67-22 +5%RAS.

Source	DF	Sum of Squares	Mean Square	F Ratio	Prob > F
Mixture Type	2	25.015900	12.5080	60.4736	0.0038*
Error	3	0.620500	0.2068		
C. Total	5	25.636400			

Table C171. Means for one-way ANOVA rutting depth for PG 67-22 +5%RAS.

Level	Number	Mean	Std Error	Lower 95%	Upper 95%
67Co	2	8.17000	0.32158	7.1466	9.1934
67-5RAS	2	3.18500	0.32158	2.1616	4.2084
67-5RAS-5P	2	5.32500	0.32158	4.3016	6.3484

Table C172. Connecting letters report rutting depth for PG 67-22 +5%RAS.

Level				Mean
67Co	A			8.1700000
67-5RAS-5P		B		5.3250000
67-5RAS			C	3.1850000

Table C173. Ordered differences report rutting depth for PG 67-22 +5%RAS.

Level	- Level	Difference	Std Err Dif	Lower CL	Upper CL	p-Value
67Co	67-5RAS	4.985000	0.4547893	3.084567	6.885433	0.0033*
67Co	67-5RAS-5P	2.845000	0.4547893	0.944567	4.745433	0.0168*
67-5RAS-5P	67-5RAS	2.140000	0.4547893	0.239567	4.040433	0.0366*

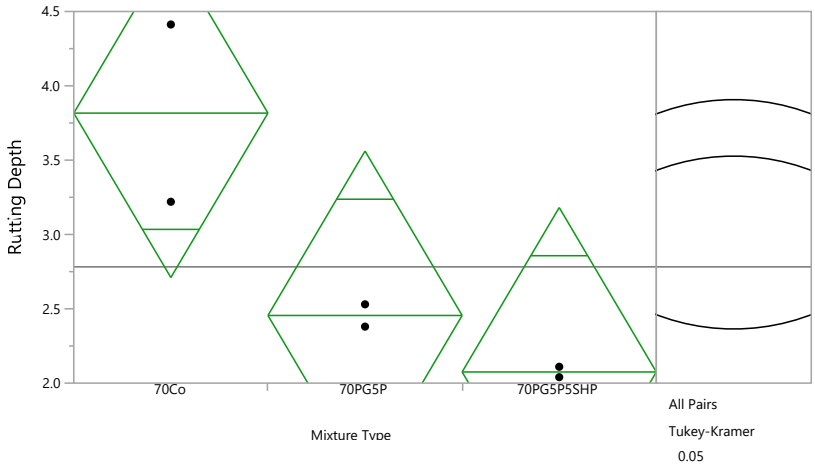

Figure C36. One-way analysis of rutting depth for PG 70-22M +5%RAS.

Table C174. Summary of fit for rutting depth for PG 70-22M +5%RAS.

Parameter	Value
Rsquare	0.822269
Adj Rsquare	0.703782
Root Mean Square Error	0.491499
Mean of Response	2.782081
Observations (or Sum Wgts)	6

Table C175. Analysis of variance rutting depth for PG 70-22M +5%RAS.

Source	DF	Sum of Squares	Mean Square	F Ratio	Prob > F
Mixture Type	2	3.3528772	1.67644	6.9397	0.0749
Error	3	0.7247138	0.24157		
C. Total	5	4.0775910			

Table C176. Means for one-way ANOVA rutting depth for PG 70-22M +5%RAS.

Level	Number	Mean	Std Error	Lower 95%	Upper 95%
70Co	2	3.81624	0.34754	2.7102	4.9223
70-5RAS	2	2.45500	0.34754	1.3490	3.5610
70-5RAS-5P	2	2.07500	0.34754	0.9690	3.1810

Table C177. Connecting letters report rutting depth for PG 70-22M +5%RAS.

Level		Mean
70Co	A	3.8162440
70-5RAS	A	2.4550000
70-5RAS-5P	A	2.0750000

Table C178. Ordered differences report rutting depth for PG 70-22M +5%RAS.

Level	- Level	Difference	Std Err Dif	Lower CL	Upper CL	p-Value
70Co	70-5RAS-5P	1.741244	0.4914990	-0.31259	3.795076	0.0759
70Co	70-5RAS	1.361244	0.4914990	-0.69259	3.415076	0.1350
70-5RAS	70-5RAS-5P	0.380000	0.4914990	-1.67383	2.433832	0.7427

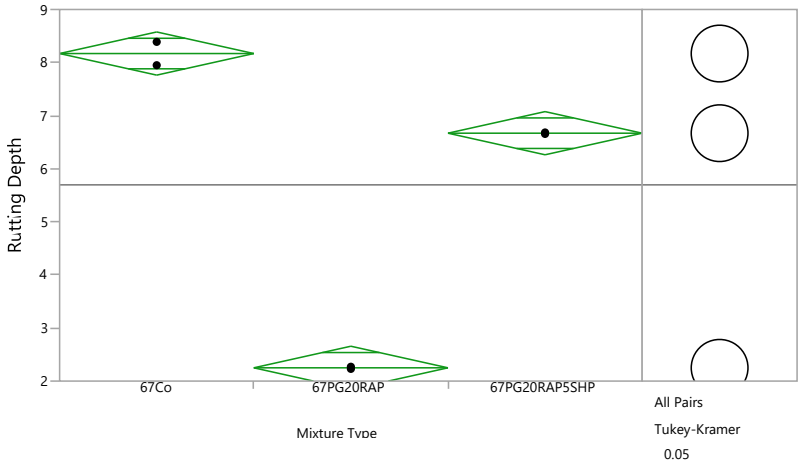

Figure C37. One-way analysis of rutting depth for PG 67-22+20%RAP.

Table C179. Summary of fit for rutting depth for PG 67-22+20%RAP.

Parameter	Value
Rsquare	0.997421
Adj Rsquare	0.995701
Root Mean Square Error	0.180715
Mean of Response	5.696524
Observations (or Sum Wgts)	6

Table C180. Analysis of variance for rutting depth for PG 67-22+20%RAP.

Source	DF	Sum of Squares	Mean Square	F Ratio	Prob > F
Mixture Type	2	37.886868	18.9434	580.0546	0.0001*
Error	3	0.097974	0.0327		
C. Total	5	37.984842			

Table C181. Means for one-way ANOVA for rutting depth for PG 67-22+20%RAP.

Level	Number	Mean	Std Error	Lower 95%	Upper 95%
67Co	2	8.17000	0.12779	7.7633	8.5767
67-20RAP	2	2.25000	0.12779	1.8433	2.6567
67-20RAP-5P	2	6.66957	0.12779	6.2629	7.0762

Table C182. Connecting letters report for rutting depth for PG 67-22+20%RAP.

Level				Mean
67Co	A			8.1700000
67-20RAP-5P		B		6.6695722
67-20RAP			C	2.2500000

Table C183. Ordered differences report for rutting depth for PG 67-22+20%RAP.

Level	- Level	Difference	Std Err Dif	Lower CL	Upper CL	p-Value
67Co	67-20RAP	5.920000	0.1807153	5.164843	6.675157	0.0001*
67-20RAP-5P	67-20RAP	4.419572	0.1807153	3.664415	5.174729	0.0003*
67Co	67-20RAP-5P	1.500428	0.1807153	0.745271	2.255585	0.0075*

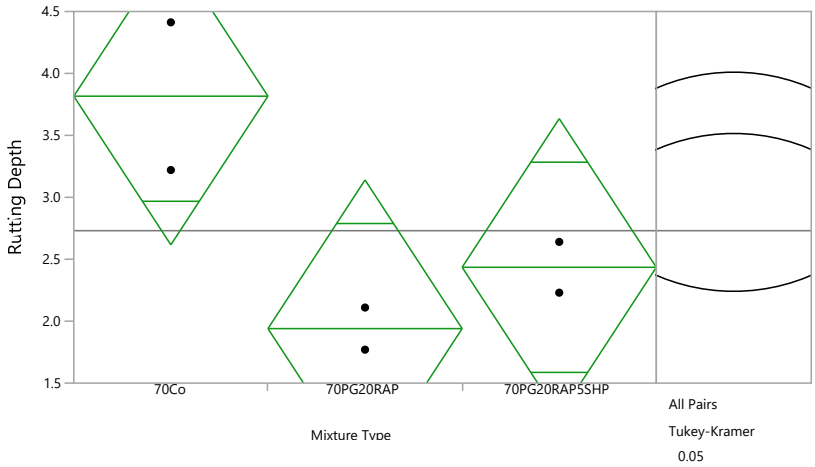

Figure C38. One-way analysis of rutting depth for PG 70-22M +20%RAP.

Table C184. Summary of fit for rutting depth for PG 70-22M +20%RAP.

Parameter	Value
Rsquare	0.815993
Adj Rsquare	0.693322
Root Mean Square Error	0.533187
Mean of Response	2.730415
Observations (or Sum Wgts)	6

Table C185. Analysis of variance for rutting depth for PG 70-22M +20%RAP.

Source	DF	Sum of Squares	Mean Square	F Ratio	Prob > F
Mixture Type	2	3.7821010	1.89105	6.6519	0.0789
Error	3	0.8528638	0.28429		
C. Total	5	4.6349648			

Table C186. Means for one-way ANOVA for rutting depth for PG 70-22M +20%RAP.

Level	Number	Mean	Std Error	Lower 95%	Upper 95%
70Co	2	3.81624	0.37702	2.6164	5.0161
70-20RAP	2	1.94000	0.37702	0.7402	3.1398
70-20RAP-5P	2	2.43500	0.37702	1.2352	3.6348

Table C187. Connecting letters report for rutting depth for PG 70-22M +20%RAP.

Level		Mean
70Co	A	3.8162440
70-20RAP-5P	A	2.4350000
70-20RAP	A	1.9400000

Table C188. Ordered differences report for rutting depth for PG 70-22M +20%RAP.

Level	- Level	Difference	Std Err Dif	Lower CL	Upper CL	p-Value
70Co	70-20RAP	1.876244	0.5331866	-0.35179	4.104277	0.0772
70Co	70-20RAP-5P	1.381244	0.5331866	-0.84679	3.609277	0.1560
70-20RAP-5P	70-20RAP	0.495000	0.5331866	-1.73303	2.723033	0.6623

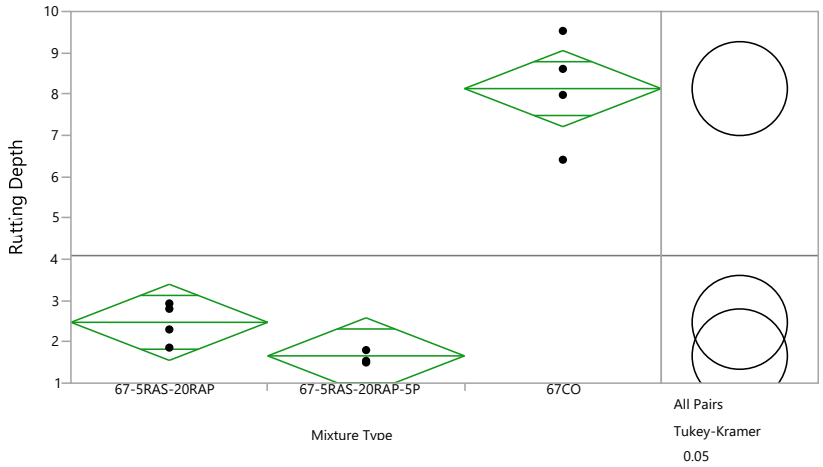

Figure C39. One-way analysis of rutting depth for PG 67-22 +5%RAS+20%RAP.

Table C189. Summary of fit for rutting depth for PG 67-22 +5%RAS+20%RAP.

Parameter	Value
Rsquare	0.943353
Adj Rsquare	0.930765
Root Mean Square Error	0.814586
Mean of Response	4.088333
Observations (or Sum Wgts)	12

Table C190. Analysis of variance for rutting depth for PG 67-22 +5%RAS+20%RAP.

Source	DF	Sum of Squares	Mean Square	F Ratio	Prob > F
Mixture Type	2	99.45202	49.7260	74.9394	<.0001*
Error	9	5.97195	0.6636		
C. Total	11	105.42397			

Table C191. Means for one-way ANOVA for rutting depth for PG 67-22 +5%RAS+20%RAP.

Level	Number	Mean	Std Error	Lower 95%	Upper 95%
67-5RAS-20RAP	4	2.47250	0.40729	1.5511	3.3939
67-5RAS-20RAP-5P	4	1.66000	0.40729	0.7386	2.5814
67CO	4	8.13250	0.40729	7.2111	9.0539

Table C192. Connecting letters report for rutting depth for PG 67-22 +5%RAS+20%RAP.

Level			Mean
67CO	A		8.1325000
67-5RAS-20RAP		B	2.4725000
67-5RAS-20RAP-5P		B	1.6600000

Table C193. Ordered differences report for rutting depth for PG 67-22 +5%RAS+20%RAP.

Level	-Level	Difference	Std Err Dif	Lower CL	Upper CL	p-Value
67CO	67-5RAS-20RAP-5P	6.472500	0.5759991	4.86430	8.080695	<.0001*
67CO	67-5RAS-20RAP	5.660000	0.5759991	4.05180	7.268195	<.0001*
67-5RAS-20RAP	67-5RAS-20RAP-5P	0.812500	0.5759991	-0.79570	2.420695	0.3760

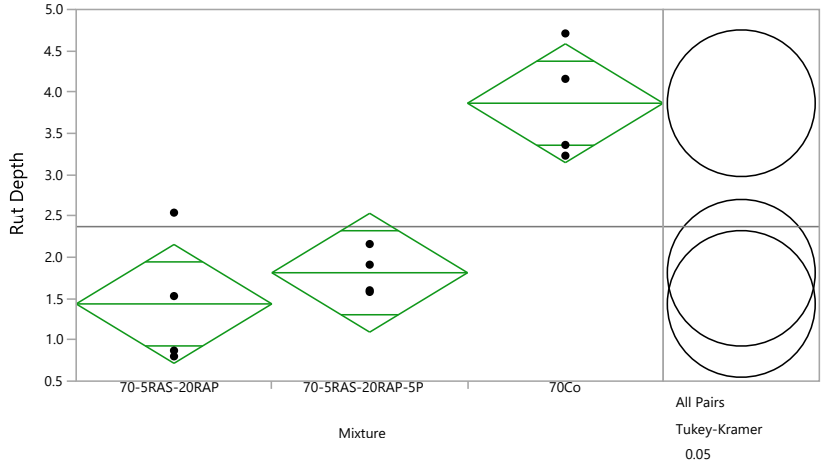

Figure C40. One-way analysis of rutting depth for PG 70-22M +5%RAS+20%RAP.

Table C194. Summary of fit for rutting depth for PG 70-22M +5%RAS+20%RAP.

Parameter	Value
Rsquare	0.789783
Adj Rsquare	0.743068
Root Mean Square Error	0.636071
Mean of Response	2.370833
Observations (or Sum Wgts)	12

Table C195. Analysis of variance for rutting depth for PG 70-22M +5%RAS+20%RAP.

Source	DF	Sum of Squares	Mean Square	F Ratio	Prob > F
Mixture	2	13.680217	6.84011	16.9064	0.0009*
Error	9	3.641275	0.40459		
C. Total	11	17.321492			

Table C196. Means for one-way ANOVA for rutting depth for PG 70-22M +5%RAS+20%RAP.

Level	Number	Mean	Std Error	Lower 95%	Upper 95%
70-5RAS-20RAP	4	1.43500	0.31804	0.7156	2.1544
70-5RAS-20RAP-5P	4	1.81250	0.31804	1.0931	2.5319
70Co	4	3.86500	0.31804	3.1456	4.5844

Table C199. Connecting letters report for rutting depth for PG 70-22M +5%RAS+20%RAP.

Level			Mean
70Co	A		3.8650000
70-5RAS-20RAP-5P		B	1.8125000
70-5RAS-20RAP		B	1.4350000

Table C197. Ordered differences report for rutting depth for PG 70-22M +5%RAS+20%RAP.

Level	- Level	Difference	Std Err Dif	Lower CL	Upper CL	p-Value
70Co	70-5RAS-20RAP	2.430000	0.4497700	1.17424	3.685762	0.0011*
70Co	70-5RAS-20RAP-5P	2.052500	0.4497700	0.79674	3.308262	0.0035*
70-5RAS-20RAP-5P	70-5RAS-20RAP	0.377500	0.4497700	-0.87826	1.633262	0.6894

C.5. Statistical Analysis for TSRST Results

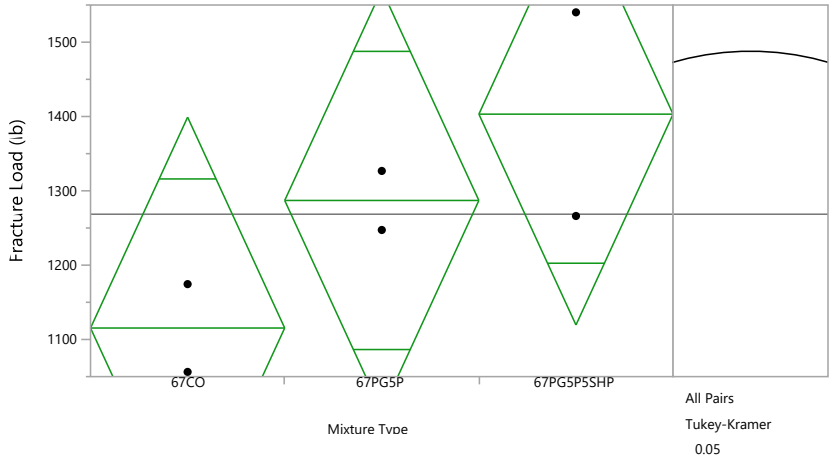

Figure C41. One-way analysis of fracture load (°C) for PG 67-22 +5%RAS.

Table C198. Summary of fit for fracture load (°C) for PG 67-22 +5%RAS.

Parameter	Value
Rsquare	0.637497
Adj Rsquare	0.395828
Root Mean Square Error	126.0568
Mean of Response	1268.523
Observations (or Sum Wgts)	6

Table C199. Analysis of variance fracture load (°C) for PG 67-22 +5%RAS.

Source	DF	Sum of Squares	Mean Square	F Ratio	Prob > F
Mixture Type	2	83833.99	41917.0	2.6379	0.2183
Error	3	47670.99	15890.3		
C. Total	5	131504.98			

Table C200. Means for one-way ANOVA fracture load (°C) for PG 67-22 +5%RAS.

Level	Number	Mean	Std Error	Lower 95%	Upper 95%
67CO	2	1115.39	89.136	831.7	1399.1
67-5RAS	2	1287.02	89.136	1003.4	1570.7
67-5RAS-5P	2	1403.15	89.136	1119.5	1686.8

Table C201. Connecting letters report fracture load (°C) for PG 67-22 +5%RAS.

Level		Mean
67-5RAS-5P	A	1403.1543
67-5RAS	A	1287.0236
67CO	A	1115.3919

Table C202. Ordered differences report fracture load (°C) for PG 67-22 +5%RAS.

Level	- Level	Difference	Std Err Dif	Lower CL	Upper CL	p-Value
67-5RAS-5P	67CO	287.7624	126.0568	-238.993	814.5176	0.2021
67-5RAS	67CO	171.6317	126.0568	-355.123	698.3868	0.4597
67-5RAS-5P	67-5RAS	116.1307	126.0568	-410.624	642.8859	0.6660

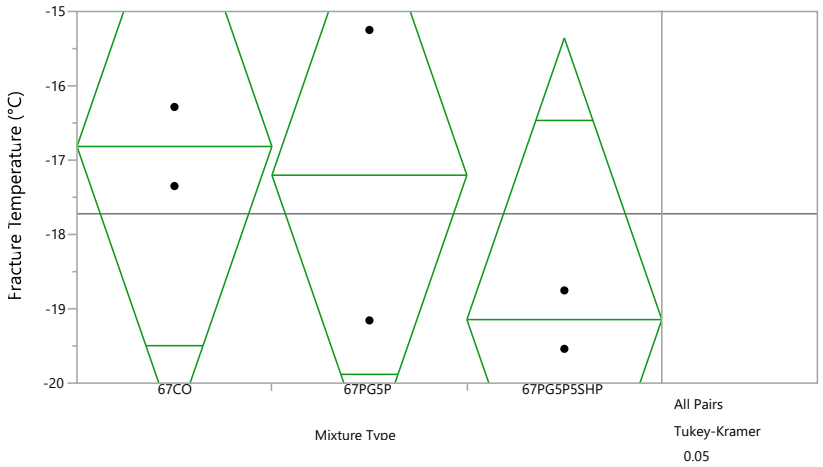

Figure C42. One-way analysis of fracture temperature (°C) for PG 67-22 +5%RAS.

Table C203. Summary of fit for fracture temperature (°C) for PG 67-22 +5%RAS.

Parameter	Value
Rsquare	0.422842
Adj Rsquare	0.038069
Root Mean Square Error	1.684008
Mean of Response	-17.7214
Observations (or Sum Wgts)	6

Table C204. Analysis of variance fracture temperature (°C) for PG 67-22 +5%RAS.

Source	DF	Sum of Squares	Mean Square	F Ratio	Prob > F
Mixture Type	2	6.232931	3.11647	1.0989	0.4385
Error	3	8.507649	2.83588		
C. Total	5	14.740580			

Table C205. Means for one-way ANOVA fracture temperature (°C) for PG 67-22 +5%RAS.

Level	Number	Mean	Std Error	Lower 95%	Upper 95%
67CO	2	-16.816	1.1908	-20.61	-13.03
67-5RAS	2	-17.202	1.1908	-20.99	-13.41
67-5RAS-5P	2	-19.145	1.1908	-22.94	-15.36

Table C206. Connecting letters report fracture temperature (°C) for PG 67-22 +5%RAS.

Level		Mean
67CO	A	-16.81636
67-5RAS	A	. -17.20238
67-5RAS-5P	A	-19.14547

Table C207. Ordered differences report fracture temperature (°C) for PG 67-22 +5%RAS.

Level	- Level	Difference	Std Err Dif	Lower CL	Upper CL	p-Value
67CO	67-5RAS-5P	2.329111	1.684008	-4.70787	9.366094	0.4510
67-5RAS	67-5RAS-5P	1.943099	1.684008	-5.09388	8.980082	0.5510
67CO	67-5RAS	0.386012	1.684008	-6.65097	7.422995	0.9717

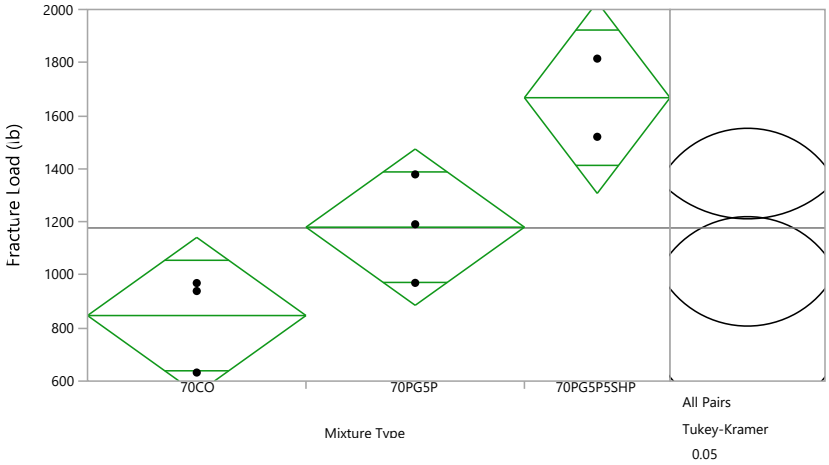

Figure C43. One-way analysis of fracture load (°C) for PG 70-22M +5%RAS.

Table C208. Summary of fit for fracture load (°C) for PG 70-22M +5%RAS.

Parameter	Value
Rsquare	0.804249
Adj Rsquare	0.725948
Root Mean Square Error	198.3469
Mean of Response	1176.955
Observations (or Sum Wgts)	8

Table C209. Analysis of variance fracture load (°C) for PG 70-22M +5%RAS.

Source	DF	Sum of Squares	Mean Square	F Ratio	Prob > F
Mixture Type	2	808177.4	404089	10.2713	0.0170*
Error	5	196707.6	39342		
C. Total	7	1004885.0			

Table C210. Means for one-way ANOVA fracture load (°C) for PG 70-22M +5%RAS.

Level	Number	Mean	Std Error	Lower 95%	Upper 95%
70CO	3	846.96	114.52	552.6	1141.3
70-5RAS	3	1179.86	114.52	885.5	1474.2
70-5RAS-5P	2	1667.60	140.25	1307.1	2028.1

Table C211. Connecting letters report fracture load (°C) for PG 70-22M +5%RAS.

Level			Mean
70-5RAS-5P	A		1667.5953
70-5RAS	A	B	1179.8590
70CO		B	846.9569

Table C212. Ordered differences report fracture load (°C) for PG 70-22M +5%RAS.

Level	- Level	Difference	Std Err Dif	Lower CL	Upper CL	p-Value
70-5RAS-5P	70CO	820.6385	181.0652	231.477	1409.800	0.0142*
70-5RAS-5P	70-5RAS	487.7363	181.0652	-101.425	1076.898	0.0928
70-5RAS	70CO	332.9021	161.9496	-194.060	859.864	0.1942

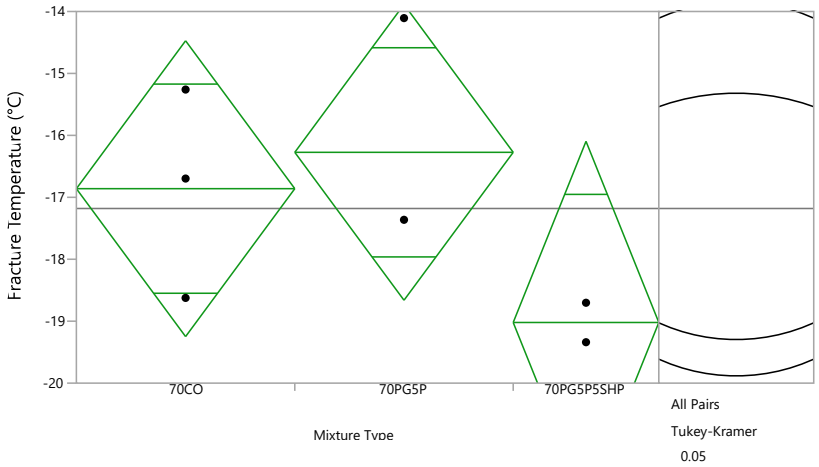

Figure C44. One-way analysis of fracture temperature (°C) for PG 70-22M +5%RAS.

Table C213. Summary of fit for fracture temperature (°C) for PG 70-22M +5%RAS.

Parameter	Value
Rsquare	0.424471
Adj Rsquare	0.19426
Root Mean Square Error	1.60896
Mean of Response	-17.1806
Observations (or Sum Wgts)	8

Table C214. Analysis of variance for fracture temperature (°C) for PG 70-22M +5%RAS.

Source	DF	Sum of Squares	Mean Square	F Ratio	Prob > F
Mixture Type	2	9.546448	4.77322	1.8438	0.2513
Error	5	12.943769	2.58875		
C. Total	7	22.490217			

Table C215. Means for one-way ANOVA for fracture temperature (°C) for PG 70-22M +5%RAS.

Level	Number	Mean	Std Error	Lower 95%	Upper 95%
70CO	3	-16.861	0.9289	-19.25	-14.47
70-5RAS	3	-16.274	0.9289	-18.66	-13.89
70-5RAS-5P	2	-19.021	1.1377	-21.95	-16.10

Table C216. Connecting letters report for fracture temperature (°C) for PG 70-22M +5%RAS.

Level		Mean
70-5RAS	A	-16.27381
70CO	A	-16.86062
70-5RAS-5P	A	-19.02078

Table C217. Ordered differences report for fracture temperature (°C) for PG 70-22M +5%RAS.

Level	- Level	Difference	Std Err Dif	Lower CL	Upper CL	p-Value
70-5RAS	70-5RAS-5P	2.746964	1.468773	-2.03222	7.526151	0.2409
70CO	70-5RAS-5P	2.160154	1.468773	-2.61903	6.939341	0.3785
70-5RAS	70CO	0.586810	1.313711	-3.68782	4.861445	0.8980

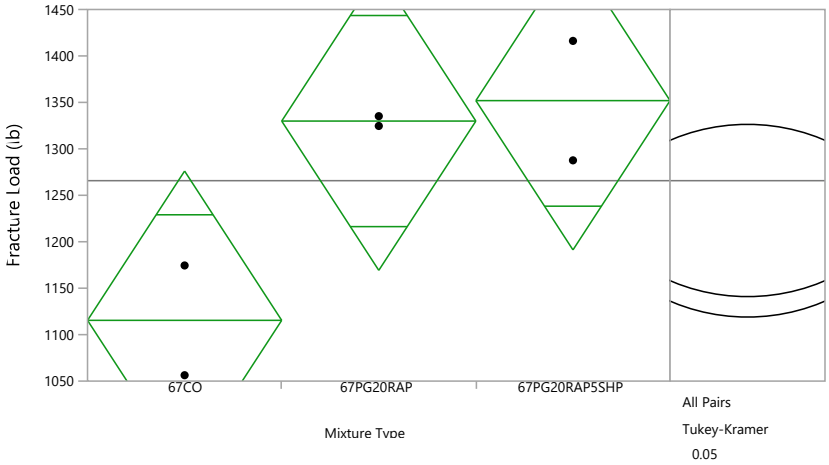

Figure C45. One-way analysis of fracture load (°C) for PG 67-22 +20%RAP.

Table C218. Summary of fit for fracture load (°C) for PG 67-22 +20%RAP.

Parameter	Value
Rsquare	0.816988
Adj Rsquare	0.69498
Root Mean Square Error	71.40551
Mean of Response	1265.725
Observations (or Sum Wgts)	6

Table C219. Analysis of variance for fracture load (°C) for PG 67-22 +20%RAP.

Source	DF	Sum of Squares	Mean Square	F Ratio	Prob > F
Mixture Type	2	68284.185	34142.1	6.6962	0.0783
Error	3	15296.239	5098.7		
C. Total	5	83580.424			

Table C220. Means for one-way ANOVA for fracture load (°C) for PG 67-22 +20%RAP.

Level	Number	Mean	Std Error	Lower 95%	Upper 95%
67CO	2	1115.39	50.491	954.7	1276.1
67-20RAP	2	1329.89	50.491	1169.2	1490.6
67-20RAP-5P	2	1351.89	50.491	1191.2	1512.6

Table C221. Connecting letters report for fracture load (°C) for PG 67-22 +20%RAP.

Level		Mean
67-20RAP-5P	A	1351.8927
67-20RAP	A	1329.8902
67CO	A	1115.3919

Table C222. Ordered differences report for fracture load (°C) for PG 67-22 +20%RAP.

Level	- Level	Difference	Std Err Dif	Lower CL	Upper CL	p-Value
67-20RAP-5P	67CO	236.5008	71.40551	-61.882	534.8838	0.0894
67-20RAP	67CO	214.4983	71.40551	-83.885	512.8813	0.1124
67-20RAP-5P	67-20RAP	22.0025	71.40551	-276.380	320.3855	0.9499

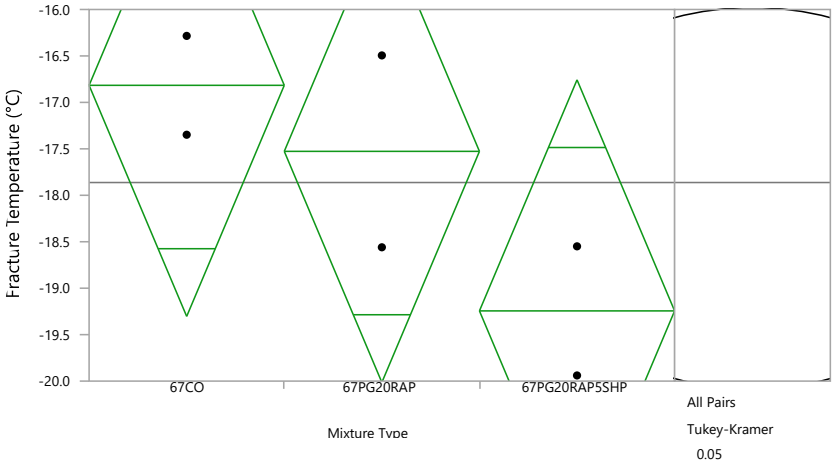

Figure C46. One-way analysis of fracture temperature (°C) for PG 67-22 +20%RAP.

Table C223. Summary of fit for fracture temperature (°C) for PG 67-22 +20%RAP.

Parameter	Value
Rsquare	0.629751
Adj Rsquare	0.382918
Root Mean Square Error	1.105218
Mean of Response	-17.8626
Observations (or Sum Wgts)	6

Table C224. Analysis of variance fracture temperature (°C) for PG 67-22 +20%RAP.

Source	DF	Sum of Squares	Mean Square	F Ratio	Prob > F
Mixture Type	2	6.2329230	3.11646	2.5513	0.2253
Error	3	3.6645215	1.22151		
C. Total	5	9.8974445			

Table C225. Means for one-way ANOVA fracture temperature (°C) for PG 67-22 +20%RAP.

Level	Number	Mean	Std Error	Lower 95%	Upper 95%
67CO	2	-16.816	0.78151	-19.30	-14.33
67-20RAP	2	-17.527	0.78151	-20.01	-15.04
67-20RAP-5P	2	-19.244	0.78151	-21.73	-16.76

Table C226. Connecting letters report fracture temperature (°C) for PG 67-22 +20%RAP.

Level		Mean
67CO	A	-16.81636
67-20RAP	A	-17.52709
67-20RAP-5P	A	-19.24437

Table C227. Ordered differences report fracture temperature (°C) for PG 67-22 +20%RAP.

Level	- Level	Difference	Std Err Dif	Lower CL	Upper CL	p-Value
67CO	67-20RAP-5P	2.428004	1.105218	-2.19038	7.046392	0.2177
67-20RAP	67-20RAP-5P	1.717280	1.105218	-2.90111	6.335667	0.3869
67CO	67-20RAP	0.710724	1.105218	-3.90766	5.329111	0.8090

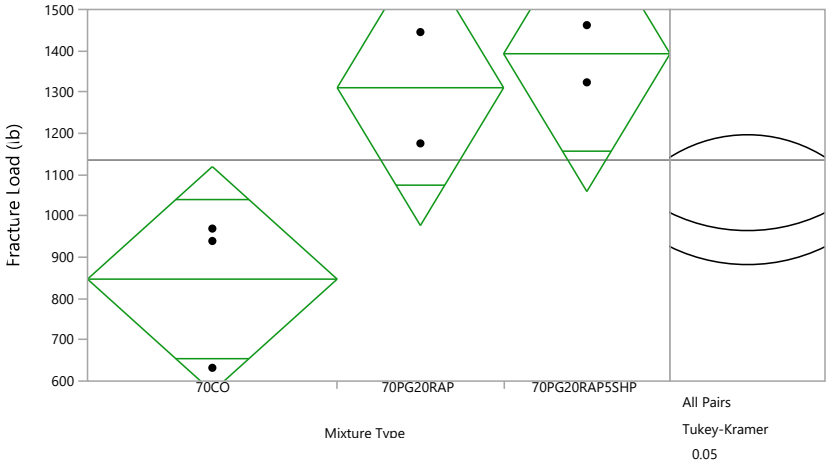

Figure C47. One-way analysis of fracture load (°C) for PG 70-22M +20%RAP.

Table C228. Summary of fit for fracture load (°C) for PG 70-22M +20%RAP.

Parameter	Value
Rsquare	0.793254
Adj Rsquare	0.68988
Root Mean Square Error	169.977
Mean of Response	1135.348
Observations (or Sum Wgts)	7

Table C229. Analysis of variance for fracture load (°C) for PG 70-22M +20%RAP.

Source	DF	Sum of Squares	Mean Square	F Ratio	Prob > F
Mixture Type	2	443419.36	221710	7.6737	0.0427*
Error	4	115568.77	28892		
C. Total	6	558988.13			

Table C230. Means for one-way ANOVA for fracture load (°C) for PG 70-22M +20%RAP.

Level	Number	Mean	Std Error	Lower 95%	Upper 95%
70CO	3	846.96	98.14	574.5	1119.4
70-20RAP	2	1310.47	120.19	976.8	1644.2
70-20RAP-5P	2	1392.81	120.19	1059.1	1726.5

Table C231. Connecting letters report for fracture load (°C) for PG 70-22M +20%RAP.

Level		Mean
70-20RAP-5P	A	1392.8094
70-20RAP	A	1310.4741
70CO	A	846.9569

Table C232. Ordered differences report for fracture load (°C) for PG 70-22M +20%RAP.

Level	- Level	Difference	Std Err Dif	Lower CL	Upper CL	p-Value
70-20RAP-5P	70CO	545.8525	155.1671	-7.161	1098.866	0.0521
70-20RAP	70CO	463.5173	155.1671	-89.496	1016.531	0.0845
70-20RAP-5P	70-20RAP	82.3352	169.9770	-523.461	688.131	0.8823

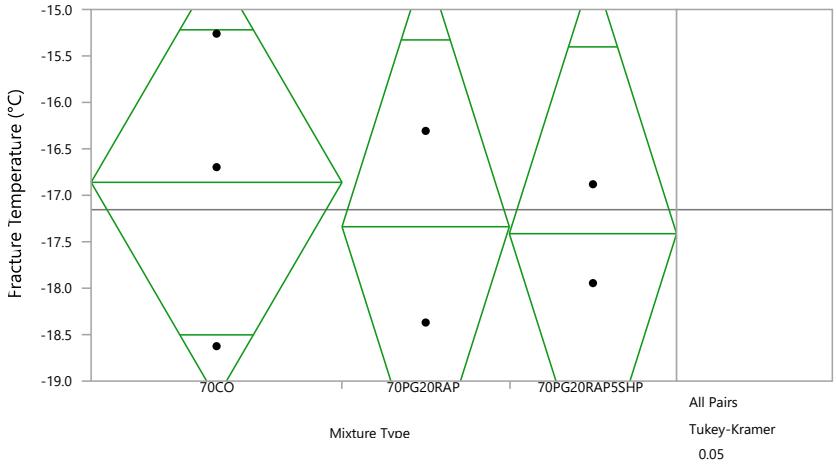

Figure C48. One-way analysis of fracture temperature (°C) for PG 70-22M +20%RAP.

Table C233. Summary of fit for fracture temperature (°C) for PG 70-22M +20%RAP.

Parameter	Value
Rsquare	0.052023
Adj Rsquare	-0.42196
Root Mean Square Error	1.448364
Mean of Response	-17.155
Observations (or Sum Wgts)	7

Table C234. Analysis of variance for fracture temperature (°C) for PG 70-22M +20%RAP.

Source	DF	Sum of Squares	Mean Square	F Ratio	Prob > F
Mixture Type	2	0.4604871	0.23024	0.1098	0.8987
Error	4	8.3910362	2.09776		
C. Total	6	8.8515233			

Table C235. Means for one-way ANOVA for fracture temperature (°C) for PG 70-22M +20%RAP.

Level	Number	Mean	Std Error	Lower 95%	Upper 95%
70CO	3	-16.861	0.8362	-19.18	-14.54
70-20RAP	2	-17.338	1.0241	-20.18	-14.49
70-20RAP-5P	2	-17.413	1.0241	-20.26	-14.57

Table C236. Connecting letters report for fracture temperature (°C) for PG 70-22M +20%RAP.

Level		Mean
70CO	A	-16.86062
70-20RAP	A	-17.33828
70-20RAP-5P	A	-17.41320

Table C237. Ordered differences report for fracture temperature (°C) for PG 70-22M +20%RAP.

Level	- Level	Difference	Std Err Dif	Lower CL	Upper CL	p-Value
70CO	70-20RAP-5P	0.5525723	1.322170	-4.15963	5.264770	0.9103
70CO	70-20RAP	0.4776583	1.322170	-4.23454	5.189856	0.9318
70-20RAP	70-20RAP-5P	0.0749140	1.448364	-5.08704	5.236868	0.9985

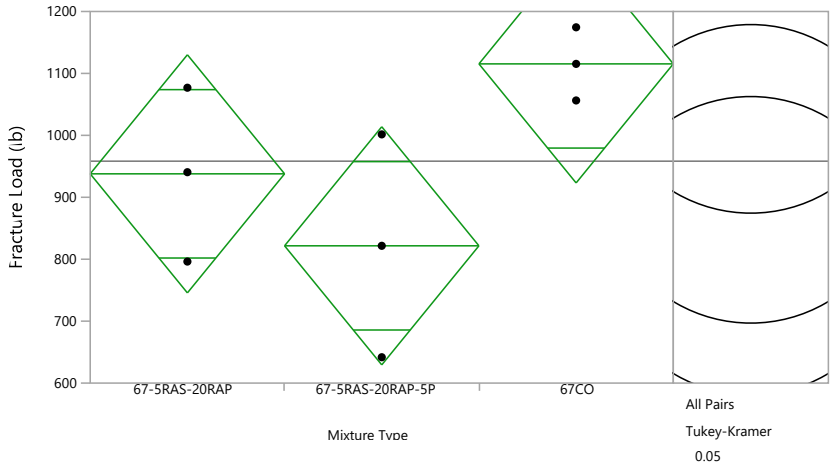

Figure C49. One-way analysis of fracture load (°C) for PG 67-22 + 5%RAS +20%RAP.

Table C238. Summary of fit for fracture load (°C) for PG 67-22 + 5%RAS +20%RAP.

Parameter	Value
Rsquare	0.54167
Adj Rsquare	0.388894
Root Mean Square Error	136.08
Mean of Response	958.3008
Observations (or Sum Wgts)	9

Table C239. Analysis of Variance for fracture load (°C) for PG 67-22 + 5%RAS +20%RAP.

Source	DF	Sum of Squares	Mean Square	F Ratio	Prob > F
Mixture Type	2	131309.71	65654.9	3.5455	0.0963
Error	6	111106.57	18517.8		
C. Total	8	242416.28			

Table C240. Means for one-way ANOVA for fracture load (°C) for PG 67-22 + 5%RAS +20%RAP.

Level	Number	Mean	Std Error	Lower 95%	Upper 95%
67-5RAS-20RAP	3	937.87	78.566	745.62	1130.1
67-5RAS-20RAP-5P	3	821.64	78.566	629.40	1013.9
67CO	3	1115.39	78.566	923.15	1307.6

Table C241. Connecting letters report for fracture load (°C) for PG 67-22 + 5%RAS +20%RAP.

Level		Mean
67CO	A	1115.3913
67-5RAS-20RAP	A	937.8666
67-5RAS-20RAP-5P	A	821.6445

Table C242. Ordered differences report for fracture load (°C) for PG 67-22 + 5%RAS +20%RAP.

Level	- Level	Difference	Std Err Dif	Lower CL	Upper CL	p-Value
67CO	67-5RAS-20RAP-5P	293.7467	111.1088	-47.152	634.6452	0.0850
67CO	67-5RAS-20RAP	177.5246	111.1088	-163.374	518.4231	0.3168
67-5RAS-20RAP	67-5RAS-20RAP-5P	116.2221	111.1088	-224.676	457.1206	0.5779

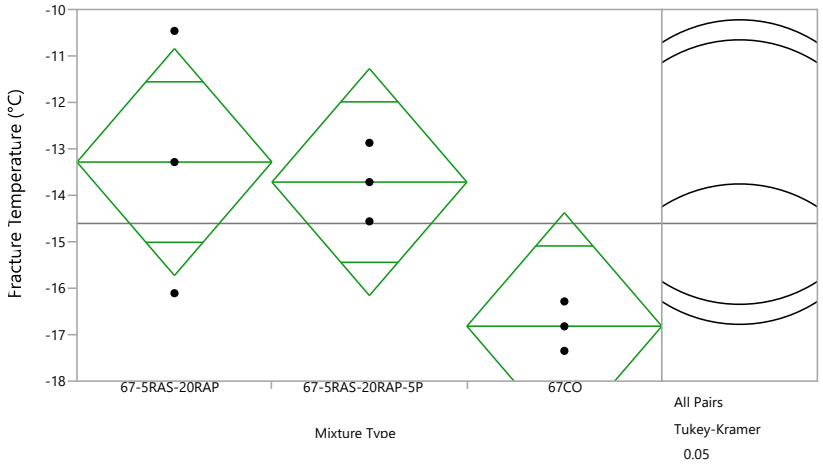

Figure C50. One-way analysis of fracture temperature (°C) for PG 67-22 + 5%RAS +20%RAP.

Table C243. Summary of fit for fracture temperature (°C) for PG 67-22 + 5%RAS +20%RAP.

Parameter	Value
R-square	0.55414
Adj Rsquare	0.40552
Root Mean Square Error	1.728968
Mean of Response	-14.6058
Observations (or Sum Wgts)	9

Table C244. Analysis of variance for fracture temperature (°C) for PG 67-22 + 5%RAS +20%RAP.

Source	DF	Sum of Squares	Mean Square	F Ratio	Prob > F
Mixture Type	2	22.291843	11.1459	3.7286	0.0886
Error	6	17.935983	2.9893		
C. Total	8	40.227826			

Table C245. Means for one-way ANOVA for fracture temperature (°C) for PG 67-22 + 5%RAS +20%RAP.

Level	Number	Mean	Std Error	Lower 95%	Upper 95%
67-5RAS-20RAP	3	-13.284	0.99822	-15.73	-10.84
67-5RAS-20RAP-5P	3	-13.716	0.99822	-16.16	-11.27
67CO	3	-16.818	0.99822	-19.26	-14.38

Table C246. Connecting letters report for fracture temperature (°C) for PG 67-22 + 5%RAS +20%RAP.

Level		Mean
67-5RAS-20RAP	A	-13.28441
67-5RAS-20RAP-5P	A	-13.71553
67CO	A	-16.81758

Table C247. Ordered differences report for fracture temperature (°C) for PG 67-22 + 5%RAS +20%RAP.

Level	- Level	Difference	Std Err Dif	Lower CL	Upper CL	p-Value
67-5RAS-20RAP	67CO	3.533169	1.411696	-0.79813	7.864465	0.1017
67-5RAS-20RAP-5P	67CO	3.102046	1.411696	-1.22925	7.433342	0.1502
67-5RAS-20RAP	67-5RAS-20RAP-5P	0.431123	1.411696	-3.90017	4.762419	0.9503

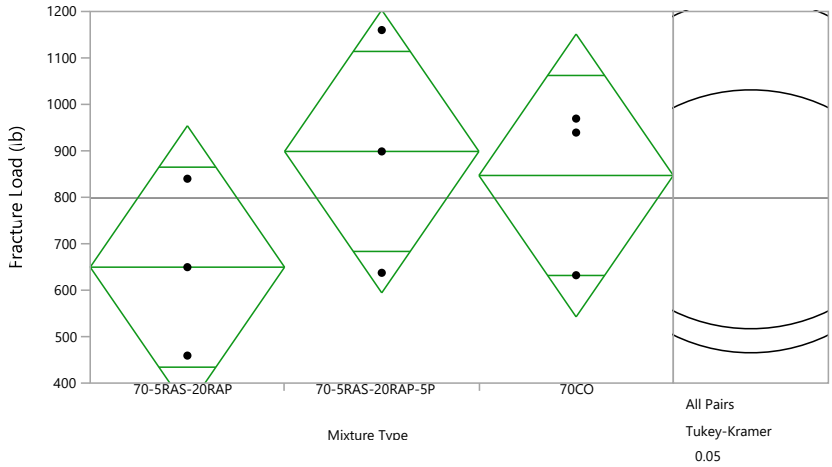

Figure C51. One-way analysis of fracture load (°C) for PG 70-22M + 5%RAS +20%RAP.

Table C248. Summary of fit for fracture load (°C) for PG 70-22M + 5%RAS +20%RAP.

Parameter	Value
Rsquare	0.271251
Adj Rsquare	0.028334
Root Mean Square Error	215.5163
Mean of Response	798.4034
Observations (or Sum Wgts)	9

Table C249. Analysis of variance for fracture load (°C) for PG 70-22M + 5%RAS +20%RAP.

Source	DF	Sum of Squares	Mean Square	F Ratio	Prob > F
Mixture Type	2	103729.93	51865.0	1.1166	0.3870
Error	6	278683.64	46447.3		
C. Total	8	382413.57			

Table C250. Means for one-way ANOVA for fracture load (°C) for PG 70-22M + 5%RAS +20%RAP.

Level	Number	Mean	Std Error	Lower 95%	Upper 95%
70-5RAS-20RAP	3	649.546	124.43	345.08	954.0
70-5RAS-20RAP-5P	3	898.707	124.43	594.24	1203.2
70CO	3	846.957	124.43	542.49	1151.4

Table C251. Connecting letters report for fracture load (°C) for PG 70-22M + 5%RAS +20%RAP.

Level		Mean
70-5RAS-20RAP-5P	A	898.70689
70CO	A	846.95686
70-5RAS-20RAP	A	649.54636

Table C252. Ordered differences report for fracture load (°C) for PG 70-22M + 5%RAS +20%RAP.

Level	- Level	Difference	Std Err Dif	Lower CL	Upper CL	p-Value
70-5RAS-20RAP-5P	70-5RAS-20RAP	249.1605	175.9683	-290.737	789.0576	0.3915
70CO	70-5RAS-20RAP	197.4105	175.9683	-342.487	737.3076	0.5365
70-5RAS-20RAP-5P	70CO	51.7500	175.9683	-488.147	591.6471	0.9538

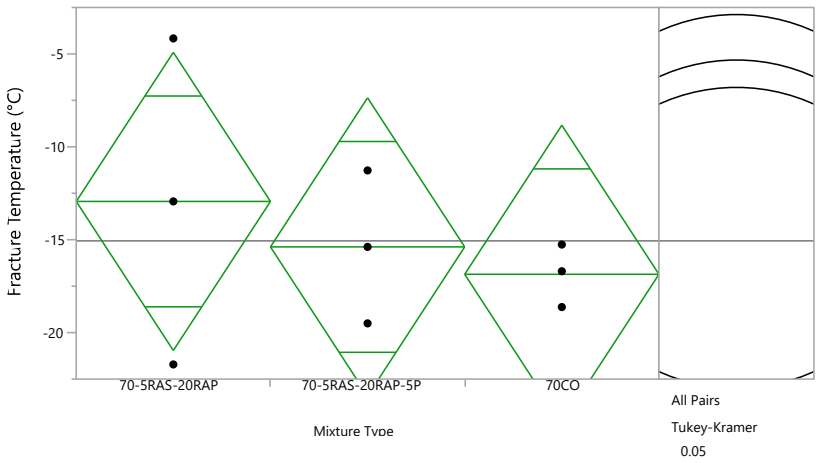

Figure C52. One-way analysis of fracture temperature (°C) for PG 70-22M + 5%RAS +20%RAP.

Table C253. Summary of fit for fracture temperature (°C) for PG 70-22M + 5%RAS +20%RAP.

Parameter	Value
Rsquare	0.108464
Adj Rsquare	-0.18872
Root Mean Square Error	5.679542
Mean of Response	-15.0618
Observations (or Sum Wgts)	9

Table C254. Analysis of variance fracture temperature (°C) for PG 70-22M + 5%RAS +20%RAP.

Source	DF	Sum of Squares	Mean Square	F Ratio	Prob > F
Mixture Type	2	23.54630	11.7731	0.3650	0.7086
Error	6	193.54321	32.2572		
C. Total	8	217.08951			

Table C255. Means for one-way ANOVA fracture temperature (°C) for PG 70-22M + 5%RAS +20%RAP.

Level	Number	Mean	Std Error	Lower 95%	Upper 95%
70-5RAS-20RAP	3	-12.939	3.2791	-20.96	-4.915
70-5RAS-20RAP-5P	3	-15.386	3.2791	-23.41	-7.362
70CO	3	-16.861	3.2791	-24.88	-8.837

Table C256. Connecting letters report fracture temperature (°C) for PG 70-22M + 5%RAS +20%RAP.

Level		Mean
70-5RAS-20RAP	A	-12.93863
70-5RAS-20RAP-5P	A	-15.38608
70CO	A	-16.86062

Table C257. Ordered differences report fracture temperature (°C) for PG 70-22M + 5%RAS +20%RAP.

Level	- Level	Difference	Std Err Dif	Lower CL	Upper CL	p-Value
70-5RAS-20RAP	70CO	3.921992	4.637327	-10.3060	18.15000	0.6908
70-5RAS-20RAP	70-5RAS-20RAP-5P	2.447445	4.637327	-11.7806	16.67546	0.8610
70-5RAS-20RAP-5P	70CO	1.474548	4.637327	-12.7535	15.70256	0.9463